Design and Physico-Chemical Properties of Cyclodextrin Incorporated Hydrogels: Application towards Controlled Delivery of Drugs

A THESIS

submitted by

SUBHRASEEMA DAS

for the award of the degree

of

DOCTOR OF PHILOSOPHY

DEPARTMENT OF CHEMISTRY
NATIONAL INSTITUTE OF TECHNOLOGY, ROURKELA
ODISHA-769 008

THESIS CERTIFICATE

This is to certify that the thesis entitled "**Design and Physico-Chemical Properties of Cyclodextrin Incorporated Hydrogels: Application towards Controlled Delivery of Drugs**" submitted by **SUBHRASEEMA DAS** to National Institute of Technology, Rourkela, for the award of the Doctor of Philosophy, is a bona fide record of research work carried out by her under my supervision. The contents of this thesis, in full or in parts, have not been submitted to any other Institute or University for the award of any degree or diploma.

Research Guide

Rourkela 769 008
Date:

Dr. U. Subuddhi
Dept. of Chemistry
NIT Rourkela

ACKNOWLEDGEMENTS

I avail this opportunity to express my deep sense of gratitude and indebtedness to my research guide **Dr. U. Subuddhi**, for her excellent guidance, constant encouragement and support throughout my research work. The vastness of her scientific knowledge and analytical approach has made a deep impression on me. The many discussions I had with her have made me think logically and have helped me improve my knowledge.

I wish to thank **Dr. N. Panda** (the present Head of the Department) and **Dr. R. K. Patel, Dr. B. G. Mishra** (former Heads of the Department) for allowing me to avail the facilities of the Department. I am thankful to all my Doctoral Committee members **Prof. P. Rath, Dr. G. Hota,** and **Dr. R. K. Patel** for their valuable suggestions throughout my research career. The financial assistance from **Department of Science and Technology, India** is highly acknowledged.

I would like to thank **Dr. S. K. Rout** of BIT, Mesra and **Prof. A. K. Mishra** of IIT Madras, for the DSC data. My sincere thanks to **Mr. B. Nayak of** CIPET, Bhubaneswar, for his kind help in DSC experiments. I wish to thank all my **teachers,** who have laid the foundation of education and inculcated the very essence of scientific temper in me.

My earnest thanks to my childhood friend **Parth** for his unconditional love and support during the difficult times of my life. I convey special acknowledgements to my dearest friend **Hirak** for his affection and encouragement during the tenure of my doctoral research. I would like to thank **Dr. S. Samantaray, Dr. A. Mahapatra, Dr. S. Pasayat** and **Dr. A. Jena** for their support and timely help. I thank all my friends **Saswati, Prakash, Sudhir, Hrushikesh, Asima, Sandip, Purabi, Jyoti**

Prakash, Shabna, Bappaditya, Smruti Ranjan, Manoj, Radharaman, Subrat, Arindam, Aniruddha, Rituraj, Himanshu Kumar, Shubham, Bhakti, Pradipta, Bedanta, Deepthi, Chaitanya, Amar, Shubhasree, Vijayalakshmi, Sasmita, Tapaswini, Shatabdi, Sudarshana, Sarita, Raghavendra, Dinesh and **Kishore Babu** for their pleasant company. A special message of thanks to my lab mate **Smruti** for being with me through thick and thin.

No words can convey my gratitude to my parents **Dr. Subhra Prakash Das** and **Dr. Somarani Chand** for their generous love and blessings, without which it would have never been possible on my part to reach so far. I thank my brother **Som** for all his affection and for uplifting my spirit in need. My heartfelt thanks are due to all my relatives for their love. I would like to add a special note of thanks for my paternal grandparents **Sri. R. C. Das** and **Smt. Laxmi Das** and maternal grandparents **Sri N. K. Chand** and **Smt. Binapani Chand** for their love, support and belief in all my endeavours.

Finally, I would like to thank all those people, who have directly or indirectly helped me at various stages of my research work.

Subhraseema Das

PREFACE

Keywords: Hydrogels, smart hydrogels, controlled drug delivery, beta cyclodextrin, solid inclusion complexes, swelling characteristics, *in vitro* drug release, cytotoxicity assay.

Hydrogels are polymeric networks with three-dimensional configuration capable of imbibing large amounts of water or biological fluids. Owing to their ability to retain a significant amount of water, hydrogels mimic the natural structure of the body's cellular makeup, which renders them important for an array of biomedical applications including tissue engineering, artificial organ and contact lens designing and most importantly in drug delivery. A truly amazing class of hydrogels that has found profound interests as drug delivery systems is the class of smart/ intelligent hydrogels. These hydrogels are endowed with the unique property to exhibit unusual volume changes in response to environmental stimuli. Efforts have focused mostly on designing hydrogel systems that make use of changes in response to pH and temperature. Despite numerous advantages, hydrogels are also associated with some inherent pharmacological limitations. The poor mechanical strength of many hydrogels results in their premature disintegration. The high water content and porous nature of the hydrogels often result in a relative rapid release of drug thereby reducing the therapeutic value.

The present study aims at addressing the above problems by incorporating preformed drug-cyclodextrin inclusion complexes (ICs) into the hydrogel matrix. Cyclodextrins are of interest in this context given their amphiphilic nature; a hydrophilic exterior and a hydrophobic pocket. The hydrophilic exterior can be useful for effective partitioning into the hydrogel matrix and maintaining the bulk hydrophilicity and swelling state of the hydrogel and the hydrophobic interior can facilitate the entrapment and controlled release of hydrophobic drugs and therapeutics. Of the parent α−, β− and

γ−cyclodextrins, β−cyclodextrin (CD) is widely employed for pharmaceutical purposes in comparison to the other two. The scope of the present study particularly emphasizes the role of CD in controlled drug delivery from hydrogels.

Chapter 1 introduces the concept of hydrogels and their numerous applications in various fields. The utility of hydrogels as target-specific drug delivery agents has been discussed at length. The importance of cyclodextrins as drug delivery agents is hereby introduced. The different strategies of integrating hydrogels and cyclodextrins to achieve improved physico-chemical properties have also been discussed. The objective of the present thesis work is also given.

Chapter 2 provides information on the materials used and the methodologies employed for the studies.

Chapter 3 demonstrates the applicability of poly(vinyl alcohol) (PVA) hydrogels containing drug−CD ICs as controlled drug delivery systems. Different compositions of pure PVA hydrogels and CD−incorporated PVA hydrogels were synthesized with varying amount of the cross-linker glutaraldehyde (GA) by the solution casting technique. Hydrogels containing the free drug and ICs were also prepared and explored for their drug releasing properties. In this study, salicylic acid (SA) and ibuprofen (IBF) were chosen as the drugs of interest. The solid ICs of the drug in CD were prepared by the co-precipitation method. The swelling evaluation of the hydrogels indicated the decreased swelling with increasing GA content for both PVA and PVA-CD hydrogels. The role of CD, the effect of nature of drug and degree of cross-linking on the drug release process has also been investigated. The probable mechanism of drug release has also been addressed by fitting the release data to various mathematical equations. Controlled release of drug was achieved from the hydrogels containing the ICs. The effect of degree of cross-linking on the release

pattern is strikingly different from hydrogels containing free drug and that with the ICs. The role of CD in the drug release process is not only because of its inclusion ability but also its effect on the polymer relaxation. GA, apart from cross-linking PVA, probably interacts with the hydroxyl groups of CDs thereby influencing the matrix structure. The nature of drug in terms of its binding efficacy with CD plays an important role. Thus the drug release is accomplished as a combination of the effects of drug diffusion, the polymer relaxation, the binding affinity of the drugs with CD and the effect of CD on the macromolecular relaxation. The cytotoxicity assay performed on the hydrogels by MTT colorimetric technique suggested a high compatibility of these hydrogels with the living tissues. Hence the strategy of incorporating pre-formed ICs into PVA hydrogels to achieve controlled delivery of drugs works quite well.

Chapter 4 presents the design of pH-responsive smart hydrogels based on chitosan (CS) and poly(acrylic acid) (PAA) for controlled drug delivery. This chapter consists of two parts; **Part I**: To explore the potential of GA cross-linked CS−PVA hydrogels towards the controlled delivery of non-steroidal anti-inflammatory drugs (NSAIDs), Naproxen (NX) and Diclofenac sodium (DS), to the intestine and **Part II**: To inspect the utility of PAA hydrogel microspheres towards controlled delivery of Dexamethasone (DX) and investigate the influence of method of preparation of IC on the drug release phenomenon from the microspheres.

Part I: pH-Sensitive CS−PVA hydrogels with varying amounts of PVA and cross-linked with GA were synthesized and explored for the delivery of NX and DS. The preformed solid NX−CD and DS−CD inclusion complexes were added directly into the CS−PVA hydrogels. With increased amount of PVA in CS−PVA hydrogels, the degree of swelling decreased due to increased hydrogel density. All the synthesized

hydrogels exhibited maximum swelling at neutral pH. The presence of CD did not have any drastic effect on the swellability of the hydrogels. The antimicrobial property of CS was not compromised in the presence of PVA and/or CD in the hydrogels. The drug release from the IPN hydrogels was much prolonged as compared to pure CS hydrogels. The hydrogels containing the ICs released the drug considerably slower than those containing the free drug. With increasing PVA content, the rate of drug release was found to decrease. The *in vitro* drug release of hydrogels in simulated gastric fluid (SGF) showed negligible release of drug over a period of 2 h while it increased significantly in the simulated intestinal fluid (SIF). This release profile is suitable for the oral delivery of the drug. The pH-specific release of NX and DS from these hydrogels can be utilised for intestine−targeted delivery. The cytotoxic assay ensured them to be non-toxic and biocompatible and suggested their potential as controlled and intestine-specific drug delivery agents. Thus, it can be proposed that the deleterious effects of NSAIDs on the epithelium of the gastrointestinal tract (GIT) could be minimized by using the IC loaded hydrogels as drug delivery system (DDS) given that they provide a controlled release resulting in a reduced concentration of free NSAIDs.

Part II: In view of the importance of microspheres in drug delivery, PVA−PAA microspheres have been synthesized and examined for the controlled delivery of the common anti-inflammatory and immunosuppressant drug DX to the intestine. To regulate the release rate of DX, preformed solid ICs of DX with CD was added to the hydrogel microspheres. In order to study the influence of the method of preparation of IC on the release behaviour, the IC was prepared by two different methods: the co-precipitation (CP) and freeze-drying (FD). The GA cross-linked PVA−PAA hydrogel microspheres containing free drug, the physical mixture and the ICs were synthesized

to investigate their drug release behaviour. The swelling characteristics of the microspheres indicated higher swelling in neutral pH than in acidic pH. The microspheres exhibited negligible drug release in pH 1.2 whereas significant release in pH 7.4. Slowest release was observed from the microspheres which contained the FD inclusion product. The drug release in SGF and SIF revealed approximately 5% of DX release during the initial 2 h in SGF and increasing significantly upon transferring to SIF. Thus the synthesized microspheres could be effectively employed for the controlled delivery of DX and their pH sensitivity could be exploited for the delivery to the intestine. Moreover, the compatibility of the synthesized microspheres with the living tissues further validates them as promising drug delivery systems.

Chapter 5 deals with regulating the delivery of the anticancer drug 5-Fluorouracil (5FU) from temperature-sensitive interpenetrating polymer network (IPN) hydrogels of guar gum (GG) and Poly (N−isopropylacrylamide) (PNIPAAm). In lieu of utilization of natural polysaccharides in drug delivery systems, GG is of particular interest because of its susceptibility to microbial degradation in the large intestine. The IPN hydrogels were synthesized using a non-toxic cross-linker, tetraethyl orthosilicate (TEOS). 5FU−CD solid ICs, prepared by freeze-drying method, were directly added to the hydrogel matrix. Incorporation of GG did not disturb the arrangement of PNIPAAm chains and the lower critical solution temperature (LCST) remained invariant. The hydrogels exhibited temperature-responsive swelling characteristics. The hydrogels also exhibited temperature dependence in their drug releasing characteristics. At higher temperature (above LCST) the release rate was considerably slower than that at lower temperature (below LCST). Presence of IC in the hydrogel matrix is capable of significantly controlling the drug release rate despite the fact that the matrix is undergoing a drastic morphological change above its LCST. The

presence of CD in the hydrogels as ICs was vital in influencing the polymer relaxation and retarding the drug release rate from the hydrogels containing the ICs. The cytotoxicity assay performed on rat fibroblasts certified these hydrogels to be safe, nontoxic and biocompatible with living tissues thereby validating their potential as controlled drug delivery systems.

Chapter 6 focuses on the evaluation and comparison of the efficacy of GG-PAA-CD hydrogels with CD as a part of their network structure, and GG-PAA hydrogel containing the preformed DX-CD IC, for the controlled delivery of DX. IPN hydrogels composed of GG and PAA have been developed by using TEOS as cross-linker by varying the ratio of GG and PAA. The corresponding GG−PAA−CD hydrogels with CD as a part of the network structure were also synthesized. The swelling characteristics revealed maximum swelling at neutral pH. Controlled release of drug was obtained from CD-incorporated hydrogels as opposed to the fast release from the hydrogels without CD. Upon comparison it was found that the hydrogels containing preformed ICs performed better in terms of controlled release characteristics than the hydrogels containing CD as a part of their network structure. The cytotoxicity study revealed the biocompatible and nontoxic nature of these hydrogels validating them as promising drug delivery systems.

Chapter 7 provides the summary of the important findings of the work and also suggests the scope for future work.

TABLE OF CONTENTS

LIST OF TABLES

LIST OF FIGURES

LIST OF SCHEMES

LIST OF ABBREVIATIONS

DDS	Drug Delivery Systems
CDDS	Controlled Drug Delivery Systems
CDs	Cyclodextrins
α−CD	Alpha Cyclodextrin
CD	Beta Cyclodextrin
γ−CD	Gamma Cyclodextrin
IC	Inclusion Complex
PM	Physical Mixture
CP	Co-precipitation
FD	Freeze-drying
NSAID	Non-steroidal Anti-inflammatory Drug
AAc	Acrylic Acid
NIPAAm	N-Isopropylacrylamide
GG	Guar Gum
HEMA	Hydroxyethyl methacrylate
HEEMA	Hydroxyethoxyethyl methacrylate
MEMA	Methoxyethyl methacrylate
EGDMA	Ethyleneglycol dimethacrylate
EGDE	Ethylene Glycol Diglycidyl Ether
EPI	Epichlorohydrin
NVP	N-vinyl-2-pyrrolidone
EG	Ethylene glycol
VAc	Vinyl acetate
PVA	Poly(vinyl alcohol)
PEG	Poly(ethylene glycol)
PPG	Poly(propylene glycol)
PLGA	Poly(lactic-co-glycolic acid)
PEO	Poly(ethylene oxide)
CS	Chitosan
HA	Hyaluronic Acid
NaAlg	Sodium alginate
PLA	Poly(lactic acid)

PAA	Poly(acrylic acid)
PNIPAAm	Poly(N-isopropylacrylamide)
PAAm	Poly(acrylamide)
PVP	Poly(N-vinyl-2-pyrrolidone)
CMC	Carboxymethyl cellulose
HPMC	Hydroxypropyl methylcellulose
PNAGA	Poly(N-acryloyl glycinamide)
PAAm	Poly(acrylamide)
PVDF	Polyvinylidene fluoride
Con A	Concanavalin A
PEG_8	8-arm PEG
UHP	Ultra High Pressure
TiO_2	Titanium Dioxide
HTCC	N-[(2-hydroxy-3-trimethylammonium) propyl] chitosan chloride
PEM	Polyelectrolyte Multilayer
BBB	Blood-Brain Barrier
PACAP	Pituitary Adenylate Cyclase Activating Polypeptide
GALP	Galanin-like Peptide
HMDI	Hexamethylene Diisocyanate
FITC	Dextran-Fluorescein Isothiocyanate
VEGF	Vascular Endothelial Growth Factor
NGF	Nerve Growth Factor
hGH	Human Growth Hormone
BSA	Bovine Serum Albumin
CNS	Central Nervous System
ADA	Adamantane
CNTs	Carbon Nanotubes
SWCNTs	Single-walled Carbon Nanotubes
MWCNTs	Multi -walled Carbon Nanotubes
DTX	Docetaxel
SA	Salicylic Acid
IBF	Ibuprofen
NX	Naproxen

DS	Diclofenac Sodium
DX	Dexamethasone
5FU	5-Fluorouracil
DOX	Doxorubicin
GA	Glutaraldehyde
TEOS	Tetraethyl orthosilicate
APS	Ammonium Persulfate
AIBN	Azo Bis Isobutyronitrile
MBA	Methylene bisacrylamide
TEMED	*N*,*N*,*N'*,*N'*-tetramethylethylene diamine
IPN	Interpenetrating Polymer Network
SGF	Simulated Gastric Fluid
SIF	Simulated Intestinal Fluid
SCF	Simulated Colonic Fluid
GIT	Gastrointestinal Tract
LCST	Lower Critical Solution Temperature
UCST	Upper Critical Solution Temperature
FTIR	Fourier Transform Infrared Spectroscopy
UV	Ultra Violet
UV-Vis	Ultra Violet Visible
XRD	X-Ray Diffraction
DSC	Differential Scanning Calorimetry
SEM	Scanning Electron Microscopy
^{1}H NMR	Proton Nuclear Magnetic Resonance
D_2O	Deuterium Oxide
TMS	Tetramethylsilane
DMEM	Dulbecco's Modified Eagle's Medium
FBS	Fetal Bovine Serum
TMS	Tetramethylsilane
MTT	3-(4,5-Dimethylthiazol-2-yl)-2,5-Diphenyltetrazolium Bromide
h	Hour
s	Second

g	Gram
°C	Degrees Centigrade
l	Litre
ml	Millilitre
M	Molar
mM	Millimolar

CHAPTER 1

INTRODUCTION

1.1 Hydrogels

Hydrogels are polymeric networks with three-dimensional configuration capable of imbibing large amounts of water or biological fluids. Hydrogels can be made from virtually any water-soluble polymer, encompassing a wide range of chemical compositions and bulk physical properties. The three-dimensional network, formed by cross-linking of polymer chains, provides resistance to the hydrogels to dissolute (Qiu and Park, 2001). They can be designed in a variety of architectures such as slabs, microparticles, coatings and films. The high hydrophilicity of hydrogels is mainly due to the presence of hydrophilic moieties such as hydroxyl, carboxyl, amino and amide groups in the backbone of the polymer strands. In general, the more hydrophilic is the polymer, the higher is the total water retention capacity of the hydrogel. The hydrogels in their dried forms are called xerogels. When dried by freeze-drying, solvent extraction or supercritical drying techniques, the resulting hydrogels are extremely porous in nature and are known as aerogels (Bhattacharya, 2000). In their fully swollen state, hydrogels are soft and have a rubbery consistency. Owing to their ability to retain a significant amount of water, hydrogels mimic the natural structure of the body's cellular makeup, rendering them important for biomedical applications *e.g.* tissue engineering, artificial organ and contact lens designing, and most importantly in drug delivery (Hoare and Kohane, 2008).

The terms 'gels' and 'hydrogels' are often misinterpreted and are used interchangeably in the world of polymer science. Both, gels and hydrogels, are polymeric networks and might be chemically similar, however they are physically very distinct. Gels are semi-solid polymeric materials comprising small amounts of solids dispersed in relatively large amounts of liquid, yet possessing more solid-like character (Kleech, 1990). Conventional gels can acquire a low level of virtual cross-linking under the

influence of shear forces, but this is reversible because of involvement of weak physical forces (Gupta *et al.*, 2002). Therefore, gels are defined as a substantially dilute cross-linked polymeric system, and are categorised principally as weak or strong depending on their flow behaviour in steady-state (Ferry, 1980). Because of the weak or virtual cross-linking, the polymer strands in gels often dissolute in aqueous environment resulting in the loss of network structure. The hydrogels, on the other hand, are cross-linked hydrophilic polymers which retain their three-dimensional structure even after absorbing large amount of water (Gehrke and Lee, 1990). Thus hydrogels are different from gels in the sense that they are already swollen matrices, and the further addition of fluids results only in their network dilution. The feature that is important to the functioning of a hydrogel is its inherent strong cross-linking. The distinct behaviour of gels and hydrogels is illustrated in Figure 1.1.

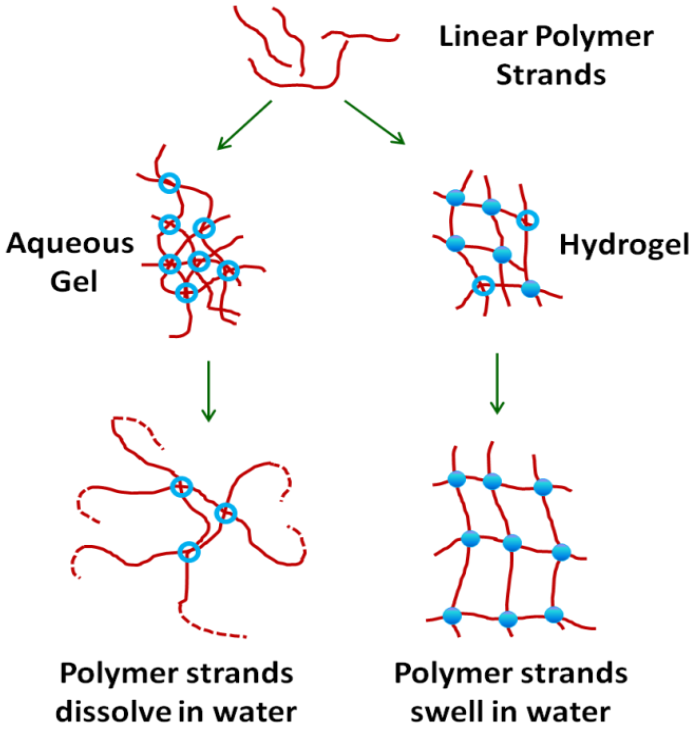

Figure 1.1. Distinct behaviour of gels and hydrogels in an aqueous environment. Solid circles represent strong covalent cross-linking while the hollow circles represent weak/virtual cross-linking (Gupta *et al.*, 2002).

1.2 Classification of Hydrogels

A proper knowledge of polymer network, quantitative features of the materials, interaction parameters, disintegration kinetic and transport phenomena are paramount to achieve a hydrogel with predetermined and well-defined physico-chemical parameters for various applications. In general, hydrogels can be classified based on a variety of characteristics. These include the source, network electrical charge, polymeric composition, network structure, type of cross-linking and responses to environmental stimuli (pH, temperature, ionic strength, glucose strength, light, enzymes *etc*.). (Peppas and Merrill, 1976; Peppas, 1986; Stauffer and Peppas, 1992; Hickey and Peppas, 1995)

Classification based on source (Zhao *et al.*, 2013):

Polymers that are generally employed for hydrogel synthesis and directed towards pharmaceutical or biomedical applications can be from natural or synthetic origins (Hoffman, 2002; Hamidi *et al.*, 2008). Typical examples of natural and synthetic polymers used in hydrogel preparations are summarized below.

Natural polymers:

- *Anionic polymers:* Hyaluronic acid, Alginic acid, Pectin, Carrageenan
- *Cationic polymers:* Chitosan, Polylysine, Gelatin, Dextran, Cellulose
- *Amphipathic polymers:* Collagen, Fibrin, Carboxymethyl chitin
- *Neutral polymers:* Agarose, Pullulan

Synthetic polymers:

- Poly(hydroxyethyl methacrylate) (PHEMA)
- Poly(ethylene glycol) (PEG) and derivatives
- Poly(vinyl alcohol) (PVA) and derivatives
- Poly(acrylic acid) (PAA) and derivatives

- Poly(ethylene oxide) (PEO)
- Poly(acrylonitrile) (PAN)
- Poly(N-isopropylacrylamide) (PNIPAAm)
- Poly(N-vinyl pyrrolidone) (PVP) and derivatives.

A summary of the monomers mostly employed in the design of hydrogels for pharmaceutical and biomedical interests are briefed in Table 1.1.

Table 1.1. List of a few monomers widely used in hydrogel preparation for biomedical applications

Monomer	**Abbreviation**
Hydroxyethyl methacrylate	HEMA
Hydroxyethoxyethyl methacrylate	HEEMA
Methoxyethyl methacrylate	MEMA
Ethyleneglycoldimethacrylate	EGDMA
N-vinyl-2-pyrrolidone	NVP
N-isopropylacrylamide	NIPAAm
Acrylic acid	AAc
Methacrylic acid	MAAc
Ethylene glycol	EG
Vinyl acetate	VAc

Classification according to network electrical charge (Hacker and Mikos, 2011):

Hydrogels may be categorized into four groups on the basis of presence or absence of electrical charge located on the cross-linked chains:

- Nonionic (neutral)
- Ionic (anionic or cationic)
- Amphoteric electrolyte (ampholytic) containing both acidic and basic groups

- Zwitterionic containing both anionic and cationic groups in each structural repeating unit

Among all, the ionic hydrogels composed of either cationic or anionic polymers are extensively investigated for various therapeutic applications. Anionic polymers have the ability to form ionic complexes with cationic biomolecules including basic peptides, blood proteins and cationic drugs (Kobayashi *et al.,* 2003; Olson and Chuang, 2002). Cationic polymers, on the other hand, form electrostatic complexes with anionic biomolecules, nucleic acids (DNA, RNA and PNA) and proteins. In addition, the inherent bioactive properties such as stimuli-responsiveness, antimicrobial, antioxidant, antitumor and anti-inflammatory properties makes cationic hydrogels more promising materials for therapeutics. Widely studied cationic polymers include poly (ethylene imine), poly-L-(lysine) and chitosan. The review article by Putnam (2006) highlights the use of cationic polymers in gene delivery applications. Samal and co-authors (2012) have also discussed the development and modification of cationic polymers into various architectures such as hydrogels, scaffolds, micelles, membranes and have addressed their therapeutic applications.

Classification based on polymeric composition (Ahmed, 2013):

Based on polymeric composition the hydrogels can be classified as:

- Homopolymeric hydrogels where the polymer network is derived from a single monomer species.
- Copolymeric hydrogels which comprise of two or more different monomer species arranged in a random, block or alternating configuration along the chain of the polymer network.
- Multipolymer interpenetrating polymeric network (IPN) hydrogels composed of two or more independent cross-linked synthetic or natural

polymers contained in a network. In semi-IPN hydrogels, one component is a cross-linked polymer and other component is a non-cross-linked linear polymer.

Classification based on network structure (Ahmed, 2013):

Hydrogels can be categorized based on their network structure as:

- Amorphous (non-crystalline): The polymer chains are randomly arranged
- Semi-crystalline: Dense regions of ordered macromolecules or crystallites present in an amorphous matrix *i.e.* a complex mixture of amorphous and crystalline phases
- Crystalline: The polymer chains are arranged in systematic manner in ordered array

Classification based on type of cross-linking (Hacker and Mikos, 2011):

Hydrogels can be classified into two categories based on the chemical and physical nature of the cross-link junctions. Chemically cross-linked networks have permanent junctions while the physically cross-linked hydrogels have transient junctions that arise from either chain entanglement of the polymers or physical interactions such as hydrogen bonds or hydrophobic interactions (Jen *et al.,* 1996).

Classification based on responses to external stimuli:

A truly amazing class of hydrogels that has found potential use for a wide variety of applications is the class of "smart" or "intelligent" hydrogels. These hydrogels exhibit changes in the gel structure in response to environmental stimuli. Smart hydrogels are a special class of hydrogels which are equipped with the exceptional property of undergoing extensive conformational changes such as reversible volume-phase transitions or sol-gel transitions, in response to very small changes in environmental factors (Rossi *et al.,* 1991). The physical stimuli include temperature, electric field,

light, pressure, and magnetic field while the chemical stimuli include pH, ions, and molecular recognition events *etc.* (Qiu and Park, 2001). The sensitivity of smart hydrogels to the minute changes in the environmental factors makes them appropriate to be used in a diversity of applications. Figure 1.2 describes the various stimuli actions on hydrogels that render them useful in diverse pharmaceutical applications and mostly as targeted drug delivery systems.

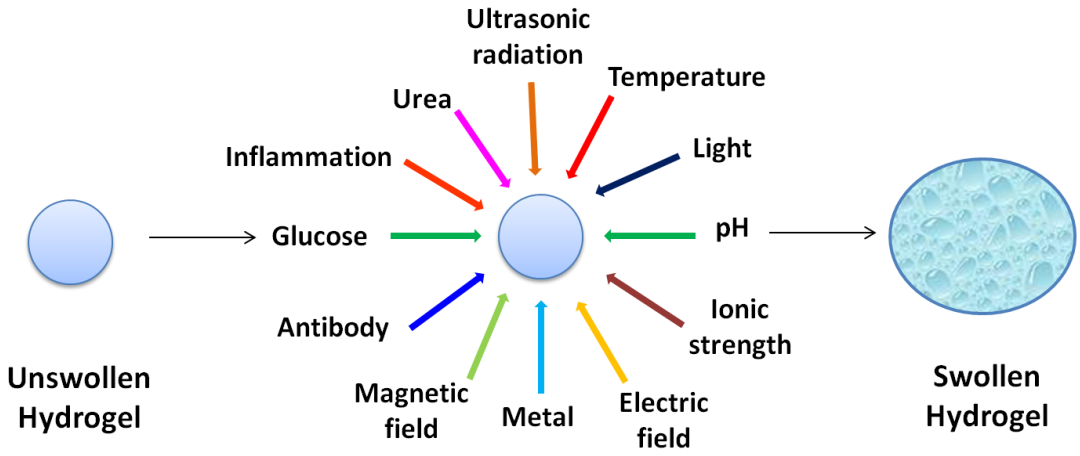

Figure 1.2. Various stimuli actions that impart stimuli-sensitivity to hydrogels.

Of the several environmental factors that render a hydrogel smart; the most common are pH, ion, temperature, glucose, electric current, light and enzymes. The properties and utilities of such smart hydrogels have been briefed below.

1.2.1 pH−sensitive Hydrogels

pH-sensitive polymers are those, whose solubility or conformation in aqueous solution changes reversibly or irreversibly as a function of environmental pH (Huh *et al.*, 2012). These polymers are a class of polyelectrolytes which have ionizable groups in the backbone of their structures, side-group or end-group and demonstrate pH-responsive physico-chemical properties. Most commonly studied ionic polymers for pH-responsive behaviour are poly(acrylamide), poly(acrylic acid), poly(methacrylic acid), poly(diethylaminoethyl methacrylate) and poly(dimethylaminoethyl

methacrylate) (Gupta *et al.*, 2002). Apart from synthetic polymers, natural polysaccharides such as chitosan, dextran, albumin and gelatin are also known to exhibit pH-sensitive behaviour (George and Abraham, 2007; Altimari *et al.*, 2012).

When the pH of the external medium is above the pK_a of the ionizable group of the anionic hydrogels, ionization occurs. This results in increased hydrophobic interactions between the polymer chains and enhances the swelling ratio. The reverse is the case with cationic hydrogels which swell at lower pH. The pH-dependent swelling/ deswelling behaviour of cationic and anionic hydrogels is demonstrated in Figure 1.3.

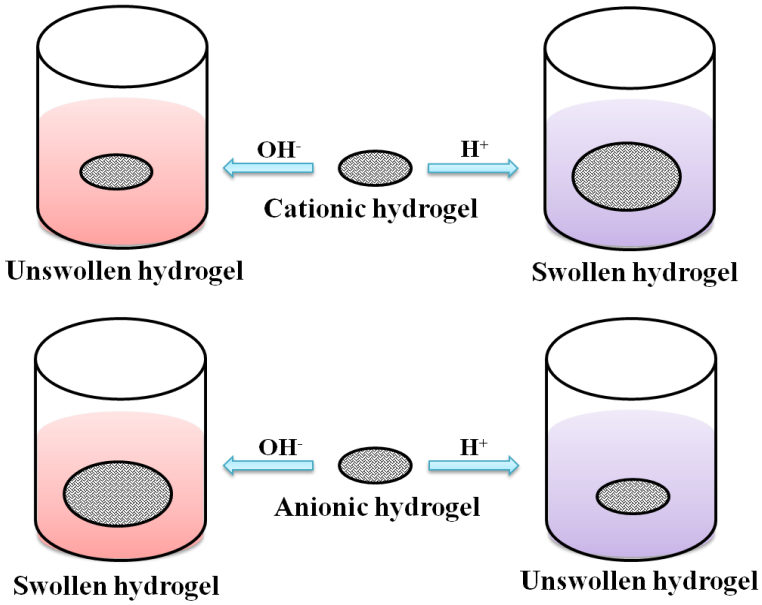

Figure 1.3. pH-responsive swelling and deswelling of ionic hydrogels.

1.2.2 Ion−sensitive Hydrogels

Ions play a crucial role in many biological processes. Thus, utilization of ion-sensitive polymeric hydrogels could be effective in drug delivery. Ionic hydrogels are swollen polymeric networks which exhibit sudden or gradual changes in their equilibrium and dynamic swelling behaviour as a result of the external ionic strength. In aqueous media of particular ionic strength, the groups ionize thereby developing a fixed charge

on the hydrogel which are responsible for the swelling or deswelling of the hydrogel. The mechanism of ion-mediated drug release from an ion-sensitive hydrogel is represented in Figure 1.4. Rasool *et al.*, (2010) designed a novel pH-, ionic strength and temperature-sensitive hydrogel composed on kappa carrageenan and AAc and investigated the delivery features for insulin. The hydrogels exhibited potential for controlled delivery of insulin.

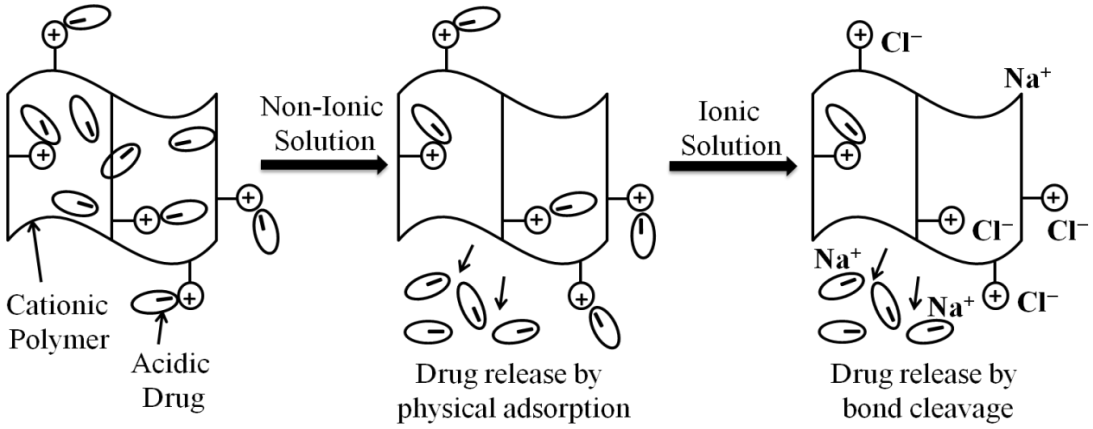

Figure 1.4. Mechanism of ion-mediated drug release at different ionic strengths (Sutani *et al.*, 2002).

1.2.3 Temperature−sensitive Hydrogels

Temperature-sensitive or thermo-sensitive hydrogels are probably the most commonly studied class of smart polymer systems in drug delivery research. The release as well as the mechanical characteristics of the hydrogels is altered with changes in the temperature of the environment (Bromberg and Ron, 1998). The common characteristic of temperature-sensitive polymers is the presence of hydrophobic groups such as methyl, ethyl or propyl groups. Of the many temperature-sensitive polymers, PNIPAAm and poly(N,N-diethylacrylamide) (PDEAAm) are widely employed because their lower critical solution temperatures (LCST) are in the range of 25−32°C, close to the body temperature which make them apt as drug delivery carriers (Qiu and Park, 2001). Most polymers have increased water-solubility with increased

temperature. But polymers with LCST have decreased water-solubility at higher temperatures. Hydrogels having LCST shrink as the temperature goes above their LCST. Such a property is known as inverse or negative temperature-dependence. These hydrogels are composed of either moderately hydrophobic groups or a mixture of hydrophobic and hydrophilic segments. At lower temperatures, the hydrogen bonding between the hydrophilic segments of the polymer backbone increases which results in an enhanced swelling of the matrix. As the temperature is increased, the hydrophobic interaction between the hydrophobic segments increases while the hydrogen bonding weakens. The net result is the shrinking of the hydrogels due to inter-polymer chain association through hydrophobic interaction. In general, negative thermo-sensitive hydrogels contract when heated above their LCST.

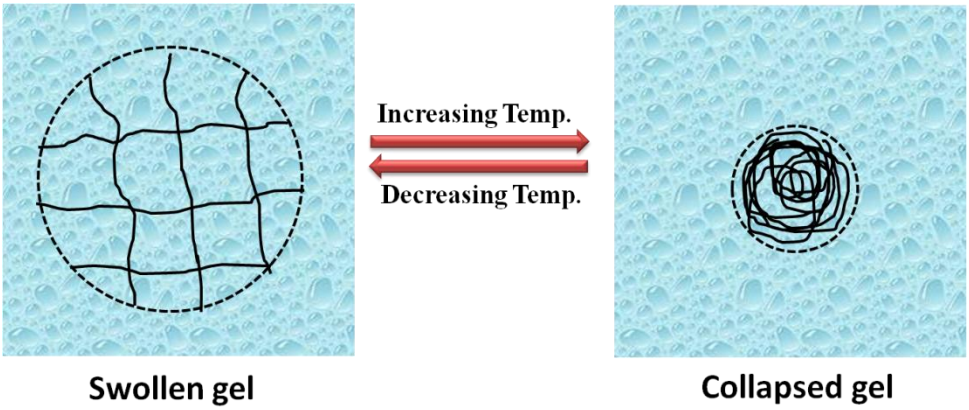

Figure 1.5. Thermo-reversible polymer showing lower critical solution temperature (LCST).

On the other hand, positive thermo-sensitive hydrogels swell at higher temperature and shrink at lower temperature (Schild, 1992). Such hydrogels are known to exhibit upper critical solution temperature (UCST). Currently, Poly(N-acryloyl glycinamide) (PNAGA) is the most studied polymer that forms sol-gel thermo-responsive systems with a UCST in aqueous media. Boustta and co-workers (2014) have designed thermo-responsive hydrogels based on the above polymer for loco-regional sustained delivery of drug. Seuring and Agarwal (2012) have focused on the applicability and

potential of polymers having UCST and also addressed the largely unknown importance of such polymers in their review article.

1.2.4 Glucose−sensitive Hydrogels

Such hydrogels are sugar-sensitive and show variability depending on the concentration of sugar present. Glucose-sensitive hydrogels are necessary for the development of self-regulated delivery systems, which can deliver therapeutic doses of insulin in response to blood sugar concentration (Kost and Langer, 1992; Ishihara and Matsui, 1986). Many hydrogel systems have been developed for modulating insulin delivery and all are equipped with a glucose sensor built in the system.

Glucose oxidase is the most widely used enzyme in glucose sensing. It oxidizes glucose to gluconic acid, resulting in a pH change of the environment (Qiu and Park, 2001). This makes it possible for the design of pH-sensitive hydrogels for insulin delivery. Hydrogels composed of polycations exhibit higher swelling at lower pH. This membrane swelling property can be utilized for the delivery of insulin (Albin *et al.*, 1985). Hydrogels made of polyanions have also been used for localized insulin delivery. Hydrogel containing polyanion such as PAA-grafted porous cellulose film and immobilised glucose oxidase was synthesized for insulin delivery in response to glucose concentration (Ito *et al.*, 1989). At neutral pH, in the absence of glucose, the repulsion between the negatively charged carboxylate groups lead to closing of the pores of the membrane. Glucose oxidase catalyzes oxidation of glucose to gluconic acid that protonates the polymer chains. This, in turn, opens up the closed pores of the membrane and thus regulates the delivery of insulin. Concanavalin A (Con A) has also been frequently used in modulated insulin delivery. Con A is a glucose-binding protein obtained from the jack bean plant, *Canavalia ensiformi.* An injectable *in-situ* forming glucose-responsive dextran and lectin Con A based hydrogels have been

synthesized to deliver the adipogenic factor of insulin to human tissues (Tan and Hu, 2012). In another formulation, insulin loaded microhydrogels fabricated from methacrylate derivatives of dextran and Con A as an insulin delivery system has been evaluated by Yin *et al.,* (2012). The results indicated that insulin release was reversibly in response to different glucose concentrations.

Hydrogels can be made to undergo reversible sol-gel phase transformations depending on the glucose concentration in the environment. The sol-gel transition of glucose-sensitive hydrogel is shown in Figure 1.6.

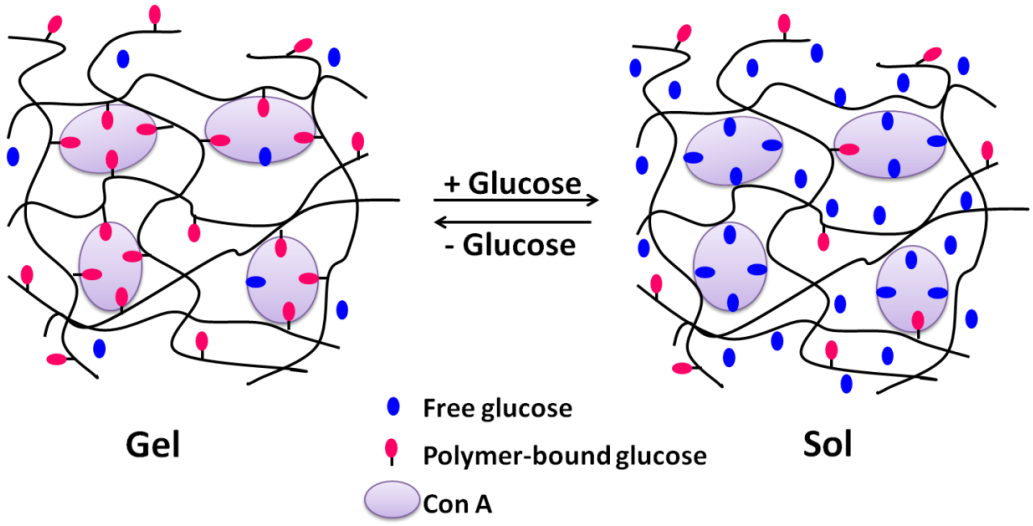

Figure 1.6. Sol-gel phase transition of a glucose-sensitive hydrogel (Qiu and Park, 2001)**.**

As the external glucose molecules diffuse into the hydrogels, individual free glucose molecules compete with the polymer-attached glucose molecules and an exchange occurs. Thus the concentrations of Con A and glucose-containing polymers can be adjusted to make hydrogels responsive at specific glucose concentrations.

1.2.5 Electric current−sensitive Hydrogels

Electro-responsive hydrogels, made of polyelectrolytes, are sensitive to electric signals and undergo shrinking or swelling in presence of an electric field. These hydrogels sometimes show swelling on one side and deswelling on the other leading

to the bending of the hydrogel. A Pluronic bis-methacrylate hydrogel modified with hydrolyzed methacrylic acid developed by Jackson *et al.,* (2013) was found to deswell uniformly without any visual deformations due to electrical bias. Recently, an electrical-sensitive hydrogel based on PVP and PAA was synthesized using potassium persulfate as the radical initiator (Jin *et al.,* 2013). The swelling behaviour indicated the bending of the hydrogel towards the cathode irrespective of the pH of buffer solution and applied voltage. Thus the utilities of these hydrogels as sensors, actuators, switches or drug delivery systems are demonstrated. Electro-conductive hydrogels based on the blends of poly(ethyleneimine) and 1-vinylimidazole were synthesized and investigated for the delivery of indomethacin (Indermun *et al.,* 2014). A natural amphoteric electroactive hydrogel based on chitosan and carboxymethyl chitosan has been prepared (Shang *et al.*, 2008). The hydrogel bended either towards anode (pH ≤ 7) or cathode (pH > 7) depending on the pH of the external medium. The report suggested improved mechanical properties and electrical sensitivity indicating potential as microsensors and actuators. Hydrogels comprising of PAA-co-poly(vinyl sulfonic acid)-polyaniline have been developed as actuator by Kim *et al.,* (2006). The hydrogels displayed a reversible change in volume on switching the electric stimulus between the positive and negative electrodes, showing a contraction and expansion of the hydrogels, respectively. The electro-sensitive behaviour of these hydrogels pointed their greater applications as actuators. Polythiophene-based conductive hydrogel has shown to undergo swelling-deswelling transition in response to an applied potential over -0.8 to 0.5 square wave potential (Irvin *et al.,* 2001). IPN hydrogels composed of PVA and PMA were prepared which exhibited electrical sensitivity behaviour (Kim *et al.,* 2004). The hydrogels showed bending behaviour in Hank's solution of pH 7.4 which is desirable in biomedical applications. In the review article by Murdan (2003),

the responses of hydrogels to external electric field and electrically-stimulated drug releases have been well summarized.

1.2.6 Photo−sensitive Hydrogels

Light-sensitive hydrogels have potential applications in optical switches, display units and ophthalmic drug delivery devices. Photo-responsive hydrogels are also potentially useful as drug delivery carriers and cell culture media. The utilization of photopolymers provides a possibility for the temporal and spatial controlling of hydrogel cross-linkers.

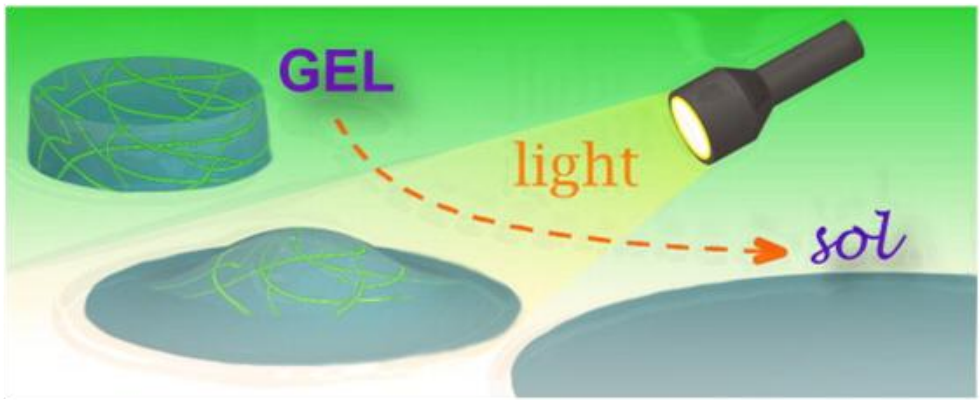

Figure 1.7. Sol-gel phase transition of a photo-sensitive hydrogel (Tomatsu *et al.,* 2011).

Torqersen *et al.*, (2012) have produced 3-D hydrogel scaffolds by means of the two-photon polymerization technique. The results demonstrated the feasibility and potential for bio-fabricating 3-D tissue constructs in the micrometer-range via near-infrared lasers in direct contact with a living organism. Wang *et al.*, (2014) have mechanically prepared strong light-sensitive hydrogels by photoinitiated copolymerization of spiropyran-containing monomer, 2-vinyl-4,6-diamino-1,3,5-triazine, hydrogen bonding polymer, oligo(ethylene glycol)methacrylate and polyethylene glycol diacrylate. It was observed that the multiple hydrogen bonding contributed to the increase in compressive strength of the photo-sensitive hydrogels.

Also selective detachment of cells was achieved by UV light illumination on the specified hydrogel surface. The hydrogels were found to be suitable platform for operating gene delivery and controlled harvesting of drugs for tissue engineering purposes. A photo-sensitive copolymer hydrogel based on polyacrylamide, poly(acrylamide-co-acrylamidoazobenzene) was synthesized in tetrahydrofuran solvent following free-radical polymerization route using azo bis isobutrylonitrile (AIBN) as an initiator (Zhao *et al.,* 2008). Photopolymerized hydrogels were evaluated for their degradation and cytocompatibility by Vermonden *et al.,* (2008). The LIVE/ DEAD cell viability/ cytotoxicity assay on goat mesenchymal cells demonstrated the biocompatibility of the synthesized hydrogels. The review articles by Tomatsu *et al.,* (2011) and Alvarez-Lorenzo *et al.,* (2009) investigate photo-sensitive hydrogels as emerging biomaterials for various applications.

1.2.7 Enzyme−sensitive Hydrogels

Biodegradable polymers are becoming increasingly important in biomedical fields because of their high potential in tissue engineering, drug delivery devices *etc*. Since some of the biodegradable polymers can be digested by specific enzymes, enzyme-sensitive hydrogels can be designed from such polymers (Miyata *et al.,* 2002). The microbial enzymes that are mostly present in the colon can be utilized for designing colon-specific drug delivery systems. Hovgaard and Brønsted (1995) focussed on the fact that microbial enzymes such as dextranases can degrade the polysaccharide dextran. Dextran hydrogels cross-linked by diisocyanate were synthesized for colon targeted drug delivery. The hydrogels were degraded by dextranases *in vivo* in rats and also in human colonic fermentation. Azoreductase is one of the most useful enzymes for colon-specific drug delivery as it is produced by the microflora of the colon. To fabricate colon-specific delivery systems, researchers have used azoaromatic bonds

which can be degraded by azoreductases (Ghandehari *et al.*, 1997; Akala *et al.*, 1998). Prodrug is another important approach for targeting drugs to colon. A large number of enzyme based prodrugs are available but azo prodrugs have clinically proven to be most efficient. The azo bonds of the prodrugs of 5-aminosalicylic acid and sulphasalazine were reduced specifically in the caecum of rats (Schellekens *et al.*, 2007).

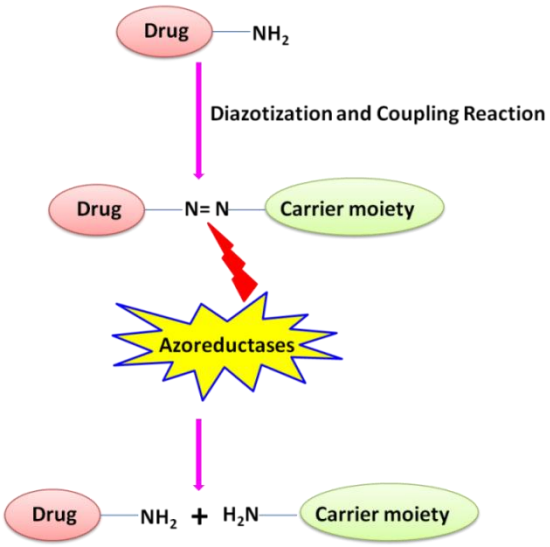

Figure 1.8. Diagrammatical representation of mechanistic aspect of azo-based prodrugs (Sharma *et al.*, 2013).

1.3 Technologies Adopted in Hydrogel Preparation

A hydrogel is simply a hydrophilic polymeric network cross-linked to produce an elastic structure to avoid dissolution of the hydrophilic polymer chains (Hennink and van Nostrum, 2002). A number of cross-linking approaches have been developed to obtain hydrogels with desired properties. The most common cross-linking methods used in hydrogel fabrication are summarized in Figure 1.9.

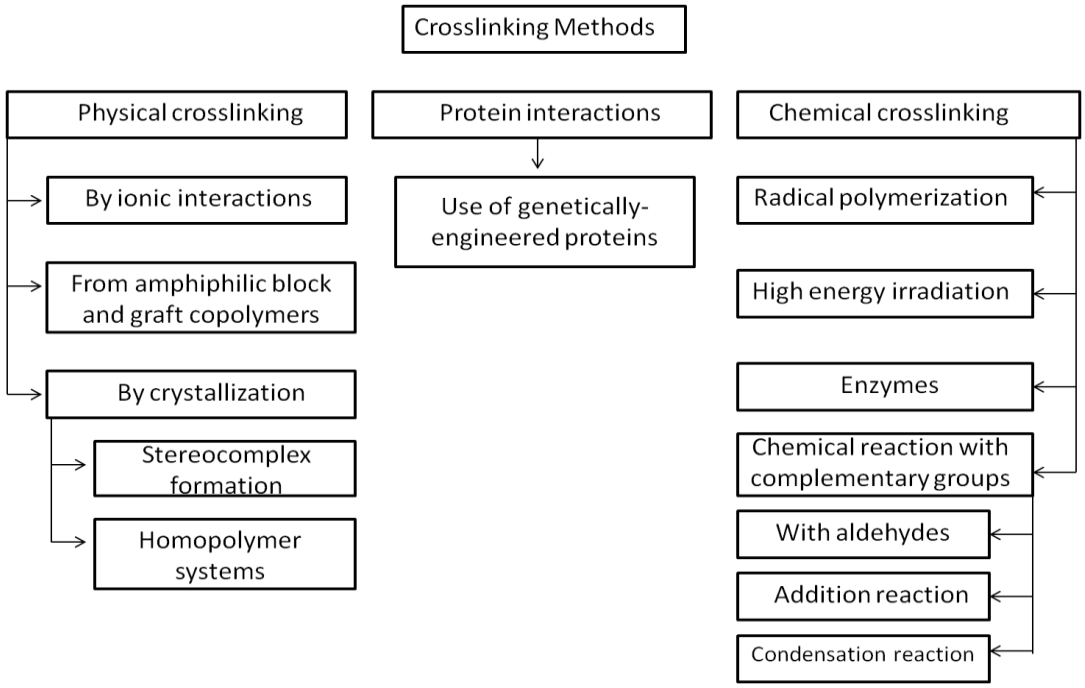

Figure 1.9. Various cross-linking approaches used in hydrogel preparation.

In chemically cross-linked hydrogels, covalent bonds are present between the polymer chains while physical interactions predominate in physically cross-linked hydrogels.

1.3.1 Chemically Cross-linked Hydrogels

Chemical cross-linking usually refers to grafting of monomers to the polymer backbone or the use of a chemical agent to link two polymer chains. Various approaches such as radical copolymerization, energy irradiation, use of enzymes and by chemical reaction with complementary groups have been adopted to design chemically cross-linked hydrogels.

Chemically cross-linked hydrogels can be obtained by radical copolymerization of low molecular weight monomers in presence of a cross-linker. The first reported PHEMA hydrogel by Wichterle and Lim (1960) was obtained by polymerizing HEMA in presence of the cross-linking agent ethylene glycol dimethacrylate (EGDMA). A great variety of other hydrogels have also been synthesized using radical polymerization procedures.

Radiation cross-linking is another widely used technique for fabrication of hydrogels (Lugao and Malmonge, 2001).

Increasing interest has also been focussed on enzyme cross-linked hydrogels mainly due to the mildness of this type of reaction. Recent research has demonstrated enzyme cross-linking as an emerging and competitive method for *in situ* formation of hydrogels within few minutes to be explored in the field of cartilage tissue engineering (Jin *et al.*, 2008; Jin *et al.*, 2010; Jin *et al.*, 2011). Yu *et al.,* (2014) have successfully synthesized injectable hyaluronic acid/ PEG hydrogel by integrating enzymatic cross-linking (tyramine hydrochloride) and Diels-Alder "click chemistry" for cartilage tissue engineering. The studies by da Silva and co-workers (2014) concerns about the gel properties and cellular responses of chitosan and tilapia fish gelatin hydrogels cross-linked by the microbial enzyme transglutaminase.

The presence of functional groups such as −OH, −COOH, $-NH_2$ are susceptible to form covalent linkages between polymer chains by reaction with complementary groups. Polymers containing hydroxyl groups such as PVA can be cross-linked using the cross-linking agent glutaraldehyde (GA) (Kudo *et al.,* 2010; Belder *et al.,* 2001). Amine containing polymers have also been cross-linked with GA under mild conditions whereby Schiff bases are formed. Condensation reactions between hydroxyl groups or amines with carboxylic acids or derivatives have been frequently employed in polymer synthesis. Such reactions have also been utilized in the preparation of hydrogels.

Michael addition reactions have become promising routes for *in situ* cross-linking of hydrogels. The fact that Michael addition can happen by simply mixing the components under mild conditions without any by-products makes it a better choice to form *in situ* cross-linked hydrogels (Pritchard *et al.,* 2011; Fu and Kao, 2011). A novel

Michael addition type *in situ* forming chitosan-ε-polylysine hydrogel was developed by Nie *et al.,* (2013). The obtained hydrogel had four times higher adhesive properties than commercial glue and found to be non-toxic to L−929 cells and exhibited prompt haemostatic property.

1.3.2 Physically Cross-linked Hydrogels

Various approaches have been adopted to design physically cross-linked hydrogels. Such approaches include ionic interactions between polymers, using multiblock copolymers or graft copolymers and stereocomplex formation between polymers.

Alginate is an exemplary polymer which can be cross-linked by ionic interactions. Alginate-chitosan-alginate multilayer hydrogel encapsulation systems were developed by Wasiak and Ciach (2014) for encapsulation of chondrocytes. The cross-linking of hydrogels occurred due to the ionic interactions between cationic chitosan and anionic alginate and calcium ions as additive.

Physically cross-linked hydrogels can also be obtained from multiblock copolymers or graft copolymers. Amphiphilic block and graft copolymers self-assemble in water to form organized structures such as polymeric micelles and hydrogels, in which the hydrophobic segments are aggregated. Albumin-conjugated pH- and thermo-responsive poly(amino urethane) multiblock copolymers were synthesized by Manokruang and Lee (2013). Novel thermo-responsive cross-linked hydrogels with controlled multiblock copolymer structure have been prepared from α,ω-diamino PPG and diepoxy-terminated PEGs (Anghelache *et al.,* 2014).

Hydrogels based on stereocomplex formation are well studied. The ability of poly(lactic acid) (PLA) to form stereocomplexes was first described by Ikada *et al.,* (1987). Biocompatible and biodegradable hydrogels composed of 2-methacryroyloxyethyl phosphorylcholine and oligo(L- or D-lactic acid) macro-

monomers have been developed into injectable hydrogel matrix (Takami *et al.,* 2011). Aqueous solutions containing the polymers along with oligo(L- or D-lactic acid) underwent spontaneous gelation upon mixing. This was attributed to the formation of stereocomplex between the lactic acid side-chains which act as cross-linking component in the hydrogel. Similarly, in another study, hydrogels were obtained by mixing aqueous solutions of dextran grafted with L-lactic acid oligomers and dextran grafted with D-lactic acid oligomers (Bos *et al.,* 2005). These hydrogels degraded *in vivo* within 15 days and showed good biocompatibility which make them suitable candidates in pharmaceuticals.

PVA being a hydrophilic polymer; PVA hydrogel possesses very low mechanical strength. Interestingly when PVA gel is subjected to freeze-thaw process, a highly elastic gel is obtained (Yokoyama *et al.,* 1986). PVA hydrogels prepared in this way were found to be stable for six months at 37°C. The crystallization that occurs during the freeze-thawing process has been cited in the literature as the primary mechanism responsible for imparting tougher mechanical properties to the resultant hydrogel. The roles of crystallization and phase separation in the formation of physically cross-linked PVA hydrogels have been discussed eloquently by Holloway and co-authors (2013).

The review article by Zhang *et al.,* (2013) addresses the recent developments in polysaccharide-based cryogels, which are a type of physical hydrogels prepared by freeze-thaw technique under mild conditions and in the absence of added cross-linking agents and organic solvents.

1.3.3 Cross-linking by Protein Interactions

The major advantage of protein engineering is that the sequence of the peptides and thus, the physical and chemical properties can be tuned into desirable properties.

Cappello and co-workers (1998) prepared for the first time copolymer containing silk-like and elastin-like blocks in which the silk-like segments are associated through hydrogen bonded beta strands or sheets. Dinerman *et al.,* (2010) synthesized networks of genetically engineered silk-elastin-like protein polymer and have investigated the influence of solute hydrophobicity and charge on partition and diffusion of the hydrogels. The results indicated the possibility of controlling solute release from the hydrogel by modifying its hydrophobicity. Recombinant protein domains have also been used to cross-link hydrogels (Chen *et al.,* 2000).

1.4 Applications of Hydrogels

The pioneering report on hydrogels dates back to more than fifty years where PHEMA was investigated for contact lens applications (Wichterle and Lim, 1960). Since then, the research in the areas pertaining to hydrogels has expanded dramatically, especially in the last decade. The utility of hydrogels can be classified broadly into two categories: (i) non-medical and (ii) biomedical and pharmaceutical applications. (Hoffman, 2001; Peppas *et al.,* 2000; Scherman, 2013; Aguilar and Roman, 2014).

1.4.1 Non-medical Applications of Hydrogels

Hydrogel technologies have been applied to various non-medical applications *e.g.* agriculture, coal dewatering, food packaging, membranes *etc.*

Hydrogels in Agriculture

Hydrogels have potential as eco-friendly water-saving materials and serve as soil conditioner for agricultural applications in sandy soil in view of their increasing water and/ or nutrition retaining capacity. Acrylamide is the major component for hydrogel designed for agricultural utilities (Singh *et al.,* 2010). Raafat and co-workers (2012) have proposed a series of superabsorbent hydrogels based on PVP and carboxymethyl cellulose (CMC) for application in agriculture. The prospective of cellulose hydrogels

in agricultural fields has been compiled in the review article by Chang and Zhang (2011).

Hydrogels for Coal-dewatering

Although water is a necessary medium in most coal preparation processes, its presence in the final product however reduces its value. Thermal drying is the only process that was used to dewater coal. The associated high operational costs and safety hazards have invited widespread reluctance for this method. Studies have now pointed to the use of superabsorbent polymers for the same. Dzinomwa *et al.,* (1997) dewatered fine coal upto 29.4% from a plant in Queensland, Australia using pH-sensitive hydrogels.

Hydrogels in Food Packaging

Bio-based polymeric hydrogels for food packaging applications have invited attention as an alternative approach to plastic packaging materials. Hydrogels constructed using PVP and CMC demonstrated promising features as food packaging material (Roy *et al.,* 2012). PNIPAAm hydrogels developed by Fucinos *et al.,* (2012) were found potential in packaging because the hydrogels provided protection to the antifungal drug pimaricin such that its controlled release regulated the presence of unnecessary fungal in food.

Hydrogels as Membranes

Poly(acrylamide) (PAAm) hydrogels are one of the most powerful tools in the analysis of biomolecules and bio-macromolecules (Chrambach and Rodbard, 1971). They have the unique property to separate molecules based on their size and electrophoretic mobility. Even PAAm membranes have been used to separate, isolate and concentrate biomolecules including the separation of monoclonal antibodies, proteins from plasma, certain recombinant proteins and viruses. Valade and co-workers (2013) have recently prepared PAAm hydrogel networks cross-linked with

poly(N,N-dimethylacrylamide)-coated Au nanoparticles. The study was found to have greater implications in the development of hydrogel membranes for nanoparticle and protein separation. Polyvinylidene fluoride (PVDF) hydrogel membranes have been potentially utilized for the removal of carbon dioxide in air (Xu et al., 2002).

1.4.2 Biomedical and Pharmaceutical Applications of Hydrogels

Hydrogel technologies have also been utilized in pharmaceutical applications *e.g.* stem cell therapy, scaffolds, sealing applications, gene delivery, implants *etc.*

Hydrogels in Stem Cell Therapy

One of the most recent clinical applications of hydrogels that has dramatically evolved into a huge territory is the area of stem cell encapsulation and their release for stem cell therapy. The major disadvantage associated with the conventional methods is the use of liquid nitrogen for effective transfer of stem cells which necessitates a small time of delivery, thus offering great challenges (Choumerianou *et al.,* 2008). Chen *et al.,* (2013) have demonstrated the use of alginate based hydrogels for encapsulation, storage and release of stem cells. Human mesenchymal stem cells and mouse embryonic stem cells were successfully stored in these hydrogels in air tight bottles. In another study, degradable and injectable alginate based hydrogel microbeads have been established to deliver stem cells for bone regeneration (Leslie *et al.*, 2013). A double stimulus-sensing hydrogel biopolymer has been reported by Tan *et al.,* (2013) for inducing stem cell aggregation and sparking their subsequent release.

Hydrogels as Scaffolds in Regenerative Medicine

Hydrogels have been developed to serve as scaffolds in regenerative medicine to regenerate numerous tissues such as nerve (Park *et al.,* 2010), bone (Patterson *et al.,* 2010), cartilage (Park *et al.,* 2009) and vasculature (Chui *et al.,* 2011). The review article by Mather and Tomlins (2010) briefly summarizes the nature of hydrogel-

structure relationships in regenerative medicine by highlighting the key attributes that modulate their functions. Hydrogels can also be readily tailored for the inclusion of biochemical cues known to guide cellular processes such as cellular adhesion peptides (*e.g.*, RGD, YIGSR, VAPG) to mimic the extracellular space or growth factors (*e.g.*, nerve growth factor (NGF)) to trigger proliferation, migration and cell survival (Zhu, 2010; Anderson *et al.,* 2009). The functionality of hydrogels in regenerative medicine has been enhanced with localized gene delivery to promote tissue morphogenesis.

Hydrogels for Sealing Applications

Hydrogels are particularly attractive for sealant applications because the mechanical properties of swollen hydrogels are comparable to native soft tissues (Shazly *et al.,* 2010). Incisional cerebrospinal fluid (CSF) leakage remains a significant complication after cranial surgery. Standard closure techniques such as sutures, grafts or collagen sponges sometimes fail to achieve watertight closure because the suture pinholes and the gaps between the sutures create defects that allow CSF seepage. Dura Seal Dural Sealant System is a PEG hydrogel based sealant approved by US Food and Drug Administration (FDA) (Osbun *et al.,* 2012; Bhatia, 2010). Preul *et al.*, (2010) have successfully utilized PEG-based hydrogel as dural sealant that prevented intra-operative CSF leaks by 100% and reduced the incidence of postoperative CSF leaks by 90%.

Hydrogels in Gene Delivery

The high water content of hydrogels supports their use for gene delivery by preserving the activity of lentiviral vectors and acting to shield vectors from any host immune response. Natural and synthetic hydrogels have been employed to provide a sustained release of viral and non-viral vectors (Quick and Anseth, 2004). Kimura *et al.,* (2007) have formed PVA−DNA hydrogels by using ultra-high pressure (UHP) technology

and studied the controlled release of DNA for gene delivery. It was found that DNA release was much less from the hydrogels prepared by the UHP technology than from the hydrogels prepared by freeze-thaw process. The cutaneous delivery of nucleic acids has a number of therapeutic applications and most notably the genetic vaccination. Unfortunately the non-viral gene expression in skin is generally inefficient and transient. Pearton *et al.,* (2008) have employed hydrogel formulations for improved delivery of plasmid DNA in skin using hydrogels composed of Carbopol polymers and thermo-sensitive PLGA-PEG-PLGA triblock copolymers. In the review article by Seidlits and co-authors (2013), the ability of hydrogels to control the transgene expression profile and also the capacity of hydrogels to protect vectors from any host immune response has been presented comprehensively.

Hydrogels as Implants

The numerous health hazards exposed by the potential use of silicone gel in breast implants have raised the need for a filler material with minimum risk and cost-effectiveness. CMC hydrogels have higher radio-translucency than silicone gel and the integrity of such hydrogels as breast implants has been clinically proven (Brunner and Groner, 2006). Polyimplant prosthesis hydrogel breast implants were successfully tested clinically for their efficacy by Choi *et al.,* (2010). Hydrogels has also been used as optical implants (Kopecek, 2009), nerve implants (Lesny *et al.,* 2002) and for skin regeneration (Miguel *et al.,* 2013).

The ever growing spectrum of functional monomers and polymers further widen the scope of applicability of hydrogels. Apart from the uses discussed above, hydrogels also find significant applications as drug delivery systems.

1.5 Hydrogels as Drug Delivery Systems

Hydrogels, as drug delivery systems, have inevitably flourished in recent years. Indeed, the benefits of hydrogels for drug delivery are plenty. Hydrogels are highly biocompatible as reflected in their successful use in the peritoneum and other sites *in vivo* (Lee and Mooney, 2001). The biocompatible nature has been attributed to the high water content and the physico-chemical similarity to the native extracellular matrix both compositionally and mechanically. Biodegradability may be designed into the hydrogels by enzymatic, hydrolytic or environmental (pH, temperature or electric field) pathways. Hydrogels are easily deformable and can conform to the shape of the surface where they are applied (Singh *et al.,* 2010). In comparison to other synthetic biomaterials, hydrogels show minimal tendency to absorb proteins from body fluids because of low interfacial tension. Moreover, the muco- or bio-adhesive properties of some hydrogels can be advantageous in immobilizing them at the site of application or in applying them in uneven surfaces. Further the ability of different molecules to diffuse into (drug loading) and diffuse out of (drug release) the hydrogel allows the possible use of the dry or swollen hydrogel matrix for oral, nasal, buccal, rectal, vaginal, ocular and parenteral drug delivery systems.

Various polymers, natural as well as synthetic, have been explored to design novel hydrogels to be utilized as drug delivery systems. A polymeric material must possess the foremost characteristic properties of biocompatibility, biodegradability and non-toxicity to be rendered as drug delivery devices. Recent advancements in polymer science have led to the development of biocompatible hydrogels employing various natural and/or synthetic polymers to be employed as delivery vehicles (El-Leithy *et al.,* 2010; Liang *et al.,* 2012; Cavalli *et al.,* 2012; Xiong *et al.,* 2013). A summary of the natural and synthetic polymers utilized for drug delivery purposes can be obtained

in the excellent review articles by Liechty *et al.,* (2010) and Kim *et al.,* (2014). Below given is a brief account of different hydrogels utilized for site specific delivery of drugs to different parts of body.

1.5.1 Hydrogels in Ocular Drug Delivery

Anatomy and physiology of the eye makes it a highly protected organ. Designing an effective therapy for ocular diseases has been a formidable task. Recently, the fabrication of drug delivery systems targeting to the anterior and posterior segments of the eyes have become more challenging. In clinical practice, the anterior segments of the eye (cornea, sclera, conjunctiva, anterior uvea) can be treated with ocular eye drop which is the most commonly used dosage form in ocular drug treatment. Unfortunately, the eye drops are rapidly drained from the ocular surface, therefore bioavailability is very low, typically less than 5%. Topical ocular medications do not reach the posterior segment drug targets. The posterior segment (retina, vitreous and choroid) are treated by high drug doses given intravenously or by intravitreal administration. However, many posterior segment diseases such as age related macular degeneration, retinitis pigmentosa, diabetic retinopathies cannot be treated with current methods (Urtti, 2006). The scope of implantable hydrogels for ocular drug delivery has thus gained momentum in recent years. Polymeric hydrogel implants are on high demand for topical applications to eyes for improved drug retention time on ocular surfaces. Silicone hydrogels have proven to be a breakthrough for traditional contact lenses. These hydrogels allow oxygen penetration three times more than conventional lenses (Raul *et al.,* 2012). Gordon *et al.,* (2010) found doxycycline hydrogels as a potential therapy for ocular vesicant injury. Hydrogels based ophthalmic drug delivery systems offer an increase in the precorneal drug

residence time to a sufficient extent such that the drug can exhibit maximum biological action (Kushwaha *et al.,* 2012; Wassmer *et al.,* 2013).

1.5.2 Hydrogels in Transdermal Drug Delivery

Hydrogels have received enormous attention for their biomedical applications for skin (Varghese and Jamora, 2012). Skin is the first line of defence for protecting the entire body against pathogens and major loss of water. Helary *et al.,* (2013) found that the fibroblasts within collagen hydrogels favour chronic skin wound healing and are found to be advantageous over the currently used gel formulations for chronic skin wound treatment. The efficacy of hydrogels as dermatological patches is well demonstrated (Onuki *et al.,* 2005; Chen *et al.,* 2013). Matsuo *et al.,* (2013) developed a glycerine based hydrogel patch, which could promote antigen penetration through stratum corneum. They have also examined its safety and efficacy in animals and humans and found positive results. Photo cross-linked PAA hydrogels containing indomethacin have been developed as anti-inflammatory dermatological patches (Nishikawa, 2008). The results evidenced a highly functional anti-inflammatory patch in terms of its adhesive properties and drug bioavailability. The development of hydrogel nanocomposites has been a breakthrough in biomedical applications for skin. Incorporation of nanocomposite fillers in the network resulted in superior hydrogel properties (Bait *et al.,* 2011). Recently, Bait and co-workers (2013) have investigated the properties of PAAm based hydrogels to be utilized in applications for skin contact. The authors have prepared poly(acrylamide-co-hydroxyethyl methacrylate) hydrogels and nanocomposite copolymer poly(acrylamide-co-hydroxyethyl methacrylate) hydrogels filled with poly(Bu-acrylate) nanoparticles, which are found to be suitable for transdermal drug delivery. Si *et al.,* (2013) have synthesized methacrylated gelatin hydrogel films with *in situ* generated TiO_2 nanoparticles. The anti-bacterial activities

of these films suggested good performance after introduction of TiO_2 nanoparticles. The cytotoxicity assay on L−929 cells indicated their biocompatible nature. A chitosan-PVP matrix loaded with TiO_2 has been studied as wound dressing material (Archana *et al.,* 2013). Compared to conventional gauze treatment; the prepared hydrogel dressing caused an accelerated healing of open excision type wounds in albino rat models. In addition, they showed excellent antimicrobial efficacy and good biocompatibility against NIH3T3 and L−929 fibroblast cells.

1.5.3 Hydrogels in Nasal Drug Delivery

The prolonged residence of drug formulation in nasal cavity is of paramount importance for intranasal drug delivery. *In situ* thermo-reversible muco-adhesive gels using blends of Poloxamer 407, Poloxamer 188 and Carbopol 934P have been developed by Parmar and Lumbhani (2012) for improving the nasal bioavailability of the antiemetic drug, metoclapramide hydrochloride. *In vitro* release of the drug from the muco-adhesive system in simulated nasal fluid was improved significantly by varying the concentrations of the polymers. The hydrogels also exhibited enhanced drug bioavailability. Chen *et al.* (2013) have established an intranasal thermo-sensitive hydrogel comprising of Pluronic F127 and Poloxamer 188. The developed nasal hydrogels showed shorter gelation time, longer mucociliary transport time and produced prolonged curcumin retention in the rat nasal cavity at body temperature. One of the major disadvantages of mucosal vaccinations is the fast mucosal self-clearance and tight arrangement of nasal epithelial cells, which eventually lead to shorter residence time of antigen in nasal cavity and hence the low antigen penetration through nasal mucosal surface. Typically cationic chitosan salts not only can bind strongly to negatively charged mucosal surfaces but can also loosen the tight conjugation between epithelial cells (Islam *et al.,* 2012). Wu *et al.,* (2012) have

developed novel thermo-sensitive hydrogels formulated with N-[(2-hydroxy-3-trimethylammonium) propyl] chitosan chloride (HTCC) and α, β-glycerophosphates and evaluated them for intranasal vaccine delivery with adenovirus based Zaire Ebola virus glycoprotein antigen. The hydrogels displayed low toxicity to nasal tissues and epithelial cells even after frequent intranasal dosing. The HTCC and α, β-glycerophosphates hydrogels have also been explored as adjuvant-free vaccine delivery system for H5N1 intranasal immunization (Wu *et al.,* 2012). In another study, an *in situ* thermo-gelling, muco-adhesive formulation based on N-trimethyl chitosan chloride has been evaluated for its potential for the trans-mucosal delivery of insulin *via* the nasal route (Nazar *et al.,* 2013). The *in vivo* potential of these formulations for the intranasal delivery of insulin has been demonstrated in a diabetic rat model and found to act as once-a-day dosage form. A broad picture on the different nasal dosage forms based on chitosan hydrogels can be obtained from the review article by Luppi *et al.,* (2010). In this review, the intranasal delivery of drugs has been discussed at length for local and systemic treatments; chitosan based hydrogels are described with a focus on their muco-adhesive and permeation-enhancing ability and a detailed discussion regarding the different nasal dosage forms are reported considering the *in vitro, in vivo* and *ex vivo* studies.

1.5.4 Hydrogels in Pulmonary Drug Delivery

Delivery of therapeutic agents through pulmonary route is expected to provide significant improvements in patient compliances and reduce systemic toxicity for a range of diseases. However, many inhalable drug formulations suffer from low respirable fractions, rapid clearance by alveolar macrophages, target non-specificity and difficulties in combining aerodynamic properties with efficient cellular water uptake (Courrier *et al.,* 2002). Hydrogel chemistry has offered the scope of

synthesizing nanoparticles incorporated with pharmaceutical moieties embedded within the hydrogel matrix. An enzyme-responsive, nanoparticles-in-microgel delivery system was devised by Wanakule *et al.,* (2012) for intracellular drug delivery to deep lung. The microgels exhibited triggered release of various nanoparticles and biologics in the presence of physiological levels of enzyme. They also showed little uptake by microphages indicating potential for increased lung residence time. El-Sherbiny *et al.,* (2010) have formulated swellable microparticles based on PEG graft copolymerized onto chitosan in combination with Pluronic F-108 and found that the microparticles delayed phagocytosis and have the potential for sustained drug delivery to deep lung. A copolymer of PLGA-PEG-PLGA developed by Gao *et al.,* (2011) provided a promising profile for local delivery of Docetaxel, a chemotherapeutic agent used for non-small cell lung cancer, to attain prolonged release with greater efficacy.

1.5.5 Hydrogels in Drug Delivery to Brain

Drug delivery to the brain is particularly challenging because systemic delivery requires high doses to achieve diffusion across the blood-brain barrier which often results in systemic toxicity. Intracerebroventricular implantation of a minipump/ catheter system provides local delivery but results in brain tissue damage and can be prone to infection. Wang *et al.,* (2012) have employed epi-cortical delivery using hyaluronan/ methyl cellulose hydrogels for the local release of erythropoietin to induce endogenous neural stem and progenitor cells of the subventricular zone to promote repair after stroke injury in the mouse brain. Caicco *et al.,* (2013) have studied the sustained epi-cortical delivery of cyclosporin A from PLGA encapsulated microspheres to the brain for stroke treatment. Hyaluronic acid hydrogels have been developed by covalently attaching antibodies *via* hydrazone linkage to deliver the antibodies to the injured brain (Tian *et al.,* 2005). Hydrophobic drugs such as

paclitaxel are in demand due to their effective loading in polymeric hydrogels. In a recent study by Torres *et al.,* (2011) the delivery of paclitaxel from hydrogels indicated that the effective therapeutic concentration of the drug could be maintained for more than 30 days. Paclitaxel-loaded PLGA hydrogel microspheres have been fabricated for the treatment of malignant brain tumour (Ranganath *et al.,* 2009). Diblock co-polypeptide hydrogels have been employed for the sustained local release of protein effector molecules to the central nervous system (CNS). The results show that the hydrogels can provide sustained delivery when injected into CNS (Song *et al.,* 2012). Stearic acid-g-chitosan hydrogels were also studied for the brain-targeted delivery of doxorubicin (DOX) (Xie *et al.,* 2012).

1.5.6 Hydrogels in Drug Delivery to Colon

Targeting of drugs to colon has received much interest recently for the local treatment of a variety of colonic diseases as well as systemic absorption of proteins and peptides. While the stomach is hostile to many drugs for its highly acidic pH; the colon, on the other hand, offers numerous therapeutic advantages as a site of drug delivery (Sharma and Harikumar, 2013). Natural polysaccharides such as pectin, chitosan, guar gum sustain the acidic environment of the stomach and remain intact in the small intestine but are degraded by the vast anaerobic microflora of the colon; thus are rendered as suitable drug carriers for colon specific delivery. Hydrogel discs of guar gum cross-linked by GA were prepared and studied for the colonic delivery of ibuprofen (Das *et al.,* 2006). Significant increase in drug release was observed in the medium containing the rat cecal content. Sinha *et al.,* (2004) studied the colonic delivery of 5-fluorouracil from guar gum and xanthan gum tablets for the treatment of colorectal cancer. The prospective of guar gum and its derivatives as colon specific and controlled drug delivery systems have been well documented by Prabaharan

(2011). Chitosan based hydrogels have also shown promising results for colonic drug delivery (Sareen *et al.,* 2013). The review article by Gulbake and Jain (2012) reflects the potential of chitosan hydrogels as colon specific drug delivery systems. This review focuses on various aspects of chitosan based formulations such as coatings, tablets, capsules, beads, gels, microparticles and nanoparticles, for the development of colonic drug delivery. Araujo *et al.,* (2013) demonstrated the colonic delivery of prednisolone and insulin from calcium alginate chitosan-coated matrices. Sustained release of antitumor drug β-lapachone was observed from alginate-chitosan hydrogel beads prepared by coacervation with prolonged gastrointestinal release and good stability in acidic medium (Torelli-Souza, 2012). Vaghani *et al.,* (2012) have synthesized pH-sensitive hydrogel composed of carboxymethyl chitosan using GA as the cross-linker and explored the colon targeted delivery efficacy for ornidazole. The *in vitro* drug release evaluation indicated maximum release in pH 6.8 and negligible release in pH 1.2, thus demonstrating both the pH-sensitivity and colon-specificity. Saboktakin *et al.,* (2010) have developed chitosan nanogels which have shown promising results for the colonic delivery of 5-aminosalicylic acid. Pectin is an edible plant polysaccharide widely employed in colonic drug delivery systems. The review by Liu *et al.,* (2007) describes the flexibility and possibility to tailor pectin macromolecules into a variety of architectures. Methoxyl citrus pectin hydrogel beads were compared for their encapsulation efficiency of indomethacin and drug release characteristics were evaluated in simulated gastric fluid (SGF) and simulated intestinal fluid (SIF) for the use in oral drug formulation targeting to colon (Jung *et al.,* 2013). A colon targeted tablet formulation using pectin as a carrier and diltiazem hydrochloride and indomethacin as model drugs has been developed (Ravi *et al.,* 2008). Gelatin, a protein based biodegradable polymer derived from collagen, is an attractive material

for preparing smart hydrogels because of its unique gelling properties and large number of functional side groups available for chemical cross-linking. Zheng *et al.,* (2013) have prepared composite hydrogel films of gelatin-chitosan-pectin and studied the release of BSA in SGF and SCF media. The dissolution and *in vitro* drug release profiles established these formulations as controlled delivery vehicles for BSA. pH-responsive gelatin based biodegradable hydrogels containing PAA were evaluated for oral colon specific delivery of ketoprofen (Raafat, 2010). Bajpai *et al.,* (2003) have synthesized hard gelatin capsules containing riboflavin-loaded PVP-PAAm hydrogels and studied for the release of vitamin B_2 and found the device to be suitable for colon targeted drug delivery.

1.6 Limitations of Hydrogels as Drug Delivery Systems

Despite numerous advantages, hydrogels are also associated with some inherent pharmacological limitations. Ease of application of hydrogels can be problematic sometimes. The poor mechanical strength of many hydrogels hinders their use in load-bearing applications and sometimes results in their premature dissolution from the targeted site. In addition, greater problems arise relating to drug delivery properties of the hydrogels when a hydrophobic drug is taken into consideration. The quantity and homogeneity of drug loading is highly doubtful, particularly for hydrophobic drugs. The high water content and large pore size of the hydrogels often result in a relative rapid release of drug thereby reducing the therapeutic value of the drug (Hoare and Kohane, 2008).

1.7 Concept of Controlled Drug Release Technology

A device that delivers therapeutic agents to desired body locations and provides timely release of these agents is highly in demand in pharmaceutical fields. Some drugs have an optimum concentration range within which maximum benefit is derived and

concentrations below or above this range can prove to be less efficient therapeutically. The very slow progress in the efficacy of the treatment of severe diseases has suggested an urgent need for a multidisciplinary approach for the delivery of therapeutic agents to the tissues. In this regard, new ideas on controlling the pharmacokinetics and pharmacodynamics of drugs have emerged. These new strategies, referred to as controlled drug delivery (CDD), are often based on interdisciplinary approaches that combine pharmaceutics, polymer science, analytical chemistry, bioconjugate chemistry and molecular biology. Controlled drug delivery is the use of formulation components and devices to release a therapeutic agent at a predictable rate *in vivo* upon administration. Controlled drug delivery occurs when a polymer, whether natural or synthetic, is judiciously combined with a drug or other active agent in such a way that the active agent is released from the material in a predesigned manner. The release of the active agent may be constant over a prolonged period, it may be cyclic over a long period or it may be triggered by environmental factors. In any case, the sole purpose behind controlling the drug delivery is to achieve more effective therapies while eliminating the adverse effects of both under- and overdosing (Uhrich *et al.,* 1999; Siegel and Rathbone, 2012).

In the past few decades, pharmaceutical formulations that target specific areas and control the rate and period of drug delivery (*i.e.* timed-release medications) have gained much impulse. Conventional drug dosage forms which include pills, tablets, capsules, injections, ointments, creams *etc.* release the drug instantaneously in a bolus form; which calls for frequent dosing and increases patience non-compliances. With conventional formulations, the drug level in the blood follows the profile shown in Figure 1.10 A.

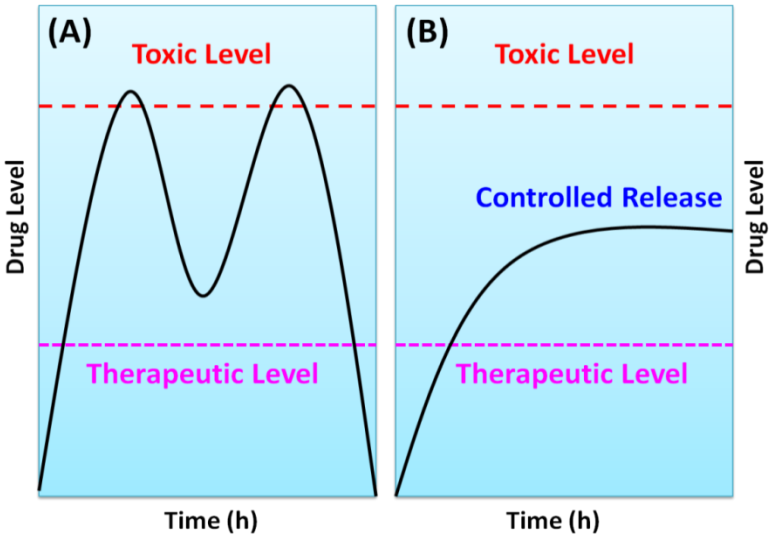

Figure 1.10. Typical pharmacokinetic profiles of (A) conventional and (B) controlled drug release formulations (Martin del Velle *et al.,* 2009).

As shown in Figure 1.10 A, the drug level rises rapidly after each administration of the drug and then decreases steeply until next administration. This might typically lead to higher concentrations of the drug in the blood plasma which represents the toxicity level. Sometimes the drug concentration lies below a particular minimum value where the drug remains mostly ineffective therapeutically. In controlled drug delivery systems (Figure 1.9 B), the drug level remains constant at an optimum level between the desired maximum and minimum, for a prolonged period of time therefore increasing the therapeutic value (Martin del Velle *et al.,* 2009). Controlled release of drugs reduces the dosing frequency, enhances activity of short half-life drugs, eliminates side-effects and drug wastage, optimizes therapy and improves patient compliances. Some of the main advantages of controlled drug release technology are listed in Figure 1.11.

Figure 1.11. Major advantages of controlled drug release technology.

Drug release mechanism from a hydrogel matrix can be broadly classified into three categories in accordance to the three main processes (Siegel and Rathbone, 2012):

- Drug diffusion from hydrogel matrix (diffusion-controlled system)
- Enhanced drug diffusion due to hydrogel swelling (swelling-controlled system)
- Drug release due to polymer degradation and erosion (erosion-controlled system)

The phenomenon of diffusion is inherent to all types of drug release systems. For a non-biodegradable polymer matrix, the drug diffusion is mainly due to the concentration gradient between the matrix and the releasing medium. For a swelling controlled release the drug diffusion happens as the water/ fluid enters the polymer network during the swelling process. For a polymer matrix prone to degradation, the drug release is controlled by the hydrolytic cleavage of polymer chains that leads to matrix erosion. The phenomena of the three classes of drug release mechanism from polymeric hydrogels are illustrated in Figure 1.12.

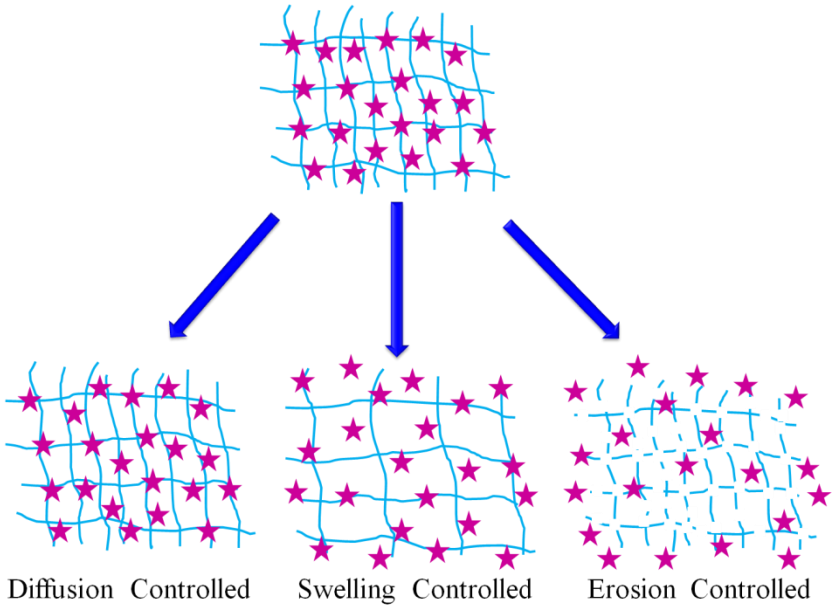

Figure 1.12. Mechanisms of drug release from polymeric hydrogels

1.8 Improving the Drug Delivery Efficacy of Hydrogels

The high water content of hydrogels often induces rapid release of drugs from the matrix. In response, a range of strategies have been explored to reduce the burst release of drugs from the hydrogel matrices. These strategies can be categorized on the basis of whether they enhance the drug-hydrogel interactions or increase the diffusive barrier to drug release from the hydrogels (Hoare and Kohane, 2008).

1.8.1 Drug−Hydrogel Interactions

Both physical and chemical methods have been utilized to enhance the interaction between the hydrogel and the drug to control the release rate.

1.8.1.1 Physical Interactions

Interactions between ionic polymers and charged drugs have often been employed as a strategy for controlling the rate of release of drug.

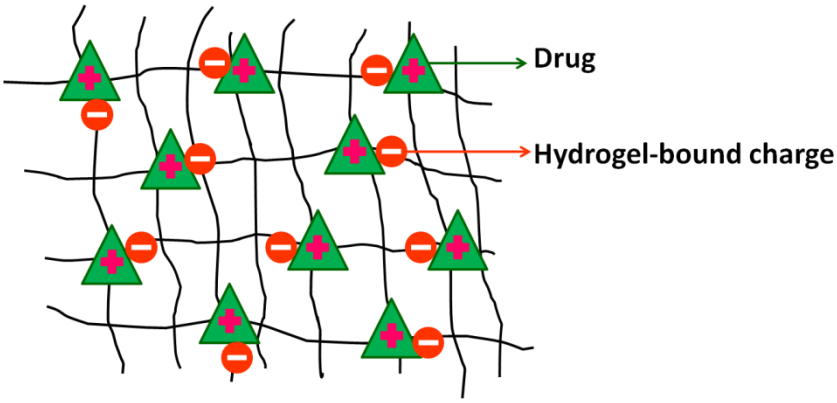

Figure 1.13. Ionic interactions between a polymer and loaded drug to control drug release.

The ability of the anionic polymer CMC sodium to influence the release of four cationic drugs (chlorpheniramine maleate, venlafaxine hydrochloride, propanolol hydrochloride and verapamil hydrochoride) from hydrophilic PEO matrices was investigated by Palmer *et al.,* (2013). Slower drug release was observed from the hydrogels as compared to the matrices of single polymers. This was mainly attributed to the ionic interaction and hydrogen bonding between anionic polymer and cationic drugs leading to a reversible drug-polymer complexation. Marras-Marquez and colleagues (2014) discussed the effect of anionic/ non-ionic surfactants such as sodium lauryl sulphate, Tween-80 and Pluronic F-68 when introduced into agarose hydrogels for the release of the hydrophilic drug theophylline and hydrophobic drug tolbutamide. Controlled drug release was observed which was attributed to the charged interactions between the drug loaded micelles and agarose and also to the hydrogel microstructure. A dual ionic interaction system composed of a positively charged polyelectrolyte complex containing human growth hormone (hGH) and anionic thermo-sensitive poly(organophosphazene) hydrogel has been developed by Park *et al.,* (2013) for sustained delivery of bioactive hGH. The hydrogels were found to suppress the initial burst release of hGH and extend the release period *in vitro* and *in vivo*. Thermo-sensitive poly(NIPAAm-co-NVP)-chitosan hydrogels were explored

for the sustained release behaviour of the anionic drug, naproxen (Li *et al.*, 2012).The strong interaction between chitosan chains and the anionic drug led to improved swelling behaviour of the hydrogels and showed a continuous naproxen release without any burst effect.

1.8.1.2 Covalent Bonding

Drugs or prodrugs can also be covalently bound to the hydrogel matrix such that the release of drug is primarily controlled by the rate of the cleavage of drug-polymer or prodrug-polymer bond.

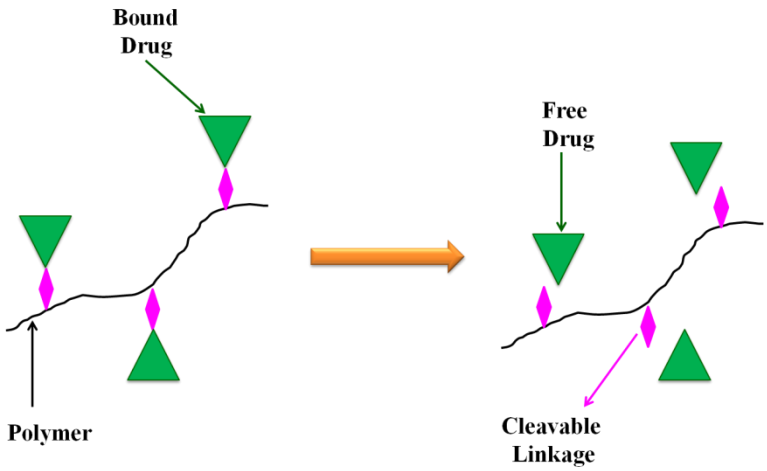

Figure 1.14. Drug-polymer interaction by covalent linkages to control drug release.

In a recent study by Ke *et al.*, (2014) DOX has been covalently conjugated with amphiphilc diblock copolymers of PEG. The release studies indicated pH-triggered intracellular drug release and established these hydrogels as promising candidates for anticancer drug delivery. Bezuidenhout and co-workers (2013) have employed a variety of techniques to locally deliver dexamethasone from injectable PEG hydrogels. The drug was acrylated, pegylated and tethered to hydrolytically degradable (acrylate based) and non-degradable (vinyl sulfone based) PEG hydrogels. Sustained release was observed in the cases where dexamethasone was covalently bonded in comparison to the controls where the drug was simply dispersed. The recently published review

article by Duncan and Vincent (2013) on "polymer therapeutics" briefly describes polymeric drugs, polymer conjugates of proteins, drugs and aptamers, with block copolymer micelles and multicomponent non-viral vectors containing covalent linkages and the subsequent applications in drug delivery .

1.8.2 Gel Engineering

Several approaches have been explored to control the rate of release of drugs from hydrogel matrices by modifying the microstructure of the hydrogel, either through the full hydrogel network or locally at the hydrogel surface. Some of the approaches are discussed below.

1.8.2.1 Interpenetrating Polymer Networks (IPNs)

An interpenetrating polymer network (IPN) is formed when a secondary polymer network is polymerized within a pre-formed polymer network. IPNs can be classified as full-IPN or semi-IPNs depending upon the presence or absence of a cross-linker. Full-IPNs are formed in the presence of a cross-linker while in the absence of the cross-linker; a semi-IPN is generated. The semi-IPN comprises of linear polymers entrapped within the original hydrogel matrix. This is illustrated in Figure 1.16.

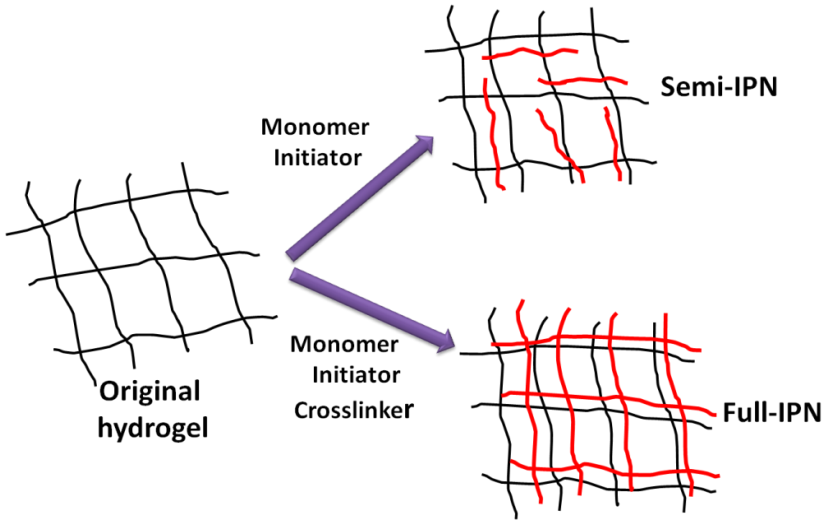

Figure 1.15. Formation of semi− and full−interpenetrating polymer networks (IPNs).

The formation of IPNs leads to denser hydrogel matrices with tougher and stiffer mechanical properties, controllable physical properties and sustained drug release characteristics than conventional hydrogels. Drug loading is also carried out in conjugation with polymerization process (Mohamadnia *et al.,* 2007). IPNs can also regulate the rate of drug release because of their ability to restrict the swelling capacity of both the polymer networks depending on the cross-linking density. For example, pH- and temperature-responsive IPN hydrogels based on soy protein and poly(NIPAAm-co-acrylate) were successfully prepared by Liu *et al.*, (2014). BSA release from the hydrogels was sustained with good pH- and temperature sensitivity. In another study, Chen and colleagues (2014) observed a controlled and pH-sensitive delivery of riboflavin from carboxymethyl chitosan/ (PNIPAAm-co-methacrylic acid) IPN hydrogels. The drug release rate from the hydrogels was very low at pH 1.2 and increased at pH 7.4 suggesting them as site-specific drug carriers. The design and applications of various IPN hydrogels have been finely addressed in the recently published review article by Dragan (2014). The influence of the second network on IPN properties, deswelling and mechanical improvements in IPN has been discussed eloquently.

1.8.2.2 Surface Grafting

Surface modification of the hydrogel is another approach that can be performed at the hydrogel surface employing a stimuli-responsive polymer. This method prevents the modification of the bulk structure of the hydrogel. The mechanism of surface grafting of hydrogels is shown in Figure 1.16.

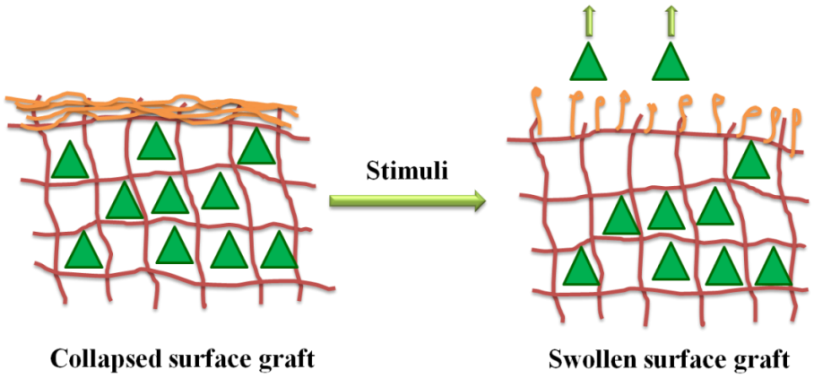

Figure 1.16. Controlling drug diffusion from a hydrogel with a stimuli-responsive surface graft.

By this method, polymers sensitive to environmental stimuli such as pH, temperature, light, ionic strength *etc.* can be grafted to the surface of the parent hydrogel network. For example, PNIPAAm or PAA can be grafted on the surface of a hydrogel to provide temperature or pH-dependent surface permeability, respectively. This, in turn, will affect the drug release kinetics. PNIPAAm oligomers were grafted onto PHEMA hydrogels and utilized as delivery devices for insulin and theophylline (Ankareddi and Brazel, 2007). Drug release was observed to be rapid at low temperatures but significantly slower at higher temperatures owing to the phase transition behaviour of PNIPAAm. Alternatively, a drug-loaded hydrogel can be coated with a polyelectrolyte multilayer (PEM) film that would limit the drug diffusion out of the hydrogel matrix. Matsusaki and co-workers (2007) prepared alginate hydrogels nano-coated with PEM films composed of chitosan and dextran sulphate. The release of vascular endothelial growth factor (VEGF) was monitored from these hydrogels. The nano-coated hydrogels were found to be more stable than the non-coated ones. The release of VEGF from the nano-coated hydrogels continued for one month, thus establishing them suitable for controlled and sustained drug delivery systems. Sakaguchi *et al.*, (2006) have also synthesized alginate hydrogels nano-coated with PEM films composed of poly(diallyldimethyl ammonium chloride) and poly(sodium 4-

sytrenesulfonate). The pH-sensitive swelling behaviour of the hydrogels indicated their potential in biomedical applications.

1.8.3 Composite/ "Plum pudding" Hydrogels

In order to overcome the inherent pharmacological limitations of hydrogels, growing interest has been focussed on the incorporation of particulate systems such as microparticles, liposomes, micelles *etc.* into the hydrogel matrix to form composite/ "plum pudding" hydrogels. This has been illustrated in Figure 1.17.

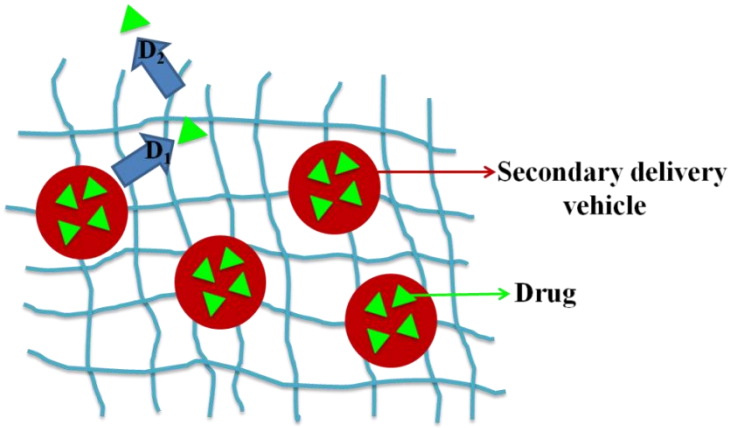

Figure 1.17. "Plum pudding"/ Composite hydrogel containing drug encapsulated in a secondary delivery vehicle; D_1 and D_2 represent the diffusion coefficients of drug out of hydrogel (D_1→ release from secondary delivery vehicle; D_2→ drug diffusion out of hydrogel).

The hydrogel template method for generation of homogenous nano/ microparticles has drawn much focus in recent years for optimal drug loading and release properties. Acharya *et al.,* (2010) first reported the hydrogel template approach for pH-sensitive gelatin hydrogels. It was observed that gelatin hydrogels could be tailored to possess various properties for microparticle encapsulation. The drug loading was found to be higher than 50% with minimal initial burst and near zero-order kinetics. In a recent study by Lu and co-authors (2014) hydrogel template method was employed to produce homogeneous PLGA microparticles that were embedded in PVA matrix and investigated for drug delivery. Drug release was found to be sustained for weeks.

Insulin-like-growth factor-1, an important growth factor in cartilage regenartion, was encapsulated within PLGA microspheres embedded in PVA hydrogels (Spiller *et al.,* 2012). Sustained release was obtained from these hydrogels which pointed their potential in cartilage tissue engineering.

Xu *et al.,* (2006) have synthesized PNIPAAm-poly(methyl methacrylate) micelles and physically incorporated the micelles into the thermo-sensitive bulk PNIPAAm hydrogel to form composite hydrogels. The composite hydrogels exhibited faster shrinking kinetics than pure PNIPAAm hydrogels. In addition, the release of prednisolone acetate was monitored from the hydrogels which showed excellent thermo-sensitivity.

Liposomes have also been entrapped in hydrogels. Liposomes embedded in PLGA-PEG-PLGA hydrogels released 2-methoxyestradiol in a prolonged manner (Xing *et al.,* 2014). Propylene glycol liposomes in Carbopol hydrogels containing metronidazole and clotrimazole were synthesized for the treatment for vaginal microbial infections (Vanic *et al.,* 2014). *In vitro* studies of drug release indicated sustained behaviour of the drugs in simulated human conditions. Chitosan containing liposomes and cubosomes have also been developed as sustained release vaccine delivery systems (Gordon *et al.,* 2014). The potential of liposomal hydrogels as wound dressing materials have been well documented in the review article by Thirumaleshwar and co-authors (2012). PNIPAAm hydrogels containing temperature-sensitive liposomes have been prepared by Han *et al.,* (2005) to obtain a hydrogel complex at room temperature. The release behaviour of calcein was explored from these hydrogels. A sustained release was observed which indicated the prospective of this system as drug delivery carriers. The review articles by Mufamadi *et al.* (2011)

and Alinaghi *et al.* (2013) summarize comprehensively the recent developments in the area of composite liposomal-hydrogel technologies.

Cyclodextrins are of particular interest in the context of designing composite hydrogel systems, given their hydrophilic exterior which is useful for maintaining the bulk hydrophilicity and swelling state of the hydrogel, and their hydrophobic interior which can facilitate entrapment and controlled release of hydrophobic drugs.

1.9 Cyclodextrins and Drug Delivery

1.9.1 Introduction to Cyclodextrins

Cyclodextrins (CDs) are a family of macrocyclic oligosaccharides linked by α−1,4 glycosidic bonds derived from starch. These are extensively studied in diverse fields since their discovery by Villiers in 1891 (Villiers, 1891). α−, β− and γ−CDs are the most common naturally occurring CDs composed of six, seven and eight glucose rings, respectively (Connors, 1995; Szejtli, 1998). The truncated cone shape of CDs possess a hollow tapered cavity of 0.79 nm depth while the top and bottom diameters increase with corresponding increase in the number of glucose units (Figure 1.18). The hydrophobic inner cavity of CDs gives them the capability to include a variety of compounds ranging from small molecules, proteins and oligonucleotides. The pharmaceutical and biomedical applications of CDs are extremely attractive due to their low toxicity and low immunogenicity. Apart from being used exhaustively in pharmaceuticals, CDs find extensive demand in the fields of cosmetics and toiletries, food industries, agricultural and chemical industries and also as adhesives and coatings (Martin del Velle, 2004).

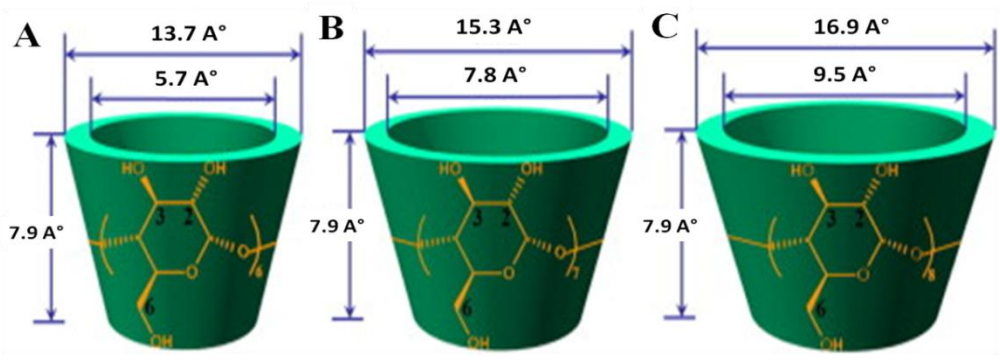

Figure 1.18. Truncated cone or torus shape of various CDs; (A) α−CD, (B) β−CD and (C) γ− CD.

The internal cavity of CDs enables to complex "guest" drug molecules and in doing so, enhance the physico-chemical properties of the drug. The guest molecules can either be included totally or partially into the CD cavity. This process occurs spontaneously in the aqueous medium, since the displacement of water from the apolar cavity and the establishment of hydrophobic, electrostatic, van der Waals or hydrogen bonding interactions with the guest, and the release of conformational strain in the CD structure lead to thermodynamically favourable balance (Liu and Guo, 2002).

The complexation of drug with CD can be defined by an association constant (K_b) which is given by the following formula:

$$K_b = \frac{[Drug - CD]}{[Drug][CD]}$$

Where, [Drug] and [CD] represent the free concentration of drug and CD and [Drug-CD] is the concentration of drug-CD inclusion complex. No covalent bonding exists between CD and the guest and the complexation is a dynamic process. High values of K_b indicate the high stability of the drug-CD complexes in aqueous solution.

The phenomenon of inclusion of guest inside CD cavity brings remarkable physico-chemical consequences (Figure 1.19).

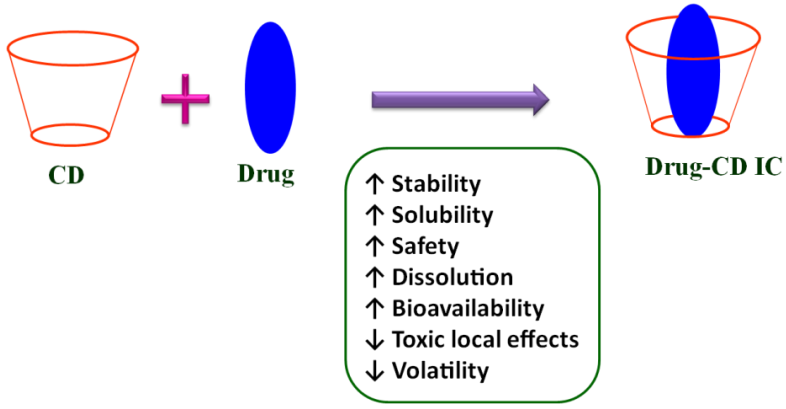

Figure 1.19. Changes in physico-chemical properties of drug caused by inclusion complex formation with CD in solution.

Advantages of CD complexation in pharmaceutical formulations are due to:

- Greater solubility and dissolution of hydrophobic moieties (Brewster and Loftsson, 2007).
- Enhanced drug absorption/ bioavailability (Vyas *et al.,* 2008).
- Reduction in drug toxicity (Challa *et al.,* 2005).
- Increase in shelf-life of drugs or increased drug stability (Larsen, 2002).
- Control of drug release (Tiwari *et al.,* 2010).

Detailed appraisal of physico-chemical properties of CDs and the usefulness of CD inclusion technology in pharmaceutical industries have been beautifully articulated in several review articles (Szejtli, 2004; Uekama, 2004; Astakhova and Demina, 2004; Loftsson *et al.*, 2005; Stella and He, 2008; Salustio *et al.,* 2011; Mura, 2014; Sharma and Baldi, 2014).

1.9.2 Applications of CDs in Drug Delivery Systems

CDs, because of their unique features, are greatly employed as drug delivery agents. Pharmaceuticals formulated using CDs have been evaluated for oral, nasal, ocular, rectal and dermal drug delivery.

1.9.2.1 Oral Drug Delivery

Oral route has always been the preferred route of drug administration because of the ease of the method. Advantages of CDs in oral drug delivery include improvement of drug bioavailability due to increased drug solubility, enhanced drug dissolution, drug stability at absorption site and reduction in drug-induced irritation (Stella and Rajeswski, 1997). CDs enhance the mucosal drug permeability mainly by increasing the free drug concentration at the absorptive surface (Yoo *et al.,* 1999). CD complexation provides better and uniform absorption of low-soluble drugs and also enhances their activity on oral administration (Veiga *et al.*, 2000; Fathy and Sheha, 2000). The review article by Perchyonok and Oberholzer (2012) focuses on the applicability of CDs as oral drug carrier molecular devices and also demonstrates the practical *in vitro* models.

1.9.2.2 Nasal Drug Delivery

Nasal drug delivery is an attractive approach for the systemic delivery of high potency drugs with low oral bioavailability due to extensive gastrointestinal breakdown and high hepatic first-pass effect. CDs have the ability to enhance drug delivery through biological barriers without affecting their barrier function, a property which makes them highly commendable for intranasal drug delivery purposes (Merkus *et al.*, 1999). The solubility of the anti-allergic drug loratadine was enhanced by complexing with β−CD and targeted for nasal delivery of the drug (Singh *et al.*, 2013). A nasal delivery system for lorazepam has been developed by Jug and Becirevic-Lacan, (2008).

1.9.2.3 Ocular Drug Delivery

The ideal route of drug administration in ocular drug delivery is the eye drop formulation due to its simple method of application. But the major disadvantage associated with this form of dosage is its inability to sustain local drug concentrations. CDs have been used to increase the solubility and chemical stability of drugs and prevent side-effects such as ocular drug irritation. Applications of CDs have also led to enhanced drug permeability by making the drug available at the ocular surface. Hydrophilic CDs, especially 2HP−β−CD and SBE−β−CD are found to be non-toxic to the eye and are well tolerated in aqueous eye drop formulations (Challa *et al.,* 2005). The review article by Kang-Mieler (2014) discusses the utility of cyclodextrins in ocular drug delivery with particular emphasis on the posterior segment.

1.9.2.4 Rectal Drug Delivery

Applications of CDs in rectal drug delivery include enhancing drug absorption from a suppository base either by enhancing the drug release from the base or by increasing drug mucosal permeability, providing sustained release and alleviating drug-induced discomfort and irritation (Matsuda and Arima, 1999). CDs enhance the rectal absorption of inabsorbable hydrophilic drugs such as antibiotics, peptides and proteins by their direct action on rectal epithelial cells. α−CD enhanced the rectal absorption of morphine and human chorionic gonadotropin by increasing their mucosal permeability and decreasing their degradation (Uekama *et al.,* 1995; Kowari *et al.,* 2002).

1.9.2.5 Colon-specific Drug Delivery

CDs are slightly absorbed in the stomach and small intestine but are absorbed in the large intestine after fermentation by the colonic microflora. This unique hydrolyzable nature of CD makes them apt in the design of colon targeted drug delivery systems. The CD based prodrug approach has been widely employed to delay the drug release

and ensure its degradation in colon. Active molecules can be covalently attached to the primary or secondary hydroxyl groups of β−CD producing prodrugs with the ability to remain intact in the upper GIT. Once these molecules reach the colon, they are subsequently cleaved to release the drug (Uekama, 2004). Moreover, the fermentation of β−CD leads to production of short chain fatty acids that contribute to the health and maintenance of the colonic epithelium (Giardina and Inan, 1998). In a recent study by Vieira *et al.,* (2013) microwave assisted diclofenac and β−CD conjugates were prepared and assessed for colonic delivery. The conjugate was found to be stable in SGF and liberated the drug in SIF which confirmed the potential of this diclofenac prodrug for colonic delivery. Macromolecular prodrug of 4-aminosalicylic acid with β−CD was prepared by Vadnerkar and Dhaneshwar (2013) and the release was studied in rat cecal/ faecal buffers. The produgs suggested the targeted delivery of the drug to the colon.

1.9.2.6 Drug Delivery to Brain (Brain Targeting)

The blood-brain barrier (BBB) restricts the transfer and delivery of most drugs to the brain. A novel lactoferrin-modified β−CD nanocarrier was designed by Ye and co-workers (2013) for brain targeting drug delivery. The results of tissue distribution indicated that the nanocarriers greatly improved BBB transport efficiency. The study also evaluated lactoferrin-β-CD nanocarriers as potential brain targeting drug delivery system for hydrophobic drugs and diagnostic reagents which normally fail to pass through BBB. The short half-life of pituitary adenylate cyclase activating polypeptide (PACAP), a potent neurotrophic and neuroprotectant, makes it difficult to be administered peripherally. Nonaka and co-workers (2012) demonstrated that therapeutic amounts of PACAP can be delivered to brain by intranasal administration by the use of CDs. It was also observed that CDs targeted the peptides to specific

regions of the brain. In another study, galanin-like peptide (GALP), which is potential in treatment of obesity and related conditions showed greater uptake with CDs (Nonaka *et al.,* 2008). The studies also proclaimed that targeting of GALP to the brain regions is possible with the use of various CDs.

1.9.3 CD-based Hydrogels for Drug Delivery

The combination of CDs and hydrogels can overcome the limitations of poor loading of drugs into hydrogels and improve the controlled delivery features of the hydrogels (Otero-Espinar *et al.,* 2010). It has been found that incorporation of CD into polymeric drug release systems could change the drug-polymer interactions and as a result, the mechanisms of drug release may be greatly modified (Bibby *et al.,* 2000). Moreover, the hydrogel phase improves the kinetic release profile of the particulate system by providing an additional diffusion barrier to drug release, extending the release period of drugs (Chen *et al.,* 2004; Barreiro-Iglesias *et al.,* 2001). Therefore, composite systems integrating hydrogels and cyclodextrins complement the advantages, while avoiding the disadvantages, of the two discrete systems, as a consequence this is used as a strategy to design more effective formulations.

CDs are pivotal in improving the loading of drugs and controlling the rate of release of drugs from the hydrogel matrix. In case of physically cross-linked hydrogels, the larger hydrodynamic radius of the drug-CD inclusion complex, than the free drug, effectively reduces the rate of drug diffusion and controls the delivery (Bibby *et al.,* 2000). When CDs are incorporated into hydrogels, they can act as binding points which can either be utilized as drug-CD interaction platform or for improving the mesh size of the hydrogels. These cross-linked networks effectively limit the entrance of physiological fluids and as a result the covalently attached CDs cannot move apart

from each other. In such an environment, the drug-CD affinity becomes the driving force to retain the drug and control the delivery.

When the hydrogels come in contact with the physiological fluids, they swell but the volume of water taken up is limited by the polymer network and consequently, the polymeric chains do not dissolve. This creates a microenvironment rich in cavities available to interact with the guest drug molecules. In such cases, the affinity of the drug molecules for the CD cavities drives the drug delivery. The covalent attachment of CDs to polymer networks might not decrease their inclusion ability but sometimes improve the same, particularly in the cases of large molecules which require one or more CD for complexation (Li *et al.,* 2004; Crini *et al.,* 1998; Layre *et al.,* 2002). Decomplexation of a drug molecule from one CD cavity makes the drug available to form complexes with the neighbouring empty CD cavity and the likelihood of recomplexation is strongly dependent on the drug-CD affinity.

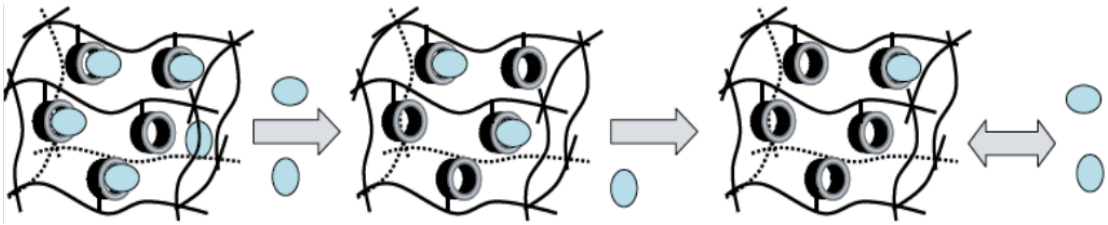

Figure 1.20. Drug release from a chemically cross-linked CD network.

Therefore, drug release from a hydrogel can be visualized as successive escapes of drug molecules from CD cavities until the drug reaches the surface (Figure 1.20). The higher the drug-CD affinity, the slower is the drug release. Figure 1.21 describes the different states in which CDs can be found in a polymeric network.

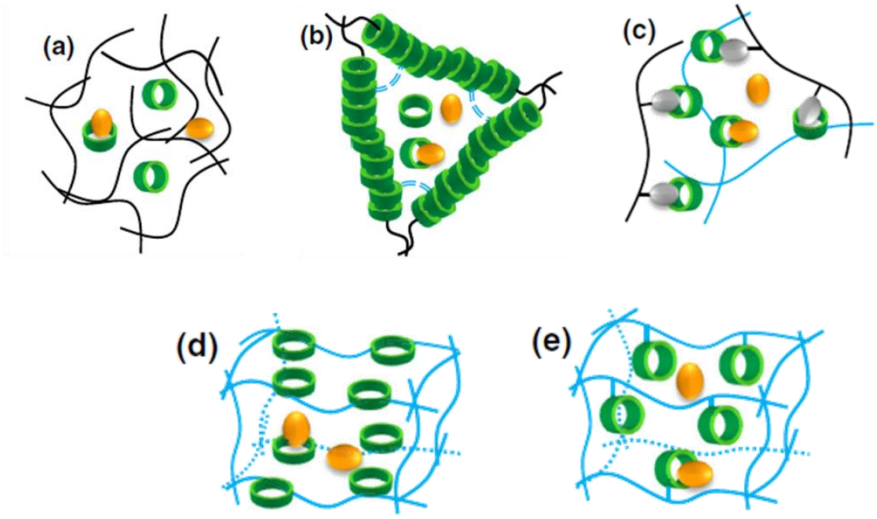

Figure 1.21. Different modes in which CDs can be found in polymeric networks; (a) movable CDs, (b) polypseudorotaxanes in which the CDs are chemically threaded, (c) CDs forming part of polymer chains to act as tie-junctions of other polymeric chains with complexable moieties, (d) CDs forming part of the polymer backbone and (e) CDs hanging from the network structure (Concheiro and Alvarez-Lorenzo, 2013).

Different synthetic strategies have been employed to prepare polymeric CD based systems. Hydrogels in which CDs form a part of the network structure can be obtained by direct cross-linking of the CDs or by copolymerization of the CDs with other monomers.

1.9.3.1 Hydrogels Obtained by Cross-linking of CDs

Although originally designed as a column material for separation chromatography, the first CD containing polymeric networks were developed in the 1980s (van de Manakker *et al.,* 2009). CD polymers and hydrogels were first obtained by the condensation reactions of the hydroxyl groups of the CDs with various cross-linking agents such as aldehydes, ketones, epoxides and epichlorohydrin (EPI) (Crini and Morcellet, 2002). Under alkaline conditions, the two reactive functional groups of EPI react with the hydroxyl groups of CDs or with other EPI molecules which results in a mixture of cross-linked CDs joined by repeating glyceryl units of polymerized EPI (Kobayashi *et al.,* 1989). EPI-CD hydrogels have been utilized as selective traps for

removal of components from food (Crini, 2008), bioremediation (Sevillano *et al.*, 2008), separation science (Scriba, 2008) and as drug delivery systems (Mok and Kim, 2014).

Studies pioneered by Szetjli *et al.,* (1978) focused on mixed networks of CDs and hydrophilic polymers such as PVA using EPI and ethylene glycol bis(epoxypropyl) ether with a rational of achieving greater hydrophilicity and better mechanical properties for biomedical applications. The hydrogels were then modified with carboxymethyl and acetyl groups to render hydrophobicity. This approach ensured that CDs retained their inclusion capability and the hydrogels demonstrated high loading capacity for drugs. A great many research has been dedicated towards EPI-CD hydrogels for diverse applications (Crini and Crini, 2013). Although EPI-CD hydrogels have demonstrated potential for pharmaceutical and biomedical applications, the relatively high toxicity of EPI and its pollutant character limits its applicability and has invited further research on alternative cross-linking agents (Mocanu *et al.,* 2001). The use of diisocyanates has received attention for preparing CD hydrogels or beads. This approach has been particularly aimed for PEG hydrogels which is a highly hydrophilic and biocompatible polymer. The PEG chains previously end-capped with isocyanate groups react with β−CD forming urethane links. The molecular weight of PEG and PEG/β−CD molar ratio was central in determining the structure of the hydrogel, its swelling properties and its capability to load naphthol by forming inclusion complexes with β−CD. PEG hydrogels were first obtained by activating the β−CD with hexamethylenediisocyanate (HMDI) in anhydrous DMSO. These hydrogels exhibited high hydrophilicity and biocompatibility and higher loading efficacy and sustained release of estradiol, quinine and lysozyme. Following a more sophisticated approach PEG-diamine networks had been created in which the tie

junctions were polyrotaxanes having isocyanate-activated β−CD groups (Ooya *et al.,* 2007). Comparative studies on the performance of CD hydrogels cross-linked with EPI, succinyl chloride and HMDI revealed the importance of the nature of the cross-linker regarding the affinity of the guest molecules for the CD cavities. The results suggested that diisocyanates lead to formation of networks of smaller mesh size and a lower swelling degree in water while the use of EPI provides longer bridges in CDs.

Condensation of CDs with poly(carboxylic acids) has been reported to be one of the clean methods to obtain cross-linked CD networks. Polyesterification of native CDs can be carried out with citric acid or PAA but not with dicarboxylic acids. These results stressed the use of poly(carboxylic acids) with at least three neighbouring carboxylic groups. A phosphate catalyser (*e.g.* NaH_2PO_4) is also required to form an intermediate cyclic anhydride of the poly(carboxylic acid) that will react with the CDs (Martel *et al.,* 2005).

One-step direct cross-linking of CDs using ethylene glycol diglycidyl ether (EGDE) has ensured hydrogel synthesis in aqueous conditions under mild conditions. EGDE is a relatively nontoxic reagent. Most of the glycidyl groups are consumed in the reaction, while washing with dilute HCl opens the remaining rings to give hydroxyl groups which give rise to highly biocompatible hydrogel (Huang *et al.*, 1998).

With the aim of modulating the mechanical properties and broadening the spectrum of applicability of CD hydrogels as drug delivery agents; linear cellulose ethers and dextran were incorporated during cross-linking. HP−β−CD−*co*−HPMC and Me−β−CD−*co*−HPMC hydrogels absorbed water 10 times their own weight and loaded upto 24 mg of estradiol per gram, which is 500 times greater than the amount of drug that can be dissolved in aqueous phase (Rodriguez-Tenreiro *et al.*, 2007). This work highlighted the major role of CD in drug loading and the high drug-CD affinity

led to the achievement of sustained delivery of estradiol for one week. The role of cellulose ethers in improving the physical properties of the hydrogels was pertinent. β−CD / HP−β−CD−*co*−HPMC cross-linked with 1, 4-butanediol diglycidyl ether have been developed to prevent wound infection (Pinho *et al.,* 2014). The hydrogels were able to incorporate high amounts of gallic acid and sustain the release for more than 48 h.

1.9.3.2 Hydrogels Obtained by Covalent Linking of Polymers and CDs

Covalently cross-linked polymeric CD systems have also been developed by coupling either modified or un-modified CDs to a wide variety of pre-existing polymers. Cross-linked networks of PAA and β-CD were obtained and the network formation was ascribed to the esterification of the hydroxyl group of the CDs with the carboxylic acid groups of PAA. Bibby and co-workers (1999) have performed this reaction in water-in-oil emulsion to get CD containing microspheres. The microspheres were then loaded with two dyes, phenolphthalein and rhodamine B, as model drugs and their release was monitored. More recently, hydrogel formation has been accomplished by a highly selective copper (I) catalyzed 1, 3-dipolar cycloaddition ("click chemistry") between alkyne-modified CD and an azide-functionalized poly(NIPAAm-*co*-HEMA) copolymer. This reaction provided several advantages including relatively mild conditions and reduced gelation rate (van Dijk *et al.*, 2009).

The most commonly employed strategy to generate CD-polymer networks is through copolymerization of vinyl- or acryloyl-modified CD monomers with other vinyl monomers such as AAc, NIPAAm or HEMA. Following this approach, several research groups have created hydrogels for pharmaceutical applications.

Wang *et al.,* (2009) reported the preparation of dual-stimuli responsive gels using the complexation of α-CD onto PEG grafts present in random copolymers of PEG-

methacrylate and 2-(dimethyl-amino) ethyl methacrylate. The α-CD slides onto the PEG side-chains of the polymer allowing for gel formation at high pH, while the pendant dimethylamino-functionality allows for pH-sensitivity leading to disruption of hydrogel structures at low pH. Based on a combination of PNIPAAm and β-CD, novel hydrogels, having both thermal and pH sensitivities were synthesized. Semi-IPN hydrogels composed of PNIPAAm and β-CD-g-polyethylenimine were prepared by radical polymerization. Propranolol as a model drug was loaded into the gels, and the release results showed that compared to that of the normal PNIPAAm hydrogel, the release time of propranolol from the CD-containing gel was prolonged (Wang *et al.*, 2007). CDs were grafted to the PVP/PEG-DMA polymer matrix that changed both the release rate and the release profile of ibuprofen (dos Santos *et al.*, 2008). Copolymerization of HEMA with a methacrylated-derivative of β-CD was evaluated to obtain hydrogels with tunable mechanical, drug loading and release properties, particularly to be used as medicated soft contact lenses. The hydrogels sustained the drug delivery for several days, the acetazolamide release rate being dependent on the β-CD content (Rodriguez-Tenreiro *et al.*, 2003). Mono-acrylated CD monomer was copolymerized with hydroxyethyl acrylate to produce a hydrogel network with CDs as pendent groups. The hydrogel showed a sustained release of N-acetyl-5-methoxytryptamine owing to the formation of drug/ β-CD inclusion complexes (Victor and Sharma, 2007). PHEMA/β-CD hydrogels have been investigated for sustained release of ophthalmic drugs. The incorporation of β-CD in the hydrogels increased the equilibrium swelling ratio and tensile strength. Puerarin was used as a model to evaluate drug loading and *in vitro* and *in vivo* release behaviour. Puerarin loading and *in vitro* release rate were dependent on β-CD content in the PHEMA/β-CD hydrogels (Liu and Fan, 2005). Liu and co-authors (2005) prepared β-CD

containing hydrogels by copolymerization of maleic anhydride-modified β-CD and NIPAAm. The resulting hydrogels were loaded with the anticancer agent chlorambucil and the drug release was investigated at pH 1.4 and 7.4 and compared to a gel without β-CD. The results indicated that increasing β-CD content led to faster release of drug. The faster release of drug from the β-CD hydrogels compared to β-CD free gels was attributed to the hydrophobic interactions between the drug and the dehydrated PNIPAAm chains which were prevented by drug-CD inclusion complexes. Anirudhan and Mohan (2014) have synthesized novel pH-switchable gelatin based hydrogel by grafting β-CD to the gelatin gel and cross-linking by oxidized dextran. This composite hydrogel was investigated for the colonic delivery of the anticancer drug 5-fluorouracil.

1.9.3.3 Self-assembled Polymer Systems Based on Host-Guest CD Inclusion Complexes

The inclusion complex forming ability of CD has also been utilized as a non-covalent binding motif for the development of a wide variety of dynamic polymeric networks and assemblies in aqueous media. Such polymeric systems have been widely recognized in pharmaceutical, biomedical and drug delivery applications. From a topological point of view, it is possible to differentiate two families of non-covalently bonded CD polymeric hydrogels: (a) polypseudorotaxane hydrogels containing CDs threaded onto one or more polymer chains and (b) hydrogels in which the polymer chains are held together by host-guest inclusion between CDs and guest molecules (Appel *et al.*, 2012).

Recently CD based polyrotaxanes and polypseudorotaxanes have led to interesting developments in the field of supramolecular hydrogels intended for drug delivery purposes. The pioneering report on the synthesis of CD based polyrotaxanes dates

back to 1992 in which the first preparation of the supramolecular compound composed of multiple α−CD rings threaded on a PEO chain and trapped by end-capping the chain with bulky end groups was described (Figure 1.22) (Harada *et al.*,1992). Since then, an overwhelming research has been devoted to the studies of supramolecular structures of polyrotaxanes and polypseudorotaxanes formed by CD threaded on polymers and their various applications as biomaterials (Li and Loh, 2008).

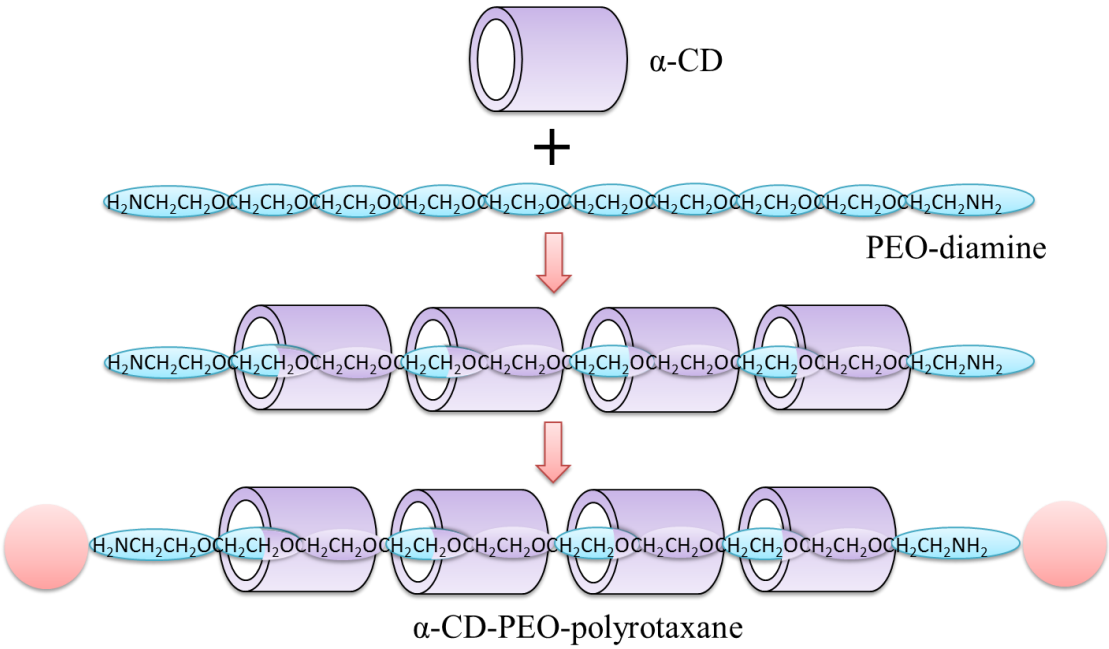

Figure 1.22. The synthesis of polyrotaxane from α−CD and PEO-diamine.

Research in CD based supramolecular hydrogels has developed since the 1990s and taken a huge leap forward in the next two decades. Cross-linking in these cases occurs from H-bonding interactions between exteriors of bound CD units and the formation of crystalline domains. Supramolecular hydrogels can be developed either by interaction of CDs with the polymer chains or by grafting copolymers onto the grafted polymer backbone (Figure 1.23 a & b).

Growing attention has been focussed on inclusion complex formation between CDs and block copolymers comprising blocks of different cross-sectional areas and properties. It was observed that CDs selectively complex with different blocks forming supramolecular structures containing partially complexed and un-complexed polymer segments. PEO and oligoethylene of various molecular weights formed inclusion complexes with α−CD to form polypseudorotaxanes in high yields. However, PPO formed inclusion complexes with β−CD and γ−CD in high yields but not with α−CD (Harada *et al.*, 1995). It was suggested that the PPO chains were too large to penetrate the cavity of α−CD.

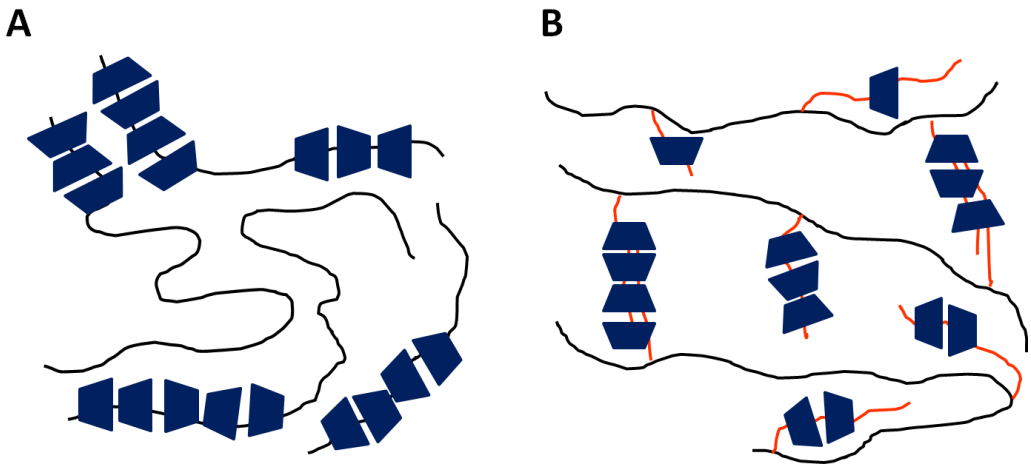

Figure 1.23. Schematic representation of polypseudorotaxane formation utilizing CD-based interactions with either (a) polymer chains or (b) grafted polymer chains from grafted copolymers as the driving force for hydrogel preparation.

Supramolecular structures formed between CDs and polymers have inspired interesting developments of novel supramolecular biomaterials. Of late, many new supramolecular CD hydrogel technologies have evolved as drug delivery systems. Supramolecular hydrogels consisting of triblock PLGA-PEG-PLGA copolymers and α-CD have been fabricated and investigated as drug delivery agents for naltrexone hydrochloride and vitamin B12 (Khodaverdi *et al.*, 2014). In a novel attempt by

Tabassi and co-workers (2014), supramolecular hydrogels based on the triblock copolymers of PCL-PEG-PCL and α-CD were developed and evaluated for their drug delivery efficacies of naltrexone hydrochloride and vitamin B12. Apart from controlled drug delivery purposes, the thixotropic nature of these hydrogels makes them injectable. The review article by Li (2010) summarizes the potential of CD-based self-assembled supramolecular hydrogels for drug and gene delivery applications. Supramolecular hydrogels based on self-assembly between PEO-PPO-PEO triblock copolymers and α-CD were prepared by Ni *et al.,* (2009) and found to be potentially suitable for drug delivery applications. The advancement in CD-based supramolecular assemblies and hydrogels has been well articulated in the recently published review by Tan *et al.,* (2014). Thermo-responsive supramolecular hybrid hydrogels formed by graphene oxide-grafted-PEG and α-CD have been developed by Kong and colleagues (2013).

Several attempts have also been made to develop hydrogels from CDs by covalently attaching a CD host to the polymer chain and mixing with a similarly-functionalized guest-containing polymer (Figure 1.24 a). Supramolecular hydrogels self-assembled by α-CD and methoxypolyethylene glycol-poly(caprolactone)-(dodecanoic acid)-poly(caprolactone)-methoxypolyethylene glycol (MPEG-PCL-MPEG) triblock polymers were prepared by Wu and co-workers (2008) for drug delivery and stem cell encapsulation. The sustained delivery of dextran-fluorescein isothiocyanate (FITC) from the hydrogels lasted for more than one month indicating the hydrogels to be promising for drug delivery application. ECV 304 and mesenchymal cells were encapsulated and the cell morphologies could be preserved during the cell culture. The *in vitro* cytotoxicity and the *in vivo* histological studies demonstrated the hydrogels as promising injectable scaffolds for tissue engineering applications. Koopmans and

Ritter (2008) presented a novel host-guest hydrogel system employing β−CD polymers and copolymers bearing adamantyl (ADA) groups. The construction of polymeric hydrogel networks through host-guest complexation between β−CD substituents and adamantyl substituents have also been reported by Wang *et al.*, (2010).

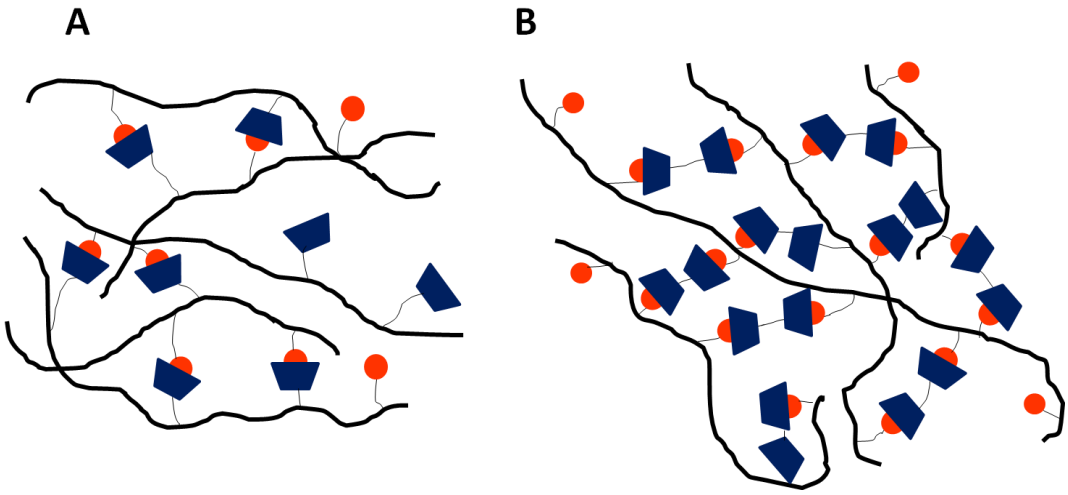

Figure 1.24. Schematic representation of hydrogel structures prepared by employing functional polymers bearing guests for CD complex formation either by (a) CD-functionalized polymers or (b) small molecule CD dimers.

A CD dimer could also be employed for fabrication of hydrogels using guest-functional polymer (Figure 1.24 b). Guan *et al.*, (2014) reported a triply stimuli-responsive hydrogel constructed by the formation of host-guest complexes between PNIPAAm containing azobenzene groups and CD dimers connected by disulfide bonds. Copolymers of NIPAAm containing adamantyl groups have been cross-linked non-covalently with CD dimers to give intelligent hydrogels (Kretschman *et al.*, 2006).

Tian *et al.*, (2014) designed an assembly of organophosphazene material based on the host-guest interactions between an ADA end-functionalized polyphosphazene and a 4-armed β−CD initiated poly(PEG- methyl ether methacrylate) branched-star type polymer. The resultant polymeric materials demonstrated useful properties including

self-aggregation, supramolecular gelation and stimuli-responsive behaviour. Rodell and co-workers (2013) have developed a shear-thinning hyaluronic acid (HA) hydrogel based on the host-guest interactions of ADA modified HA (guest macromer) and β−CD modified HA (host macromer). The hydrogel sustained the release of BSA for more than 60 days and showed potential as a minimally invasive injectable hydrogel for biomedical applications. Kandoth and co-authors (2013) developed a hydrogel by the spontaneous self-assembly of a poly-β−CD polymer, hydrophobically modified dextran and nitric oxide (NO) photo-donor bearing an adamantyl group. The formation of the hydrogel was attributed to a "lock-and-key" mechanism in which the adamantly moiety forms inclusion complexes with β−CD cavities. The utility of this photo-releasing NO platform showed highly effective and strictly light-dependent bactericidal activity against Gram-negative *E.coli*. A novel star-star supramolecular architecture self-assembled between a star-shaped adamantyl-terminated 8-arm PEG and a star-shaped PNIPAAm with a β−CD core has been designed which self-aggregates into a 3D network that induces thermo-responsive hydrogel formation (Zhang *et al.,* 2013). Liu *et al.,* (2014) obtained supramolecular assemblies with a bottle-brush structure by utilizing β−CD modified chitosan as host. The supramolecular hydrogels were formed by the host-guest inclusion of the ADA-modified methoxy-PEG into the β−CD cavity on the chitosan chain. The hydrogels can be used to realize the biomimetic structure of the articular cartilage proteoglycan. Supramolecular hydrogels, without using a cross-linker, were prepared by the polymerization of the inclusion complexes between β−CD acrylamide and ADA acrylamide (Kakuta *et al.,* 2013). The hydrogels demonstrated high performance physical properties in terms of elasticity and toughness.

Besides ADA moieties, other molecules have also been utilized as guests for the formation of CD inclusion complexes. Self-assembling PEG hydrogel system based on the inclusion complexes of β−CD and cholesterol have been described by van de Manakker and colleagues (2013). The hydrogels were formed after the hydration of a mixture of star-shaped 8-arm PEG (PEG_8) end-modified with β−CD groups and cholesterol. The hydrogels offered excellent biocompatibility and potential for various biomedical applications. The authors have reported the degradation and protein release behaviour from the β−CD and cholesterol-derivatized PEG_8 hydrogels (van de Manakker *et al.,* 2009). The high tunability, unique protein release mechanism and ease of preparation makes these useful as injectable drug delivery devices and scaffolds. In another approach, the PEG_8 hydrogels were obtained by an alternate strategy (van de Manakker *et al.,* 2010). In this system, the PEG_8−cholesterol was combined with 0.5 to 4 equivalent of free β−CD which led to hydrogel formation that were 5-10 folds stronger than the gels composed of PEG_8−β−CD and PEG_8−cholesterol.

In recent days, carbon nanotubes (CNTs), either single-walled (SWCNTs) or multi-walled (MWCNTs), have invited much attention because of their unique thermal, electronic and mechanical properties. They have been invariably utilized as carriers for therapeutic molecules. Since the CNTs are entirely built of carbon, the major limitation, besides their non-degradability, is their solubility in aqueous solvents. To improve the aqueous solubility, CNTs have been modified with β−CD. PEG-g-MWCNTs were synthesized and formed inclusion complexes after selective threading of the PEG segment of the PEG-g-MWCNT through α−CD cavities (Sui *et al.,* 2010). A chemically responsive supramolecular SWCNT hydrogel has been constructed by using the host-guest interactions of hybrids of SWCNTs and β−CDs (Ogoshi *et al.,*

2007). SWCNTs were incorporated into a Pluronic supramolecular hydrogel containing α−CD exploiting the inclusion efficacy of α−CDs with SWCNTs (Wang and Chen, 2007).

Efforts are still being made to incorporate CDs into various polymer matrices in order to explore and improve current drug release systems.

1.10 OBJECTIVES

The present research work aims at employing a simple and easy strategy for incorporating CDs to hydrogel matrix by loading preformed drug−CD ICs directly into the hydrogel to design an array of controlled delivery systems and exploring this possibility in greater details. CDs have the potential to reduce the release rate of drug from hydrogels even without any covalent linking to the matrixes, for they diffuse in the gel much slower than small molecule drugs probably due to their higher excluded volumes, low water-solubility, and hydrogen bonding ability.

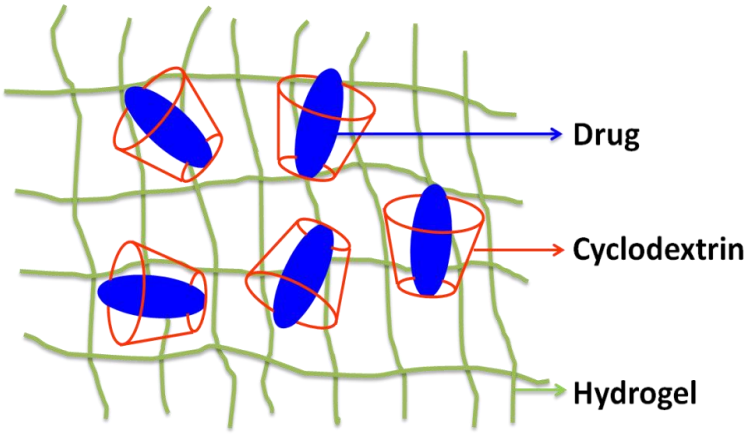

Figure 1.25. Drug−CD inclusion complex incorporated hydrogels for controlled delivery of hydrophobic drugs.

The specific objectives are:

- To explore the controlled drug releasing characteristics of PVA hydrogels containing drug-β-CD inclusion complexes. To investigate the role of CD, the effect of nature of drug (hydrophilic/ hydrophobic) and degree of cross-linking on the drug release process and to know the probable mechanism of drug release.
- To examine the utility of pH-sensitive CS-PVA hydrogels containing drug-CD ICs for controlled delivery of non-steroidal anti-inflammatory drugs; naproxen (NX) and diclofenac sodium (DS), to the intestine.
- To study the behaviour of PVA-PAA microspheres towards pH-responsive sustained release of dexamethasone (DX) and to further inspect the influence of method of preparation of the inclusion complexes on the drug release phenomenon.
- To study the drug delivery behaviour from thermo-sensitive Guar gum–PNIPAAm hydrogels containing 5-fluorouracil-CD solid inclusion complexes.
- To evaluate and compare the efficacy of GG-PAA-CD hydrogels with CD as a part of their network structure and GG-PAA hydrogel containing the preformed DX-CD inclusion complexes, for the controlled delivery of DX.

CHAPTER 2

MATERIALS AND METHODS

2.1 MATERIALS

2.1.1 Polymers and Monomers Employed for Hydrogel Preparation

Poly (vinyl alcohol) (PVA) having molecular weight of 85,000 − 1, 24,000 and degree of hydrolysis 86−89% was purchased from S. D. Fine Chemicals, India and employed in the preparation of hydrogel films. Another grade of PVA (M_w = 89,000 − 98,000 and 99.0% hydrolyzed) was received from Sigma-Aldrich, India and utilized in the synthesis of hydrogel microspheres. Chitosan (CS) (deacetylation degree > 75%, bulk density = 0.15−0.3 g/ cm^3 and viscosity > 200 cP) was obtained from Sigma-Aldrich, India. Guar gum (GG) was purchased from Merck India Ltd.

N-isopropylacrylamide (NIPAAm), the monomer for poly (N-isopropylacrylamide) (PNIPAAm), was obtained from Sigma-Aldrich, India and Acrylic acid (AAc), the monomer for poly (acrylic acid) (PAA), was received from SRL, India.

2.1.2 Medium Components

β−cyclodextrin (CD), ammonium persulfate (APS), tetraethyl orthosilicate (TEOS), *N*,*N*,*N*′,*N*′- tetramethylethylene diamine (TEMED) and analytical grade acetic acid were procured from Sigma-Aldrich, India and used as received. Glutaraldehyde (GA) was supplied as a 25% (w/w) aqueous solution by Spectrochem Pvt. Ltd., Mumbai, India. Ceric ammonium nitrate (CAN), light liquid paraffin oil and hydrochloric acid were obtained from S. D. Fine Chemicals, Mumbai, India. Tween-80 was received from Merck, India. Dulbecco's Modified Eagle's Medium (DMEM), Fetal Bovine Serum (FBS), Penicillin–streptomycin antibiotic solutions, 0.25% Trypsin and 0.02% EDTA solutions, MTT (3-(4,5-dimethylthiazol-2-yl)-2,5-diphenyltetrazolium bromide), RPMI-1640, Luria Bertani (LB) agar medium required for the biological studies were procured from Hi-Media, India.

2.1.3 Drugs

Ibuprofen (IBF), Dexamethasone (DX) and Naproxen (NX) were obtained from Sigma-Aldrich, India. Analytical-reagent grade Salicylic acid (SA) was received from Merck India Ltd. 5-Fluorouracil (5FU) was acquired from Spectrochem Pvt. Ltd., Mumbai, India. All the drugs were used as received.

2.1.4 Solvents and Buffers

Triply distilled water was utilized for the hydrogel syntheses and drug−CD inclusion complex preparation processes. Hexane and ethanol were obtained from Merck, India. D_2O, employed in the ^1H NMR studies, was obtained from Sigma-Aldrich, India. The phosphate buffers were prepared using sodium monohydrogen phosphate and sodium dihydrogen phosphate according to standard methods. Simulated gastric fluid (SGF) (pH 1.2, NaOH= 34.2 mM) containing pepsin (0.1 mg/ ml) and Simulated intestinal fluid (SIF) (pH 7.4, NaOH= 34.8 mM, NaCl= 68.62 mM) containing pancreatin were prepared according to standard methods reported in *United States Pharmacopeia* (Marques *et al.,* 2011).

2.2 INSTRUMENTS

Following instruments were used for the studies:

- Shimadzu UV−Vis spectrophotometer (UV−1800) for absorption studies.
- Horiba Jobin-Yvon Fluoromax-4P spectrofluorimeter for fluorescence measurements.
- Perkin Elmer RX I spectrophotometer for recording the Fourier Transformed Infrared (FTIR) spectra.
- PANalytical X−Ray diffractometer for the X−Ray diffraction (XRD) studies.
- Mettler Toledo DSC822 and Netzsch DSC200 instruments for carrying out Differential Scanning Calorimetry (DSC) studies.

- Microscopic observations were performed under an optical microscope (Olympus BX-51).
- Morphological studies were carried out on a JEOL Scanning Electron Microscope (SEM), model JSM 6480LV and Nova Nano 450 Field Emission SEM (FESEM).
- Bruker 400 MHz NMR Spectrometer for Nuclear Magnetic Resonance (^{1}H NMR) studies.
- LabTech and Scanvac Coolsafe Lyophilizers for freeze-drying purposes.
- Temperature related experiments were carried out in a Heidolph temperature control instrument working in the temperature window of −10°C to 100°C with an accuracy of ±0.1°C.

2.3 METHODS

2.3.1 Studies on Inclusion Phenomenon in Solution Phase

The inclusion phenomenon of drug in CD was studied in the solution phase by Phase solubility studies, UV−Vis, Fluorescence and ^{1}H NMR spectroscopic techniques.

2.3.1.1 Phase Solubility. Phase solubility studies were carried out in aqueous medium at room temperature according to the reported method by Higuchi and Connors (1965). An excess amount of drug (20 mg) was added to 5 ml of aqueous solution containing various concentrations of CD (0−10 mM) in sealed glass containers. The suspensions were shaken on a mechanical shaker for 7 days at room temperature to achieve equilibrium. After equilibrium was achieved, the samples were filtered through 0.22 μm syringe filters (Himedia, India) and properly diluted. The concentration of the drug was determined spectrophotometrically from the absorbance at appropriate λ_{max} of the drug and comparing it with the calibration plot of the drug. The apparent stability constant K_s was calculated from the phase solubility diagram

(plot of solubility of drug against concentration of CD) according to the following equation:

$$K_s = \frac{slope}{S_0(1-slope)} \qquad (1)$$

where S_0 is the solubility of the drug in absence of CD.

2.3.1.2. UV−Vis and Fluorescence Spectroscopy. For the UV-Vis and fluorescence studies appropriate concentration of the drug of interest was chosen. The CD concentration was varied from 0 to 20×10^{-3} M. After preparation, the solutions were left undisturbed for at least 2 h to ensure equilibrium. The absorption and emission spectra were then recorded. For the emission spectra the excitation wavelength was set at the absorption maximum.

The binding constant (K_b) for the drug and the CD complexation was calculated from the absorbance and fluorescence data using the modified Benesi-Hildebrand equation (Velaz *et al.,* 1997; Li and Zhang, 2011):

$$\frac{1}{(A-A_o)} = \frac{1}{([CD]\alpha K_b)} + \frac{1}{\alpha} \qquad (2)$$

$$\frac{1}{(F-F_o)} = \frac{1}{([CD]\alpha K_b)} + \frac{1}{\alpha} \qquad (3)$$

Here A_0 and A represent the absorbance of drug in absence of CD and at each CD concentration respectively, F_0 and F represent the fluorescence intensity of the drug in absence of CD and at each CD concentration respectively and α is a constant. From the double reciprocal plot of [1/ ($A-A_o$)] or [1/ ($F-F_o$)] against 1/ [CD], the ratio of the intercept to the slope was calculated which provided the value of K_b.

2.3.1.3. ^{1}H NMR. ^{1}H NMR experiments of CD, drugs and the inclusion complexes were carried out in D_2O at 298 K. Tetramethylsilane (TMS) was used as an internal reference. All data have been shown by fixing the D_2O peak at 4.69 ppm.

In the present thesis work, drug-CD inclusion complexes have been prepared by using β−CD. Henceforth, CD represents β−CD in all the work chapters.

2.3.2 Preparation of Solid Drug-CD Inclusion Complex (IC)

All the drugs employed in this study are found to form 1:1 solid IC with CD. There are various methods of preparation of inclusion complexes of drug in CD; namely, physical mixing, kneading, co-precipitation, freeze-drying, spray-drying, microwave irradiation *etc.* The ICs employed in this thesis work have mostly been prepared by the co-precipitation and/or the freeze-drying/ lyophilization processes.

2.3.2.1 Physical Mixture

A physical mixture (PM) of drug and CD was obtained in 1:1 molar ratio by homogeneous blending of the components in a mortar for 15 min.

2.3.2.2 Co-precipitation Method

Briefly, calculated amount of CD was dissolved in distilled water at 50°C for 1 h. Desired amount of drug was solubilized in ethanol and slowly added to the CD solution with continuous stirring. The molar ratio of drug to CD was maintained at 1:1. The final solution was left undisturbed at room temperature for 3 days. The precipitated complex (CP) was recovered by filtration and washed with ethanol to remove the uncomplexed drug. The residue was vacuum−dried and utilized for further studies.

2.3.2.3 Freeze−drying/ Lyophilization Method

Desired amount of drug was solubilized in ethanol and slowly added to the CD solution with continuous stirring. After agitation for 24 h, the solution was filtered through 0.22 μm syringe filter. The clear solution was frozen at −20°C for 6 h and then freeze−dried at −55°C for 48 h in a Freeze Dryer. The product was ground and stored in air tight bottles for further uses.

2.4 Characterization of Solid Drug−CD ICs

2.4.1 FTIR Studies. The FTIR spectra were recorded in the scanning range of 4000 to 400 cm^{-1} using KBr as reference at room temperature. The samples were triturated with dry KBr, compressed to pellets and then scanned.

2.4.2 XRD Studies. The XRD profiles were collected on an X-Ray diffractometer using Nickel-filtered Cu K_α radiation and scanned from 5° to 50° at room temperature at a scan rate of 3°/min.

2.4.3 DSC Studies. DSC was performed on 5−10 mg of powdered samples under N_2 atmosphere (purging rate: 40 mL/ min) from 50°−300°C at a heating rate of 10°C/ min.

2.4.4 Optical Microscopic Studies. Microscopic observations of the powdered samples were performed under an optical microscope. The samples were mounted on glass slides and viewed under normal light.

2.4.5 SEM Studies. The surface morphology of the samples was investigated by SEM. The powder samples were gold-coated and directly observed under SEM.

2.5 Hydrogel Preparation

The objective of the present thesis is to design pH-sensitive and thermo-sensitive smart hydrogels to be utilized as controlled delivery vehicles for different drugs. The detailed methodologies involved in the fabrication of the different hydrogel systems are given below.

2.5.1 Synthesis of PVA Hydrogels

10 wt% PVA was dissolved in water by heating at 80°C for 6 h. To the clear PVA solution, desired amount of GA as cross-linking agent and concentrated HCl as catalyst were added and the mixture was stirred at room temperature for an hour. To this mixture, desired amount of drug or preformed drug-CD IC was added and stirred

briefly at 200 rpm. The mixture was then poured onto a clean and dried glass petri dish of known surface area to obtain a film. The quantity of GA was varied so as to get a series of cross-linked hydrogels. GA cross-linked PVA and PVA-CD hydrogels without containing drug or ICs were also synthesized and used for characterization and swelling studies.

2.5.2 Design of pH-sensitive Hydrogels

pH-sensitive hydrogels were prepared by using two pH-responsive polymers: CS (natural) and PAA (synthetic). Individually both CS and PAA lack mechanical strength; therefore IPN hydrogels such as CS−PVA, GG−PAA and PVA−PAA were prepared.

2.5.2.1 Synthesis of CS−PVA IPN Hydrogels

2% (w/v) CS was dissolved in 0.1 M aqueous acetic acid solution under continuous stirring for 48 h. PVA was dissolved in distilled water for 6 h at 80°C to obtain the desired final concentration of PVA. The mixture of CS and PVA solutions was stirred for a brief period of time followed by drop-wise addition of the cross-linking reagent GA (1 wt %) and the solution was stirred for an hour. To this solution, desired amount of free drug or the preformed solid IC was added and stirred for 24 h. Further, the solution was added to known area glass petri dishes and allowed to dry at room temperature *in-vacuo*. GA cross-linked CS−PVA and CS−PVA−CD hydrogels, in absence of drug or IC, were also synthesized and used for characterization and swelling studies.

2.5.2.2 Synthesis of GG−PAA IPN Hydrogels

A weighed amount of GG was allowed to hydrate by overnight stirring in a round-bottomed flask at 40°C. The solution was cooled down to room temperature. An appropriate weight of AAc monomer was added into the GG solution according to the

desired ratio. The solution was purged with nitrogen to eliminate dissolved oxygen. APS as initiator and TEMED as activator (each at 1 wt% with respect to AAc monomer) were added into the reaction mixture under the nitrogen atmosphere. This was then followed by the addition of the cross-linking agent, TEOS (2 wt %) and CD (0.2 g). The reaction vessel was transferred to an oil bath maintained at 60°C and the reaction was carried out for 24 h. Subsequently, the resulting homogenous polymer solution was cooled to room temperature and was evenly cast on petri plates to form films. In a similar fashion, hydrogels without containing CD were also synthesized for comparison. For the drug containing hydrogels, drug (10 mg) was added to the polymer solution at room temperature and magnetically stirred for 30 min to ensure proper mixing and then the films were casted.

2.5.2.3 Synthesis of PVA−PAA Hydrogel Microspheres

Synthesis of PVA-PAA microspheres was carried out according to reported method by Kurkuri and Aminabhavi, (2004). CAN have been used as an initiator for the polymerization of AAc (Mino and Kaizerman, 1958; Jana, Maiti and Biswas, 2000). 10 wt% PVA solution was prepared by dissolving in distilled water at 80°C for 6 h. Requisite amount of AAc monomer (10 wt%) was taken in distilled water and added drop-wise to the PVA solution maintained at 50°C with continuous stirring. Then 0.2 g CAN was dissolved in 10 ml water and added to the above solution and stirred vigorously. The solution was cooled down to room temperature followed by the addition of free drug or the IC and stirred for 30 min to get a homogeneous mixture. The entire solution was emulsified to form water-in-oil (w/o) emulsion in 100 ml of light liquid paraffin oil containing 2% (w/v) Tween- 80, 1 ml of 0.1 M HCl and 1 ml of 0.1 M GA and stirred for 5 h. The microspheres formed were centrifuged and washed repeatedly with hexane and water to remove the excess of reactants. The

microspheres were dried under vacuum and stored in desiccator for further use. Blank microspheres without containing any drug were also synthesized. The schematic illustration for the formation of microspheres by the emulsion cross-linking method is presented in Scheme 2.1.

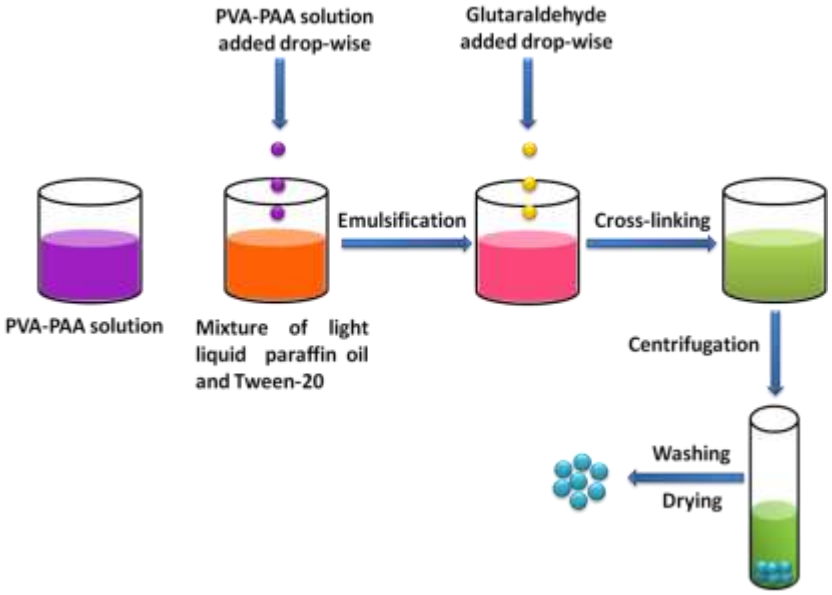

Scheme 2.1. The preparation process of PVA−PAA microspheres by the emulsion cross-linking method.

2.5.3 Design of GG−PNIPAAm Temperature-Sensitive Hydrogels

An appropriate weight of NIPAAm monomer was added into GG solution according to the desired ratios. The solution was purged with nitrogen for 30 min to eliminate oxygen. APS as initiator and TEMED (30 µl) as activator were added into the reaction mixture under the nitrogen atmosphere. This was then followed by the addition of the cross-linking agent, TEOS (2 wt %) and stirred for 24 h. To this solution, desired amount of free drug or the preformed IC was added and stirred to get a homogeneous mixture. Subsequently, the resulting polymer solution was evenly cast on petri plates to form a film. Hydrogels with different feed compositions were synthesized. Blank hydrogels without any free drug or IC were also synthesized for characterization purpose.

2.6 Characterization of Hydrogels

2.6.1 FTIR Studies. The FTIR spectra of the hydrogels were recorded in the scanning range of 4000 to 400 cm^{-1} using KBr as reference at room temperature. The hydrogels were properly ground with KBr so as to form a homogeneous mixture, pressed to form a pellet and then scanned.

2.6.2 XRD Studies. The XRD profiles were collected on a X−Ray diffractometer scanned from 5° to 50° at room temperature at a scan rate of 3°/min.

2.6.3 DSC Studies. Dried hydrogel samples weighing around 5 mg were taken in Al crucibles, sealed with Al-lid and then placed in DSC instrument. All the samples were first heated over the temperature range from 25°C to 200°C (first heating cycle); then cooled to 25°C followed by heating again up to 300°C (second heating cycle), all at a heating rate of 10°C/ min under nitrogen environment (purging rate: 40 ml/ min). The reported results were taken from the second heating runs of the experiments in order to avoid experimental effects arising from the previous thermal history, structural relaxation and incomplete chemical reactions.

2.6.4 SEM Studies. The surface morphology of the samples was investigated by SEM. The hydrogels were either swollen in distilled water or in phosphate buffers of desired pH till equilibrium. They were frozen at −20°C for 6 h and lyophilized at −55°C for 48 h. The lyophilized samples were gold-coated and then observed under SEM directly.

2.7 Drug Loading Efficiency and Drug Content

To study the drug encapsulation efficacy of the hydrogels, dry hydrogel films were put inside vials containing the saturated drug solution in hydroalcoholic medium (1:1), which was subjected to mechanical shaking for 30 min and the films were left in the

drug solution for 24 h at room temperature. The drug concentration was determined spectrophotometrically by comparing with standard calibration curve.

The drug content of the microspheres was performed in accordance with the procedure reported by Angadi *et al.,* (2011). Microspheres of known weight (10 mg) were finely ground using a mortar, extracted with 50 ml of distilled water and sonicated for 30 min (Electrosonic Industries, India). The solution was centrifuged (Remi Research Centrifuge, India) to remove the polymeric debris and the clear supernatant was analyzed spectrophotometrically. The percent drug content was calculated as:

$$\% \text{ drug content} = \frac{\text{weight of drug in microspheres}}{\text{weight of microspheres}} \times 100 \qquad (4)$$

The values reported are the mean of the three independent measurements.

2.8 Equilibrium Swelling Measurement of Hydrogels

The swelling characteristic of all the prepared hydrogels was studied. The dried and pre-weighed samples were immersed in distilled water or buffer solution of appropriate pH (for pH dependence studies) at 37°C till equilibrium swelling was achieved. They were taken out at regular intervals and their weight was measured after gentle wiping with tissue paper to remove excess surface water. The degree of swelling was calculated as:

$$Degree\ of\ Swelling(\%) = \frac{Ws - W_d}{W_d} \times 100 \qquad (5)$$

where W_s and W_d are the weights of the swollen and dried hydrogels, respectively. The pH- dependent and temperature-dependent swelling of the hydrogels was also studied. The pH-responsive swelling behavior of the hydrogels was investigated by immersing them in solutions of different pH (2.0−11.0). Samples were allowed to swell in the buffer solution of desired pH till equilibrium and weighed after gentle wiping with tissue paper. The swollen gel was then slowly dried to constant weight. The swelling percentage was calculated using the above formula (Eq. 5).

The swelling response of the hydrogel microspheres was also investigated as a function of time at pH 1.2 (dilute HCl) and pH 7.4 (phosphate buffer). The microspheres were allowed to swell and weighed at regular intervals of time till a constant weight was achieved. The percentage equilibrium swelling was then calculated.

The temperature-responsive swelling characteristics of the hydrogels were evaluated by immersing in phosphate buffer (pH 7.4) solutions maintained at the desired temperature (15°C – 50°C). At regular time intervals, samples were taken out, gently wiped with filter paper to remove the excess surface water and weighed and their swelling parameters were evaluated.

The data have been expressed as the mean value of three independent experiments and the standard deviations are presented as error bars.

2.9 *In vitro* Drug Release Studies

Calibration plots were constructed spectrophotometrically by monitoring the absorbance of the drug solutions at the respective λ_{max} of the drugs as a function of concentration. *In vitro* release studies of the drug was carried out by placing the drug loaded hydrogels in 50 ml of the releasing medium at 37°C and taking out aliquots of 3 ml at particular time intervals. The withdrawn aliquots were replenished with equal volumes of fresh buffer solution to simulate physiological conditions. For the pH-responsive hydrogels release studies have been carried out at pH 1.2 (dilute HCl) and pH 7.4 (phosphate buffer). In order to imitate the conditions of the human gastrointestinal tract (GIT), the drug loaded hydrogels were immersed in SGF for 2 h and then transferred to SIF and the drug release was monitored. The concentration of the drug released was estimated from the calibration plots. Drug release experiments have also been conducted at 25°C in order to test the thermo-sensitivity of

GG–PNIPAAm hydrogels. The release data shown are expressed as the mean value of three independent experiments and the standard deviations are represented as error bars.

2.10 Drug Release Kinetics

Accurate prediction of the mechanism of drug release from swellable hydrogel matrices is very complicated. Several factors such as hydrogel swelling (water diffusion into the polymer matrix), polymer relaxation, diffusion of drug inside and from the swollen matrix, drug-polymer interaction and its effect on the drug diffusion, changes in the geometry and/or dimensions of the hydrogel, and many more such factors influence the drug release kinetics from a hydrogel matrix. In the present study the drug−CD interaction and its effect on the drug diffusion from the hydrogels containing drug−CD ICs also needs to be considered in order to have a clear understanding of the release mechanism. However to garner an approximate idea about the probable mechanism of the drug release from the hydrogels, the release data were analyzed according to four basic kinetic models. These models are valid for the initial 60% of drug release (Serra *et al.*, 2006). All data were analyzed using OriginPro 7 (OriginLab Corporation).

Model 1 is based on the Higuchi equation that describes the Fickian diffusion of a drug (Higuchi, 1963):

$$M_t/M_\infty = k.\ t^{0.5} \qquad (6)$$

where M_t/M_∞ is the fractional drug release at time t and k is the kinetic constant.

Model 2 is described by the Ritger–Peppas equation (Ritger & Peppas, 1987):

$$M_t/M_\infty = k'.\ t^n \qquad (7)$$

where *k'* is the kinetic constant, *t* is the release time and *n* is the diffusional exponent that explains the drug transport mechanism. Table 2.1 summarizes the different values of *n* for drug delivery systems of different geometries and their significance.

Table 2.1. Diffusion exponent and solute release mechanism.

Diffusion exponent (*n*)			Mechanism
Film	Cylinder	Sphere	
0.50	0.45	0.43	Fickian diffusion
$0.50 < n < 1.00$	$0.45 < n < 0.89$	$0.43 < n < 0.85$	Anomalous transport
1.00	0.89	0.85	Case II transport

For hydrogel films, when $n = 0.5$, the drug release mechanism is Fickian diffusion which occurs due to the molecular diffusion of the drug. When $n = 1$, Case II transport occurs, which is associated with the relaxational release of drug leading to zero-order kinetics. When *n* lies between 0.5 and 1, anomalous transport is observed where both Fickian and relaxational phenomena contribute to the drug release. And $n > 1$ implies super Case II transport mechanism which is due to a large increase in osmotic pressure driving forces, followed by relaxation and swelling of polymers.

Model 3 is based on the Peppas–Sahlin equation, accounting for the coupled effects of Fickian diffusion and Case II transport (Peppas & Sahlin, 1987):

$$M_t/M_\infty = k_1 . t^m + k_2 . t^{2m} \qquad (8)$$

The first term on the right hand side of Eq. 8 represents the contribution of Fickian diffusion and the second term refers to the macromolecular relaxation contribution on the overall release mechanism. k_1 is the diffusion and k_2 is the relaxation rate constant. The coefficient *m* is the Fickian diffusional exponent which also depends on the geometry of the device. The values of *m* for different types of drug delivery devices are known to be 0.5 (film), 0.45 (cylinder) and 0.43 (sphere).

Using the estimated values of k_1 and k_2 obtained from fitting the experimental data to Eq. (8), the ratio of relaxation (R) and Fickian (F) contributions was calculated using Eq. (9) as:

$$R/F = (k_2/k_1)\, t^m \qquad (9)$$

The release time is related to the fraction of drug release; thus *R/F* is represented as a function of fraction of drug released.

Model 4 is the zero−order drug delivery kinetics equation given as:

$$M_t/M_\infty = k''.\, t \qquad (10)$$

Where *k''* represents the zero-order kinetic rate constant.

2.11 Antimicrobial Assay

Antimicrobial activity of the synthesized hydrogels obtained directly after synthesis (without drying) was evaluated against *E. coli* (Gram−negative) and *S. aureus* (Gram−positive) by the disc diffusion method (Vimala *et al.*, 2009). The nutrient agar medium was prepared by using peptone (5.0 g), yeast extract (3.0 g) and NaCl (5.0 g) in 1000 ml distilled water. The pH was adjusted to 7 and agar (15.0 g) was added to this solution. The agar medium was sterilized in a conical flask at a pressure of 15 lbs for 15 min. This nutrient agar medium was transferred into sterilized petri dishes. After the medium was solidified, 9 mm wells were bored using a cork borer. The bacterial culture was swabbed on the solid surface of the medium to obtain a lawn culture. To the inoculated petri dishes, one drop of gel particle solution was added and incubated for 48 h at 37°C in the incubation chamber. After incubation, the zone of inhibition was measured in mm.

2.12 Cytotoxicity Assay

Cytotoxicity of the hydrogels was studied by the direct contact method and the indirect MTT colorimetric assay technique. Cytotoxicity was tested on mouse

fibroblast L−929 cells procured from National Centre for Cell Science, Pune, India. Cultures were maintained at 37°C under 5% CO_2 in RPMI-1640 medium. Prior to the cytotoxicity evaluation, the hydrogel samples were sterilized at 15 lb/ in^2 steam pressure, 121°C for 1 h in an autoclave.

2.12.1 Direct Contact Method

The fibroblast cells, 1 x 10^5 cells/ ml, were seeded in RPMI-1640 medium and directly incubated with the hydrogel samples at 37°C. After 48 h of incubation, the number of cells was counted and their physical appearance was observed.

2.12.2 Indirect Method: MTT Colorimetric Assay

Cell viability was measured by the MTT colorimetric assay. For this test, reference fibroblast cells and cells containing the hydrogel samples dispersed in phosphate buffer were added to RPMI-1640 medium and incubated at 37°C in 5% CO_2 atmosphere for 24 h. The absorbance was monitored at 575 nm. The untreated cells were considered as control (100% viability). The percentage cell viability of the samples was calculated as $[O.D.]_{sample}/ [O.D.]_{control}$ x 100. All experiments have been performed in triplicate.

CHAPTER 3

EXPLORING POLY(VINYL ALCOHOL) HYDROGELS CONTAINING DRUG–CYCLODEXTRIN INCLUSION COMPLEXES AS CONTROLLED DRUG DELIVERY SYSTEMS

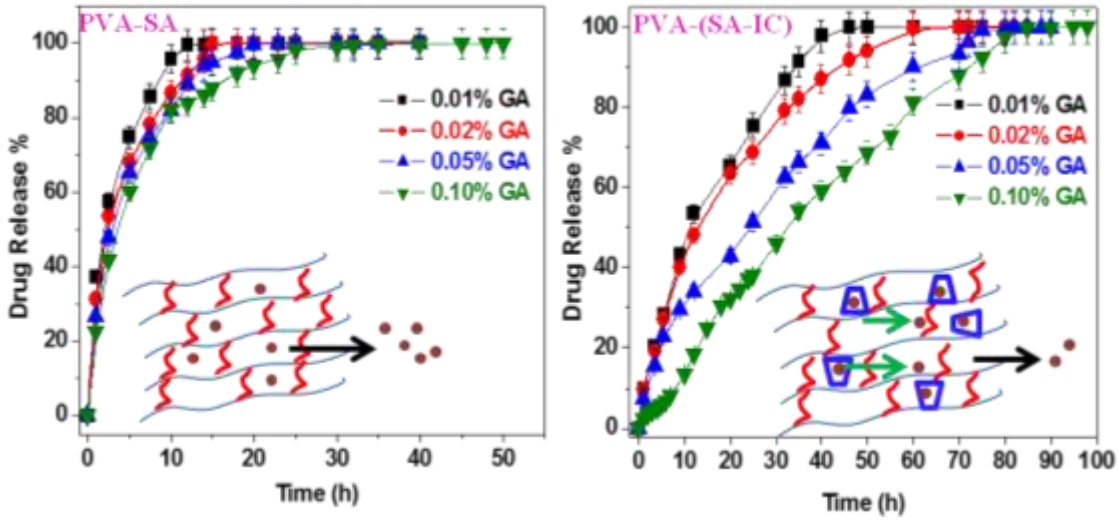

3.1 INTRODUCTION

Poly(vinyl alcohol) (PVA) is a neutral, synthetic and water soluble hydrogel forming polymer produced by the partial or full hydrolysis of poly(vinyl acetate) (Scheme 3.1). The primary raw material used for the synthesis of PVA is vinyl acetate monomer instead of vinyl alcohol because the latter is unstable in nature. The degree of hydrolysis or the content of the acetate groups in the polymer determines the physical characteristics, chemical properties and the mechanical behaviour of the resulting PVA polymer. The resistance of PVA against organic solvents and its high aqueous solubility makes it suitable for various applications (Tubbs, 1966). FDA has approved PVA to be applicable in food packaging industries because of its excellent barrier properties. In pharmaceutical fields, PVA is used as a biomaterial due to its biocompatible, non-toxic, non-carcinogenic and swelling characteristics. Moreover, its low protein adsorption properties results in low cell adhesion which makes it highly attractive for pharmaceutical purposes (Hassan and Peppas, 2000).

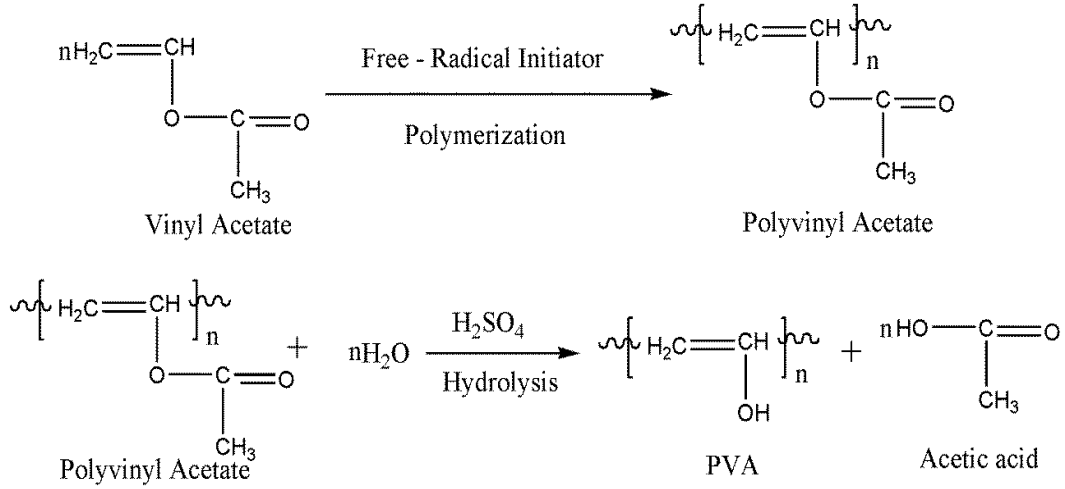

Scheme 3.1. Synthetic scheme of PVA by hydrolysis of poly(vinyl acetate)

The versatility of PVA is paramount in the fabrication of a variety of architectures including films, microgels, microspheres, microbubbles and microcapsules. Owing to their good film forming ability, long-term temperature and pH stability and excellent

biocompatibility, PVA hydrogels are much in demand in the areas pertaining to biomedical research. The pharmaceutical and biomedical utilities of PVA hydrogels has been well documented in the review article by Kobayashi and Hyu (2010). PVA hydrogels and membranes have been developed for numerous biomedical applications such as contact lenses, artificial pancreases, hemodialysis, synthetic vitreous humor and implantable medical materials to replace cartilage and meniscus tissues (Peppas, 1986). PVA shows higher elongation than conventional HEMA hydrogels when employed in contact lens fabrication, thus extending the wearing time without inducing hypoxia to cornea (Peppas, 1986). It has been used to treat vascular embolisms in the particulate form and as hydrophilic coatings to improve neurologic regeneration and tissue adhesion barriers (Baker *et al.*, 2012). On the drug delivery front, PVA has been exploited as a preferred material for the fabrication of ocular inserts and films, nanoparticles, microspheres, floating microspheres, mucoadhesive and targeted drug delivery systems like rectal, colonic, transdermal, buccal, *etc*. The review article by Gajra and co-authors (2010) briefly summarizes the relevance and importance of PVA in DDS.

Despite all the meritorious effects, pure PVA films are known to be very fragile in nature. They possess lower mechanical strength and dissolute totally upon swelling in aqueous medium or any other biological fluids because of their high hydrophilic characteristics. Thus their applicability is greatly hindered. Chemical or physical cross-linking methods are common strategies employed to impart tougher mechanical properties to the conventional PVA hydrogel. In the chemical cross-linking method, certain chemical agents such as GA, EPI, acetaldehyde and other monoaldehydes are usually employed (Xiao and Zhou, 2003). Cross-linking can also be achieved by the use of UV radiation, electron beam and γ-radiation (Hassan and Peppas, 2000). PVA

hydrogels can also be physically cross-linked by the freeze/ thaw process (Hassan and Peppas, 2000). The molecular weight of PVA, its concentration, the time of freezing and thawing and the number of freeze/ thaw cycles affect the properties of the generated PVA hydrogel. These cross-linking techniques generally improve the mechanical strength of the otherwise fragile pure PVA hydrogel.

As drug delivery carriers, the major drawback that is inevitably associated with PVA hydrogel is its inefficacy to control the initial burst release of drugs. For many medications, the burst release has been known to cause patient non-compliances. Further, the burst release is a wasteful process since too high a burst will reduce the efficacy of the delivery device, leading to loss in effectiveness both therapeutically and economically. Moreover, excessive initial release rates can result in drug levels close to or exceeding toxic threshold levels (Huang and Brazel, 2001). For this reason, one of the goals in drug delivery systems is to reduce the initial burst effect and to achieve a constant release rate. In order to substantiate PVA hydrogels as controlled drug delivery devices, "composite" hydrogels have been designed as useful tools. Nugent and Higginbotham (2007) have developed freeze-thawed composite PVA−AAc hydrogel and demonstrated the controlled delivery for theophylline. It was observed that the composite hydrogel released the drug in a sustained manner in comparison to the pure one. Bai and co-workers (2010) have synthesized graphene oxide−PVA composite hydrogel and utilized for controlled drug delivery at physiological pH. The recent review article by Gonzales and Alvarez (2013) summarizes the current developments in composite PVA hydrogels towards applications in biomedicine and drug delivery.

Incorporation of particulate systems (liposomes, micelles, microparticles, *etc.*) into the PVA hydrogel matrix has also been utilized to achieve a sustained drug release

profile. DDS have been constructed from aspirin and DOX dispersed PVA hydrogels loaded with poly(L-glutamic acid)-b-poly(propylene oxide)-b-poly(glutamic acid) (GPG) micelles (Wei *et al.,* 2009). Aspirin had short term release while the release of DOX was sustained. Wei and colleagues (2011) have also utilized GPG micelles for encapsulating paclitaxel and then loaded onto the PVA hydrogel. Controlled release of paclitaxel was observed from the composites. Assimilation of microparticles has also been recognized as another strategy to fabricate PVA hydrogels as controlled delivery vehicles. Uniform PLGA microparticles have been produced by PVA hydrogel template method for delivery of risperidone, methylprednisolone acetate and paclitaxel (Lu *et al.,* 2014). An enhanced drug loading was observed by this method in comparison to the microparticles prepared by the conventional emulsion method. For all the three drugs, release was sustained for weeks. Spiller and co-workers (2012) have encapsulated insulin-like growth factor-1 (IGF-1) in PLGA microparticles embedded in PVA hydrogels. The release of IGF-1 was found to be sustained for over 6 weeks *in vitro*.

Integration of β−cyclodextrin (CD) to PVA hydrogels has also been performed with an aim to improve the drug release characteristics of the hydrogels. CD has been blended with PVA hydrogels and it was found that the presence of CD in the matrix prolonged the release of salicylic acid (Sreenivasan, 1997). Microspheres of PVA−cyclodextrin have been synthesized by Constantin and co-workers (2004) and estimated for the inclusion and separation of drugs. Chemically modified PVA hydrogels containing methacrylated-CD prepared by UV-induced polymerization have been studied for sustained release of the ocular therapeutics, puerarin and acetazolamide (Xu *et al.,* 2010). The amount of drug loaded into the hydrogels increase with the increase in CD content. The incorporation of CD effectively reduced

the initial burst of acetazolamide and the release was sustained for 15 days. Efforts are still being made to incorporate CDs into various polymer matrices in order to explore and improve current drug-release systems.

In the present chapter, GA cross-linked PVA hydrogels containing solid drug-CD ICs have been explored as potential controlled drug delivery systems. Salicylic acid (SA) and Ibuprofen (IBF) (Figure 3.1) are employed as two model drugs. SA and IBF are commonly used anti-inflammatory, antipyretic and analgesic drugs. SA is monohydroxybenzoic acid and is best known for being a key ingredient in topical skin care products for the treatment of acne, psoriasis, corns, calluses, warts, ichthyosis *etc*. IBF (α-methyl-4-[isobutyl] phenylacetic acid), on the other hand, is a non-steroidal anti-inflammatory drug (NSAID) that is available in a variety of preparations. It is commonly used for the treatment of pain and inflammation in rheumatoid arthritis and other musculoskeletal disorders. The formulation for IBF is quite problematic because of its poor solubility in water (Manzoori, and Amjadi, 2003). The strategies that are usually employed to increase drug solubility include salt formation, microenvironment pH control, solubilization with surfactants, complexation with cyclodextrins, solid dispersions, lipid based formulations and nanoparticles formulations (Salustio *et al.,* 2011). Belyakova and co-authors (2006) have studied the inclusion of SA in CD and observed that encapsulation of SA in CD cavity improves its thermal stability. However, an elaborate discussion on the inclusion phenomenon of SA with CD is still lacking. The inclusion of IBF in CD improves the drug loading (Salustio *et al.,* 2009). Hladon *et al.,* (2000) have demonstrated an increase in IBF solubility by complexation with CD.

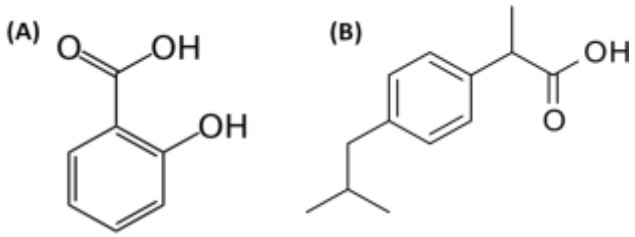

Figure 3.1. Chemical structures of (A) Salicylic acid (SA) and (B) Ibuprofen (IBF).

OBJECTIVES

In this context, achieving controlled drug release from PVA hydrogels containing preformed solid drug-CD ICs becomes an important strategy to explore. Investigation of the effect of nature of the drug, extent of cross-linking, influence of CD complexation on the drug release characteristic from PVA matrices becomes interesting. The inclusion studies of IBF, which is a relatively hydrophobic drug (solubility of IBF at 25°C ≈ 0.552 x 10^{-4} M) (Garzon and Martinez, 2004), in comparison to SA (solubility of SA at 25°C ≈ 2.2 x 10^{-3} M) (Shalmashi and Eliassi, 2008) and their subsequent release from GA cross-linked PVA hydrogels necessitates an elaborate discussion.

The specific objectives of the present work are to:

- prepare solid inclusion complexes (ICs) of SA and IBF with CD and affirm the formation of ICs by various spectroscopic techniques,
- synthesize various compositions of GA cross-linked PVA and PVA−CD hydrogels and their characterization,
- synthesize hydrogels containing free drug and the ICs and explore their release characteristics,
- study the effect of nature of drug and the role of CD on the drug release phenomena,
- address the preliminary kinetics of drug release from the hydrogels,

- assay the cytotoxicity of the synthesized hydrogels for biomedical applications.

The feed compositions and designations of the hydrogels are given in Table 3.1.

Table 3.1. Compositions of synthesized hydrogels

Sample Number	PVA (wt %)	CD (wt %)	GA (v/v)	Sample Designation
1	10	0	0.01%	P1
2	10	0	0.02%	P2
3	10	0	0.05%	P3
4	10	0	0.10%	P4
5	10	1	0.01%	P1-CD
6	10	1	0.02%	P2-CD
7	10	1	0.05%	P3-CD
8	10	1	0.10%	P4-CD

The PVA hydrogels having free drug hydrogels are designated as P1-D, P2-D, P3-D and P4-D and the ones with the drug-CD ICs are labelled as P1-IC, P2-IC, P3-IC and P4-IC. Here 'D' can be either SA or IBF and has been indicated in parentheses whenever needed. The amounts of drug released from the hydrogels were determined spectrophotometrically by observing absorbance at λ_{max} = 296 nm for SA and λ_{max} = 276 nm for IBF.

3.2 RESULTS AND DISCUSSION

3.2.1 Characterization of Solid Drug-CD ICs

Solid inclusion complexes of SA and IBF with CD were prepared by co-precipitation method and characterized by different techniques.

3.2.1.1 FTIR Analysis

The FTIR spectrum of CD (Figure 3.2) shows the characteristic CD peaks which include the broad band with a maximum at 3377 cm^{-1} due to the stretching vibrations of the hydroxyl groups, an absorption band at 2917 cm^{-1} attributed to the C−H stretching, a band at 1647 cm^{-1} assigned to the bending vibrations of O−H bonds in

COH groups and/or in water molecules and a band at 1412 cm^{-1}owing to the bending vibration of C−H bonds in CH_2OH and CHOH groups (Gao and Zhao, 2005).

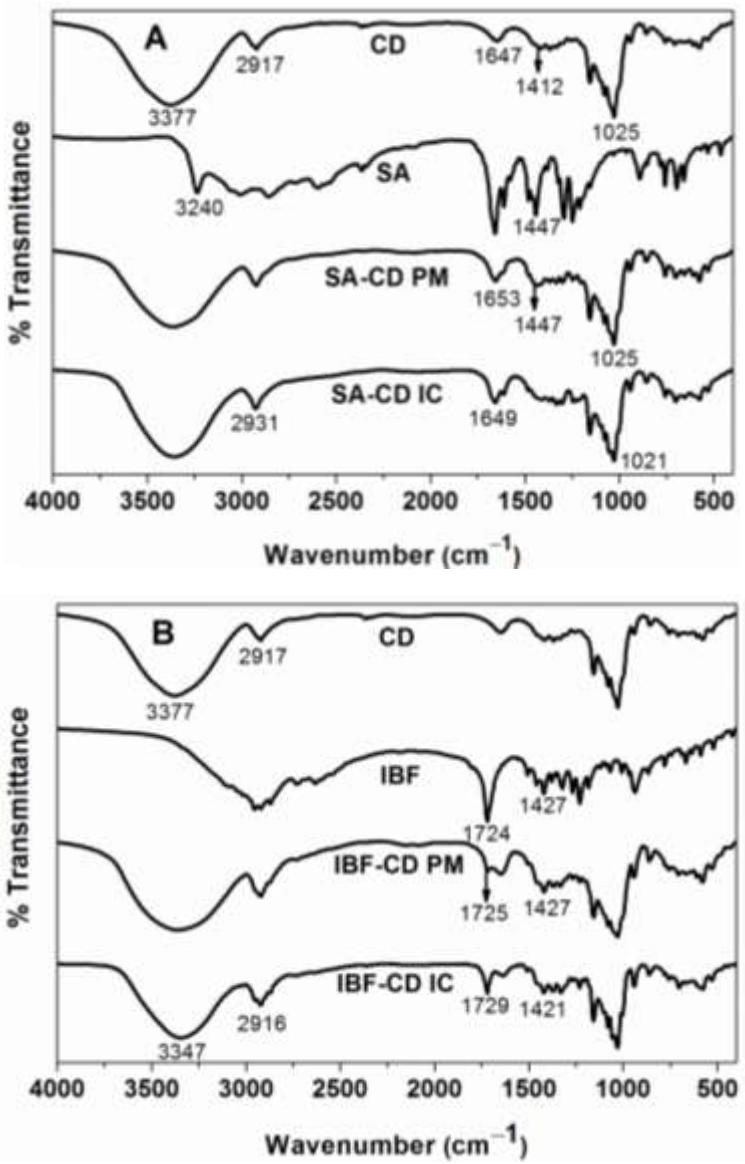

Figure 3.2. FTIR spectra of (A) CD, SA, SA-CD physical mixture, SA-CD inclusion complex and (B) CD, IBF, IBF-CD physical mixture and IBF-CD inclusion complex.

(A) *Salicylic Acid:*

The FTIR spectrum of SA (Figure 3.2 A) presents the bands attributed to the phenyl O−H stretching vibrations at 3240 cm^{-1}, C−H bending vibrations of aromatic protons at 1295 cm^{-1}, stretching of C=O bonds at 1647 cm^{-1} and C=C bonds of benzene rings (1607, 1439, 1495 cm^{-1}). The FTIR spectrum of the SA-CD PM is superposition of

the spectra of CD and SA. However, major shifts occurred in the spectrum of SA-CD IC. The shift in the absorption of the hydroxyl group to 3347 $cm^{-1}$and the carbonyl group to 1666 cm^{-1} was witnessed. These changes suggested the inclusion of the benzene ring of salicylic acid into CD cavity (Belyakova *et al.,* 2007).

(B) *Ibuprofen:*

The FTIR spectrum of IBF (Figure 3.2 B) shows the presence of a band at 1724 cm^{-1} corresponding to the carbonyl stretching. Two bands arising from C=O stretching and O−H bending appear in the spectrum at 1427 and 1231 cm^{-1}. The spectrum of IBF-CD PM shows the presence of the key peaks of both CD and SA. A shift in the characteristic acid carbonyl stretching in the IBF-CD IC to higher frequency (1729 cm^{-1}) was indicates the inclusion of IBF into the CD cavity (Hussain *et al.*, 2007; Mura *et al.,* 1998).

3.2.1.2 XRD Analysis

X−Ray diffraction has been employed as one of the useful tools to judge drug−CD complexation. The diffraction profile of the inclusion complex is generally different from those of the individual components (Zhou *et al.*, 2013). The XRD profile of CD (Figure 3.3) include peaks at 9.1° (101), 12.54° (111), 21.2° (410) which suggests CD adopts a cage type structure (Harata, 1998).

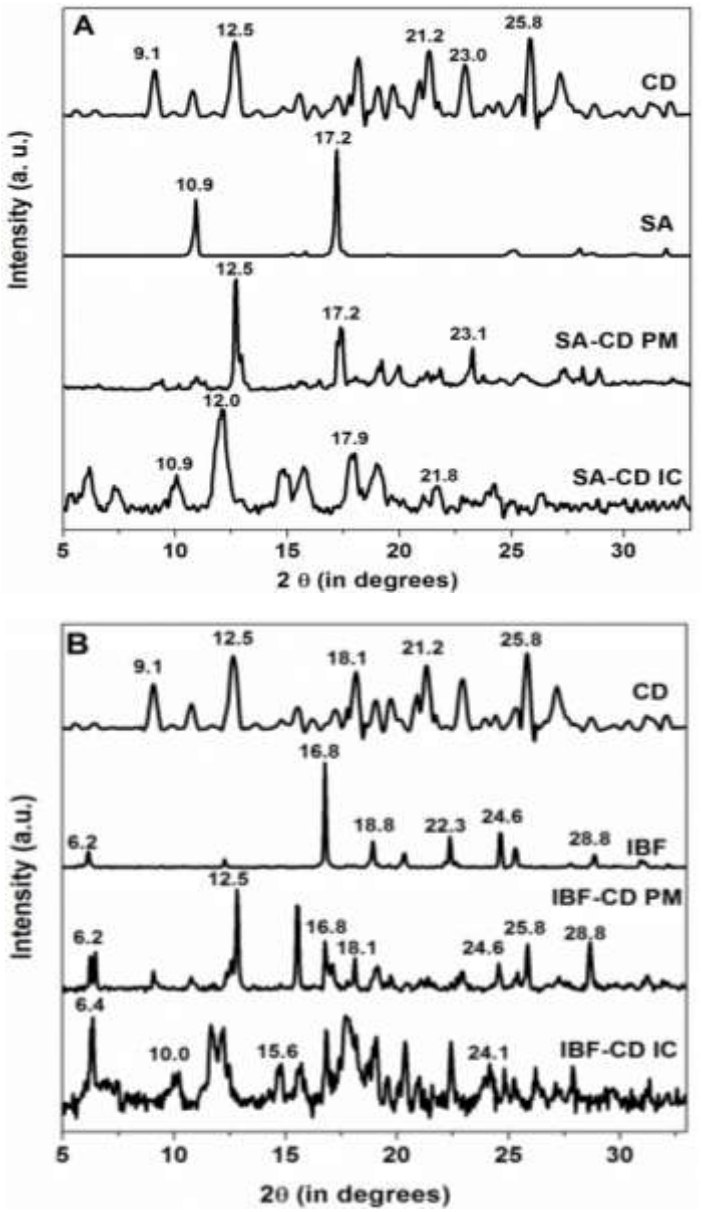

Figure 3.3. XRD profiles of (A) CD, SA, SA-CD physical mixture, SA-CD inclusion complex and (B) CD, IBF, IBF-CD physical mixture and IBF-CD inclusion complex.

(A) *Salicylic Acid:*

The X-ray diffraction profile of SA (Figure 3.3A) comprises of two sharp peaks at 10.9° and 17.2° that indicates its crystalline nature. The physical mixture (SA-CD PM) represents a superposition of the XRD patterns of individual components. However, in the XRD profile of SA-CD IC, the shift in peak positions to 10.1°, 12.2°, 17.9° and 21.9° were observed, which suggests the formation of new phases probably due to the inclusion of SA into CD cavity (Belyakova *et al.,* 2007).

(B) *Ibuprofen:*

The XRD profile of IBF (Figure 3.3B) exhibited numerous distinct peaks at 6.2°, 12.2°, 16.8°, 18.8°, 20.1°, 22.3° and 24. ° that clearly points towards the crystalline nature of the drug. Principal peaks from IBF and CD were present in the IBF-CD PM. The diffraction profile of IBF-CD IC presented a completely different pattern with new peaks at 6.4°, 10.1°, and 17.7° which indicated the formation of new entities of inclusion complex (Salústio *et al.*, 2009).

3.2.1.3 DSC Analysis

DSC has been established as an important criterion for the recognition and characterization of CD inclusion complexes. When guest molecules are embedded in CD cavities; their melting or sublimating points generally shift to different temperatures or disappear completely (Marques *et al.*, 1990). Figure 3.4 A presents the DSC traces of CD, SA, SA-CD PM and SA-CD IC and Figure 3.4 B represents that for CD, IBF, IBF-CD PM and IBF-CD IC.

The thermogram of CD exhibits a broad endotherm around 130°C due to the dehydration process.

(A) *Salicylic Acid:*

The thermogram of SA was typical of a crystalline anhydrous substance with a sharp endotherm at 153°C indicating its melting temperature (Rotich *et al.*, 2003). In the endotherm of SA-CD PM, the dehydration endotherm from CD and the melting endotherm from free SA are both seen. On the contrary, the endotherm of SA-CD IC presents a shift in the CD endotherm and lacks the characteristic SA melting peak. Thus the DSC studies suggest the inclusion of SA in CD cavity.

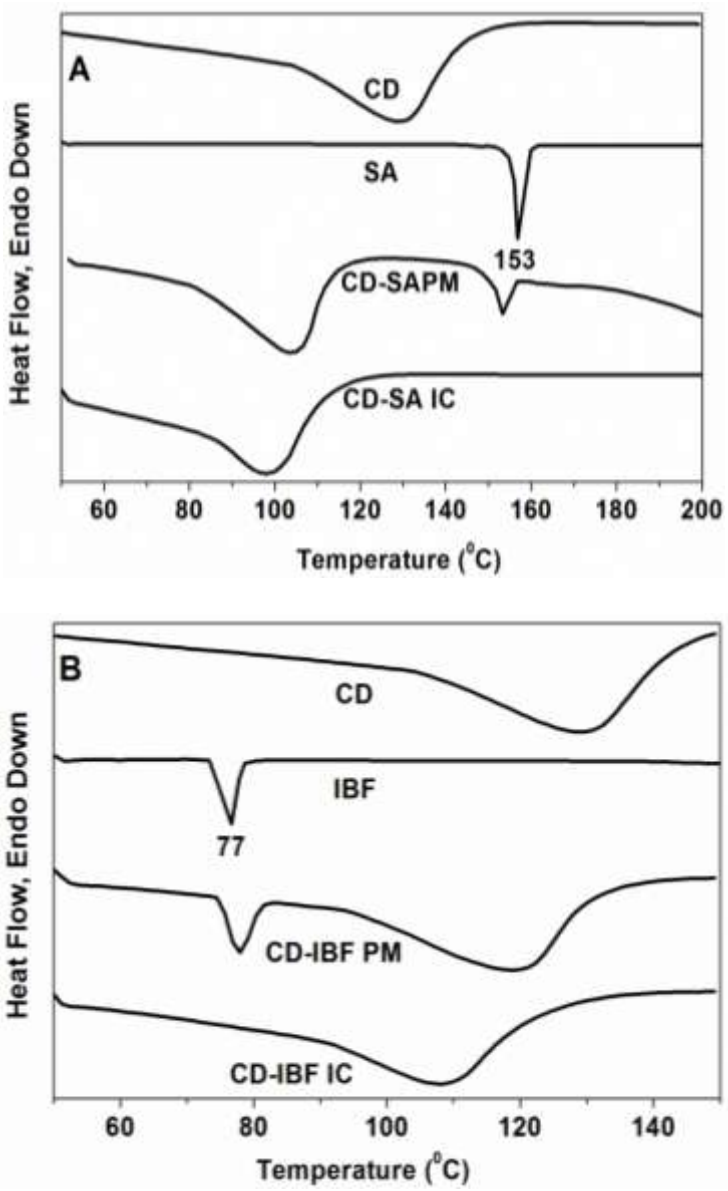

Figure 3.4. DSC thermograms of (A) CD, SA, SA-CD physical mixture, SA-CD inclusion complex and (B) CD, IBF, IBF-CD physical mixture and IBF-CD inclusion complex.

(B) *Ibuprofen:*

The melting of IBF was observed as a sharp endotherm at 77°C. The IBF-CD PM exhibits the endotherms of both CD and free IBF. The absence of free IBF melting endotherm in the IBF-CD IC and the shift of the CD endothermic transition to lower temperature range indicate the formation of the inclusion complex of IBF in CD (Salústio *et al.*, 2009).

3.2.1.4 Optical Microscopic Analysis

The morphology of CD, drugs, the physical mixtures and the ICs was visualized by optical microscopy. The images of CD (Figure 3.5A), SA (Figure 3.5B) and IBF (Figure 3.5E) indicate their crystalline nature. The photographs of the physical mixtures, SA-CD PM (Figure 3.5C) and IBF-CD PM (Figure 3.5F) show the presence of both the drug and CD crystals. However, the images of the ICs (Figures 3.5D & G) clearly demonstrate the formation of new entities possibly due to the inclusion complexation.

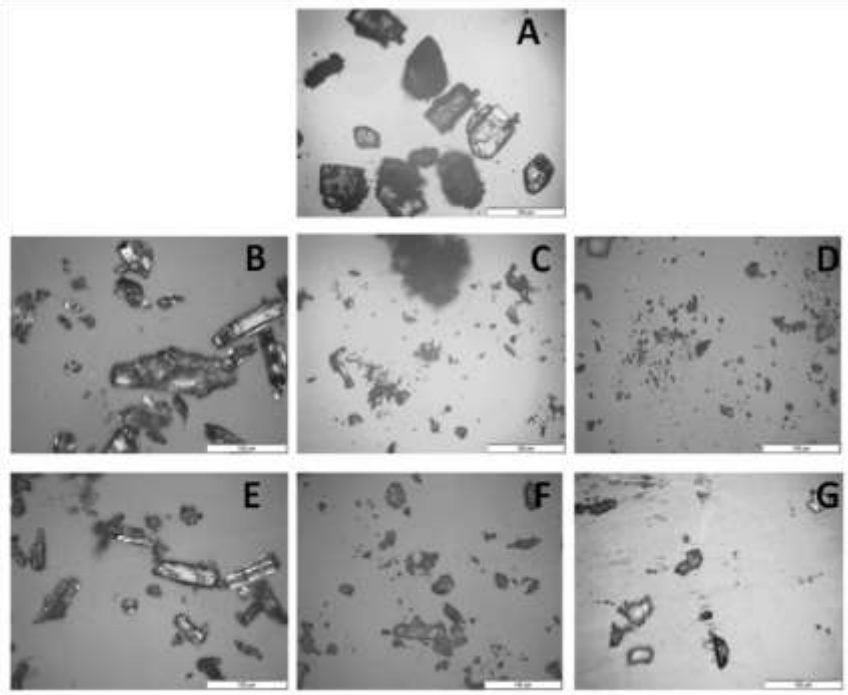

Figure 3.5. Optical microscopic images of (A) CD, (B) SA, (C) SA-CD physical mixture (D) SA-CD inclusion complex; and (E) IBF, (F) IBF-CD physical mixture, (G) IBF-CD inclusion complex.

3.2.1.5 ^{1}H NMR studies

^{1}H NMR spectroscopy is one of the most useful techniques for investigating the CD complexes, particularly in the solution state. NMR spectra obtained from most of the CD complexes represent concentration weighted averages since proton exchange between the free and complexed guest molecule is usually fast in the NMR time scale.

The major advantage consists in the possibility to use several independent signals for the evolution of association constants, so being less prone to misinterpretations caused by minor impurities (Schneider *et al.*, 1998).

Direct evidence for the formation of drug-CD ICs can be obtained from ^{1}H NMR studies. It is well known that CD has the topology of a hollow cone with H−3 and H−5 being the inner protons. The hydrophobic guests get included in the toroidal cavity of CD thereby affecting the inner protons of the macrocycle (Figure 3.6). The change in chemical shifts of H−3 [Δ(δH−3)] and H−5 [Δ(δH−5)] between the protons of CD and IC suggest the inclusion process; when Δ(δH−3) > Δ(δH−5), the inclusion of the guest inside the cavity is partial, while Δ(δH−3) ≤ Δ(δH−5) indicates total inclusion of guest inside CD cavity (Greatbanks and Pickford, 1987).

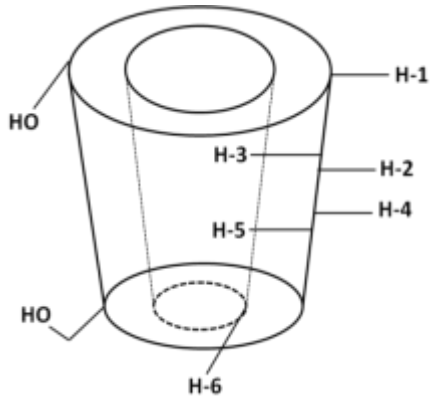

Figure 3.6. Truncated cone shape of CD cavity showing the positions of its protons.

The ^{1}H NMR spectra of CD, SA-CD IC and IBF-CD IC are shown in Figure 3.7 and the chemical shifts (δ) of the CD protons are listed in Table 3.2.

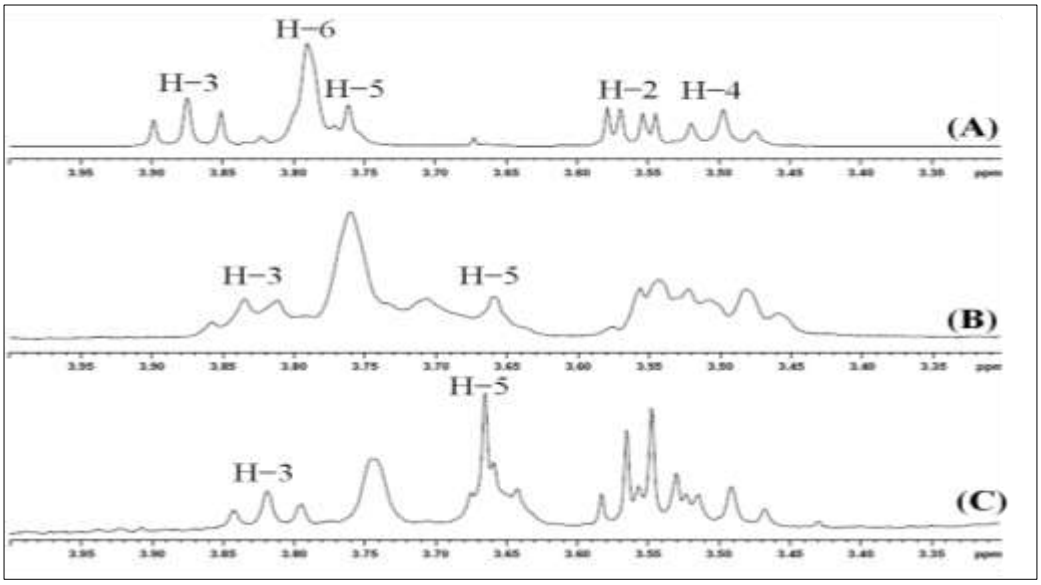

Figure 3.7. ^{1}H NMR spectra of (A) CD, (B) SA-CD inclusion complex and (C) IBF-CD inclusion complex in D_2O at 298K.

Table 3.2. δ and Δδ of protons in CD, SA-CD IC and IBF-CD IC

Protons	δ_{CD}	SA−CD IC		IBF−CD IC	
		δ	Δδ	δ	Δδ
H−1	4.991	5.012	0.021	5.015	0.024
H−2	3.561	3.532	0.029	3.563	0.002
H−3	3.874	3.813	0.061	3.818	0.056
H−4	3.496	3.471	0.025	3.522	0.026
H−5	3.761	3.660	0.101	3.676	0.085
H−6	3.790	3.760	0.030	3.744	0.046

From Table 3.2, it is noteworthy that the H−3 and H−5 protons shifted *ca.* 0.061 ppm and 0.101 ppm in SA-CD IC and 0.056 ppm and 0.085 ppm in IBF-CD IC with respect to the native CD. Considering the changes in the chemical shifts of H−3 and H−5 of CD and the ICs, total inclusion of both SA and IBF in CD cavity are confirmed.

3.2.2 Characterization of Hydrogels

The reaction scheme for cross-linking of PVA by GA in presence of HCl is represented in Scheme 3.2. The cross-linking occurs by the formation of acetal bridges between the pendant hydroxyl groups of PVA chains.

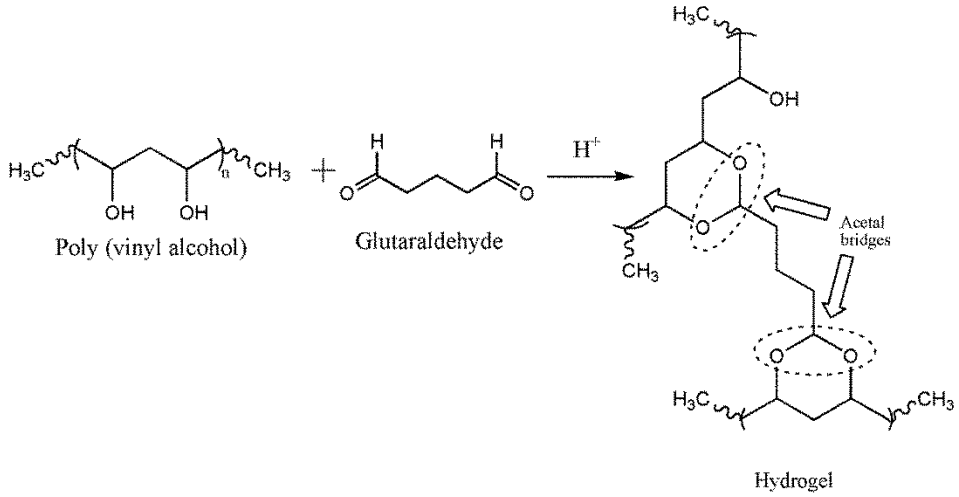

Scheme 3.2. Cross-linking scheme of GA with PVA.

3.2.2.1 FTIR Analysis

Figure 3.8 A presents the FTIR spectra of P1 and P1-CD hydrogels. The FTIR spectrum of P1 hydrogel shows all the characteristic peaks of PVA. A large band at around 3400 cm^{-1} is due to O-H stretching. The C-H stretching from alkyl group regions is observed at around 2935 cm^{-1} and the peak at 1720 cm^{-1} is attributed to the C=O stretching. The peak at 1140 cm^{-1} is attributed to crystalline C=O stretching due to the semi-crystalline nature of PVA. The FTIR spectrum of P1C hydrogel showed the characteristic O-H and C-H peaks. However, the carbonyl stretching has been modified and the crystalline C=O peak is considerably reduced indicating the reduction in the crystallinity of the hydrogel upon incorporation of CD. Figures 3.8 B and C display the FTIR spectra of P1, P2, P3, P4 and P1-CD, P2-CD, P3-CD and P4-CD hydrogels, respectively. It is evident that as cross-linking increases, there is a reduction in the crystalline nature of the hydrogels.

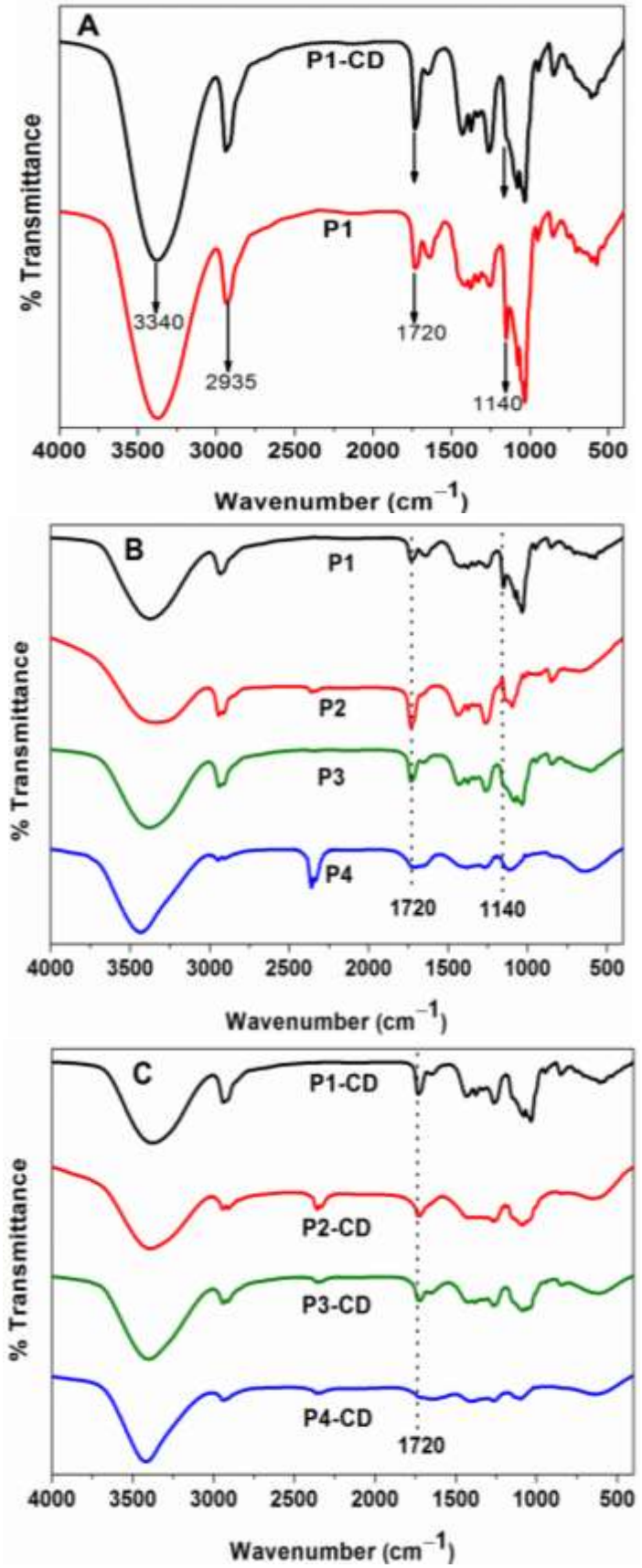

Figure 3.8. FTIR spectra of (A) P1 and P1-CD, (B) P1, P2, P3, P4 and (C) P1-CD, P2-CD, P3-CD, P4-CD hydrogels.

3.2.2.2 XRD Analysis

Figure 3.9 A illustrates the wide-angle X-Ray diffraction traces of P1, P2, P3, P4 and Figure 3.9 B represents that of P1-CD, P2-CD, P3-CD, P4-CD hydrogels.

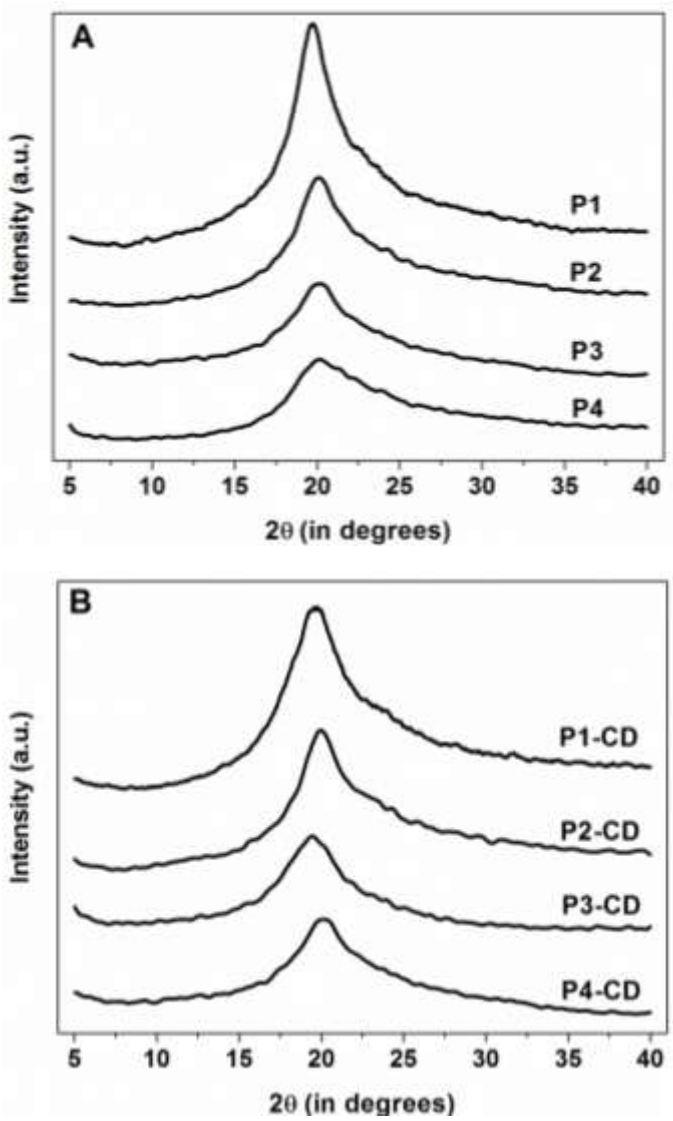

Figure 3.9. XRD profiles of (A) P1, P2, P3, P4 and (B) P1-CD, P2-CD, P3-CD, P4-CD hydrogels.

The PVA hydrogel with the lowest GA content (P1) shows a peak at around diffraction angle (2θ) of 19.8° similar to that of pure PVA, which is associated with the crystalline phase of PVA, PVA being a semi-crystalline polymer. With further increase in GA content, there is remarkable decrease of the crystalline reflection from PVA (Figure 3.9 A). It is well established that GA disrupts the crystalline phase of

PVA (Hari and Sreenivasan, 2001). Similar effect was also observed for CD containing hydrogels (Figure 3.9 B). These samples show a broad diffraction pattern. Hence it can be concluded from the FTIR and XRD data that higher content of GA and CD prevent the self-association of PVA chains rendering somewhat amorphous nature to the otherwise semi-crystalline PVA matrix.

3.2.2.3 DSC Analysis

Figures 3.10 A and B represent the DSC thermograms of P1, P2, P3, P4 and P1-CD, P2-CD, P3-CD, P4-CD hydrogels, respectively.

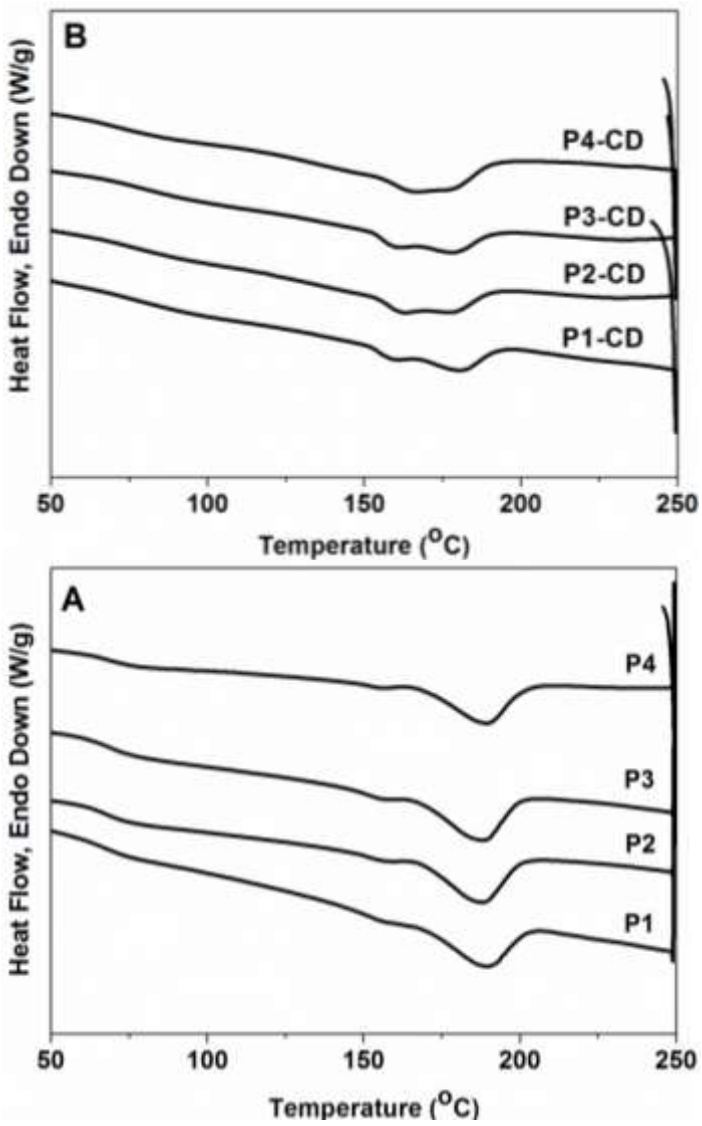

Figure 3.10. DSC thermograms of (A) P1, P2, P3, P4 and (B) P1-CD, P2-CD, P3-CD, P4-CD hydrogels.

In the thermograms, the glass transition temperature (T_g) and melting temperature (T_m) are clearly seen. The glass transition temperature was found to decrease with increase in the GA content ($T_g \approx 68.7\ ^oC$ for P1, $T_g \approx 67.5\ ^oC$ for P2, $T_g \approx 67.2\ ^oC$ for P3 and $T_g \approx 65.8\ ^oC$ for P4), which implies that the increased cross-linking density results in a limited mobility of the polymer chains (Figueiredo *et al.*, 2009). The melting enthalpy decreased with increasing GA content (Table 3.3). This property is related to the membrane crystallinity. The addition of GA to the polymer increases the distance between the chains, which makes the organization of PVA in crystalline lattices difficult resulting in the decrease in the melting enthalpy. This is also clear from the decreased degree of crystallinity with increasing cross-linking.

The degree of crystallinity of the hydrogels has been calculated from the given equation:

$$X = \frac{\Delta H}{\Delta H_c}$$

Where ΔH is the heat of melting of PVA hydrogels and ΔH_c is the heat of melting of 100% crystalline PVA which is 138.60 J/g (Peppas and Merrill, 1976; Hassan and Peppas, 2000).

Table 3.3. Values of T_m, ΔH and X of hydrogels

Sample	T_m (°C)	ΔH (J/g)	X (%)
P1	189.55	26.88	19.4
P2	187.75	24.68	17.8
P3	187.31	24.34	17.6
P4	187.11	24.11	15.6
P1-CD	181.00	25.77	18.6
P2-CD	177.90	24.15	17.4
P3-CD	177.79	22.17	16.0
P4-CD	177.45	19.59	14.3

The P1-CD, P2-CD, P3-CD and P4-CD hydrogels show lower melting temperature as compared to the corresponding hydrogel without CD *i.e.* P1, P2, P3 and P4, respectively (Table 3.3). This can be due to the decreased crystallinity of the PVA matrix in presence of CD as evident from the degree of crystallinity values. For a given amount of GA; the degree of crystallinity of the PVA matrix without CD is relatively higher than that of the corresponding hydrogel with CD. The melting temperature (T_m) of these hydrogels was also found to decrease with increasing GA content, which can be attributed to the restricted mobility of chains due to combined effect of CD and increased matrix density due to cross-linking.

3.2.2.4 SEM Analysis

The SEM images of the lyophilized P1, P2, P3, P4, P1-CD, P2-CD, P3-CD and P4-CD hydrogels were captured under a voltage of 15 kV and 1000X magnification. The SEM images (Figure 3.11) revealed the morphological dependence of the synthesized hydrogels on the extent of cross-linking. As the concentration of GA was increased, a distinct difference in the morphology of the hydrogels was observed. The P1 and P2 hydrogels (Figure 3.11 A and B respectively) exhibited highly porous network structures with a spongy appearance. The morphology of P3 hydrogel (Figure 3.11 C) was more of a fibrillar kind. However, the matrix structure tightened in presence of 0.1% of GA. As evident, the P4 hydrogel (Figure 3.11 D) is relatively denser and compact as compared to others. Similar morphological behaviour was observed for the P1-CD, P2-CD, P3-CD and P4-CD hydrogels. The P1-CD and P2-CD hydrogels (Figure 3.11 E and F respectively) appeared to be porous while the P3-CD hydrogel (Figure 3.11 G) was observed to be somewhat fibrillar. The P4-CD hydrogel (Figure 3.11 H) was found to be compact in nature, similar to that of P4 hydrogel.

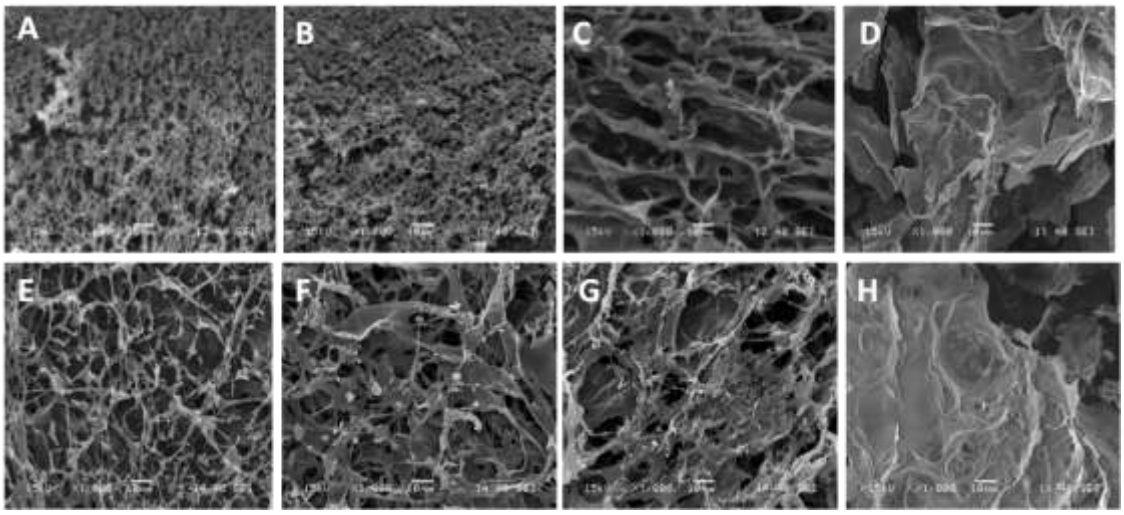

Figure 3.11. SEM images of (A) P1, (B) P2, (C) P3, (D) P4, (E) P1-CD, (F) P2-CD, (G) P3-CD and (H) P4-CD hydrogels.

3.2.3 Equilibrium Swelling Studies

The swelling characteristic of hydrogels has significant influence on the diffusion behaviour of small molecules and is an important parameter in deciphering the nature of hydrogels for drug delivery applications. Figure 3.12 A shows the equilibrium swelling of P1, P2, P3, P4 and Figure 3.12 B shows that of P1-CD, P2-CD, P3-CD and P4-CD hydrogels. With the increasing cross-linker percentage, there is a gradual decrease in the degree of swelling observed for both types of hydrogels. This can be rationalized by considering the morphological dependence of these hydrogels on the cross-linker concentration. As evident from the SEM studies, the hydrogels with lower degree of cross-linking are porous in nature and therefore can accommodate more water in their capillary pores resulting in higher swelling ability. The decrease in swelling with increased cross-linker concentration can be due to the increased matrix density, which restricted the inward flow of solvent molecules.

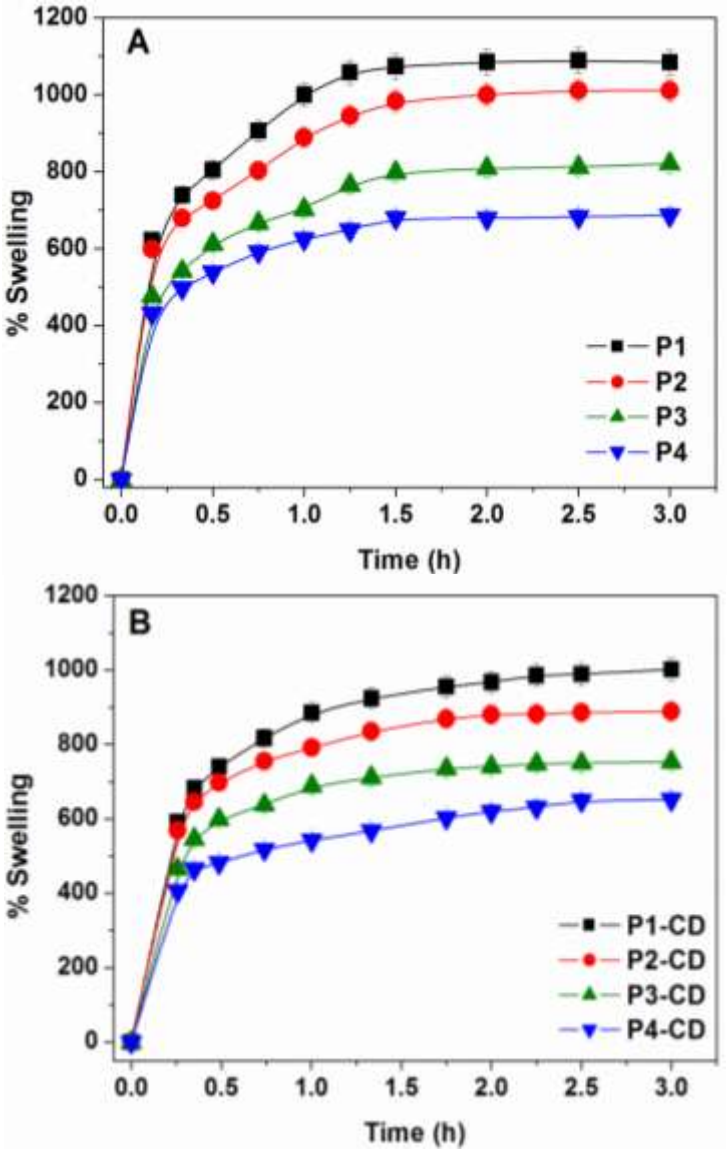

Figure 3.12. Swelling behaviour of hydrogels at pH=7.4 and 37°C, (A) P1, P2, P3, P4 and (B) P1-CD, P2-CD, P3-CD, P4-CD hydrogels.

For a given cross-linker concentration, the swellability of pure PVA hydrogel is slightly higher than that of PVA hydrogels containing CD. This might be due to the formation of somewhat rigid hydrogel matrix upon incorporation of CD because of the hydrogen bonding interaction between the CD and PVA or the CDs getting cross-linked to some extent in the presence of GA.

3.2.4 *In Vitro* Drug Release and Kinetics Studies

3.2.4.1 Drug Release from Hydrogels

Figure 3.13 shows the drug release profiles of SA from P4-D and P4-IC hydrogels. As evident, the release patterns differ significantly from the two hydrogel matrices.

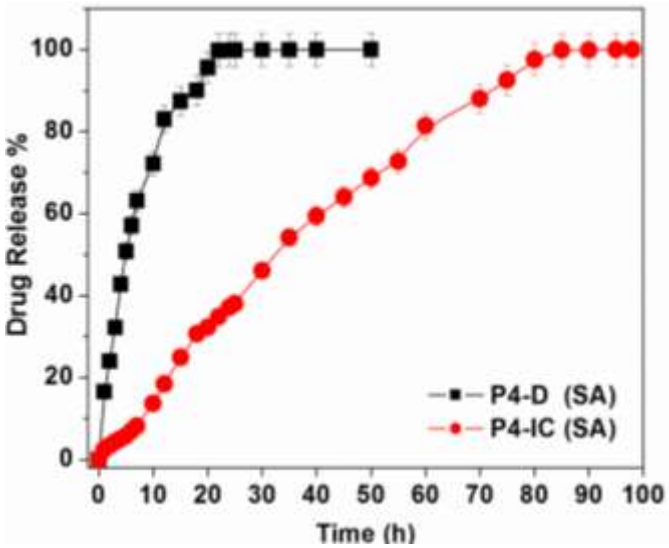

Figure 3.13. Release profiles of SA from P4-D and P4-IC hydrogels in pH 7.4 at 37°C.

P4-D film shows almost a burst type release of drug and total drug release is observed in a short period. The presence of CD significantly prolonged the release of SA showing a sustained release pattern from P4-IC hydrogel. In the P4-D hydrogel, the drug is freely dispersed in the polymer matrix and the drug being a small molecule can easily diffuse to the releasing medium as the hydrogel swells. On the other hand, the P4-IC hydrogel contains the drug in the form of an inclusion complex with CD. For drug release process to be accomplished from P4-IC hydrogel, the bound SA must first be released to the polymer matrix followed by the diffusion of the free drug from the matrix. Thus the difference in release rates observed between the above two hydrogels can be attributed to the diffusion barrier imposed by CD in terms of inclusion process, resulting in a slow release of the drug from the CD containing hydrogel. However, it is known that even with simple blending of CD with PVA, it is

possible to achieve prolonged release of drug (Sreenivasan, 1997). In order to verify whether the inclusion property of CD is solely responsible for the slow release of drug from the hydrogels, drug release studies were carried out from PVA hydrogels keeping the CD and dug content same but varying the cross-linker concentration *i.e.* P1-IC, P2-IC, P3-IC and P4-IC hydrogels. The release studies from PVA hydrogels in absence of CD at varying cross-linker concentration (P1-D, P2-D, P3-D and P4-D hydrogels) were also carried out for comparison (Figure 3.14).

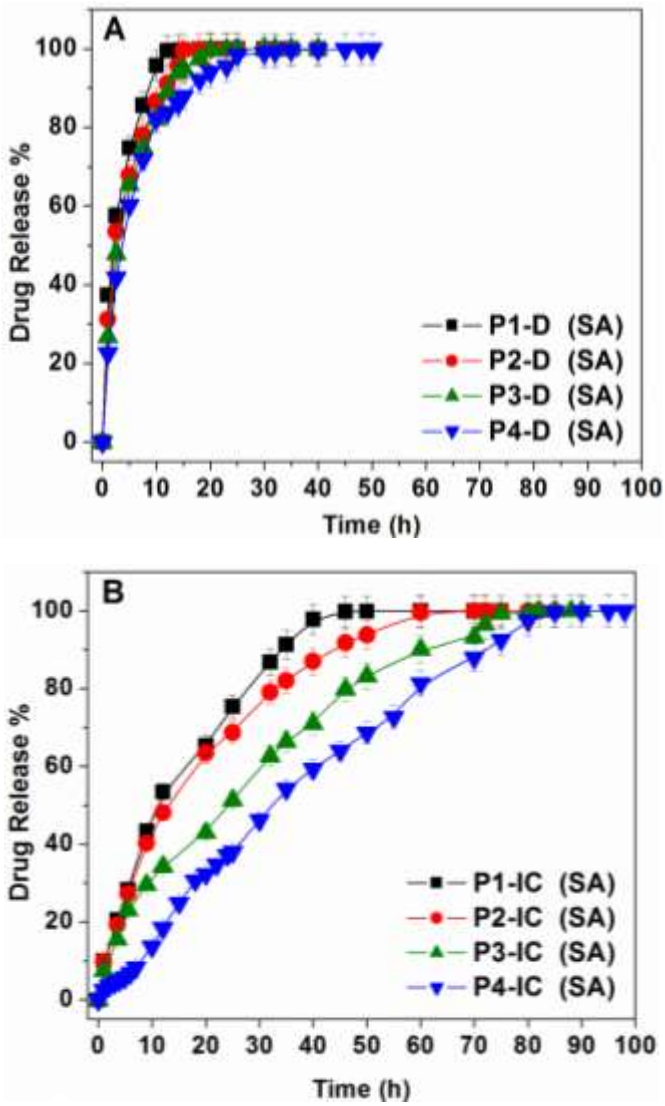

Figure 3.14. SA release profiles from (A) P1-D, P2-D, P3-D, P4-D and (C) P1-IC, P2-IC, P3-IC, P4-IC hydrogels.

Figure 3.14 A depicts the SA release profiles from the P1-D, P2-D, P3-D and P4-D hydrogels and Figure 3.14 B from that of PVA hydrogels containing SA-CD IC (P1-IC, P2-IC, P3-IC and P4-IC hydrogels). As evident from the figures, there is a striking difference in the release patterns as the GA concentration is varied. The drug release profiles from the hydrogels containing SA-CD IC show a strong dependence on the degree of cross-linking. With increasing GA concentration the drug release is found to be considerably slower. On the other hand, for the hydrogels containing free drug, the effect of GA concentration on the release rate is almost insignificant and there is only a nominal decrease in the release rate with the increased GA concentration. Release of drug from any hydrogel is governed by various factors such as hydrogel swelling, diffusion of drug from the swollen matrix and polymer relaxation. Therefore any change in the hydrogel that affects the above factors can influence the drug release process. If hydrogel swelling and drug diffusion from the swollen matrix are the governing factors, then both types of hydrogels are expected to show similar release patterns with respect to varying cross-linker concentration since they exhibit similar swelling behaviour with increasing GA percentage. Thus the observed difference in the release patterns from these hydrogels with change in GA concentration can be rationalized only when the presence of CD is somehow influencing the polymer relaxation which in turn affects the drug release rate. Apart from cross-linking PVA, GA probably interacts with the hydroxyl groups of CDs and further cross-links the matrix. Thus, with increasing GA concentration more and more CDs get cross-linked, as a result the polymer matrix is modified and the drug release rate is reduced. Among all the hydrogels studied, P4-IC was found to show the slowest release of SA and hence can be utilized as a controlled delivery system.

In order to study the effect of the nature of drug on the release process, the release of IBF, a relatively hydrophobic drug (Garzon and Martinez, 2004) in comparison to SA (Shalmashi and Eliassi, 2008) was monitored from P4-D and P4-IC hydrogels.

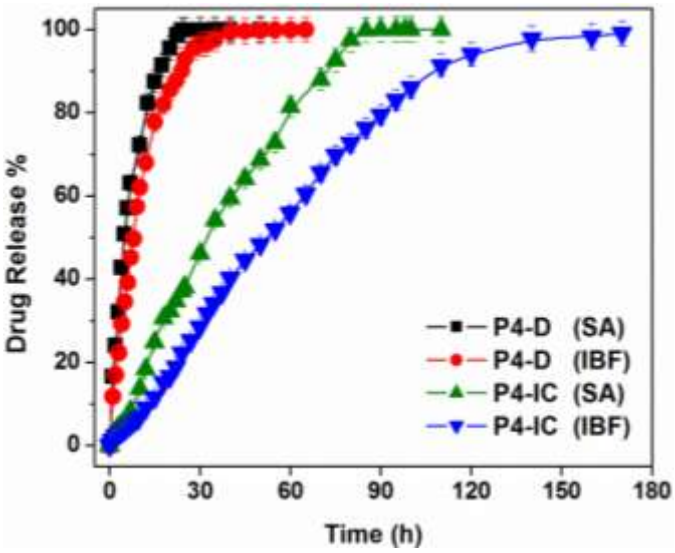

Figure 3.15. Comparison of release profiles of SA and IBF from P4-D and P4-IC hydrogels.

Figure 3.15 shows the release profiles of IBF from P4-D and P4-IC hydrogels; the release profiles of SA from the same hydrogels are also included for comparison. As expected, a sustained release for IBF was obtained from the P4-IC hydrogel as opposed to burst release from the P4-D hydrogel similar to that of SA. When SA and IBF releases are compared from P4-D hydrogel, there is not much of difference but from the P4-IC hydrogel the release of IBF is further prolonged than that of SA. The difference in the rates of release of IBF and SA can be explained by taking into account the binding efficiencies of the two drugs with CD. The association constant for IBF with CD ($K_{IBF\text{-}CD} \approx 10^3$ M^{-1}) is almost an order higher than that for SA ($K_{SA\text{-}CD}$ = 119 ± 6 M^{-1}) (Belyakova and Lyashenko, 2008; Hergert and Escandar, 2003; Manzoori and Amjadi, 2003). Stronger the binding efficiency between the CD and the drug, slower is the diffusion of drug from the CD resulting in the slower release of drug from the hydrogel matrix. Thus the nature of drug in terms of its binding

efficiency with CD plays an important role in the drug release process from these hydrogels.

3.2.4.2 Drug Release Kinetics

The fundamental kinetic analyses of the drug release data can reveal the probable mechanism of release from the hydrogels. The release data showed the best fit to Ritger-Peppas and Peppas-Sahlin models in all cases (Table 3.4). The values of the diffusional exponent (*n*) lie between 0.5 and 1 for all the hydrogels except for P4-IC. The value of *n* between 0.5 and 1 indicates the anomalous nature of drug release from these hydrogels, where both diffusion and relaxation processes contribute. From the Peppas-Sahlin equation, it was discovered that the diffusion kinetic constant (k_1) dominates over the relaxation kinetic constant (k_2) for P1-D, P2-D, P3-D and P4-D hydrogels.

It is not possible to know exactly the contribution of the Fickian and Case II mechanism from the estimated values of k_1 and k_2 alone (Peppas and Sahlin, 1989), hence the ratio of the relaxational over Fickian contributions (R/F) was calculated for the hydrogels and plotted against the fraction of the drug released from these hydrogels (Figure 3.16).

Table 3.4. SA and IBF release parameters fitting to various mathematical models

Sample	**Higuchi**		**Ritger–Peppas**			**Peppas-Sahlin**			**Zero-Order**	
	k ($h^{-0.5}$)	R^2	n	k' (h^{-n})	R^2	k_1 ($h^{-0.5}$)	k_2 (h^{-1})	R^2	k'' (h^{-1})	R^2
P1-D (SA)	0.358	0.951	0.55	0.347	0.986	0.337	0.014	0.982	0.238	0.631
P2-D (SA)	0.324	0.947	0.62	0.298	0.984	0.242	0.057	0.980	0.217	0.796
P3-D (SA)	0.286	0.957	0.65	0.25	0.992	0.194	0.056	0.988	0.170	0.855
P4-D (SA)	0.218	0.915	0.74	0.149	0.995	0.103	0.052	0.995	0.098	0.933
P1-IC (SA)	0.141	0.953	0.63	0.103	0.982	0.102	0.011	0.978	0.038	0.815
P2-IC (SA)	0.133	0.959	0.64	0.093	0.994	0.091	0.012	0.992	0.036	0.848
P3-IC (SA)	0.102	0.977	0.69	0.077	0.992	0.079	0.005	0.992	0.021	0.815
P4-IC (SA)	0.073	0.818	1.00	0.015	0.994	-0.002	0.015	0.994	0.015	0.994
P4-D (IBF)	0.169	0.891	0.81	0.094	0.995	0.058	0.042	0.997	0.064	0.968
P4-IC (IBF)	0.056	0.796	1.00	0.007	0.994	-0.006	0.01	0.995	0.009	0.992

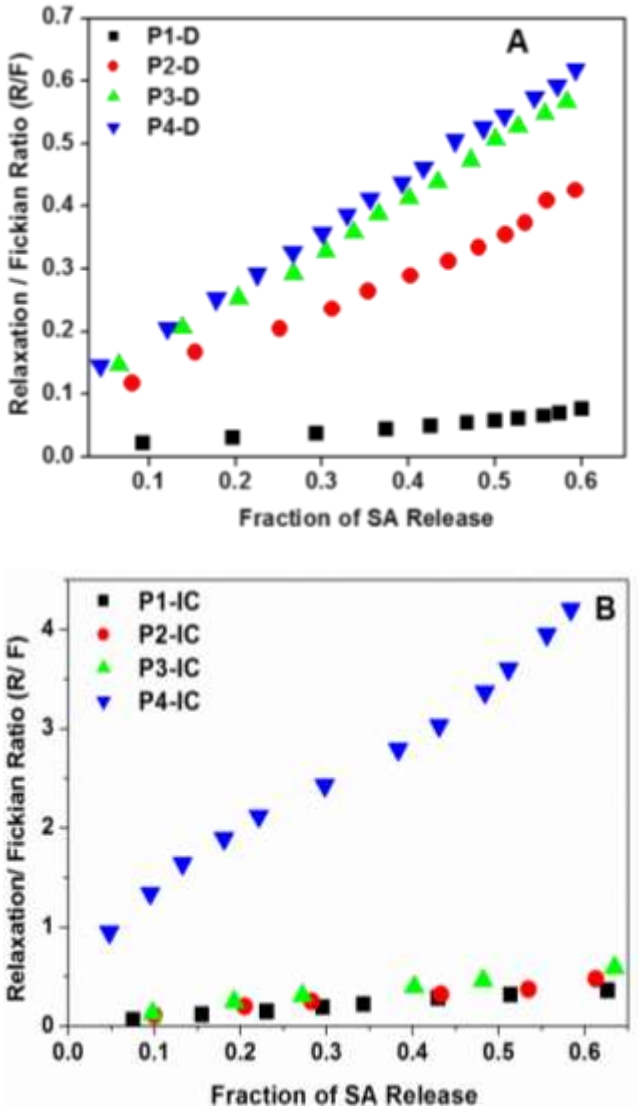

Figure 3.16. Plot of ratio of relaxation to the Fickian contribution (R/F) with the fraction of SA release for (A) P1-D, P2-D, P3-D P4-D and (B) P1-IC, P2-IC, P3-IC, P4-IC hydrogels.

The values of R/F for the P1-IC, P2-IC, P3-IC, P4-IC hydrogels were found to be higher than the corresponding P1-D, P2-D, P3-D, P4-D hydrogels. The fractional values of R/F clearly indicate the predominance of the diffusion process over the relaxation process and with the increased GA content, the R/F value also increases. The high value is suggestive of the greater polymer relaxation of the P4-IC hydrogel than others. For a given GA percentage the value of *n* is slightly higher for the hydrogels containing drug-CD IC as compared to those containing free drug. For P1-

IC, P2-IC and P3-IC hydrogels the diffusion kinetic constant (k_1) dominates over the relaxation kinetic constant (k_2) very similar to that observed for P1-D, P2-D, P3-D and P4-D hydrogels. And with the increased GA concentration the R/F value was found to increase. The P4-IC hydrogel, however, showed Case II transport mechanism (n =1) associated with the dominant relaxational release of drug which is evident from the lower magnitude and negative values of diffusion rate constant k_1 for both SA and IBF release. This is further supported by the fact that the release data from this film fit quite well to the zero-order kinetics. Thus the presence of CD at high cross-linker concentration influences the relaxation rate of the polymer chains, and further slows the release of the drug from the hydrogel matrix. This can be explained by taking into account that GA not only cross-links the PVA chains but also interacts with the hydroxyl groups of CDs thereby influencing the matrix structure (Bibby *et al.,* 2000). Thus from the above studies it is clear that the role of CD in the drug release process is not only because of its inclusion ability but also its effect on the polymer relaxation. In other words, it is the combined effect of drug diffusion and polymer relaxation that controls the overall drug release process from the hydrogels containing IC.

3.2.5 Cytotoxicity Assay

While designing a material for drug delivery purposes, it is of utmost importance to characterize it in terms of cytotoxicity. *In vitro* cell culture studies are quite useful in assessing cytotoxicity. The effects of cells exposure to chemical agents at different concentrations and times can be determined by assessing cytotoxicity. In the biocompatibility evaluation of any biomaterial, *in vitro* tests should be conducted prior to *in vivo* tests in order to reduce animal suffering. Though the *in vitro* cytotoxicity assays reveal only the effects on cells during the initial 12−48 h after exposure to the

test substances, these assays provide a general idea about the biocompatibility and toxicity of the synthesized biomaterial.

In order to test the biocompatibility of the prepared hydrogels, cytotoxicity assay was performed on P4-CD hydrogel. As shown in Figure 3.17, direct contact between L-929 cells and P4-CD hydrogel sample did not reveal any adverse effect. No cell death or effect on cell morphology was observed under the microscope. This suggested a high compatibility of the hydrogels with the living tissues thereby validating them as potential drug delivery systems.

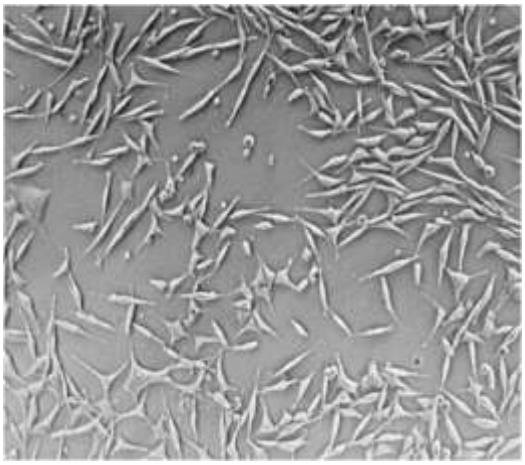

Figure 3.17. Optical Micrographs of L-929 cells cultured after 48 h incubation with P4-CD hydrogel.

3.3 CONCLUSIONS

- PVA and PVA−CD hydrogels were synthesized with varying amounts of the cross-linker GA. Hydrogels were characterized by FTIR, XRD, DSC and SEM.
- The solid ICs of SA and IBF in CD were prepared *via* co-precipitation method and affirmed from FTIR, XRD, DSC, Optical microscopy and ^{1}H NMR studies.

- The swelling evaluation indicated the decreased swelling with the increasing cross-linker content for both PVA and PVA-CD hydrogels. For a given GA concentration, the swellability of PVA hydrogel is slightly higher than that of PVA-CD hydrogels.
- The presence of IC in the hydrogel resulted in the sustained release of drug for a prolonged period of time. With increase in GA content, the rate of drug release was found to reduce. The influence of cross-linking was more pronounced in the hydrogels containing the ICs of the drug.
- The rates of release of SA and IBF also varied greatly from the P4-IC hydrogel because of the difference in their binding efficiencies with CD. Higher is the binding of the drug with CD, slower is the release.
- The preliminary kinetic analysis revealed the anomalous nature of drug release from the P1-D, P2-D, P3-D, P4-D, P1-IC, P2-IC and P3-IC hydrogels indicating the importance of drug diffusion over polymer relaxation. The P4-IC hydrogel, however, showed Case II transport mechanism indicating the dominant relaxational process.
- GA, apart from cross-linking PVA, probably interacts with the hydroxyl groups of CDs thereby influencing the matrix structure.
- The drug release is accomplished as a combination of the effects of drug diffusion, the hydrogel polymer relaxation, and the binding affinity of the drugs with CD.
- The cytotoxicity tests performed on the hydrogels ensured the hydrogels as biocompatible hence can be utilised as controlled drug delivery systems.
- Hence the strategy of incorporating pre-formed ICs into PVA hydrogels to achieve controlled delivery of drugs works quite well.

CHAPTER 4

pH−RESPONSIVE SMART HYDROGELS FOR CONTROLLED DELIVERY OF DRUGS TO THE INTESTINE

4.1 INTRODUCTION

Oral route of drug administration accounts for about 80% of the available drugs worldwide. It is the most preferred form of drug formulation, because of the ease of administration. However, the conventional oral formulations lack the feature of controlled drug delivery and site-specificity. Thus, the oral drug delivery systems targeting the lower part of the GIT, including the intestine and colon, has attracted much interest for the local treatment of a variety of colonic diseases and the delivery of an array of therapeutic agents (Jose *et al.*, 2009). The intestine as well as colon, are susceptible to various disorders such as Crohn's disease, irritable bowel syndrome (IBD), ulcerative colitis, colon cancer, polyps *etc.* that require localized drug therapy (Chourasia and Jain, 2003). Thus, proper site-specific delivery of drugs is beneficial in the effective treatment of such diseases. Additionally, the lower gut offers various therapeutic advantages as a site of drug delivery due to its near neutral pH and longer transit time as compared to stomach, where a harsh environment is experienced due to the low pH. Colon is often regarded as an ideal site for both systemic and local delivery of drugs. It is also favourable for systemic absorption of proteins and peptides because the proteolytic activity of the colonic mucosa is much less than that observed in the small intestine.

For targeted delivery of drugs to the intestine or colon, the dosage must be formulated by taking into account the hindrances offered by the upper GIT. The successful delivery of a therapeutic to the lower part of the GIT lies not only in the protection of the drug from its premature degradation in the extreme conditions of the stomach but also ensuring its release in the proximal colon (Vats and Pathak, 2013). Various drug delivery systems are in the pipeline to deliver a drug quantitatively to the intestine and then trigger the release in therapeutic doses. The delivery systems targeting to the

intestine and colon mainly include (i) time-dependent delivery systems based on gastric emptying time and small intestine transit time, (ii) microbial-triggered delivery systems which make use of the fact that the degradability of the delivery device occurs by the microflora present in the colon and (iii) pH-sensitive delivery systems based on the changes in the pH of the GIT (Yin *et al.,* 2001).

Stimuli-sensitive polymers have become quite an important class of polymers and have received much attention in the areas of pharmaceutics and related research fields. Also termed as "smart" or "intelligent" or "environment-sensitive", these polymers exhibit dramatic conformational changes in response to small changes in the external factors such as pH, temperature, light, electric field, ionic strength, *etc*. In particular, such polymers have found great utility in the fields of controlled and self-regulated drug delivery. Thus stimuli-responsive polymers can be designed to produce specific and desired response according to the variations in the physiological environment of human body. Proton concentration (pH) is an imperative stimulus and has intrinsic variations depending on the differences in the pH of the human body. pH-responsive drug delivery systems are endowed with the unique ability to sense macro- or micro-environments in organs, tissues, cells and subcellular compartments *viz.* blood (pH 7.35 ~ 7.45), stomach (pH 1.0 ~ 3.0), duodenum (pH 4.8 ~ 8.2), colon (pH 7.0 ~ 7.5), early endosomal (pH 6.0 ~ 6.5), late endosomal (pH 5.0 ~ 6.0), lysosome (pH 4.0 ~ 4.5), golgi (pH 6.4), extratumoral (pH 7. 2 ~ 6.5), *etc*. (Huh *et al.,* 2012). Drug delivery studies with particular interests in the human GIT have been most pronounced due to pH fluctuations (pH 1 ~ 8) and have led to the development of an assortment of controlled delivery formulations. Prodrugs, liposomes, micelles, microchips *etc.* have been designed to respond to different pH environments and facilitate controlled delivery of therapeutics. Although new technologies have

evolved, pH-sensitive polymers still remain the most popular entities for drug delivery development. Due to their flexibility in terms of design, synthesis and cost effectiveness, these polymers are accountable for most of the drug delivery formulations. pH-responsive polymers can be sculpted into various architectures including tablets, capsules, microbeads, microspheres, nanoparticles, micelles, nanobeads, liposomes and hydrogels *etc*. The review article by Yoshida and co-authors (2013) discusses about pH-responsive polymers and their specific properties that can be exploited for targeted delivery of drugs.

In this context, pH-responsive smart hydrogel is both an outstanding innovation and contribution to pharmaceutical arenas in general, and drug delivery in particular. Over the past few decades, a great many research has been dedicated for the development of pH-sensitive hydrogels (Gupta *et al.*, 2002; Gil and Hudson, 2004; Puoci and Curcio, 2013). Many natural and synthetic polymers have been utilized in the fabrication of pH-sensitive hydrogels as controlled drug delivery systems. The pH-responsive polymers are either equipped with a pendent acidic group (carboxylic/ sulfonic acids) or basic group (*e.g.* ammonium salts) that accept or release protons in response to changes in the environmental pH. These pendant acidic or basic groups undergo ionization which ultimately affects the swellability of the hydrogel. Thus the pH-responsiveness can be tailored by using different polymers as per requisites.

Numerous pH-sensitive polymeric hydrogels containing linear polymers, grafted polymers, IPNs, semi-IPNs, *etc.* have been developed and investigated for pharmaceutical purposes. Some of the commonly used pH-responsive polymers employed in the design of pharmaceutical formulations are listed in Table 4.1.

Table 4.1. Commonly employed pH-sensitive polymers

Charge Type	Polymer Name
Anionic	**Natural:** Hyaluronic acid, Alginic acid, CMC, poly(aspartic acid), carboxymethyl dextran *etc.*
	Synthetic: poly(acrylic acid), PHEMA, polystyrene sulfonate, sulfoxyethyl methacrylate, *etc.*
Cationic	**Natural:** Chitosan, Polylysine, Polyhistidine *etc.*
	Synthetic: poly(*N, N′*− diethylaminoethyl methacrylate), PAAm, diallyldimethyl ammonium chloride, poly (*N, N′*− dimethylaminoethyl methacrylate) *etc.*

Among all the polymers listed above, the natural polymer chitosan has been extensively employed in the design of pH-sensitive hydrogels while poly(acrylic acid) finds greater demand as a pH-responsive synthetic polymer.

4.1.1 CHITOSAN

Chitosan (CS) is a well-known pH-responsive natural polymer. CS [α (1→4) 2−amino−2−deoxy−β−D−glucan] is a cationic polymer obtained by the alkaline N−deacteylation of the naturally occurring polymer, chitin. Chitin, the supporting material of crustaceans, insects and fungal mycelia is comprised of 2−acetamido−2-deoxy−β−D−glucose through a β (1→4) linkage. Chitin is a highly insoluble, hard and inelastic nitrogeneous polysaccharide resembling cellulose in its solubility and chemical reactivity. Chitin may be regarded as cellulose with the hydroxyl position at C−2 replaced by an acetamido group. Both chitin and CS are of commercial significance due to their high percentage of nitrogen as compared to synthetically substituted cellulose (Muzzarelli, 1973). The chemical structures of cellulose, chitin and CS are shown in Figure 4.1.

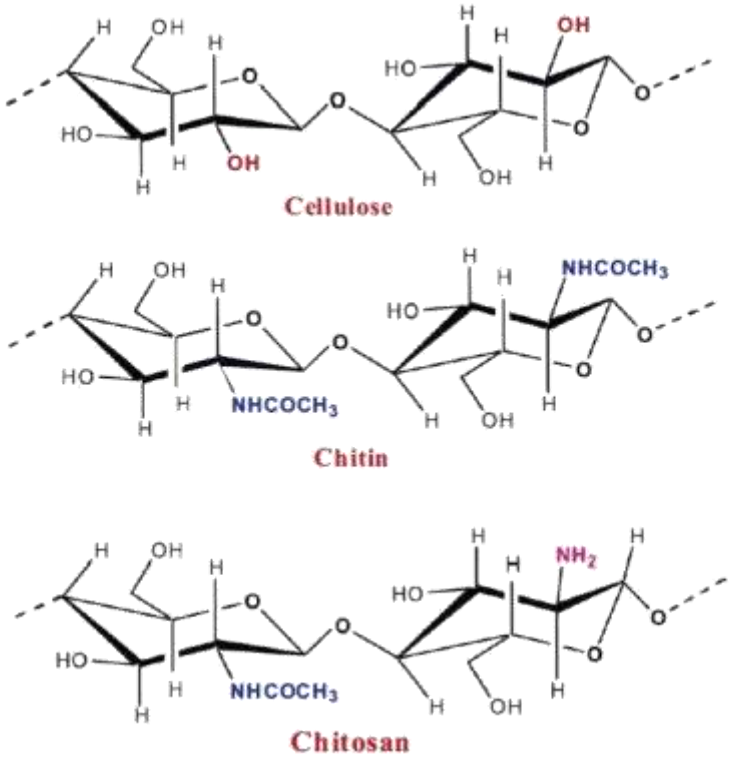

Figure 4.1. Chemical structures of cellulose, chitin and chitosan (CS).

The degree of N−deacetylation of CS is the deciding factor for its properties. This N−deacetylation degree is the ratio of the 2−acetamido−2−deoxy−D−glucopyranose to the 2−amino−2−deoxy−D−glucopyranose structural units. This ratio has a remarkable effect on the solubility and the properties of CS. It is soluble in dilute acids such as formic acid, acetic acid and hydrochloric acid. The nitrogen content of CS in the form of primary aliphatic amino groups makes it a highly reactive polymer. It undergoes the typical reactions of amines such as N−acylation, Schiff base formation and chelation with metal ligands. On the biological front, CS has the advantages of being biodegradable, biocompatible, non-toxic, bioabsorbable, mucoadhesive and possessing antimicrobial and wound healing properties (Bhattarai *et al.*, 2010).

The principal relevance of CS in pharmaceutical fields is in surgical sutures, dental implants, artificial skin, bone regeneration and contact lenses (Ravi Kumar, 2000).

Apart from these, CS shows promising features as an auxiliary agent in drug delivery. In contrast to all other biodegradable polymers having a monograph in a pharmacopeia, CS is the only one exhibiting a cationic character that makes it unique among others. This cationic character is due to its primary amino groups that are responsible for its various properties. These amino groups can easily be protonated in acidic medium thus making it soluble. This property therefore renders pH-sensitiveness to CS. The mucoadhesive properties, permeation enhancing effect and *in situ* gelling nature of CS are based on its cationic character. The mucoadhesive nature of CS has proven beneficial for the absorption of drugs, especially at neutral pH. CS has recently been explored for tissue engineering applications including cartilage, bone, liver and nerve tissues (Croisier and Jerome, 2013). Tissue engineering is aimed at developing biocompatible substitutes to restore, maintain or improve biofunction of dysfunctional human tissues or organs. Since CS is biodegradable and non-toxic, it has been formulated into films, gels or powders to improve the cell seeding (Dash *et al.,* 2011). In bone tissue engineering, CS has been shown to promote cell growth and mineral rich matrix deposition. In cartilage tissue engineering, glycosamine glycans (GAGs) play a vital role in modulating chondrocytes morphology, differentiation and function (Grande *et al.,* 1997). CS, bearing structural similarity to GAGs, is chosen as the preferred scaffold material for cartilage tissue engineering. In liver tissue engineering, the bio-artificial liver requires an extracellular matrix for surrounding the liver stem cells (Wang *et al.,* 2005). CS serves as the scaffold material for the hepatocytes culture due to its resemblance to the extracellular matrix. In nerve tissue engineering, artificial tubes are the effective means to repair injured nerves. CS is suitable for nerve regeneration because of its biocompatible, biodegradable and bioadhesive properties (Dash *et al.,* 2011).

In the areas of wound-healing, an ideal dressing should protect the wound from bacterial infection, provide a moist and healing environment, and be biocompatible (Wu *et al.,* 2003). CS, as a wound-healing agent, induces wound-healing on its own and produces less scarring. It enhances the vascularisation and the supply of chito-oligomers at the lesion site. CS hydrogels can also deliver drugs to the local wound and facilitate the healing process. While acute wound-healing can be enhanced by CS alone, due to its attractive properties for neutrophils, chronic wounds have also been healed by CS. Here the slow release of growth factors can produce more effective results. A CS hydrogel scaffold impregnated with β−fibroblast growth factor-loaded microspheres has been developed by Park *et al.,* (2009) that accelerates wound closure in the treatment of chronic ulcers.

CS has effectively been utilized in drug delivery as a hydrogel system, drug conjugate, biodegradable release system and polyelectrolyte complex for many systems. CS based hydrogel systems are used for the delivery of proteins/ peptides, growth factors, antibiotics, anti-inflammatory drugs, as well as in gene therapy and bio-imaging applications. CS is degraded by the normal microflora of the colon and is not digested in the upper gastrointestinal tract (Cheng *et al.,* 1994). By making use of this colon−specific degradation, CS has been discovered as a useful tool in order to guarantee a site specific delivery. CS hydrogels are favoured in the development of numerous drug delivery systems for various application sites which include oral, ocular, nasal, buccal, parenteral, transdermal, vaginal, rectal, intravesical and colonic areas (Ravi Kumar, 2000; Bhattarai *et al.,* 2010; Hu *et al.,* 2013; Uchegbu *et al.,* 2014).

4.1.2 POLY(ACRYLIC ACID)

Poly(acrylic acid) (PAA) has been widely employed as a synthetic pH-sensitive polymer for drug delivery applications. Acrylic based hydrogels are generally regarded as safe excipients. Moreover the mucoadhesive properties of these polymers make them suitable for increasing the drug residence time of the delivery device at the absorbing tissue thereby increasing the drug bioavailability (Cheddadi *et al.,* 2011). The pH-sensitivity of PAA is attributed to the ionization of the carboxylic acid groups in its backbone. Such polymers that consist of a large number of ionizable groups in their backbone are called as polyelectrolytes. Figure 4.2 shows the pH-dependent ionization behaviour of PAA which is ionized in higher pH. This ionization behaviour tend to make the apparent dissociation constant different from that of the corresponding monoacid or the monobase. The presence of ionizable groups also affects the swellability of the hydrogels. Since the swelling of these hydrogels is greatly influenced by the electrostatic repulsions among the charges present in the polymer chain, any change in the pH of the medium affects the extent of swelling.

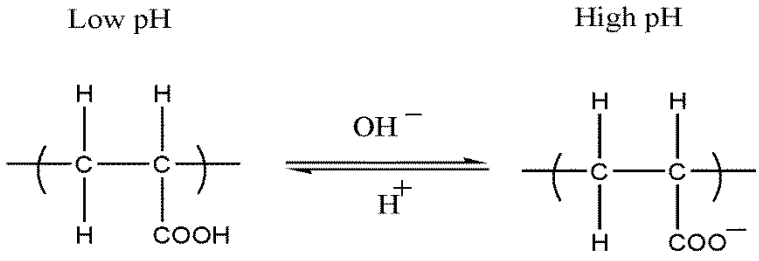

Figure 4.2. pH-dependent ionization of PAA.

However, the application of pure PAA is limited because of the fast release of the drug due to its extensive swelling in water. Moreover, PAA tend to dissolve at high pH solution. The most commonly used strategy to alleviate these problems is to prepare three-dimensional polymeric network by physical or chemical cross-linking or incorporation of PAA in an IPN (Abd El-Rehim *et al.,* 2007). PAA has been blended

with many polymers to fabricate IPN hydrogels with improved mechanical and chemical characteristics. Polymers such as CS (Wang *et al.,* 2009), PVA (Ray *et al.,* 2010), PEG (Doulabi *et al.,* 2013), PNIPAAm (Li and Liu, 2008) and others have been successfully employed to design such hydrogels.

Hydrogels composed of PAA can be used for formulations that can deliver drugs at neutral pH. To render colon specificity to such hydrogels, PAA has been cross-linked with azoaromatic cross-linkers. The magnificence of these hydrogels lies in the fact that there occurs minimal swelling in the gastric region thereby restricting the drug release. As it moves down the intestinal region, the swelling increases which releases the drug. Moreover, the azo cross-links can only be degraded by the azoreductase enzymes synthesized by the colonic microflora. Thus, PAA hydrogels can be tailored into a variety of formulations to ensure optimal drug release.

Hydrogels comprised of 2-vinyl pyridine and AAc were developed by Maziad and co-workers (2009) to study the release of water-soluble chloramphenicol drug. Recently, in a novel approach by Jiang *et al.,* (2013), pH-sensitive organic-inorganic copolymers based on polyhedral oligomeric silsesquioxane (POSS) and PAA were developed as DDS for theophylline. Low amount of drug was released in SGF and the addition of POSS prolonged the drug release time significantly. Poly[(NVP-AAc)-PEG] hydrogels were prepared by free radical polymerization and employed for the delivery of 5-Fluorouracil (Ravichandran *et al.,* 1997). The hydrogels swelled extensively in SIF than SGF suggesting possible applications of localized drug delivery. Biodegradable thermo- and pH-sensitive hydrogels based on hydroxypropyl cellulose-g-AAc have been developed for controlled delivery applications of the protein BSA (Zhang *et al.,* 2011). Hosseinzadeh and coworkers (Hosseinzadeh, 2010) have investigated the controlled release of diclofenac sodium from carrageenan-g-PAA

superabsorbent hydrogel and found favourable release profiles in SIF. Singh and Sharma (2010) have exploited the potential of psyllium-PVA-AAc based hydrogels for the delivery of the antibiotic drug tetracycline HCl. CD cross-linked microspheres of PAA have been constructed for controlled delivery of dyes (Bibby *et al.,* 1999) and drugs (Kutyla *et al.,* 2013). Microsphere of copolymers containing PAA and CD have also been studied for sorption studies (Guo and Wilson, 2012).

OBJECTIVES

The objective of this chapter is to design pH-responsive smart hydrogels based on CS and PAA for controlled drug delivery. This chapter consists of two parts;

- **Part I**: To explore the potential of GA cross-linked CS−PVA hydrogels towards the controlled delivery of NSAIDS, Naproxen and Diclofenac sodium, to the intestine.
- **Part II**: To inspect the utility of PAA hydrogel microspheres towards controlled delivery of Dexamethasone and investigate the influence of method of preparation of IC on the drug release phenomenon from the microspheres.

PART–I

CHITOSAN–POLY(VINYL ALCOHOL) INTERPENETRATING POLYMERIC NETWORK HYDROGELS FOR SUSTAINED RELEASE OF NON-STEROIDAL ANTI-INFLAMMATORY DRUGS

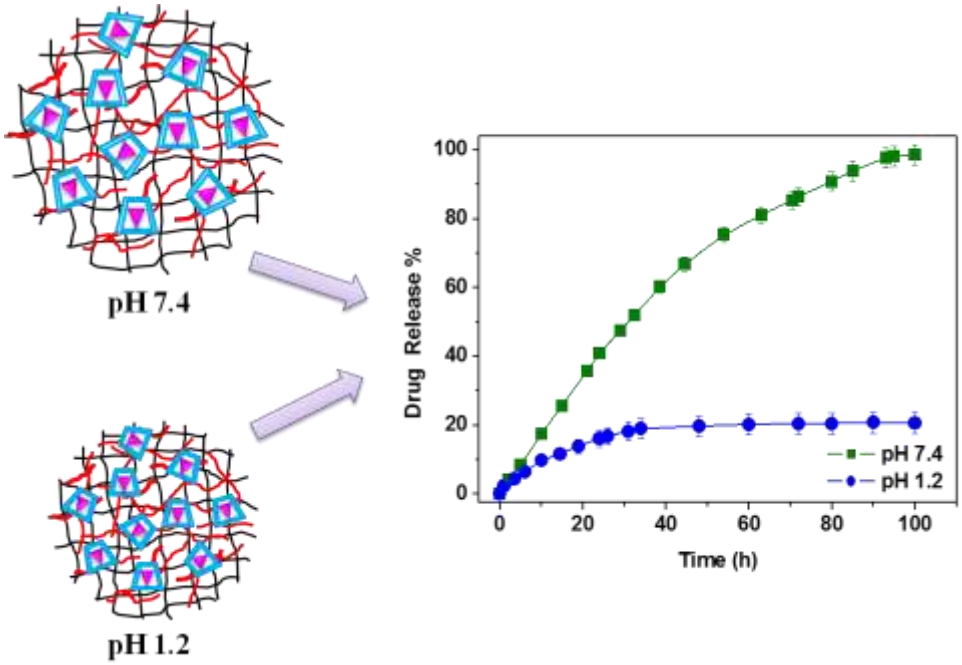

4.2 INTRODUCTION

The potential applications of CS as drug carriers have been quite well acknowledged. The principal uses of CS in oral formulations and also in parenteral drug delivery devices are also well listed. The relevance of CS hydrogels in nasal, ophthalmological, renal, rectal and colon drug delivery has been aptly justified (Bhattarai *et al.,* 2010). However, the inherent shortcomings associated with pure CS hydrogels cannot be ignored. They are highly porous, lack mechanical strength and tend to absorb moisture (Don *et al.,* 2002). Moreover as CS precipitates at pH > 6.5; it loses its mucoadhesive and permeation enhancing properties in the distal segments of the intestine. This effect reduces its applicability for drugs having their absorption window in the proximal segment of the GIT.

Incorporation of CS in an IPN hydrogel improves the mechanical strength of the conventional hydrogel. In the IPNs, CS is incorporated with either hydrophilic polymers or with hydrophilic monomer(s) treated to bring about *in situ* copolymerization in the presence of a suitable cross-linking agent. The formation of IPN produces an advanced multi-component polymeric system with superior physico-chemical properties.

PVA, because of its ease of film formation, long-term temperature and pH stability, has established itself as a potential supporting material in IPN fabrication. Hydrogels based on PVA and CS have emerged as one of the promising biodegradable materials due to their highly controllable and other advantages of non-toxic, non-carcinogenic and bioadhesive properties. Huge efforts have been made to prepare CS−PVA hydrogels and their potential in drug delivery systems is being extensively studied. CS−PVA hydrogels cross-linked by tetraethyl orthosilicate (TEOS) have been developed by Islam and co-workers (2013) and their structural and visco-elastic

properties were evaluated. The potential of the developed hydrogels in drug delivery was also investigated from the *in vitro* release studies of progesterone. The cytotoxicity evaluation on human fibroblast cells demonstrated the hydrogels to be nontoxic and biocompatible in nature. Khan and Ranjha (2014) have recently prepared low viscous CS−PVA hydrogels cross-linked by GA and inspected the effect of cross-linking on the swelling and drug release behaviour of the hydrogels. Diphenhydramine HCl was chosen as the model drug and its release characteristics were observed in buffer solutions of pH 1.2, 5.5 and 7.5. The developed hydrogels were found to be suitable for the oral delivery of the chosen drug. In a very recent study by Lejardi *et al.* (2014), CS−PVA hydrogels were synthesized by cross-linking with glycolic acid. The hydrogels were found to possess enhanced rheological properties and their thixotropic behaviour can be utilized as injectable materials for biomedical applications. CS−PVA IPN hydrogels cross-linked by GA and also by γ−irradiation were tested for their delivery efficacy for 5FU (Abdelaal *et al.*, 2007). The release of the drug from both types of hydrogels was found to be directly dependent on the PVA content indicating a slow release in neutral medium. Blend hydrogel microspheres of PVA and succinyl CS produced by water-in-oil emulsion cross-linked with GA were explored for delivery of nifedipine (Kajjari *et al.,* 2013). The review article by Ranjha and Khan (2013) discusses the biomedical applicability of CS−PVA IPN hydrogel networks at length.

The focus of this chapter is to design pH-sensitive CS−PVA hydrogels towards controlled and intestine-targeted delivery of NSAIDS, NX and DS. NSAID, as the name implies are compounds of non-steroidal origin, with the capability of inhibiting or reducing inflammatory responses associated with tissue injury due to physical trauma, noxious chemicals or microorganisms. NSAIDs are widely used for the

purpose of anti-inflammation, antipyretic and analgesia. They are also used for the alleviation of pain, fever, and inflammation associated with rheumatoid arthritis, gouts, fractures, sports injuries and musculoskeletal pain. Naproxen ((S)−6−methoxy−β-methyl−2−napthalene acetic acid) (NX) (Figure 4.3A), a member of the family of the arylpropionic acids and diclofenac sodium (sodium− (o− ((2,6−dichlorophenyl)− amino)− phenyl)− acetate) (DS) (Figure 4.3B), a phenylacetic acid derivative, are potent NSAIDs. NX and DS are commonly employed in everyday life as anti-inflammatory agents.

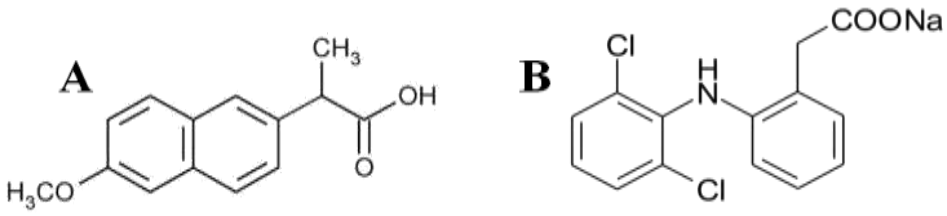

Figure 4.3. Chemical structure of (A) Naproxen (NX) and (B) Diclofenac Sodium (DS).

However, the use of NSAIDs is usually associated with the deleterious effects on the epithelium of the GIT. Thus, targeting of the NSAIDs to the intestine reduces the risks of gastrointestinal irritation and also ensures the proximal delivery of the drug.

OBJECTIVES

The specific objectives of the present study are:

- Preparation of solid ICs of NX and DS with CD and affirm the formation of ICs by various spectroscopic techniques
- Synthesis of GA cross-linked CS−PVA and CS−PVA−CD hydrogels of varying composition and their characterization
- Study of the antimicrobial properties of CS−PVA hydrogels
- To evaluate the pH-responsive swelling characteristics of the hydrogels.

- To explore the drug release behaviour of the hydrogels containing free drug and the ICs.
- To investigate the pH-responsive drug delivery behaviour in SGF and SIF for the oral delivery of the drugs.
- To address the preliminary kinetics and the effect of CD on the drug release mechanism of the hydrogels.

The compositions of various CS−PVA hydrogels are shown in Table 4.2.

Table 4.2. Compositions of synthesized hydrogels

Sample	CS: PVA (wt%)	Sample Designation			
		CS−PVA	CS−PVA−CD	CS−PVA−Drug	CS−PVA−IC
1	1:0	CS	CS-CD	CS-D	CS-IC
2	1:1	CP11	CP11-CD	CP11-D	CP11-IC
3	1:3	CP13	CP13-CD	CP13-D	CP13-IC
4	1:5	CP15	CP15-CD	CP15-D	CP15-IC

The CS-PVA hydrogels containing free NX are represented as CP11-NX, CP13-NX and CP15-NX while the hydrogels containing the free DS are labelled as CP11-DS, CP13-DS and CP15-DS. For the NX release studies IC represents the NX-CD IC and for the DS release studies IC represents the DS-CD IC.

4.3 RESULTS AND DISCUSSION

4.3.1 Characterization of CS−PVA Hydrogels

In the present study, GA has been employed as the cross-linking agent. It reacts with the hydroxyl groups of PVA and amino groups of CS producing a cross-linked network. The cross-linking reaction between CS and GA, which is a typical Schiff base reaction, is dominant to form the three-dimensional cross-linked network of CS−PVA hydrogel. The reaction scheme for the cross-linking of CS and PVA with GA is shown in Scheme 4.1.

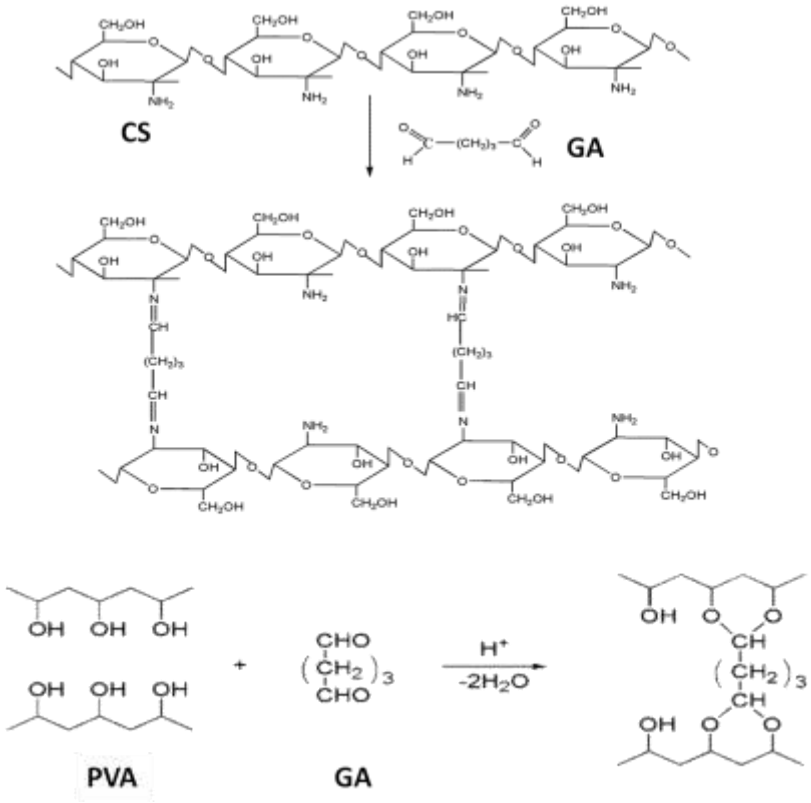

Scheme 4.1. Cross-linking reaction scheme of CS and PVA with GA.

4.3.1.1 FTIR Analysis

The FTIR spectra of pure CS, pure PVA, CP11, CP13 and CP15 hydrogels are presented in Figure 4.4.

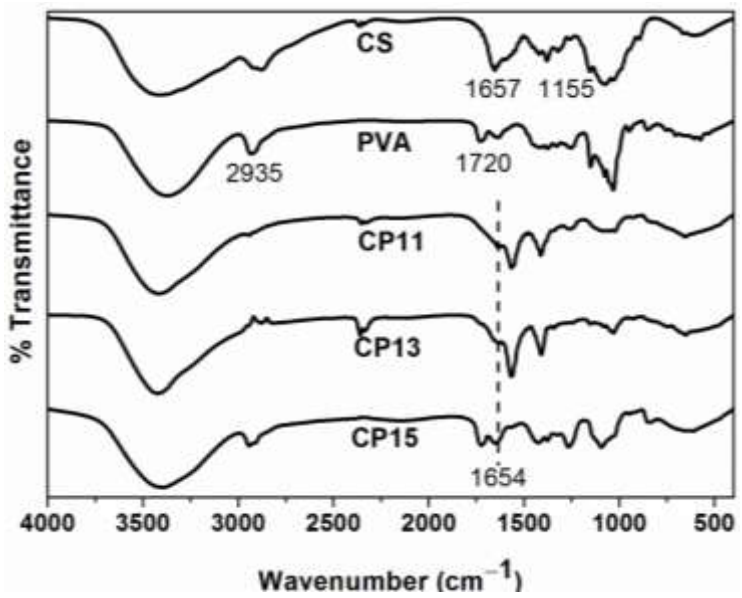

Figure 4.4. FTIR spectra of pure CS, PVA, CP11, CP13 and CP15 hydrogels.

The characteristic CS peaks include the peaks at 893 cm^{-1} and 1155 cm^{-1} due to the pyranose ring and saccharin structure of CS. The broad band around 3300−3000 cm^{-1} is due to the N–H stretching. The bands at 2922 and 2810 cm^{-1} represent the C−H aliphatic stretching vibrations. The three bands appearing at 1657, 1560 and 1254 cm^{-1} are assigned to amide−I, amide−II and amide−III of chitosan (Angadi *et al.,* 2010). The typical PVA peaks include a large band at 3400 cm^{-1} (O−H stretch), the peaks at 2395 cm^{-1} (C−H stretch from alkyl groups), 1720 cm^{-1} (C=O stretch) and 1140 cm^{-1} (crystalline C=O stretch of semi-crystalline PVA). In the FTIR spectra of the IPN hydrogels, the amide groups of CS are still evident and the key PVA peaks are also seen but with a small shift in their positions. A peak at 1654 cm^{-1} is observed in all the IPN samples which is associated with the imine group formed by the nucleophilic reaction of the amine of CS with GA. The characteristics carbonyl peak of PVA is visibly modified in the IPN hydrogels which can be due to the cross-linking reaction. The peak at 1140 cm^{-1} of PVA has reduced significantly indicating the loss in the regularity of PVA polymer chains due to inter-polymer interaction.

4.3.1.2 XRD Analysis

Figure 4.5 A projects the diffraction profiles of PVA and CS. PVA shows a broad peak centred at 2θ value of 19.8° due to its semicrystalline nature. Pure CS shows a typical strong diffraction around 20° and a relatively weak diffraction peak at around 9.5° (Kolhe and Kannan, 2003). The XRD profiles of CP11, CP13 and CP15 hydrogels are depicted in Figure 4.5 B. The IPN hydrogels showed single broad peak of relatively lower intensity as compared to pure CS and PVA hydrogels. This indicates that the IPN hydrogels exhibit somewhat reduced crystallinity. The weak diffraction peak of CS around 9.5° is completely missing in the IPN hydrogels indicating the proper blending of the two polymers in the IPN. The relative shifts in

the 2θ positions in the IPN hydrogels with respect to the pure components suggested that the intermolecular interaction disturbed the regularity of the component polymers (Tang *et al.*, 2009).

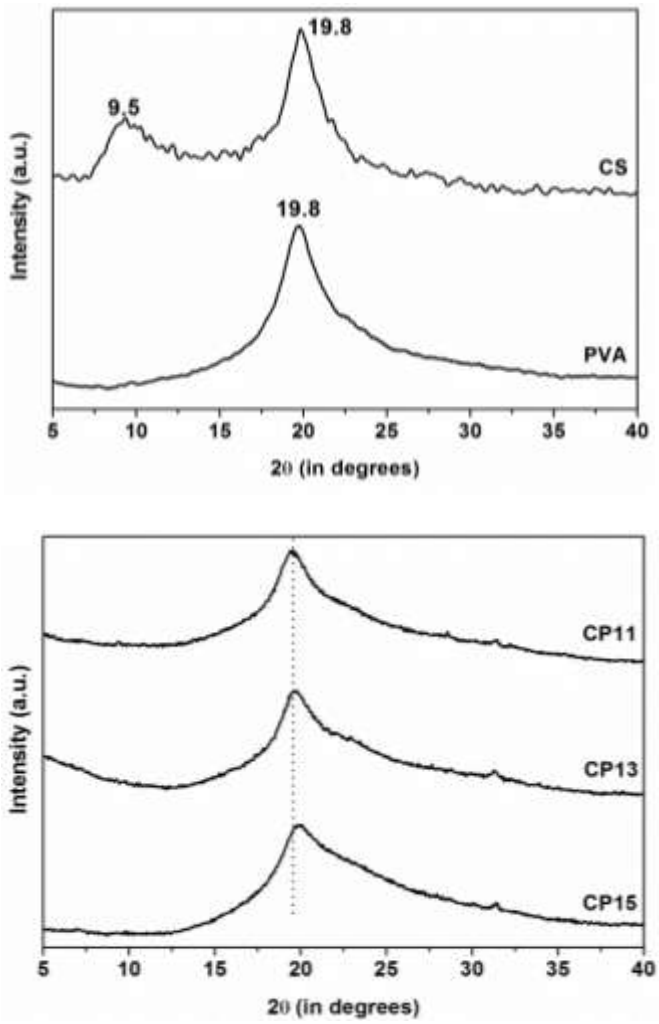

Figure 4.5. XRD profiles of (A) CS, PVA and (B) CP11, CP13, CP15 hydrogels.

4.3.1.3 DSC Analysis

DSC analysis is an important criterion to determine the miscibility of two polymers. The DSC thermograms of neat PVA, CP11, CP13 and CP15 hydrogels are shown in Figure 4.6. CS crystallinity could not be detected by DSC analysis, though it presents some crystallinity when analysed by certain other techniques. As reported by Lee and

co-workers (2000), CS has a rigid-rod backbone having strong inter- and/ or intra-molecular hydrogen bonding and its thermal transitions could not be detected by DSC.

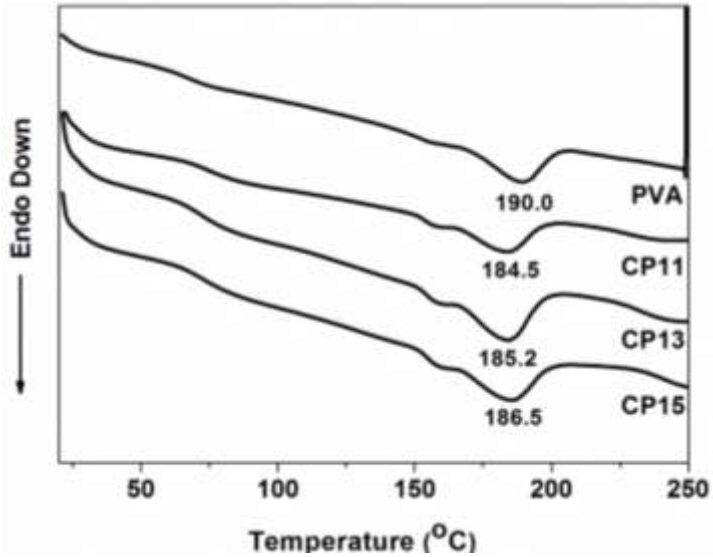

Figure 4.6. DSC thermograms of pure PVA, CP11, CP13 and CP15 hydrogels.

Neat PVA exhibited a melting temperature (T_m) at around 190°C. From the DSC traces of CP11, CP13 and CP15 IPN hydrogels; it was evident that the T_m shifted to slightly lower temperatures as compared to pure PVA. This indicates that the ordered association of the PVA chains was somewhat perturbed in presence of chitosan in the IPNs. Moreover, the presence of cross-linking is also known to cause a decrease in the polymer chain mobility that results in lowering of T_m. For the IPN hydrogels the T_m was found to increase with increase in PVA content *i.e.* CP15 > CP13 > CP11. From the DSC thermograms, it is clear that in the IPN hydrogels the two polymers have good miscibility.

4.3.1.4 Morphological analysis

The morphology of the freeze-dried CS and the IPN hydrogels were observed under SEM. The hydrogels were freeze-dried so as to maintain their bulk structure and prevent the collapse of the matrix networks. The SEM images of the hydrogels are presented in Figure 4.7. Pure CS exhibits a highly porous structure (Figure 4.7 A). The

effect of PVA content on the hydrogel morphology was examined. The photographs clearly illustrate the dependence of hydrogel morphology on the PVA content.

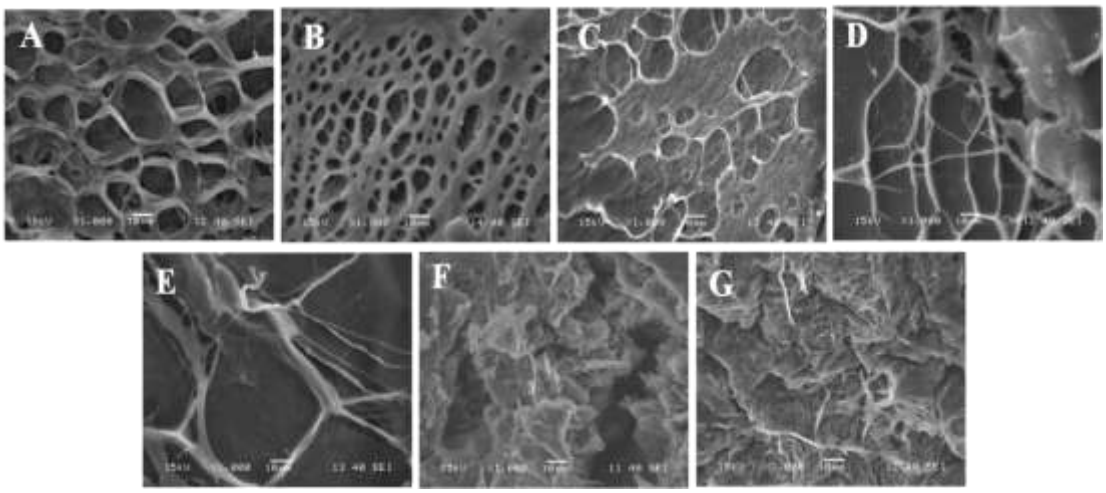

Figure 4.7. SEM micrographs of (A) CS, (B) CP11, (C) CP13, (D) CP15, (E) CP15-CD and after release (F) CP15, (G) CP15-CD hydrogels.

With increasing PVA content, (Figure 4.7 B−D); the porosity diminishes making the hydrogel relatively compact. This can be explained by the enhanced entanglement between CS and PVA with increased PVA content (Tang *et al.,* 2007). CP15-CD exhibits more or less a similar morphology as that of CP15, which indicates that presence of CD did not induce any significant alteration in the hydrogel morphology (Figure 4.7 E). The morphology of the CP15 and CP15-CD hydrogels after drug release was also visualized (Figures 4.7 F & G). Interestingly the CP15-CD film was intact and eroded less even after prolonged exposure to the releasing medium; whereas the CP15 film had some wear and tear. Thus, it could be inferred that the CP15-CD hydrogel possessed the most dense and rigid matrix network structure in comparison to the other hydrogels.

4.3.2 Swelling Response of Hydrogels

4.3.2.1 Swelling in Water

Time dependent swelling behaviour of the hydrogels in deionized water was studied. The CS film was very brittle in nature and exhibited less mechanical strength; upon swelling it disintegrated and resulted in a gel-like mass (Figure 4.8). With increasing amount of PVA, the stability of the hydrogels was found to increase indicating increased mechanical strength. The CP15 and CP15-CD hydrogels were found to be the most stable ones and were intact even after prolonged exposure to swelling.

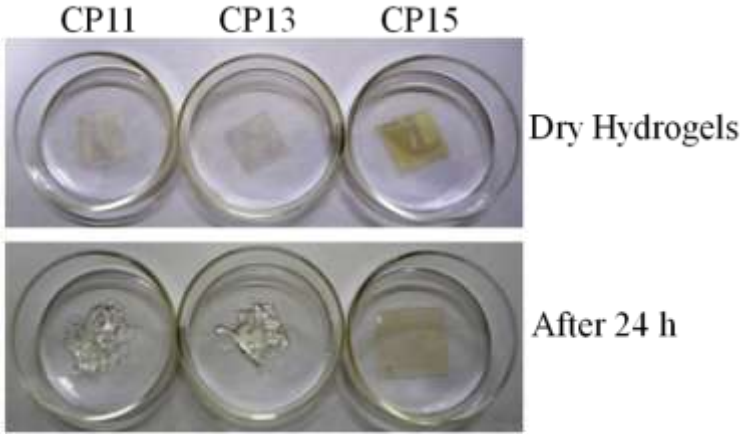

Figure 4.8. Photographs depicting the physical stability of hydrogels after swelling in water for 24 h.

The swelling profiles of CP11, CP13 and CP15 hydrogels in pH 7.4 and 37°C over a prolonged time period are shown in Figure 4.9 A. The swelling ability of the hydrogels was found to decease in the order CP11 > CP13 > CP15, which can be due to the increased compactness and rigid network structure of the hydrogels with increasing PVA content. This feature has previously been revealed by the SEM studies.

The swelling profiles of both CP15 and CP15-CD hydrogels were found to be similar in nature (Figure 4.9 B). However the swelling capacity of the CP15-CD hydrogel was

found to be a little lower than that of CP15. This could be possibly explained by considering the slightly compact nature of CP15-CD as compared to CP15 due to the presence CD, which has also been seen from the SEM images of the respective hydrogels. Thus it could be concluded that the presence of CD did not reveal any drastic effect on the swelling abilities of the hydrogel.

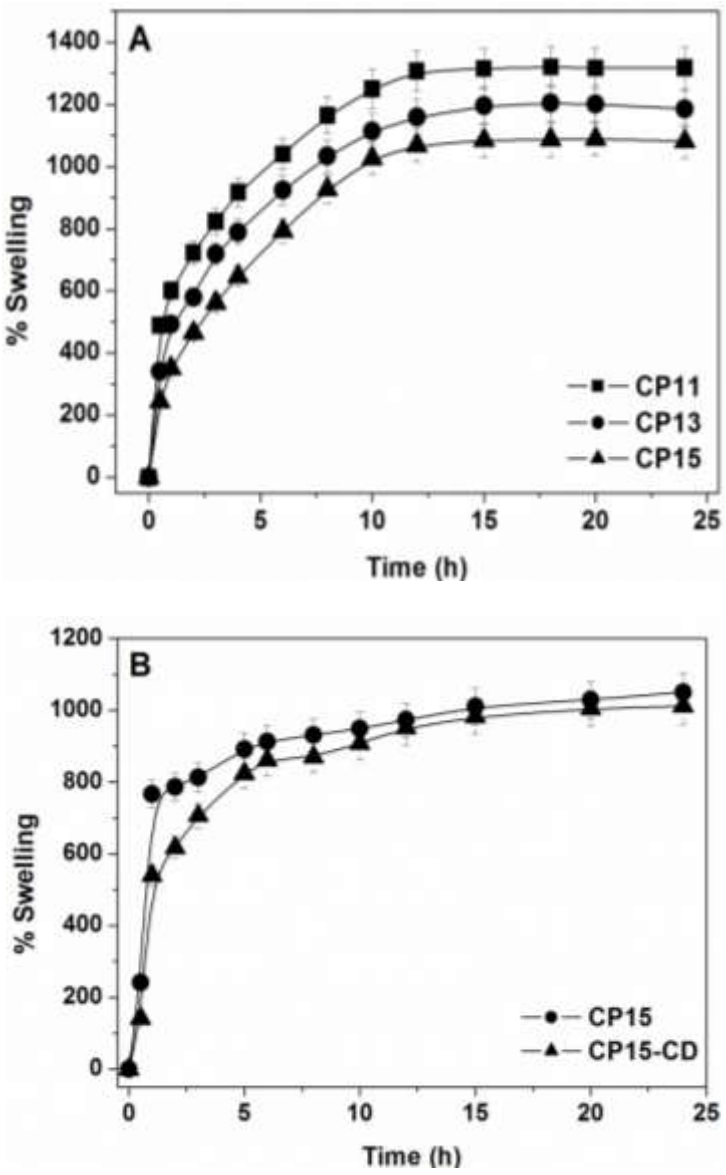

Figure 4.9. Time-dependent swelling profiles of (A) CP11, CP13, CP15 hydrogels and (B) CP15, CP15-CD hydrogels in pH 7.4 at 37°C.

4.3.2.2 pH-responsive Swelling

The swelling response of the hydrogels was also investigated at different pHs. The effect of pH on the swelling of the CP11, CP13, CP15 hydrogels and that of CP11-CD, CP13-CD, CP15-CD hydrogels is shown in Figure 4.10 A and B, respectively. The hydrogels exhibited pH-sensitive swelling with maximum swelling at neutral pH and lower swelling at acidic and alkaline pHs. Due to protonation of amino groups ($-NH_2$) in CS at lower pH, strong electrostatic repulsion occurs between the polymer chains. The flow of counter ions into the hydrogel matrix takes place to localize near the ammonium groups and the overall electrostatic potential is neutral. Thus, the increased osmotic pressure inside the hydrogel results in a reduced water uptake capacity. At neutral pH, the deprotonation of $-NH_3^+$ occurs and intra-chain hydrogen bonding can take place in the polymer matrix as a result the hydrogel can accommodate more water around hydrogen bonded groups and capillary pores, resulting in maximum swelling. At basic pH, due to complete deprotonation of $-NH_3^+$ groups, the degree of ionization of the hydrogels is lowered and there is a possiblity of stronger and extensive hydrogen bonding in the hydrogel matrix, which results in a more compact structure and swelling is hindered (Islam and Yasin, 2012; Islam *et al.,* 2012).

The degree of swelling was found to decease in the order CP11 > CP13 > CP15. This can be explained considering the increased matrix density with increasing amount of PVA in the hydrogel. The overall swelling behaviour of CP11-CD, CP13-CD and CP15-CD hydrogels were found to be very similar to the corresponding hydrogels without CD but with a slight decrease in the degree of swelling. This indicates that the presence of CD did not have any significant effect on the pH-sensitivity of the hydrogels. This has been clearly illustrated in Figure 4.10 C.

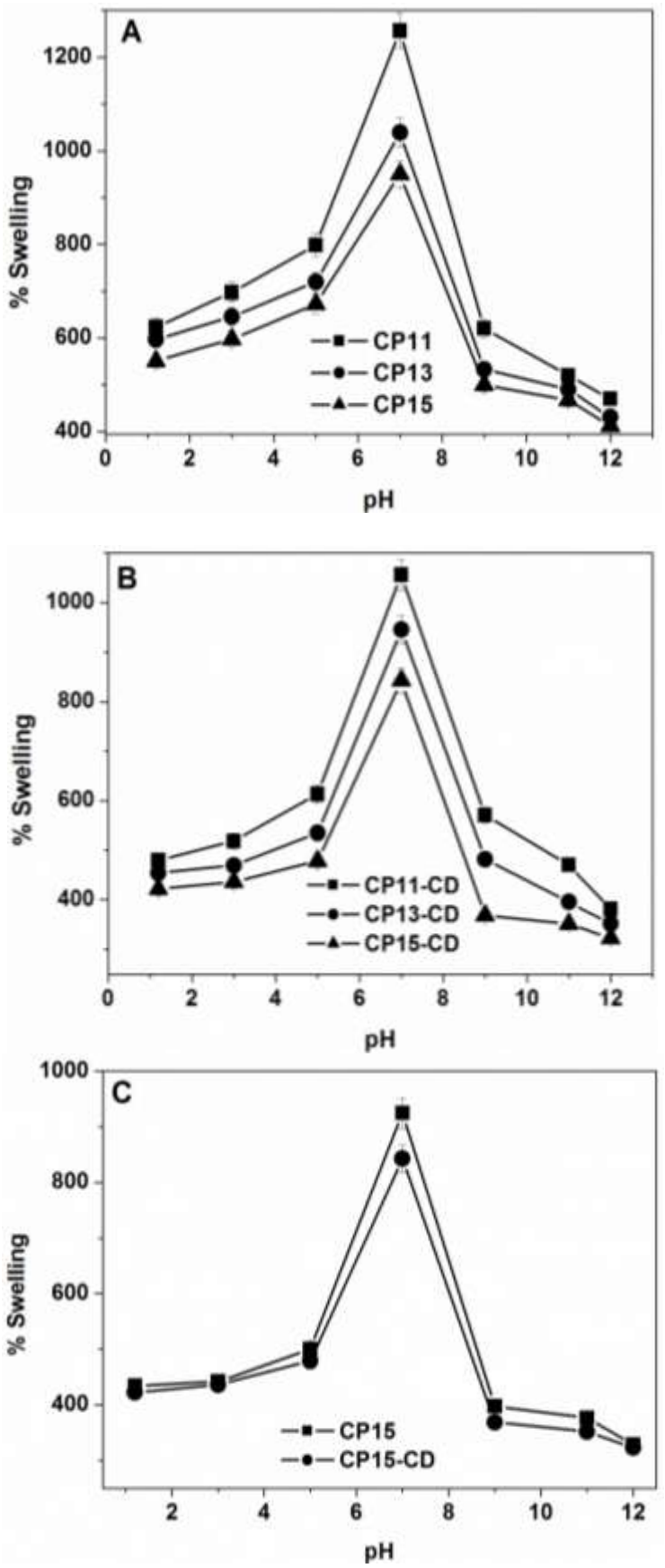

Figure 4.10. pH dependent swelling of (A) CP11, CP13, CP15; (B) CP11-CD, CP13-CD, CP15-CD and (C) CP15 and CP15-CD hydrogels in buffer.

4.3.3 Antimicrobial Activity of Hydrogels

CS has been studied in terms of its bacteriostatic/ bactericidal activity to control growth rate of algae and to inhibit viral multiplication. Three models have been proposed to describe the antibacterial mode of action of CS (Kong *et al.*, 2009); the most acceptable being the interaction between the positively charged CS and the negatively charged bacterial cell wall. Another proposed mechanism is the binding of CS with microbial DNA which leads to inhibition of mRNA and protein synthesis *via* the penetration of CS into the nuclei of the microorganisms. However, Raafat and co-workers (2008) found out that the probability of it occurring is rather low. The third mechanism is the chelation of ligands, suppression of spore elements and binding to essential nutrients to contribute to cell death. There are certain controversies regarding the bacterial effectiveness of CS on Gram−positive and Gram−negative bacteria. It has been demonstrated that the high hydrophilic characteristics in Gram-negative bacteria make them more sensitive to CS (Chung *et al.*, 2004). Although the exact mechanism of antimicrobial activity of CS is yet to be established, however the growth of *E. coli* is known to be inhibited in the presence of CS (Abdel-Mohsen *et al.*, 2011). In the present study, the synthesized CS−PVA hydrogels were tested for their antibacterial activity against *E. coli* in absence and in presence of CD. Figure 4.11 shows the antibacterial effects of CS and the IPN hydrogels against *E. coli.* The results indicated that the hydrogels are not compromised in their antimicrobial characteristics even after addition of PVA and/or CD in the matrix. The antimicrobial assay on the hydrogels also demonstrated the probable applicability of the synthesized CS−PVA IPN hydrogels as wound-healing agents.

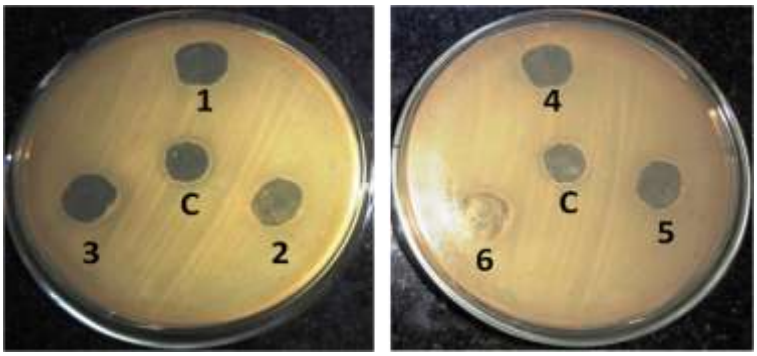

Figure 4.11. Antibacterial activity of pure CS (Control(C)), (1) CP11, (2) CP13, (3) CP15, (4) CP11-CD, (5) CP13-CD and (6) CP15-CD hydrogels against *E. coli.*

Controlled Delivery of Naproxen from CS−PVA IPN Hydrogels

4.4 CS−PVA IPN Hydrogels as Controlled Release Platforms for Delivery of NX

Naproxen, marketed under the trade names Anaprox and Naprosyn, finds wide employment for the treatment of osteoarthritis. NX is typically used in the treatment of rheumatoid and gouty arthritis that require prolonged supply of the drug for cure. The chronic exposure of the patient to the drug raises the concerns of side effects which include dizziness, drowsiness and nausea. NX has also been known to induce photosensitivity in some patients and is capable of causing photo-cleavage of DNA. Moreover, the bioavailability of NX is also limited because of its extremely low aqueous solubility (about 27 mg L^{-1} at 25°C) and causes undesirable effects on the gastric mucosa when orally administered, thereby leading to patient non-compliances (Mura *et al.*, 2005). Additionally, gastrointestinal ulcerative damages are common adverse reactions of NX. Thus, delivery of NX generally demands lower doses over prolonged period and targeted to the intestine. Cyclodextrins, in this context, play a vital role as drug delivery media in enhancing the aqueous solubility, stability and bioavailability of NX (Mura *et al.*, 2005). Complexation of NX with CD also has the

advantages of reduction in ulcerogenicity (Otero-Espinar *et al.,* 1991), improved anti-inflammatory properties (Ramı´rez *et al.,* 2006) and decreased photoreactivity of the drug (Valero *et al.,* 2004).

Thus, in order to reduce the adverse effects of free NX in the GIT, ICs of NX with CD were first prepared. The ICs were then added to the CS−PVA hydrogels and their delivery potential was explored. By taking advantage of the pH-responsive swelling characteristics of the CS−PVA hydrogels the delivery of NX could be directed to the intestine.

4.4.1 Inclusion Studies of NX in CD

The interaction of NX with CD in solution state was studied by UV-Vis and Fluorescence techniques. The solid ICs of NX with CD were prepared by the co-precipitation method and characterized by various analytical techniques.

4.4.1.1 UV−Vis Study

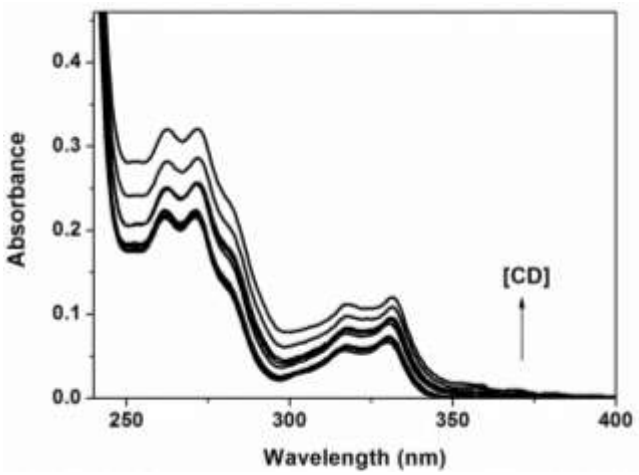

Figure 4.12. Absorption spectra of NX at varying concentrations of CD, [NX] = 5×10^{-5} M, [CD] = 0−20 $\times10^{-3}$ M, pH=7.4.

The solution phase NX−CD inclusion complexation behaviour was studied using spectrophotometric titration method. As illustrated in Figure 4.12, the absorbance of NX gradually increased with the addition of CD, which can be attributed to the increased solubility of NX in presence of CD due to formation of inclusion complex.

However, this increase is not that significant to estimate the binding constant (K_b) therefore fluorescence study was carried out.

4.4.1.2 Fluorescence Analysis

Fluorescence studies provide a better scope for understanding the formation of CD inclusion complexes because of the higher sensitivity of the technique. The solution phase inclusion efficiency of NX with CD was evaluated by fluorescence measurements using the intrinsic fluorescence of the drug. The emission spectra were recorded with excitation at 280 nm and scanned between 300 and 500 nm. Figure 4.13 A displays the fluorescence emission spectrum of NX as a function of [CD] in aqueous medium (pH=7.4). The fluorescence intensity of NX was very sensitive to the addition of CD; the addition of CD produced an increase in the fluorescence intensity. Once the drug is incorporated in the cavity of CD, it is protected from solvent induced quenching of fluorescence, which results in an increased quantum yield. Thus the fluorescence study suggests that a stable complex is formed between NX and CD.

It is important to know the binding constant of the drug−CD complex because the process of drug incorporation within a CD will be effective in reducing the concentration of free drug only if the binding constant (K_b) of the drug in the IC is sufficiently large, which is essential to minimize the undesired side effects of the free drug in the GIT. The K_b for the IC was found to be $1.67(8) \times 10^3$ M^{-1} from the double reciprocal plot of $[1/ (F-F_o)]$ against 1/ [CD] (Figure 4.13 B).

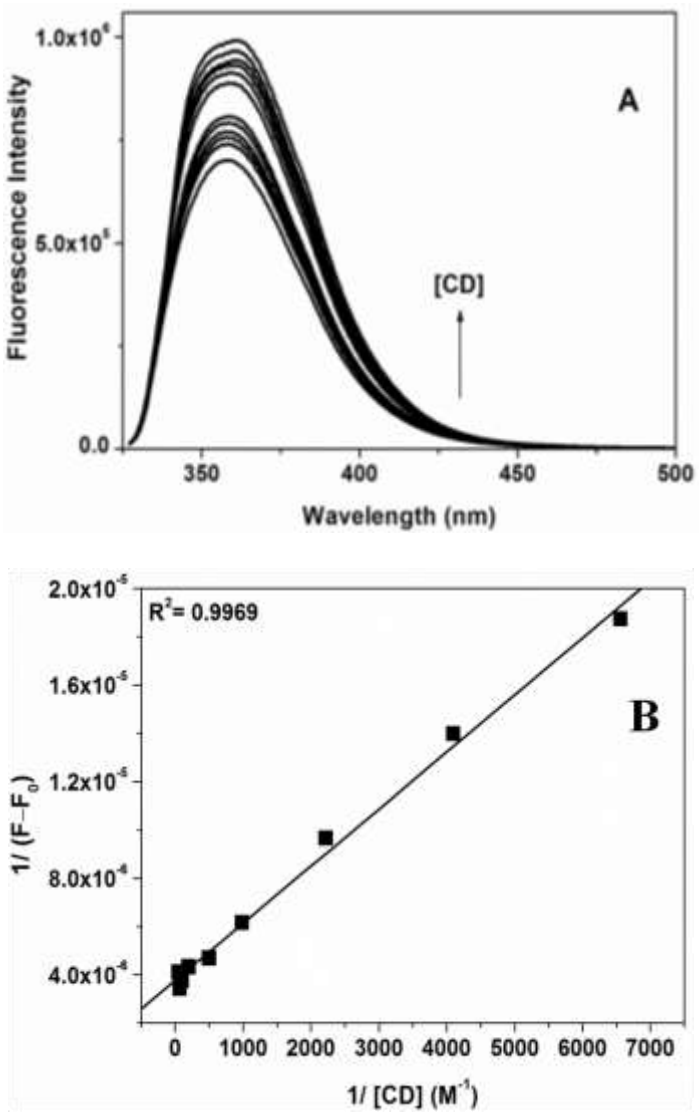

Figure 4.13. (A) Emission spectra of NX at varying concentrations of CD, [NX] = 5×10^{-5}M, [CD] = 0−20 $\times10^{-3}$ M, pH=7.4, (λ_{ex} = 280 nm); and (B) Benesi-Hildebrand plot for NX-CD interaction.

4.4.1.3 FTIR Analysis

The FTIR spectra of CD, NX, PM and IC are represented in Figure 4.14. The key NX peaks include 856 cm^{-1}(C−O−C bonds), 1728 cm^{-1} (C=O stretch), 1392 cm^{-1}(C=C stretch) and 1228 cm^{-1}(−O− stretch). The characteristic CD peaks include the asymmetric R−O−R stretch at 1158 cm^{-1}, C−OH stretch at 1025 cm^{-1}, broad band at 3377 cm^{-1} (O–H stretch). The FTIR spectrum of the PM is superposition of both CD and NX spectra. The characteristic aromatic C=C stretching band of NX at 1392 cm^{-1}

shifted to 1402 cm^{-1} in the inclusion complex (IC). The shift of the O−H band to higher frequency region (3396 cm^{-1}) in the IC indicated the cleavage of hydrogen bonding, probably due to inclusion phenomenon (Mura *et al.*, 2005).

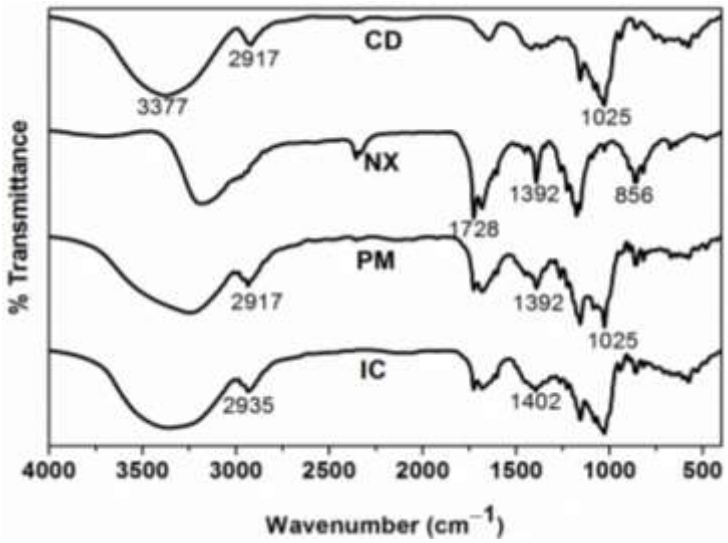

Figure 4.14. FTIR spectra of CD, NX, PM and IC.

4.4.1.4 XRD Analysis

The X-ray diffraction profiles of CD, NX, PM and IC were collected and illustrated in Figure 4.15.

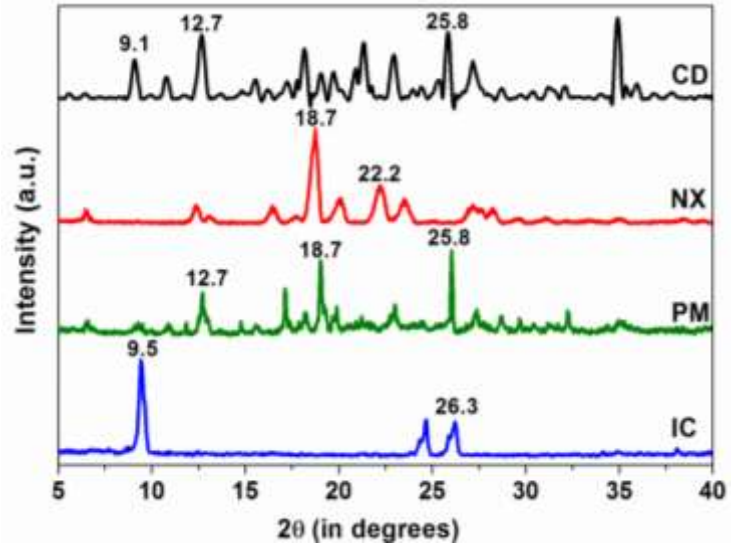

Figure 4.15. XRD profiles of CD, NX, PM and IC.

NX showed sharp diffraction peaks at 2θ values 16.5°, 18.7°, 20.1°, 22.2° and 27.2° indicating a highly crystalline nature. Crystalline nature of CD was also indicated by sharp diffraction peaks. PM showed almost all the peaks of NX and CD. In contrast, the characteristics peaks of NX and CD disappeared for the IC and new diffraction peaks appeared around 2θ values 9.5°, 24.7° and 26°, which indicate formation of new phases and confirm the inclusion of NX in the CD cavity.

4.4.1.5 DSC Analysis

The DSC curves of CD, NX, PM and IC were collected and shown in Figure 4.16. The DSC traces of CD exhibited a broad endothermic effect around 130°C due to the dehydration process. The thermal curve of NX was typical of a crystalline anhydrous substance, showing a sharp endothermic peak at 156°C due to the drug melting. The individual characteristic thermal profiles of CD and the drug were observed in the physical mixture. On the contrary, the complete disappearance of the drug thermal profile in the IC affirmed the encapsulation of NX in CD cavity (Mura *et al.*, 2005).

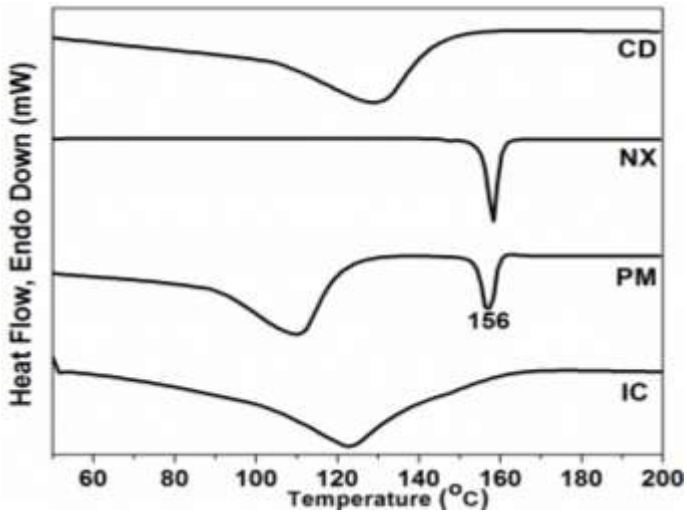

Figure 4.16. DSC thermograms CD, NX, PM and IC.

4.4.1.6 Optical Microscopic Images

Optical microscopic images were collected for the CD, NX, PM and IC to visualize their morphology. The images of CD (Figure 4.17 A) and NX (Figure 4.17 B) indicate

their crystalline nature. The photograph of PM (Figure 4.17 C) shows presence of both NX and CD crystals. However, the image of the IC clearly point towards the formation of a new crystals of ICs (Figure 4.17 D).

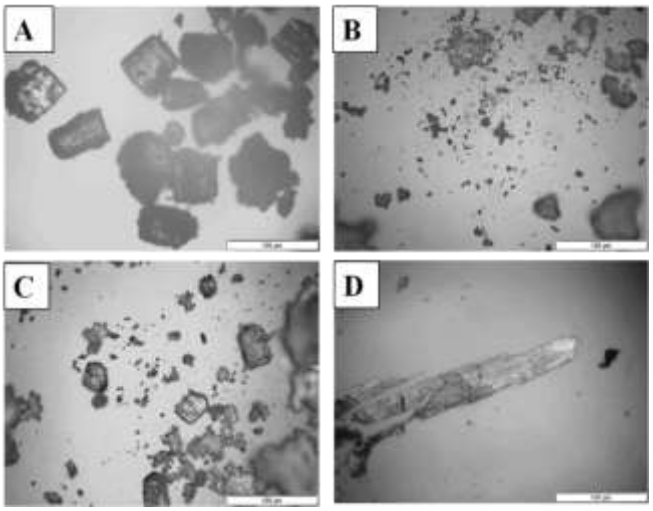

Figure 4.17. Optical microscopic images of (A) CD, (B) NX, (C) PM and (D) IC.

4.4.1.7 ^{1}H NMR Analysis

The ^{1}H NMR spectra of CD and NX-CD IC are shown in Figure 4.18. The values of chemical shifts δ, for different protons in CD and NX-CD IC are listed in Table 4.3.

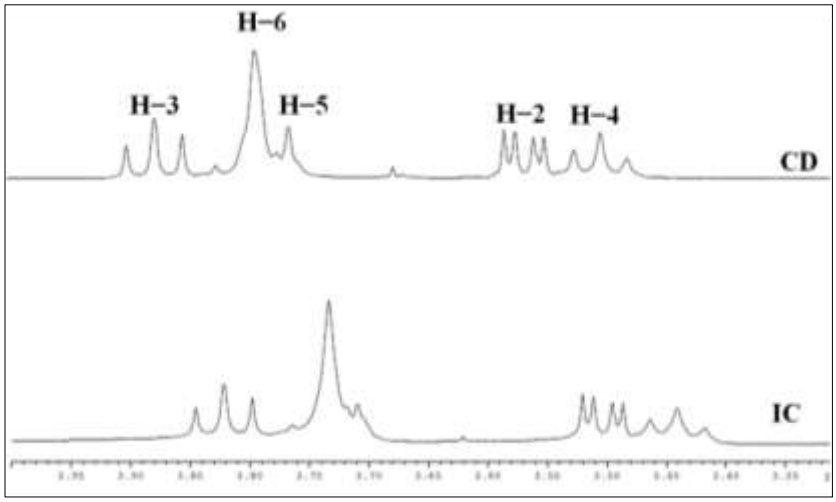

Figure 4.18. ^{1}H NMR spectra of CD and NX-CD inclusion complex in D_2O at 298 K.

Table 4.3. A. δ and Δδ of protons in CD and NX-CD IC

Protons	δ_{CD}	δ_{IC}	Δ (δ_{CD} and δ_{IC})
H−1	4.991	4.880	0.111
H−2	3.561	3.504	0.027
H−3	3.874	3.832	0.042
H−4	3.496	3.441	0.035
H−5	3.761	3.709	0.052
H−6	3.790	3.756	0.034

Table 4.3. B. Chemical shift δ and Δδ of protons of NX in free NX and IC

	Ar-H	
NX	7.125−7.737	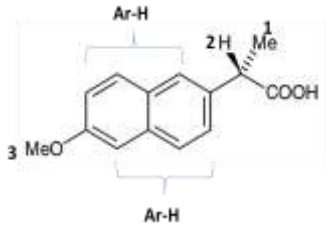
IC	7.144−7.825	
Δδ	0.019−0.088	
Comment	Down field	

The values of chemical shifts, δ for the aromatic protons in NX and IC complex are listed in Table 4.3 B. The shift in aromatic protons (7.125−7.737 to 7.144−7.825) of NX indicates the inclusion of the naphthalene ring in the CD cavity. From Table 4.3. A, by comparing the differences in the chemical shifts of the H−3 and H−5 protons of CD and IC the total inclusion of NX in CD cavity is clearly indicated (Banik *et al.*, 2012).

4.4.2 NX Release Studies

Figure 4.19 shows the release profiles of NX from CS-NX, CS-IC, CP15-NX and CP15-IC hydrogels at pH 7.4 and 37°C. NX release from CS films (CS-NX and CS-IC) was found to be very fast and complete drug release takes place in a short period of time. This can be explained by considering the high porosity and extensive swelling of CS hydrogel that leads to the fast release of the encapsulated drug. Moreover, it is known that CS precipitates at pH above 6.5. Since the CS matrix itself is undergoing

such drastic changes, the presence of CD did not have any significant effect on the drug releasing behaviour of CS-IC hydrogel.

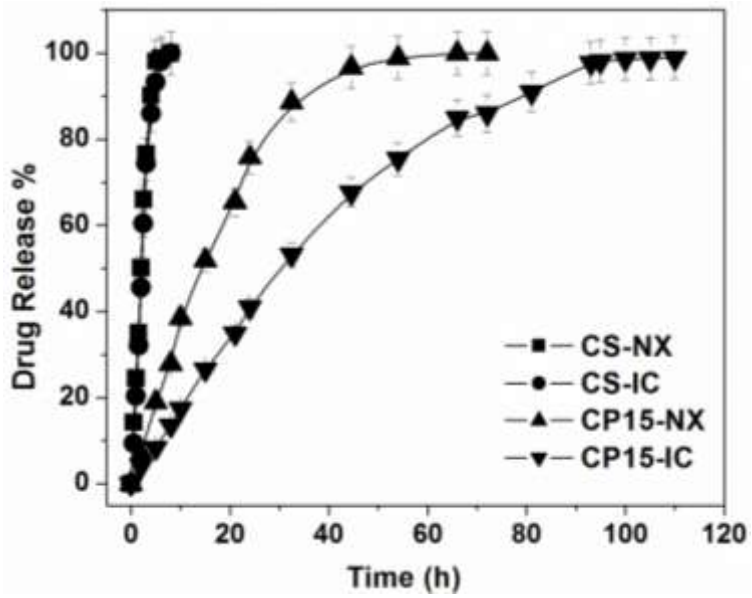

Figure 4.19. Drug release profiles of CS-NX, CS-IC, CP15-NX and CP15-IC hydrogels in pH 7.4 and at 37°C.

The drug release from the IPN hydrogels (CP15-NX and CP15-IC) was much prolonged as compared to the pure CS-NX and CS-IC hydrogels. The CP15-IC hydrogel released the drug at a much slower rate as compared to the CP15-NX hydrogel. The release of drug from a hydrogel is essentially because of swelling, polymer relaxation and diffusion of drug from the swollen matrix. However, for the CP15-IC hydrogel another important factor that needs to be considered is the strong binding (K_b = 1.67(8) × 10^3 M^{-1}) of the drug with CD. Thus for drug release process to be accomplished from CP15-IC hydrogel, the bound NX must first be released to the polymer matrix followed by the diffusion of the free drug. Again the presence of CD also influences the polymer relaxation, which in turn can affect the drug release rate. It is quite evident that at any given time the free drug concentration is considerably lower when CP15-IC is employed than CP15-NX.

The effect of PVA content on the rate of NX release from the hydrogels was also investigated. Figures 4.20 A and B illustrate that the rate of drug release from the hydrogels show significant dependence on the PVA content.

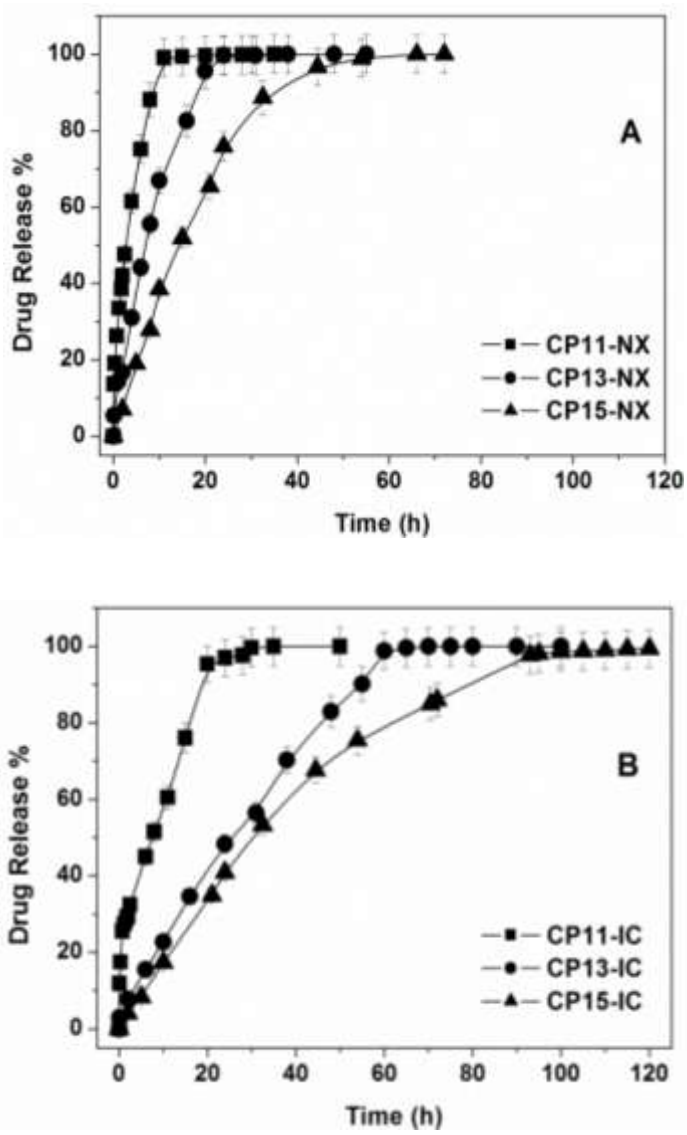

Figure 4.20. Drug release profiles of (A) CP11-NX, CP13-NX, CP15-NX and (B) CP11-IC, CP13-IC, CP15-IC hydrogels in pH 7.4 at 37°C.

As the PVA content increases, the rate of drug release decreases. This can be explained by considering the dependence of rate of release of drug from the swollen hydrogels on the nature of the hydrogel matrix. Due to increased PVA content the hydrogel changes from a porous to a denser matrix and the swelling rate decreases, which inhibit the faster release of the drug. Similar results were also obtained for the

IC incorporated hydrogels. The effect of PVA content is more pronounced in the IC containing hydrogels. This can be due to the synergistic effect of the added CD and increased PVA content on the hydrogel matrix density, hence reducing the free volume available for the drug diffusion, which in turn decreases the release rate. The CP15-IC hydrogel was found to be the best among all the synthesized hydrogels for controlled delivery of NX.

The drug release behaviour of the hydrogels was also studied in different pH conditions owing to their pH-responsive nature. Figure 4.21 depicts the drug release pattern from CP15-IC hydrogel in pH 7.4 and pH 1.2 media at 37°C

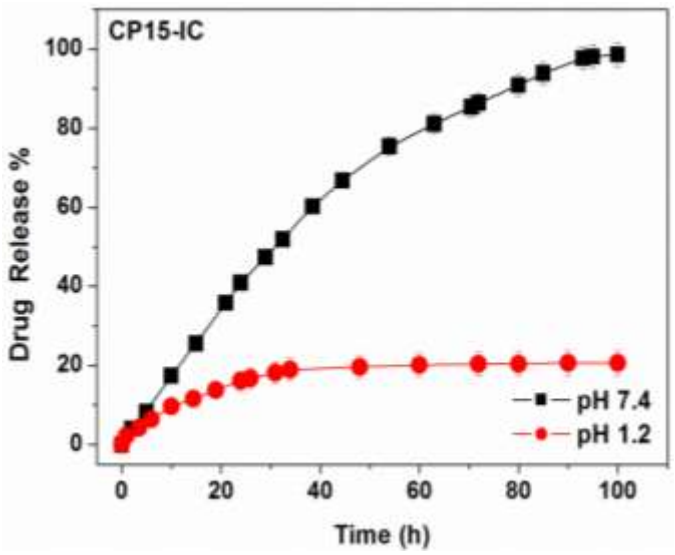

Figure 4.21. Drug release profiles CP15-IC hydrogels in pH 7.4 and pH 1.2 media at 37°C.

The maximum amount of NX released in pH 1.2 is much lower than that in pH 7.4 even after prolonged exposure of the CP15-IC hydrogel to the releasing medium. This indicated the pH sensitivity of the hydrogels which can be utilized to emulate the conditions of the GIT for the delivery of NX.

For further simulating the GIT conditions; CP15-NX and CP15-IC hydrogels were immersed in the SGF for 2 hours, then they were transferred to the SIF and the drug release was monitored. Figure 4.22 depicts the release pattern of NX from CP15-NX

and CP15-IC hydrogels in SGF and SIF conditions. Less than 5% of NX is released from CP15-NX and CP15-IC hydrogels during the initial 2h in SGF. However, when the hydrogels were transferred to the SIF the amount of NX release increased gradually. This release profile fulfils the requirements of USP XXIV, according to which, maximum 10% release in SGF is acceptable for the oral delivery of drug.

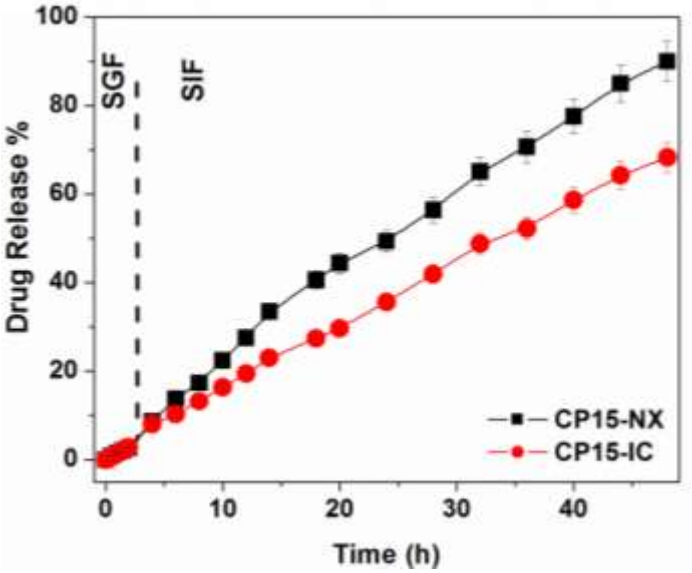

Figure 4.22. Drug release profiles of CP15-NX and CP15-IC hydrogels in SGF and SIF at 37°C.

Comparing all the release data, it is found that NX release is much more controlled from CP15-IC than any other hydrogel and at any given time the free drug concentration is considerably lower when CP15-IC is employed. Thus, it can be proposed that the deleterious effects of NX on the epithelium of the GIT could be minimized by using the CP15-IC as a DDS given that it provides a controlled release resulting in a reduced concentration of free NX. Again the pH-specific release of NX from these hydrogels can be utilized for the intestinal-targeted delivery of NX.

Controlled Delivery of Diclofenac Sodium from CS−PVA IPN Hydrogels

4.5 CS−PVA IPN Hydrogels as Controlled Release Platforms for Delivery of DS

DS is another important NSAID advocated for its use in rheumatoid arthritis, degenerative joint disease, ankylosing spondylitis and allied conditions, and in the treatment of pain resulting from minor surgery, trauma and dysmenorrhoea. DS has been demonstrated to have antipyretic activity and to be an effective analgesic in patients with rheumatoid arthritis or pains of varying origin. DS is also known to be quite an effective antibacterial agent (Mazumdar *et al.,* 2009). It exhibits remarkable inhibitory action against both drug-sensitive and drug-resistant clinical isolates of various Gram-positive and Gram-negative bacteria. The antibacterial action of DS has been attributed to its inhibition towards bacterial DNA synthesis (Dutta *et al.,* 2007). Though DS has better tolerability than moderate doses of NX, gastrointestinal side effects such as peptic ulceration, bleeding *etc.* are the most frequently reported adverse effects. Also, the very low aqueous solubility of DS, especially in gastric juice (about 15µg/ ml) causes deleterious effects on the gastric mucosa when orally administered. Its biological half-life is very short, about 1−2 h. Thus controlled delivery of DS to the intestine is generally warranted to reduce its adverse side-effects and improve its properties for better therapeutic outcome. Complexation of DS with CD has been reported to enhance the various physico-chemical properties of the drug (Manca *et al.,* 2005). The excellent performance of CS−PVA hydrogels towards the delivery of NX encouraged us to examine the hydrogels for the controlled delivery of DS to the intestine. For this the DS−CD ICs were prepared and loaded to the CS−PVA hydrogels and their drug releasing profiles were studied.

4.5.1 Inclusion Studies of DS in CD

Prior to the preparation of the solid ICs of DS and CD, the interaction of DS with CD was first studied by UV-Vis spectroscopy.

4.5.1.1 UV−Vis Study

Figure 4.23 illustrates the absorption spectrum of DS as a function of CD. DS exhibits a characteristic absorption peak at 272 nm (Figure 4.24 A).

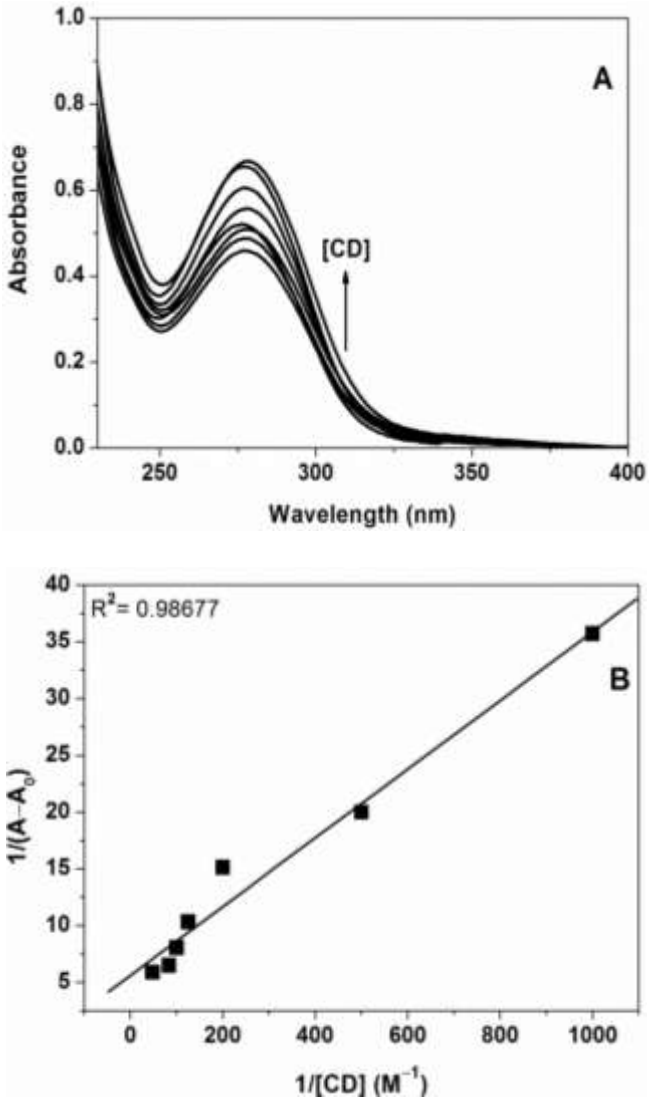

Figure 4.23. (A) Absorption spectra of DS at varying concentrations of CD, [DS] = 5×10^{-5} M, [CD] = $0–20\times10^{-3}$ M, pH=7.4 and (B) Benesi-Hildebrand plot for DS-CD interaction.

The absorbance was found to increase gradually with the step-wise addition of CD. A slight blue shift was observed in the spectra upon the increase in CD content. This

could be due to the inclusion of the drug into the hydrophobic CD cavity. From this study, the interaction of DS with CD was established. The K_b was calculated from the absorption data and found to be around 185 M^{-1} (Figure 4.24 B).

In order to know the stoichiometry of interaction of DS with CD, phase solubility studies were further carried out.

4.5.1.2 Phase Solubility Studies

The phase solubility plot of DS−CD binary system is shown in Figure 4.24. As clearly evident, the aqueous solubility of the drug increased linearly as a function of CD. This type of phase solubility profile can be considered as A_L type, thereby suggesting a 1:1 stoichiometry according to Higuchi and Connors (1965). The value of the stability constant was found to be 172 ± 4 M^{-1}. The value of the stability constant obtained in the range of 100 and 1000 M^{-1} is considered an ideal value, since smaller values are indicative of poor interaction between drug and CD while larger values suggest incomplete drug release from the IC (Mohit *et al.,* 2010).

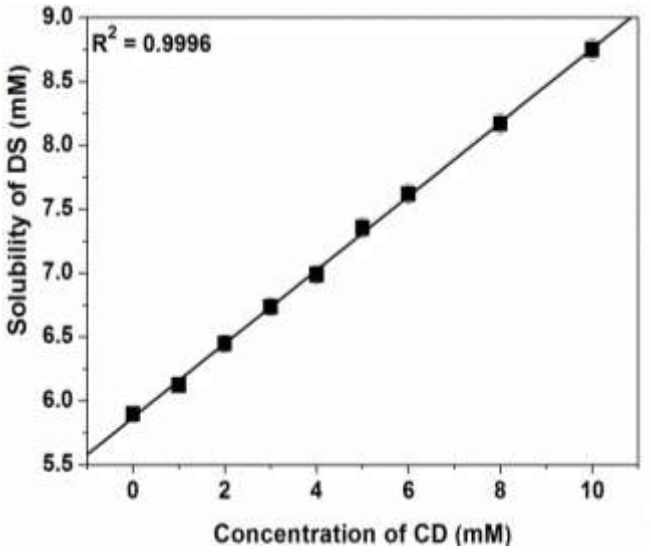

Figure 4.24. Phase solubility profile of DS−CD in water.

The solid ICs of DS with CD were prepared in 1:1 molar ratio by freeze drying method and the formation of IC was affirmed from various analytical techniques.

4.5.1.3 FTIR Analysis

Figure 4.25 represents the FTIR spectra of CD, DS, PM and IC. The most important peak of DS was observed at 1600 cm^{-1} which is attributed to the carbonyl stretching. The FTIR spectrum of the PM exhibited both the characteristics features of CD and DS.The spectrum was found to be the superposition of the parent components. However, in the FTIR spectrum of IC, the characteristic peak of DS was totally absent. Even the C−H stretching band was shifted in the IC (2921 cm^{-1} in CD; 2942 cm^{-1} in IC). These modifications in the IC are indicative of the entrapment of the drug inside the CD cavity (Manca *et al.,* 2005).

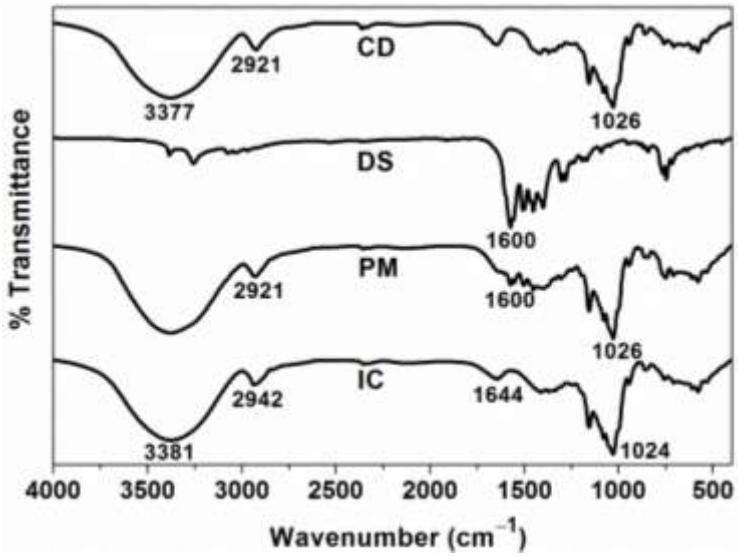

Figure 4.25. FTIR spectra of CD, DS, PM and IC.

4.5.1.4 XRD Analysis

Figure 4.26 presents the wide-angle XRD profiles of CD, DS, PM and IC. The CD and DS diffractograms display a series of sharp intense which reveal their crystalline nature. The diffraction profile of the PM revealed the features of both CD and DS which suggests that no new crystal has been formed. The diffraction profile of IC revealed a somewhat amorphous nature due to the freeze drying method of

preparation. The diffraction profile of the IC is completely different from the parent compounds. Thus the formation of an IC is also supported by the XRD data.

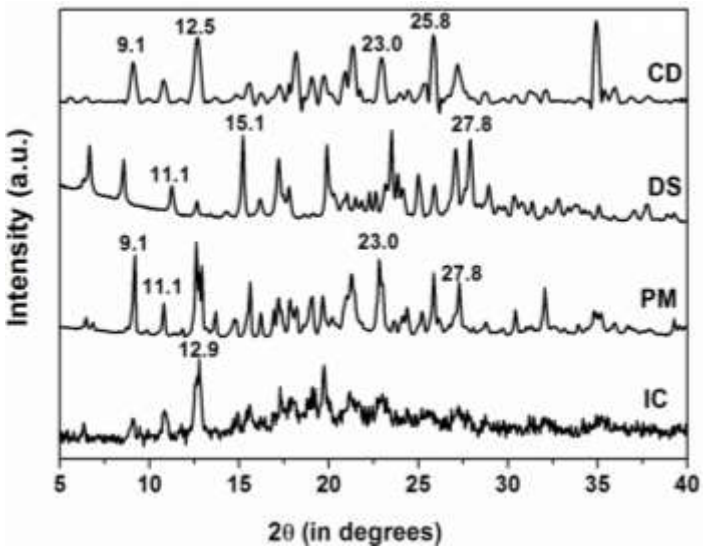

Figure 4.26. XRD profiles of CD, DS, PM and IC.

4.5.1.5 DSC Analysis

The DSC curves of CD, DS, PM and IC are illustrated in Figure 4.27. The thermogram of DS showed a sharp peak at 280°C indicating its melting point. The PM exhibited both the melting traces of CD and DS. The thermogram of IC revealed the total disappearance of the drug melting peak and a shift in the CD peak. The absence of drug peak in the IC signified the inclusion of DS in CD cavity.

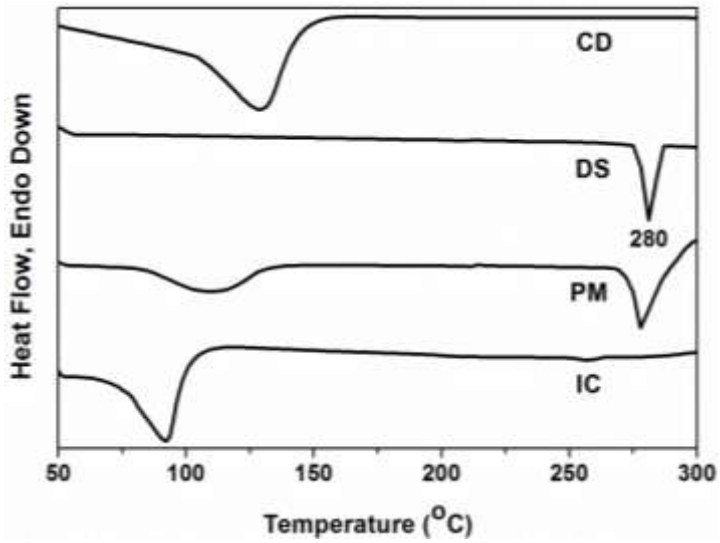

Figure 4.27. DSC thermograms of CD, DS, PM and IC.

4.5.1.6 SEM Analysis

SEM is a qualitative method to study the morphological aspects of CD and drugs and inclusion products The SEM images of CD, DS, PM and the IC are displayed in Figure 4.28.

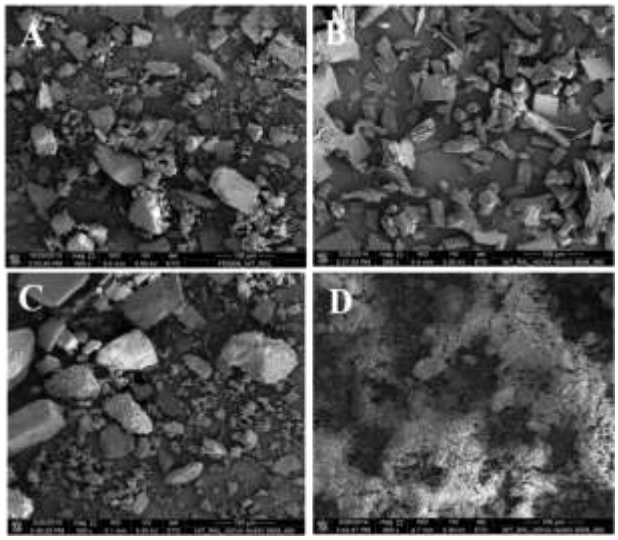

Figure 4.28. SEM images of (A) CD, (B) DS, (C) PM and (D) IC.

The particles of CD (Figure 4.28 A) and DS (Figure 4.28 B) were found to be highly crystalline in nature. The SEM image of PM (Figure 4.28 C) reveals that it is composed of both the particles of CD and DS. The SEM image of IC (Figure 4.28 D) however was found to be very different from the parent compounds and the sample appeared flaky in nature. Thus the formation of a new entity is also verified from the SEM images.

4.5.1.7 ^{1}H NMR analysis

The ^{1}H NMR spectra of CD, DS and the IC collected in D_2O at 25°C, are illustrated in Figure 4.29 A. Figure 4.29 B clearly demonstrates the differences in the positions of the protons in CD and IC while Figure 4.29 C displays the differences in the positions of protons of DS and IC. The values of chemical shifts δ, for the protons of CD and those of the IC were calculated and listed in Table 4.4.

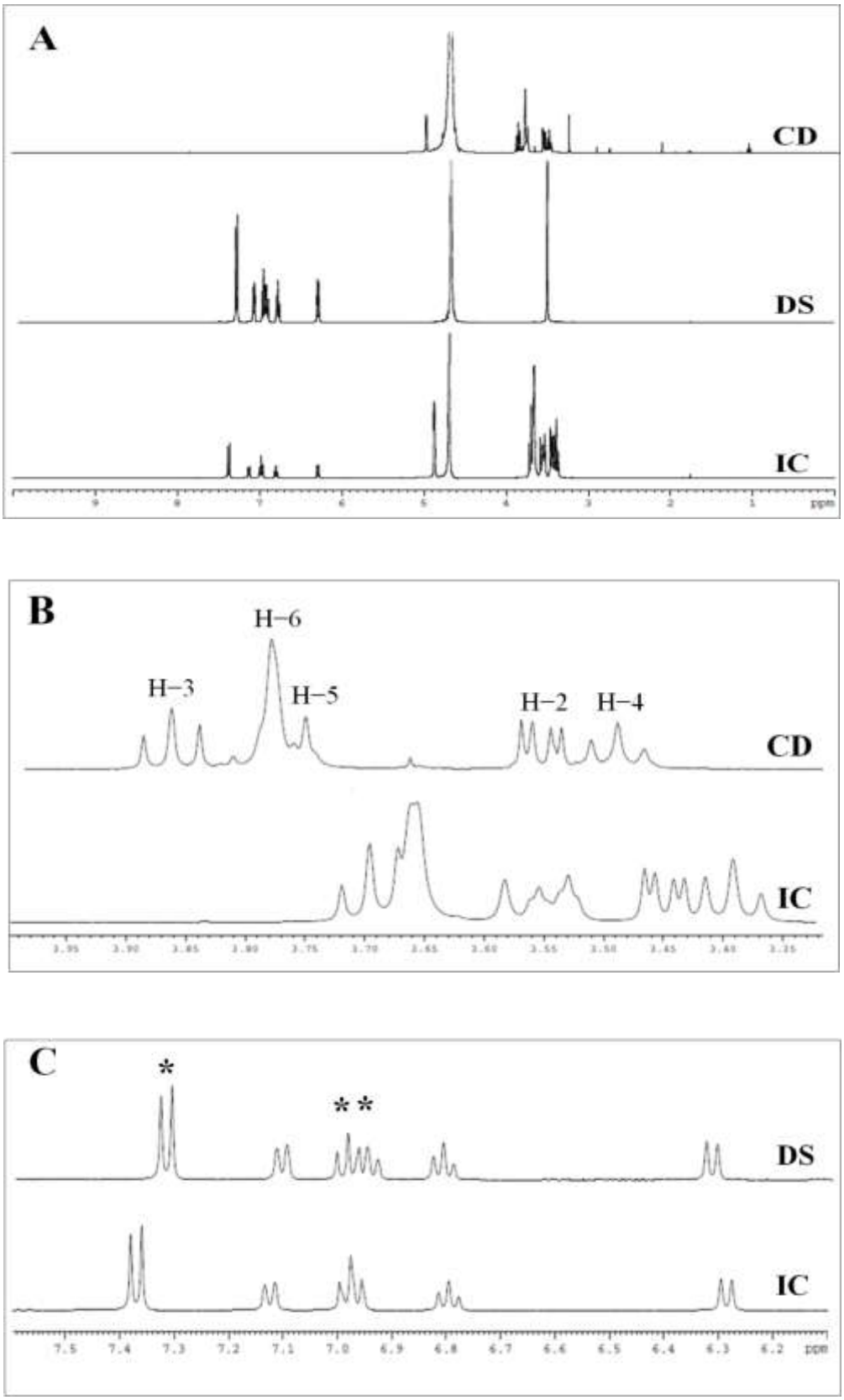

Figure 4.29. ^{1}H NMR spectra of (A) CD, DS and IC; Partial ^{1}H NMR spectra of (B) CD and IC; (C) DS and IC in D_2O at 298 K; * and ** represent the phenylacetic and dichlorophenyl protons of DS, respectively.

Table 4.4. δ and Δδ of protons in CD and DS-CD IC

Proton	δ_{CD}	δ_{IC}	$\Delta(\delta_{CD}$ and $\delta_{IC})$
H−1	4.991	4.881	0.110
H−2	3.561	3.447	0.114
H−3	3.874	3.696	0.178
H−4	3.496	3.389	0.107
H−5	3.761	3.529	0.232
H−6	3.790	3.658	0.132

By comparing the differences in the chemical shifts of the H−3 and H−5 protons of CD and IC; total inclusion of drug in CD cavity was evident. Molecular simulation studies by Abdoh and authors (2007) have also revealed similar possibility of total inclusion of DS in CD cavity.

The inclusion phenomenon was also confirmed by comparing the chemical shifts of the protons of DS and that of IC (Figure 4.29 C). The phenylacetic protons of DS (≈ 7.298 ppm) exhibit downfield shifts upon inclusion with CD (≈ 7.373 ppm in IC). This indicates the effective encapsulation of this moiety into the CD cavity. Also, the dichlorophenyl protons of DS (6.985−6.912 ppm) show downfield shifts in the ^{1}H NMR spectrum of IC suggesting the inclusion of this group. Thus the ^{1}H NMR spectral studies confirms the formation of an IC.

4.5.2 DS Release Studies

Figures 4.30 A and B illustrate the drug release profiles of CP11, CP13 and CP15 hydrogels containing DS and the IC, respectively. The drug release from the CP11-DS, CP13-DS and CP15-DS hydrogels were found to be very rapid in comparison to CP11-IC, CP13-IC and CP15-IC hydrogels. For the CP11-DS hydrogel, almost 80% of the drug has been released in the initial 5 h. On the other hand, the drug release amounted to a mere 40% from the CP11-IC hydrogel in the same time span. Similar type of slow drug release was also observed from CP13-IC and CP15-IC hydrogels with respect to CP13-DS and CP15-DS hydrogels. Since DS is in the bound state in

the IC (K_b =172 M^{-1}), it offers an additional diffusional barrier for the drug release to be accomplished from CP11-IC, CP13-IC and CP15-IC hydrogels, which delays the release time, and a slow release is witnessed from these hydrogels containing the ICs.

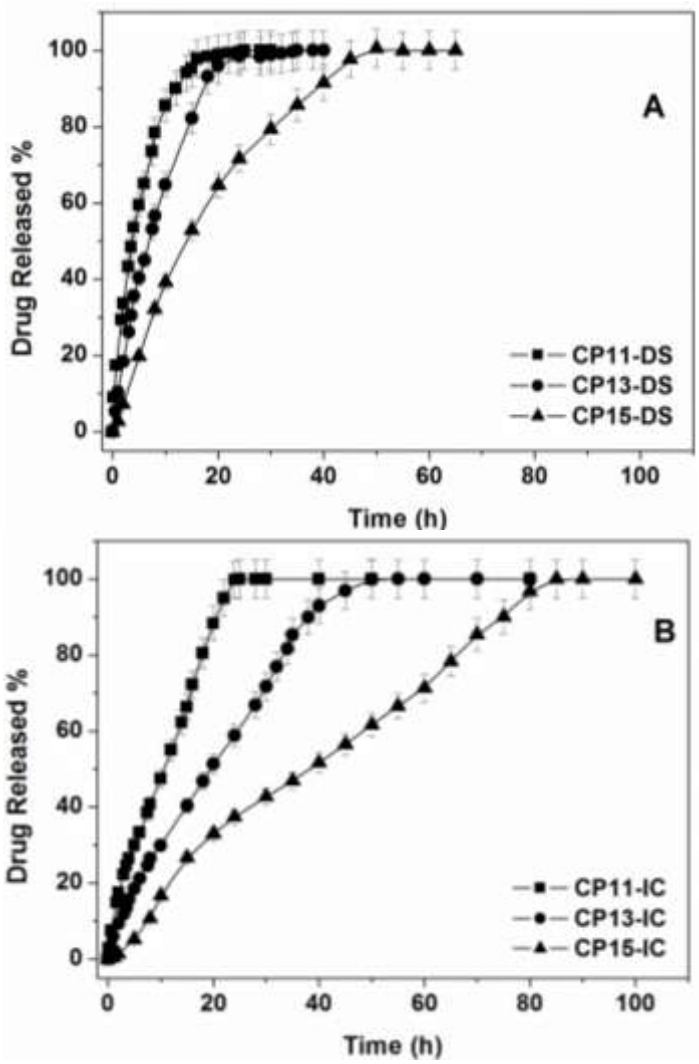

Figure 4.30. Drug release profiles of (A) CP11-DS, CP13-DS, CP15-DS; (B) CP11-IC, CP13-IC, CP15-IC hydrogels in phosphate buffer (pH 7.4) at 37°C.

The dependence of the rate of drug release on the PVA content in the hydrogels is also demonstrated from Figures 4.30 A and B. As the PVA content was gradually increased, the rate of drug release was found to decrease accordingly. Similar effect of PVA was also observed in case of NX release from these hydrogels. The rate of drug release from the hydrogels containing either the free DS or the IC was found to decrease in the order of CP11 > CP13 > CP15. However, at any time, the amount of

DS released was always less in case of the hydrogels containing the ICs. The CP15-IC hydrogel was found the best of the lot with the slowest drug releasing characteristics.

In order to study the effect of pH on the drug release phenomenon, experiments were carried at two different pHs of 1.2 and 7.4.

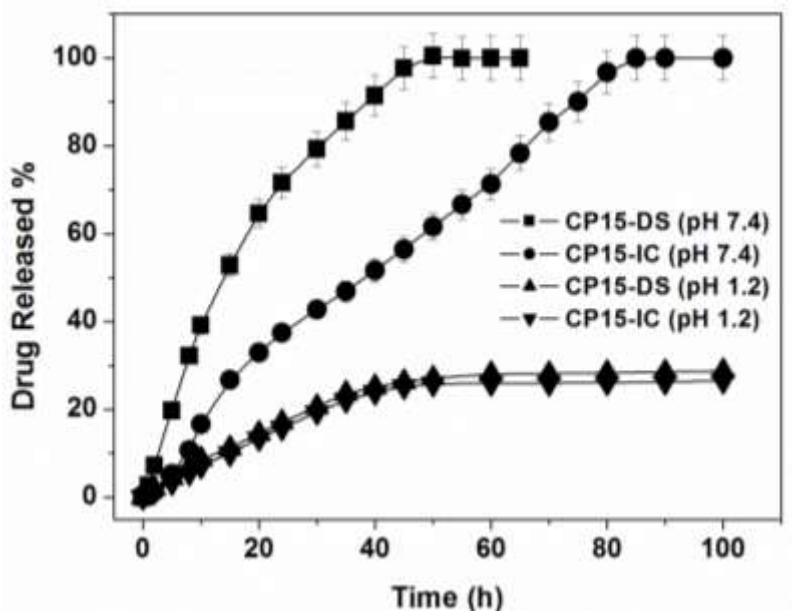

Figure 4.31. Drug release profiles of CP15-DS, CP15-IC at pH 1.2 and pH 7.4 and 37°C.

Figure 4.31 shows the drug release profiles from CP15-DS and CP15-IC hydrogels at pH 7.4 (phosphate buffer) and pH 1.2 (dilute HCl) and 37°C. At pH 1.2, the amount of DS released was much lower than the release amount at pH 7.4, even upon prolonged exposure to the releasing medium. This can be attributed to the difference in extent of swelling of these hydrogels in the above two pH conditions. The evaluation of the swelling parameter had revealed the higher swellability of the hydrogels in pH 7.4 medium and a relatively lower swelling in acidic (pH 1.2) medium. Since normal gastric emptying time is about 2 h, it is desirable for negligible or very low drug release during this period for targeting the drug release in the intestine. The drug release profile of the CP15-IC hydrogel in pH 1.2 clearly displays negligible drug release occurring here in the initial time period. Thus, the pH-sensitive release

characteristics of the CP15-IC hydrogels indicate its potential for controlled delivery of DS to the intestine.

To further confirm this, the drug release study was carried out in simulated fluids mimicking the GIT condition. Figure 4.32 depicts the release pattern of DS from CP15-DS and CP15-IC hydrogels in SGF and SIF conditions. Less than 5% DS is released from both the hydrogels during the initial 2h in SGF. But the amount of DS release increased significantly when the hydrogels were transferred to the SIF. This release profile fulfils the requisites of USP XXIV for the oral delivery of drug. It was also observed that the amount of DS released from CP15-IC hydrogel was always lower than CP15-DS hydrogel at any given time. Thus the potential of the CP15-IC hydrogel as an oral controlled delivery vehicle for delivery of DS to the intestine is well supported from the above studies.

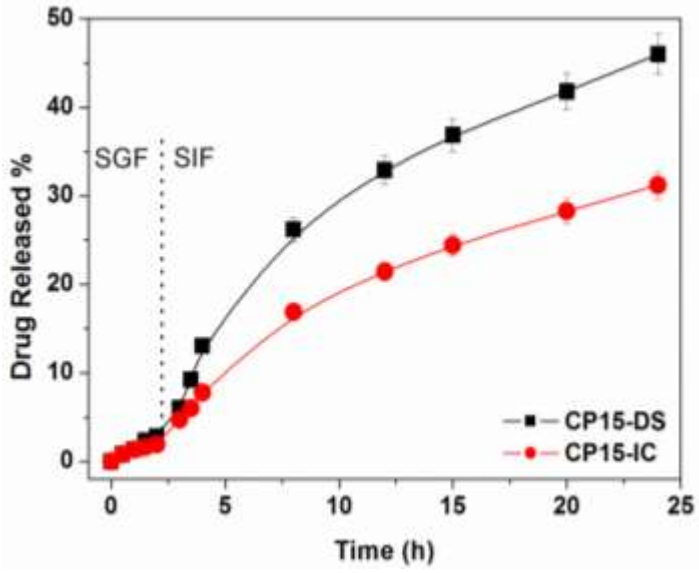

Figure 4.32. Drug release profiles of CP15-DS and CP15-IC in SGF and SIF at 37°C.

4.6 Drug Release Kinetics

Table 4.5 summarises the kinetic parameters for NX release data from the hydrogels. From the data analysis it was found that the naproxen release data showed the best fit to the Ritger−Peppas and Peppas−Sahlin equations in almost all the cases. For the CS-

NX and CS-IC hydrogels, the diffusional exponent (*n*) value was found to be 1.065 and 1.191 respectively, suggesting the super case II transport mechanism for the release of naproxen from these hydrogels. The relative contribution from the diffusion and relaxation processes calculated from the Peppas−Sahlin equation shows the predominant effect of the relaxation kinetic constant (k_2). The lower magnitude and negative values of k_1 indicate the non-significant diffusion process as compared to the relaxation mechanism. From the swelling studies it was observed that these hydrogels undergo extensive hydration and swelling in a very short period of time, which can be due to the rapid polymer relaxation followed by water diffusion. Thus, the drug release from these hydrogels is controlled mostly by relaxation rate of the polymer chains. Since Higuchi model is applicable to a purely diffusion controlled mechanism, the release data did not show good fit to this equation whereas they fitted reasonably well to zero-order kinetic equation. As the PVA content increased the value of the diffusional exponent (*n*) also increased for the hydrogels. For CP13-NX, CP15-NX, CP13-IC and CP15-IC the *n* values lie between 0.5 and 1 indicating the anomalous nature of drug release, where both diffusion and relaxation processes contribute. From the Peppas-Sahlin analysis it is found that for the CP11-NX and CP11-IC hydrogels the relaxation kinetic constant (k_2) values are negative indicating the non-significance of the relaxation process and the dominant effect of the Fickian diffusion mechanism in the drug release process. For the CP11-NX film, the release data fit well to the Higuchi model, which complies with the above observation. With increased PVA content both diffusion kinetic constant (k_1) and relaxation kinetic constant (k_2) become equally important. The release data from the CP15-NX and CP15-IC films in the SIF were also analyzed and the fitting parameters were found to be very similar to that of the respective films in the non-buffered solutions.

From Table 4.6, it was found that the DS release data showed the best fit to the Ritger-Peppas and Peppas-Sahlin equations in almost all the cases. The values of the diffusional exponent (*n*) lie between 0.6 and 0.8 indicating the anomalous nature of drug release, where both diffusion and relaxation processes contribute.

Table 4.5. NX release parameters fitting to various mathematical models

Sample	**Higuchi**		**Ritger–Peppas**			**Peppas-Sahlin**			**Zero-Order**	
	k ($h^{-0.5}$)	R^2	n	k' (h^{-n})	R^2	k_1 ($h^{-0.5}$)	k_2 (h^{-1})	R^2	k" (h^{-1})	R^2
CS-NX	0.337	0.868	1.065	0.243	0.999	−0.024	0.272	0.994	0.254	0.993
CS-IC (NX)	0.302	0.832	1.191	0.201	0.999	−0.090	0.295	0.999	0.229	0.990
CP11-NX	0.303	0.989	0.466	0.311	0.985	0.312	−0.006	0.989	0.186	0.717
CP13-NX	0.186	0.944	0.778	0.110	0.992	0.073	0.043	0.996	0.073	0.967
CP15-NX	0.124	0.902	0.855	0.050	0.991	0.031	0.025	0.992	0.033	0.983
CP11-IC (NX)	0.194	0.922	0.353	0.248	0.984	0.262	−0.026	0.971	---	---
CP13-IC (NX)	0.091	0.948	0.773	0.040	0.998	0.037	0.012	0.997	0.020	0.976
CP15-IC (NX)	0.086	0.901	0.898	0.023	0.998	0.014	0.014	0.997	0.016	0.991
CP15-NX (in SIF)	0.095	0.834	0.892	0.030	0.994	0.018	0.017	0.994	0.021	0.985
CP15-IC (in SIF)	0.078	0.834	0.924	0.019	0.999	0.011	0.013	0.999	0.015	0.994

Table 4.6. DS release parameters fitting to various mathematical models

Sample	**Higuchi**		**Ritger–Peppas**			**Peppas-Sahlin**			**Zero-Order**	
	k ($h^{-0.5}$)	R^2	n	k' (h^{-n})	R^2	k_1 ($h^{-0.5}$)	k_2 (h^{-1})	R^2	k'' (h^{-1})	R^2
CP11-DS	0.254	0.978	0.62	0.222	0.997	0.183	0.038	0.997	0.135	0.872
CP13-DS	0.183	0.917	0.75	0.116	0.995	0.007	0.046	0.992	0.072	0.946
CP15-DS	0.127	0.905	0.78	0.060	0.997	0.030	0.026	0.994	0.035	0.979
CP11-IC (DS)	0.145	0.954	0.68	0.101	0.997	0.091	0.018	0.997	0.049	0.900
CP13-IC (DS)	0.102	0.921	0.75	0.055	0.999	0.047	0. 148	0.999	0.026	0.942
CP15-IC (DS)	0.077	0.937	0.73	0.034	0.995	0.011	0.009	0.991	0.013	0.981

The ratio of the relaxational to the Fickian contributions (R/F) was calculated for the samples and plotted against the fraction of the drug released from the hydrogels.

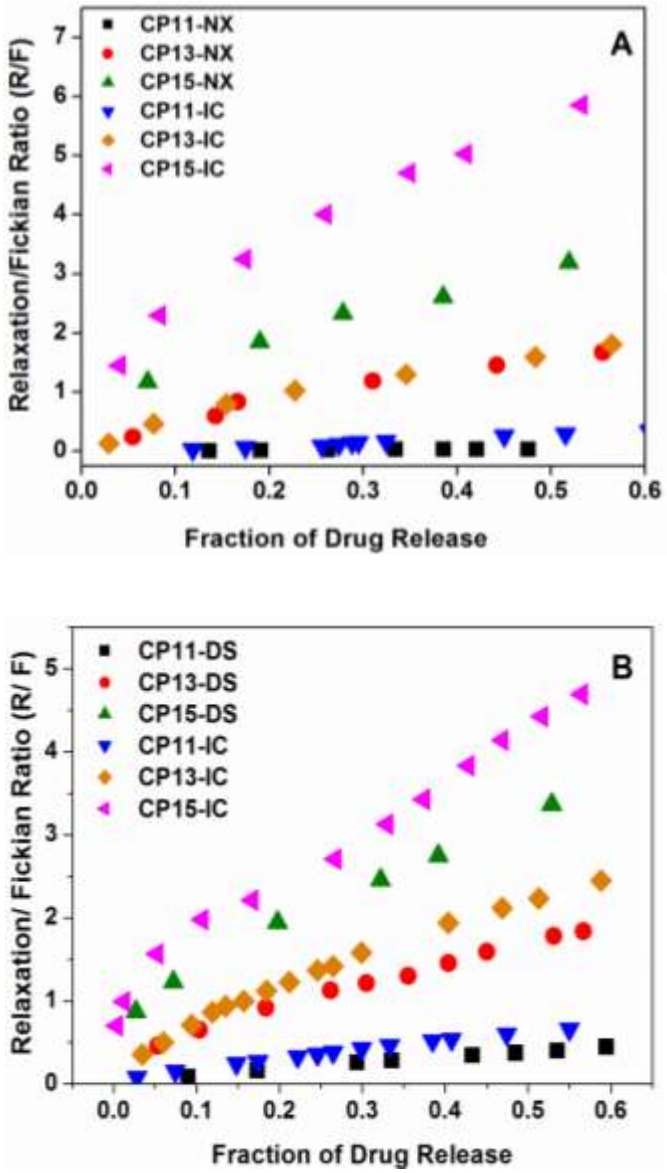

Figure 4.33. Plot of ratio of relaxation to the Fickian contribution (R/F) with the fraction of dug release for the hydrogels; (A) Naproxen and (B) Diclofenac sodium release.

It is quite evident that as the PVA content is increased the relaxation process prevails over the diffusion process. For a given PVA concentration the relaxation contribution was found to be higher for the CD containing film as compared to the one without the CD. Thus it could be inferred that the presence of CD influences the relaxation rate of the polymer chains, leading to slow release of the drug from the hydrogel matrix as

observed earlier in PVA hydrogels in chapter 3. This can be explained by considering either the presence of hydrogen bonding interaction between the CDs and polymers and/or the CDs getting cross-linked to some extent in the presence GA (Bibby *et al.*, 2000). Among all the hydrogels, the relaxation contribution was found to be maximum for CP15-IC hydrogel leading to an almost Case II type of transport, which is further supported by the fact that the release data from this film fit fairly well to the zero-order kinetics.

4.7 Cytotoxic Assay of Hydrogels

From the above studies, the CP15 hydrogel was found to be the most suitable for controlled delivery of the drugs. Since all the studies have been carried out *in vitro*, it is important to know whether this hydrogel would be compatible *in vivo*. Thus cytotoxic analysis of this hydrogel was assayed by MTT colorimetric technique and shown in Figure 4.34.

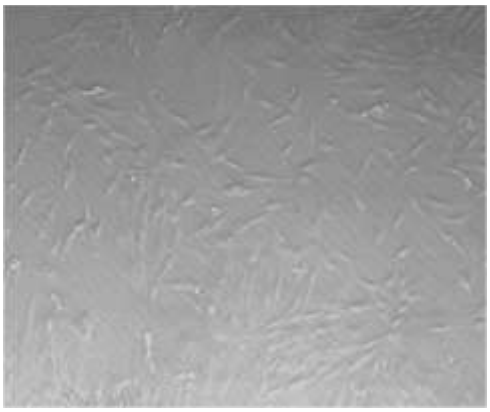

Figure 4.34. Optical micrographs of L-929 cells cultured after 48h incubation with CP15 hydrogel.

Direct contact between L-929 cells and the hydrogel did not reveal any adverse effect after 48 h incubation. This suggested the compatibility with the living tissues and non-toxicity of the hydrogel thus validating these as possible drug delivery systems.

4.8 CONCLUSIONS

- pH-Sensitive CS−PVA hydrogels, cross-linked with GA, with varying amount of PVA were synthesized and explored for the delivery of two NSAIDs.
- Solid ICs of NX and DS in CD were prepared. The inclusion phenomenon of the drugs in CD was confirmed by various analytical techniques.
- The hydrogels were characterized by FTIR, XRD, DSC and SEM analytical techniques.
- The hydrogels exhibited pH-responsive swelling characteristics and exhibited maximum swelling at neutral pH. With increased amount of PVA in CS−PVA hydrogels, the degree of swelling decreased due to increased hydrogel density. The presence of CD did not have any drastic effect on the swellability of the hydrogels.
- The antimicrobial activity of CS was not compromised in the presence of PVA and/or CD in the hydrogel.
- A remarkable controlled delivery of the drugs could be achieved from the hydrogels by incorporating preformed solid ICs.
- The hydrogels loaded with ICs showed less than 5% of drug release over a period of 2 h in SGF and upon transfer to SIF, the amount of drug released increased significantly.
- The preliminary kinetic analyses revealed that the presence of CD influences the relaxation rate of the polymer chains, leading to slower release of the drug.
- The pH-specific release from these hydrogels can be utilised for the intestinal delivery of NX and DS.
- The cytotoxic assay performed on the hydrogels ensured them to be nontoxic and biocompatible.

PART–II

CONTROLLED RELEASE OF DEXAMETHASONE FROM POLY(VINYL ALCOHOL)–POLY(ACRYLIC ACID) MICROSPHERES

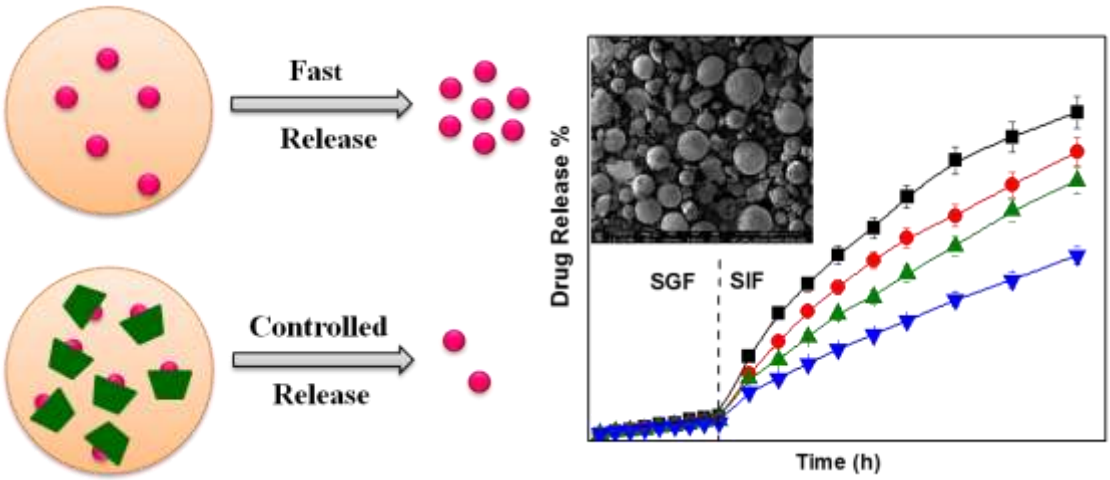

4.9 INTRODUCTION

With advances in genomics, combinatorial chemistry and biotechnology, a wide variety of potent therapeutics are being developed. Because of some common problems such as low solubility, poor stability and bioavailability of most of the drugs, new methods of drug delivery are constantly on the rise for their better administration (Vert *et al.,* 2012). The method of drug delivery can greatly impact the efficacy and the potential of commercialization. Thus there is a higher need for safe and effective methods/ devices for drug delivery. Drug delivery systems designed to provide therapeutics in the right amount, at the right location with minimal side effects and increased patient compliances have gained much attention.

While a myriad of formulations have been devised for controlled delivery of drugs, biodegradable polymeric microspheres are one of the most common types and hold various advantages. Microspheres are furnished with the exceptional property to encapsulate many types of drugs ranging from small molecules, proteins and nucleic acids. They can be ingested or injected and can be tailored for desired release profiles. They are usually biocompatible, provide high bioavailability and are capable of sustaining releases for longer periods of time (Freiberg and Zhu, 2004). Microspheres are characteristically free flowing powders and ideally having particle size less than 200 μm. Size is very crucial in delivery of therapeutics to the targeted site in a sustained and regulated fashion (Ma, 2014). The many advantages of microspheres in drug delivery include protection of unstable drugs prior to their availability at the target, enabling slow release of drug, improving the cellular interaction of the drug and ensuring uniform distribution in the tissues (Yan *et al.,* 2014). Polymeric microspheres can be made of either natural polymers such as CS, starch, GG, pectin, alginate, dextran, *etc.* or synthetic polymers like PVA, PAA, epoxy polymers, *etc.*

Several types of processes commonly used for the fabrication of microspheres include interfacial polymerization, solvent extraction/ evaporation, polymer extrusion, spray drying and coacervation or precipitation (Varde and Pack, 2004). The method of interfacial polymerization usually employs a mixture of monomer and an initiator which are polymerized in such a way that the growing polymer is constrained to form particles. This method involves suspension, emulsion and dispersion polymerizations. Emulsion-solvent extraction/ evaporation is one of the most extensively used methods to generate microspheres from preformed polymers. This method is widely accepted because of its relative ease. The extrusion method forms microspheres by forcing the raw components through an orifice or nozzle.

Controlled release microspheres have been used for a wide range of applications such as in vaccines, encapsulated protein therapeutics, DNA encapsulation *etc*. More so, their applications in drug delivery have greatly improved in recent years. Since it is often desirable for target-specific delivery of therapeutic agents, it is also important to understand the basic mechanism of drug release from microspheres. A complicated array of factors affect the rate of drug release from the microspheres which include the nature of the polymer, the molecular weight of the polymer, the copolymer composition, the nature of excipients added (for stabilization of the therapeutics) and the size of the microspheres (Varde and Pack, 2004; Dasan and Rekha, 2012).

- Polymer type: Depending on the rate of the hydrolysis, polymers can be classified as bulk-eroding and surface-eroding. Bulk-eroding polymers such as PLGA, readily allow the permeation of water into the matrix network. Thus, microspheres fabricated from bulk-eroding polymers degrade throughout the matrix and the drug is released to the surrounding medium from the spheres (Figure 4.35 A). Surface-eroding polymers are composed

of hydrophobic entities, *e.g.* polyanhydrides (Zhang *et al.*, 2003). These polymers resist the entry of water into the polymer bulk while degrading at the polymer/ water interface (Figure 4.35 B).

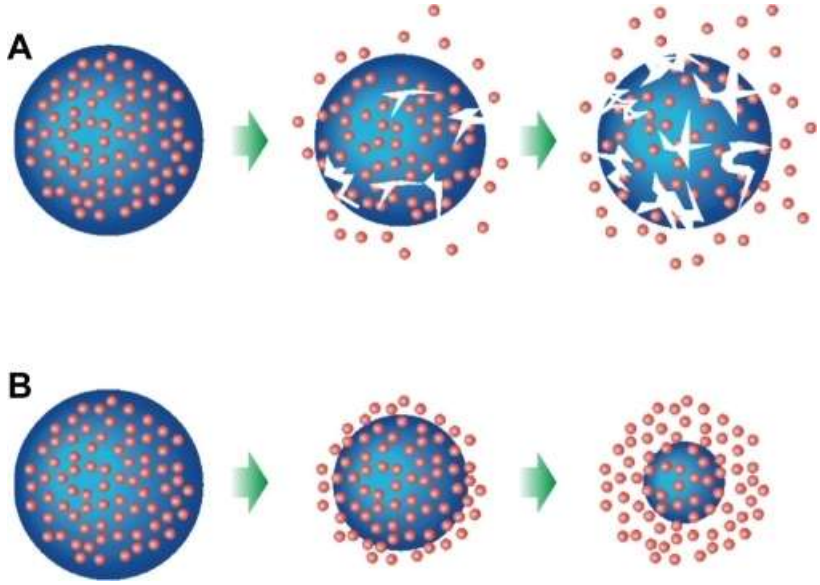

Figure 4.35. Polymer erosion and drug release from microspheres due to (A) bulk-erosion and (B) surface-erosion.

- Polymer molecular weight: Most of the studies agree that an increase in molecular weight decreases the rate of drug release from the microspheres (Le Corre *et al.*, 1994).
- Copolymer composition: Usually, in a copolymer, the relative ratio of each monomeric unit affects the relative release rate. Studies have indicated that increasing the content of the more rapidly degrading polymer enhances the release rate (Shen *et al.*, 2002).
- Drug-polymer interaction: Interactions between the encapsulated therapeutics and the polymeric microspheres may also influence the release rate. An attractive interaction will lead to slow release rate (Orienti *et al.*, 2001).

- Excipients: A range of excipients have been added to stabilise the emulsion during microsphere fabrication and also to stabilize the drug during the release (Jain *et al.,* 2000).
- Microsphere size: The effect of microsphere size on the release rate is significantly complicated. In general, as the size of the microsphere decreases, the surface area-to-volume ratio increases. Thus, the rate of flux of drug out of the sphere matrix will increase with decreasing particle size (Berkland *et al.,* 2003).

Hydrogels composed of natural polysaccharides such as CS or synthetic polymers like PAA and poly(methacrylic acid) have been employed in the fabrication of pH-sensitive formulations for intestine targeted delivery (Qiu and Park, 2001). Literature suggests overwhelming researches devoted to microsphere formulations and subsequent applications in drug delivery. IPN microspheres of locust bean gum and PVA have been developed by Kaity *et al.,* (2013) by the emulsion cross-linking method using GA as cross-linker and explored for the controlled delivery of the drug buflomedil hydrochloride. Semi-IPN microspheres of dextran-g-acrylamide and PVA have been synthesized and utilized for delivery of abacavir sulphate (Sullad *et al.,* 2011). The utility of microspheres in controlled drug delivery has been briefly reviewed by Dasan and Rekha (2012).

PAA finds great applications as a synthetic pH-sensitive polymer for drug delivery purposes because of its strong mucoadhesive and biocompatible properties. The mucoadhesive properties of PAA make it quite suitable for increasing the residence time of the device at the absorbing tissue thereby increasing the drug bioavailability (Cheddadi *et al.,* 2011). However, the application of pure PAA is limited because of the fast release of the drug due to its extensive swelling in water. Moreover, PAA tend

to dissolve at high pH solution. The most commonly used strategy to alleviate the inherent drawbacks of PAA is to prepare three-dimensional polymeric network by physical or chemical cross-linking or incorporation of PAA in an IPN with other polymers such as PVA, PEG, CS *etc.* (Abd El-Rehim *et al.,* 2007). Hydrogels based on PVA and PAA have emerged as promising materials in biomedical applications due to their highly tunable chemical and physical properties. pH-responsive hydrogel microspheres from the blends of PVA with AAc-g-guar gum matrices were synthesized for the controlled delivery of isoniazid (Sullad *et al.,* 2010). Higher drug release was evidenced in pH 7.4 than pH 1.2 media and the hydrogels were found to be suitable for the oral delivery of the drug. Park and others (2003) studied the release behaviour of insulin from pH-sensitive poly(vinyl alcohol-g-methacrylic acid) and poly(vinyl alcohol-g-acrylic acid) hydrogels prepared by gamma irradiation. The hydrogels sustained insulin release in SIF thus affirmed the oral delivery of insulin. PVA-PAA IPN hydrogels and microspheres have been prepared by Ray *et al.,* (2010) and compared for the controlled delivery of diltiazem HCl. The results demonstrated that the hydrogel microspheres had better potential than the normal hydrogel to be employed as drug carrier.

In this regard, evaluation of PVA-PAA microspheres containing drug-CD ICs towards controlled delivery of DX appears exciting. DX is one of the most preferred corticosteroid to treat inflammatory bowel disease, Crohn's disease and ulcerative colitis, which need its topical administration and often administered as enema. But in this method the drug gains access only to the rectum and the descending colon. Therefore, a number of approaches are being developed to deliver steroids to the intestine and colon *via* the oral route (McLeod *et al.,* 1994; Fedorak *et al.,* 1995). While DX is highly active in the treatment of virtually every type of B-cell

malignancy, significant side-effects such as immunosuppression, hyperlipidemia, proximal muscle wasting and osteoporosis are invariably associated with it (Mao *et al.*, 2013; Lasa *et al.*, 2001). In addition, it is a lipophilic drug (log *P* = 1.9) with extremely low aqueous solubility (0.16 mg/ml). As a result the bioavailability of DX is lowered and its efficiency is hindered (Cavalli *et al.*, 2006). Thus the formulation for this drug particularly is more challenging and warrants a delivery system that can deliver DX at a controlled rate to the specific site.

OBJECTIVES

With this rationale, we aimed at designing a delivery system for controlled delivery of DX to the intestine. To achieve specific delivery to the intestine, pH-sensitive hydrogel microspheres comprising of PVA and PAA were synthesized using GA as cross-linker by free radical polymerization and sequential IPN technology. The solid ICs of DX with CD were added to the hydrogel matrix in order to get a controlled release. The physico-chemical properties of the drug-CD ICs have been found to be strongly dependent on the method of preparation (Priya *et al.*, 2013; Chadha *et al.*, 2011; Mohit *et al.*, 2010; Manca *et al.*, 2005). Therefore, in this regard, it would be interesting to find out the influence of the method of preparation of IC on the drug release process from the synthesized PVA-PAA hydrogel microspheres.

The specific objectives of the present study comprise:

- Preparation of DX-CD solid ICs by co-precipitation and freeze-drying methods.
- Characterization of the solid ICs and the PM by FTIR, XRD, DSC, SEM and ^{1}H NMR spectroscopic techniques.
- Synthesis of pH-sensitive sequential IPN hydrogel microspheres comprising of PVA and PAA using GA as cross-linker and their characterization.

- Exploring the drug delivery efficacy of the microspheres containing the ICs, free DX and PM, in phosphate buffers and also in simulated fluids.
- Investigating the influence of the method of preparation of the inclusion complex on the drug release phenomenon from the microspheres.
- A look at the preliminary kinetics of the drug release phenomenon from the microspheres and the mechanism of drug transport.
- Assay of the cytotoxicity and biocompatibility of the synthesized microspheres on L−929 rat cells by MTT colorimetric technique.

The designation and compositions of the synthesized microspheres are listed in Table 4.7.

Table 4.7. Composition and designation of PVA−PAA microspheres

Sample	Composition	Designation
1	PVA−PAA	MS1
2	PVA−PAA−DX	MS2
3	PVA−PAA−PM	MS3
4	PVA−PAA−CP	MS4
5	PVA−PAA−FD	MS5

The amount of DX released was estimated spectrophotometrically by observing absorbance value at λ_{max} = 242 nm and comparing with the calibration plot.

4.10 RESULTS AND DISCUSSION

4.10.1 Characterization of Solid DX-CD ICs

The solid ICs of DX with CD were prepared by co-precipitation and freeze-drying methods. The formation of ICs was confirmed from the analyses of various analytical techniques.

4.10.1.1 FTIR Analysis

Figure 4.36 shows the FTIR spectra of CD, DX, PM, CP and FD. The key DX (Figure 4.36 b) peaks are observed at 1662 cm^{-1} (C=O vibration) and 1610 cm^{-1} (C=C vibration). The PM (Figure 4.36 c) exhibited a spectrum corresponding to the superposition of parent components. However the FTIR spectrum of both the inclusion products (CP and FD) showed shifts in the characteristics hydroxyl and carbonyl absorption positions. A shift in the hydroxyl absorption position from 3377 cm^{-1} to 3392 cm^{-1} and 3348 cm^{-1} in the spectral profiles of CP (Figure 4.36 d) and FD (Figure 4.36 e), respectively was evident. Similarly the carbonyl stretching in CP and FD were observed at 1664 and 1658 cm^{-1}, respectively. These spectral shifts in the CP and FD indicated the encapsulation of DX in CD cavity due to the formation of ICs (Vianna *et al.*, 1997; Doile *et al.*, 2008).

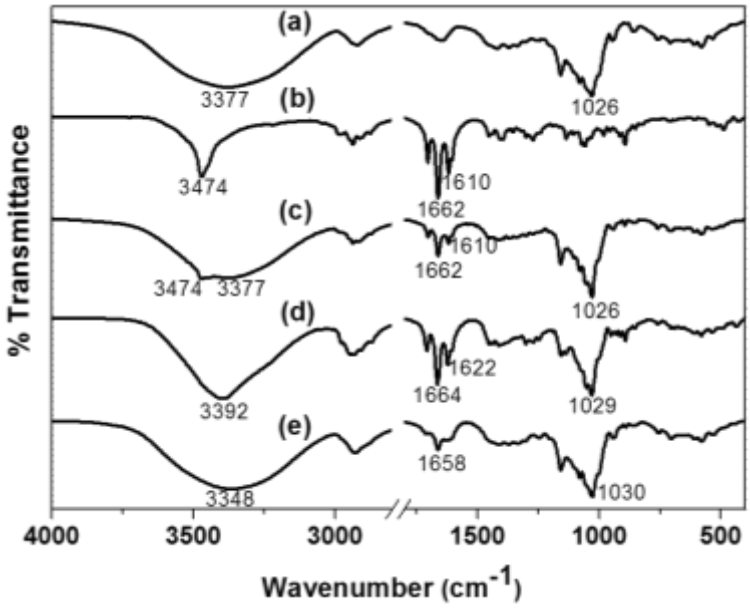

Figure 4.36. FTIR spectra of (a) CD, (b) DX, (c) PM, (d) CP and (e) FD.

4.10.1.2 XRD Analysis

Figure 4.37 presents the wide-angle XRD profiles of CD, DX, PM and the CP and FD inclusion products. The CD (Figure 4.37 a) and DX (Figure 4.37 b) diffractograms display a series of intense peaks indicating their crystalline nature. DX exhibited sharp

peaks at 2θ of 13.66°, 15.5° and 17.81° which represent the highly crystalline nature of the drug. The diffraction profile of the PM (Figure 4.37 c) revealed the features of both CD and DX suggesting that no new crystal has been formed. On the contrary, the diffractograms of CP and FD exhibited completely different features relative to the parent components. CP (Figure 4.37 d) presented new and distinct peaks at 6.72°, 13.42° and 20.13° which propose that highly crystalline particles of the inclusion complex have been formed in this method. The diffraction profile of FD (Figure 4.37 e) showed a somewhat amorphous nature of these particles in comparison to CP particles. It has been seen that the freeze-drying method of preparation of IC generally results in the amorphization of drug (Riekes *et al.*, 2007).

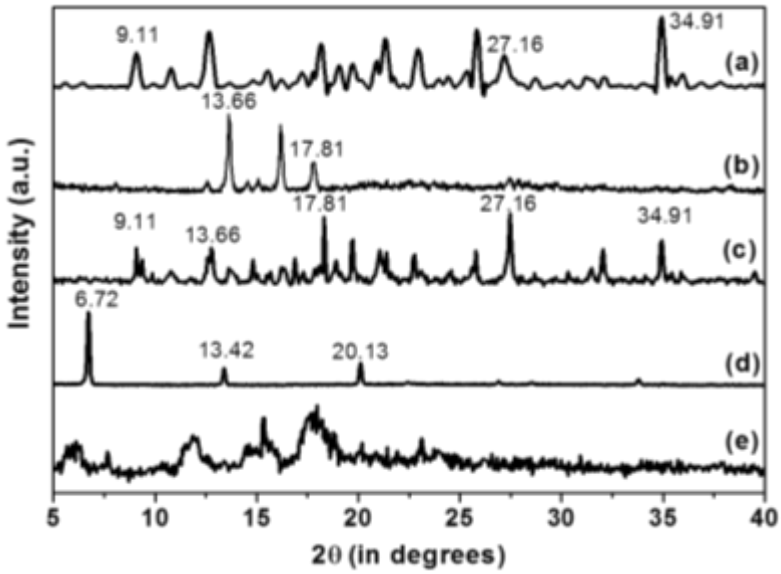

Figure 4.37. XRD profiles of (a) CD, (b) DX, (c) PM, (d) CP and (e) FD.

4.10.1.3 DSC Analysis

The DSC thermograms of CD, DX, PM, CP and FD are shown in Figure 4.38. The DSC curve of CD (Figure 4.38 a) showed a broad endothermic effect around 130°C which is associated with its dehydration process. The thermogram of DX (Figure 4.38 b) was typical of a crystalline anhydrous substance with a sharp endotherm around 270°C indicating its melting point. For the PM (Figure 4.38 c), the

endotherms corresponding to both the dehydration of CD and DX melting were observed. The DSC curves for CP and FD (Figure 4.38 d and e respectively) revealed the disappearance of the DX melting peak and only the peak from CD was observed. These results signified the inclusion of DX in CD cavity in the CP and FD.

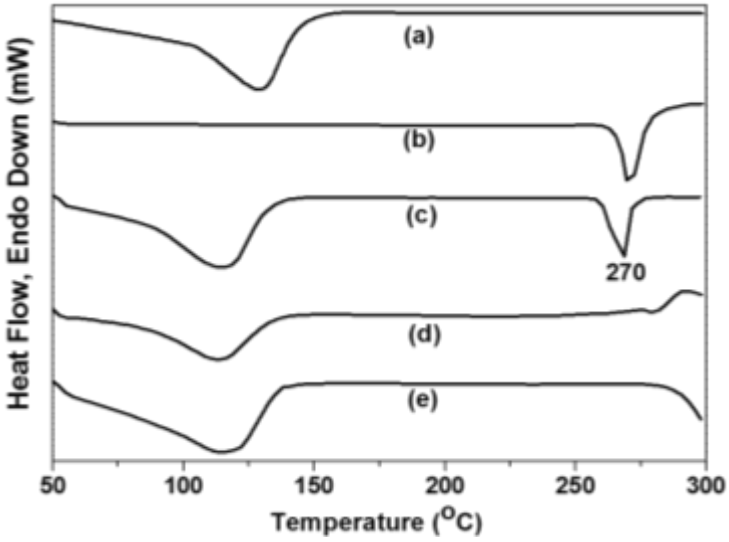

Figure 4.38. DSC thermograms of (a) CD, (b) DX, ((c) PM, (d) CP and (e) FD.

4.10.1.4 SEM Analysis

The SEM images of CD, DX, PM, CP and FD are shown in Figure 4.39. The photographs were taken under a voltage of 20 kV at 500X magnification. CD (Figure 4.39 a) crystallizes in larger polyhedral shapes, while DX (Figure 4.39 b) appears as crystalline particles with smaller dimensions. The micrograph of PM (Figure 4.39 c) presents the crystals of both the parent components. However, the crystals of the CP (Figure 4.39 d) appear as larger blocks which are much different from the sizes and shapes of CD and DX. The FD (Figure 4.39 e) gave rise to particles with flaky appearance, unlike the morphologies of CD and DX. This agrees with the XRD studies which had shown the amorphous nature for the freeze dried product. Thus the SEM analyses clearly point towards the formation of new entities by the co-

precipitation and freeze-drying processes due to the formation of the inclusion complex of DX with CD.

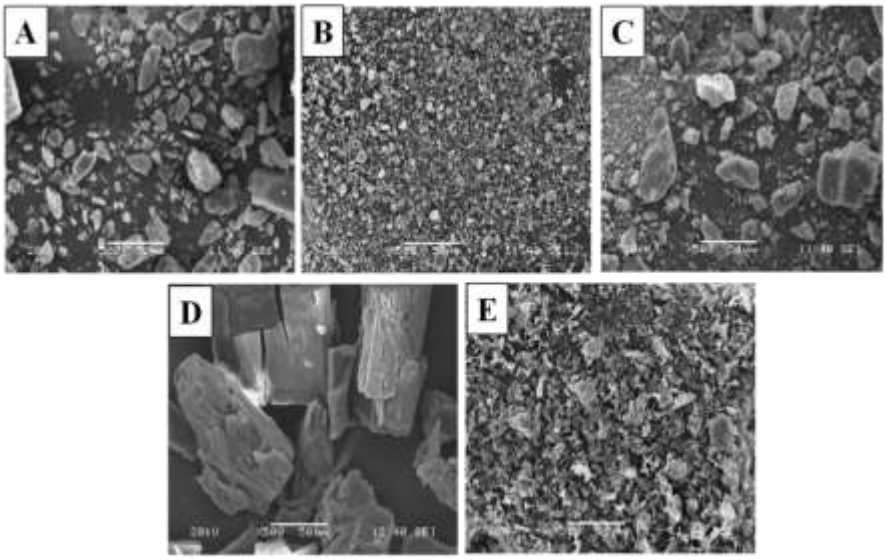

Figure 4.39. SEM images of (a) CD, (b) DX, (c) PM, (d) CP and (e) FD.

4.10.1.5 ^{1}H NMR Analysis

The ^{1}H NMR spectra for CD, freeze dried and co-precipitated inclusion products are shown in Figure 4.40.

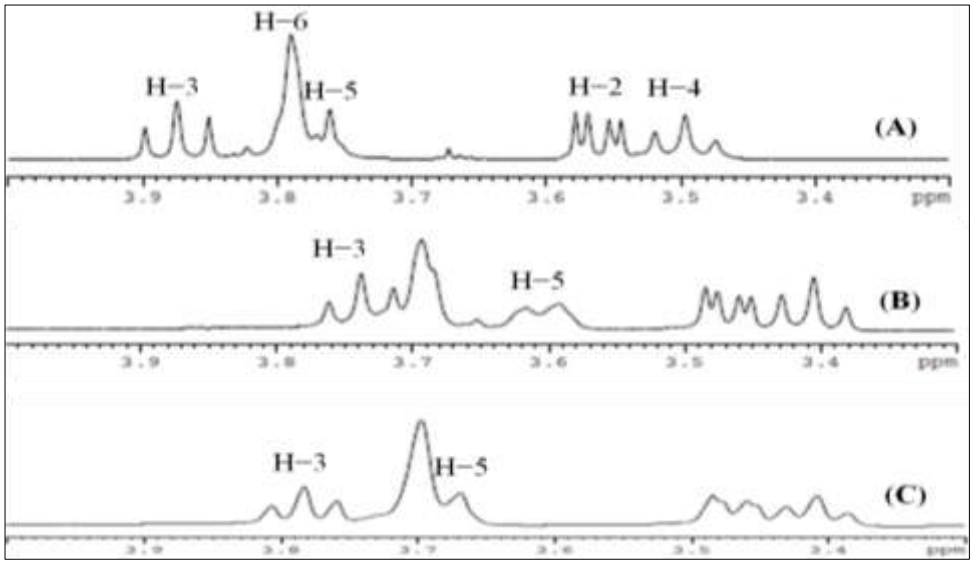

Figure 4.40. ^{1}H NMR spectra of (A) CD, (B) FD and (C) CP in D_2O at 298K.

The values of chemical shifts (δ) for the protons of CD and those of CP and FD are listed in Table 4.8. It is noteworthy that for both FD and CP, total inclusion of drug in CD cavity is indicated.

Table 4.8. δ and Δδ of protons in CD, DX-CD FD and DX-CD CP

Proton	δ_{CD}	FD		CP	
		δ	Δδ	δ	Δδ
H−1	4.982	4.880	0.102	4.891	0.091
H−2	3.561	3.468	0.093	3.469	0.092
H−3	3.874	3.737	0.137	3.782	0.092
H−4	3.496	3.405	0.091	3.408	0.088
H−5	3.761	3.604	0.157	3.669	0.092
H−6	3.790	3.693	0.097	3.697	0.093

The magnitudes of chemical shifts are relatively higher in case of FD as compared to that in CP, which points towards a somewhat stronger interaction between the drug and CD in FD than in CP complexes. Inclusion complexes prepared by freeze-dried method are often known to be physically more stable than co-precipitated products (Zingone and Rubessa, 2005).

4.10.2 Characterization of Microspheres

4.10.2.1 FTIR Analysis

The FTIR spectra of pure PVA, MS1, MS2, MS3, MS4 and MS5 microspheres are displayed in Figure 4.41. The FTIR spectrum of pure PVA shows a large band at around 3400 cm^{-1} due to hydroxyl stretching. The C−H stretching from alkyl group regions is observed at around 2941 cm^{-1} and the peak at 1740 cm^{-1} is attributed to the C=O stretching. The peak at 1140 cm^{-1} is associated with the crystalline nature of PVA.

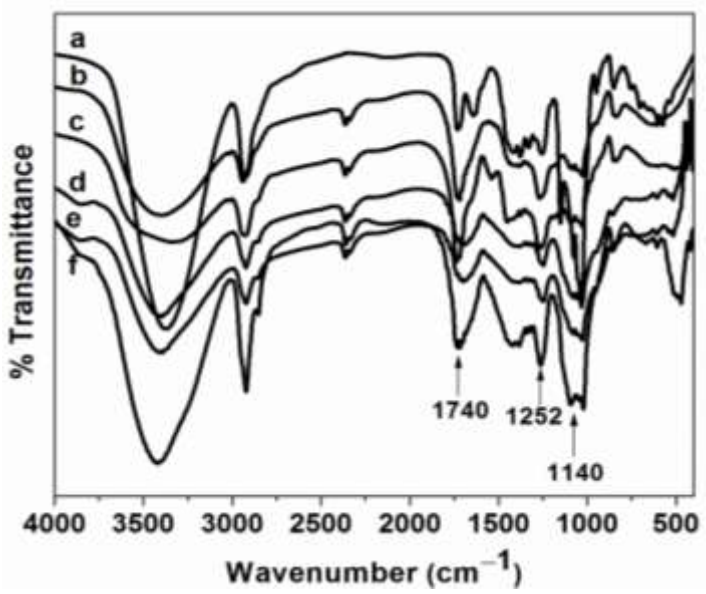

Figure 4.41. FTIR spectra of (a) pure PVA (b) MS1 (c) MS2 (d) MS3 (e) MS4 and (f) MS5 microspheres.

In the spectra of microspheres, the carbonyl stretching and the region between 1020−1080 cm^{-1} have been modified indicating the formation of acetal ring by the cross-linking reaction between the hydroxyl groups of PVA and aldehydic groups of PAA (Wang *et al.*, 2007; Lu *et al.*, 2009). The peak at 1252 cm^{-1} which is due to C−O stretching vibrations of PAA is enhanced in the spectra of microspheres. This evidenced the incorporation of PAA in the matrices of the synthesized microspheres. In addition, the decrease in intensity in the 1140 cm^{-1} peak in the microspheres indicates a decrease in crystallinity.

4.10.2.2 XRD Analysis

The X-ray diffraction profiles of pure PVA, MS1, MS2, MS3, MS4 and MS5 microspheres are demonstrated in Figure 4.42. All samples show almost similar diffraction pattern, a broad peak around 19.8°. Pure PVA hydrogel shows a peak around diffraction angle (2θ) of 19.8°, which is associated with the crystalline phase of PVA. The relative broadness and decreased intensity observed in the diffraction profiles of the microspheres indicates a decrease in crystallinity in the samples, which

might be because of the interpolymer interaction and cross-linking of PVA that prevents the PVA chains from self-associating and crystallizing.

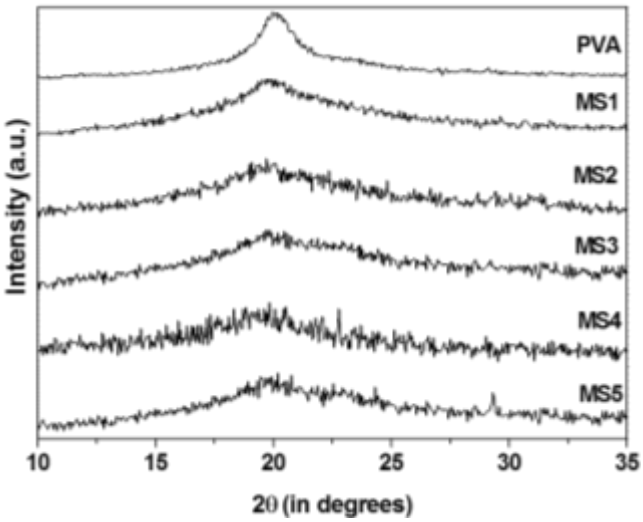

Figure 4.42. XRD profiles of pure PVA and MS1, MS2, MS3, MS4 and MS5 microspheres.

In MS2, the peaks for pure DX are absent and only the peaks for the polymer can be seen. This confirms the molecular dispersion of DX in the polymer matrix and the absence of drug crystallinity (Angadi *et al.*, 2011). The diffraction profiles of MS3, MS4 and MS5 exhibited more or less similar features and did not show any characteristic CD or DX or inclusion complex peaks. This indicated that the physical mixture and the inclusion complexes are properly blended with the hydrogel matrix.

4.10.2.3 Morphology Analysis

Figures 4.43 A−E show the SEM images of MS1, MS2, MS3, MS4 and MS5 microspheres. And Figures 4.43 F−J present the SEM images of a single MS1, MS2, MS3, MS4 and MS5 microspheres. The microspheres were found to be polydispersed in size. They are spherical in shape and formed without any agglomerations. The mean sizes of the microspheres were calculated by considering the average sizes of fifty microspheres of each sample. The mean sizes were found to be 131 ± 23 µm (MS1), 139 ± 24 µm (MS2), 140 ± 22 µm (MS3), 139 ± 21 µm (MS4) and 140 ± 21 µm

(MS5). There was no significant difference observed in the morphology of the drug free and drug loaded microspheres. This indicates that the presence of DX or PM or inclusion complex did not have any remarkable effect on the morphology or the size of the microspheres.

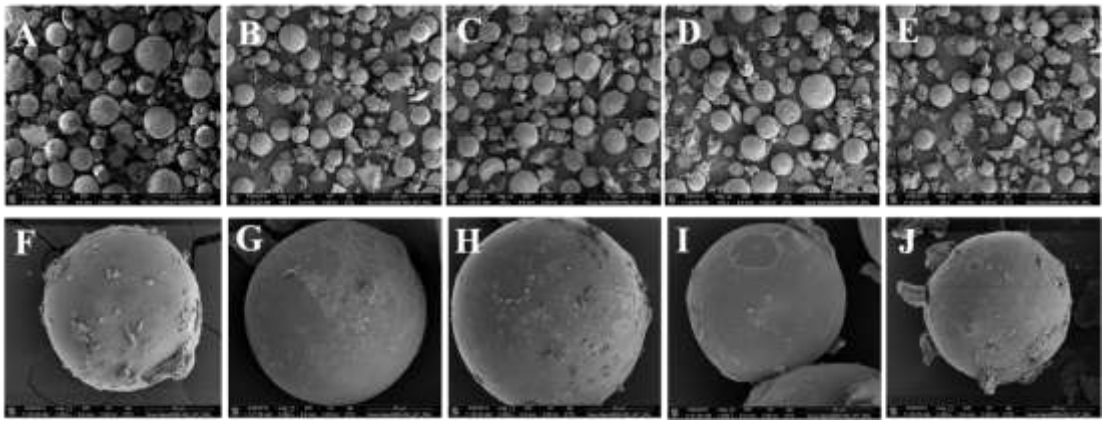

Figure 4.43. SEM images of (A) MS1, (B) MS2, (C) MS3, (D) MS4, (E) MS5 microspheres at 150X magnification and single (F) MS1, (G) MS2, (H) MS3, (I) MS4, (J) MS5 microspheres at 2000X magnification.

4.10.3 Drug Content of the Microspheres

The percentage drug content of the MS2, MS3, MS4 and MS5 microspheres were found to be 11.5 ± 0.5, 12.1 ± 0.7, 15.3 ± 0.8 and 17.2 ± 0.7 %, respectively. The drug loading efficacies of the microspheres demonstrated an increase with the addition of the inclusion complexes of the drug in comparison to the free drug. The MS5 microspheres exhibited highest drug loading capacity probably due to better inclusion complex formation by the freeze-drying method.

4.10.4 Swelling Studies

The swelling studies of the MS1 microspheres in gastric and intestinal pH conditions (pH 1.2 and pH 7.4 respectively) revealed the dependence of the swelling on the pH of external medium. The microspheres exhibited higher swelling at neutral pH as compared to that at acidic pH (Figure 4.44). The pH-sensitivity of these microspheres is mainly attributed to the presence of the carboxylic acid group in PAA which is a

weak acid with an intrinsic pK_a of around 4.28. At pH 1.2, the ionization of carboxylic groups is suppressed and there can be hydrogen bond interaction between the two polymers which reduces the flexibility of the polymer chains. Thus the swelling capacity is lowered. As the pH of the external medium rises above 4.28 (at pH 7.4), the carboxylic groups within the network tend to ionize as a result the inter-polymeric repulsion increases thus increasing the free volume in the polymer matrix which in turn increases the swelling ratio. Additionally, the negative charge in the polymer matrix drives the flow of cations into the hydrogel as a result of which the ionic swelling pressure increases resulting in an increase in swelling (Byun *et al.*, 1996; Fei *et al.*, 2002; Quintero *et al.*, 2010).

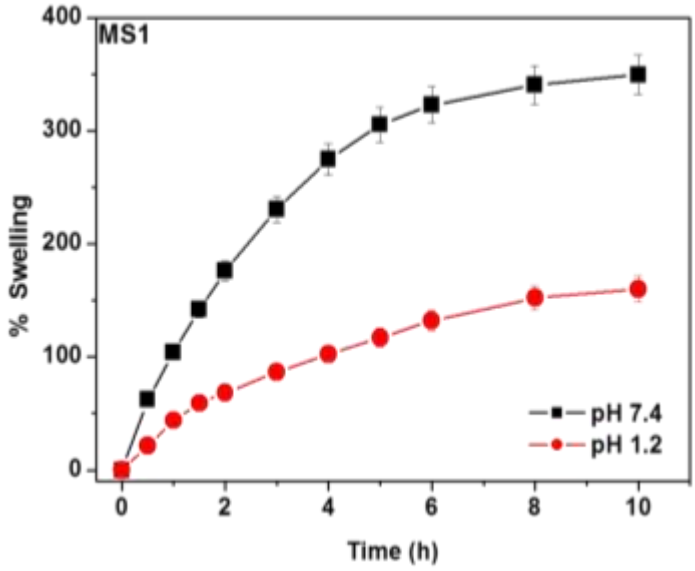

Figure 4.44. Swelling profiles of MS1 microspheres at pH 7.4 and pH 1.2.

4.10.5 *In vitro* DX Release Studies and Kinetics

4.10.5.1 *In vitro* DX Release Studies

Figure 4.45 demonstrates the release profiles of DX from MS2, MS3, MS4 and MS5 microspheres at pH 7.4 and pH 1.2 and 37°C. As evident, a pronounced difference is observed in the release rates of DX at pH 1.2 and pH 7.4. At pH 1.2, the amounts of

DX released from all microspheres were much lower than the release amounts at pH 7.4, even upon prolonged exposure to the releasing medium. This can be attributed to the difference in extent of swelling of these hydrogels in the above two pH conditions. Thus, the pH sensitive release characteristics of these hydrogels make them suitable candidates for intestine specific drug delivery systems.

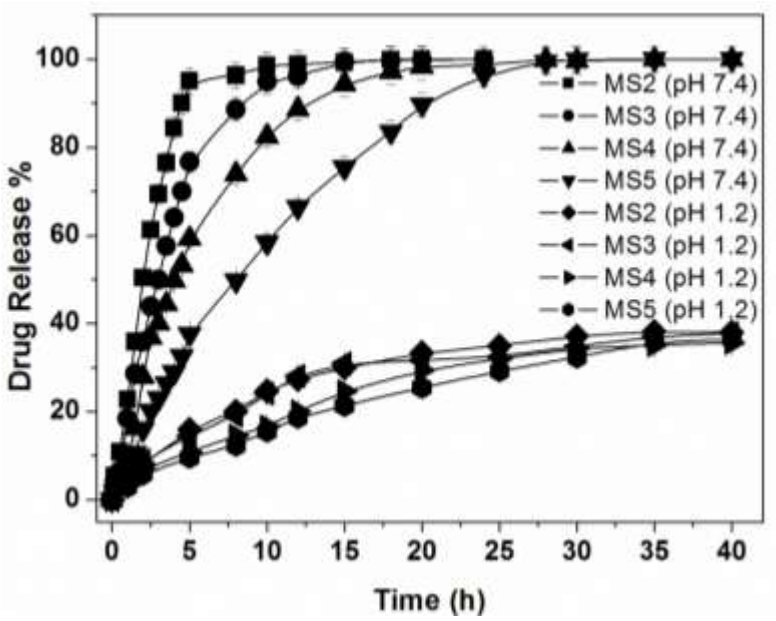

Figure 4.45. Drug release profiles of MS2, MS3, MS4 and MS5 microspheres in pH 7.4 and pH 1.2 at 37°C.

At pH 7.4 the rate of release of DX from these hydrogels follows the order: MS2 > MS3 > MS4 > MS5. DX release from the MS2 microspheres was found to be very rapid and almost 80% of the drug has been released in the initial 3 h. However, the release was much prolonged from the MS4 and MS5 microspheres. As discussed earlier, the release of a drug from a polymer matrix is generally governed by the combined effects of network swelling, polymer relaxation and diffusion of drug from the hydrogel matrix. The observed differences in the release patterns of these microspheres can be rationalized by taking into consideration the physical state of the drug in the hydrogel matrices. The MS2 microspheres contain the uncomplexed drug

which is dispersed freely in the hydrogel. But the drug is present in the form of inclusion complex in MS4 and MS5 microspheres. And, in MS3 microspheres, the drug is dispersed along with a blend of CD. The drug release from MS2 microspheres is expected to occur due to the simple diffusion of drug from the hydrogel network to the releasing medium as the hydrogel swells. Whereas in the other three microspheres, the presence of CD in the hydrogel network greatly directs the drug release profiles. For the MS3 microspheres, though the drug release is driven by diffusion, the presence of CD in the hydrogel matrix plays a pivotal role in the achievement of relatively slower drug release rate as compared to that from MS2 containing the free drug. Similar decrease in release rate has also been seen for the release of salicylic acid from CD blended PVA hydrogel as compared to pure PVA hydrogel (Sreenivasan, 1997). This can be explained by considering the following possibilities that can influence the drug release rate: (i) a few of the drug molecules getting complexed with the CD during the hydrogel synthesis and/or (ii) presence of H-bonding between CD and the polymer matrix influencing the polymer relaxation. For the drug release from MS4 and MS5 microspheres, apart from all the above mentioned factors, one major aspect that needs to be considered is the strong binding of DX with CD (K_b = 700 ± 40 M^{-1}) (Sadlej-Sosnowska, 1997). Thus for the drug release process to be accomplished from these two microspheres, the bound DX must be released from the CD cavity to the hydrogel matrix followed by the diffusion of free drug. Additionally, the presence of CD in these microspheres can also influence the polymer relaxation rate which in turn affects the drug release rate. Thus a sustained release of DX is observed from these microspheres in contrast to the burst type release from MS2 microspheres.

A pronounced difference in the release rates from the microspheres containing the CP and FD, *i.e.* from MS4 and MS5 is observed. The drug release from MS5 was much more controlled and continued for longer time than MS4 microspheres. These two microspheres are very similar in all aspects except for the type of DX-CD inclusion complex. Thus, the observed difference in the drug release kinetics between MS4 and MS5 suggests towards a strong influence of the method of preparation of drug-CD IC on the drug release kinetics from the hydrogel matrix. In the present study, MS5, the microsphere containing the DX-CD FD, is found to be the best system for the slow release of dexamethasone. Thus, it can be proposed that the adverse side-effects of DX in the GIT could be minimized by using the MS5 microspheres as delivery vehicles since they provide controlled release of DX over a prolonged period.

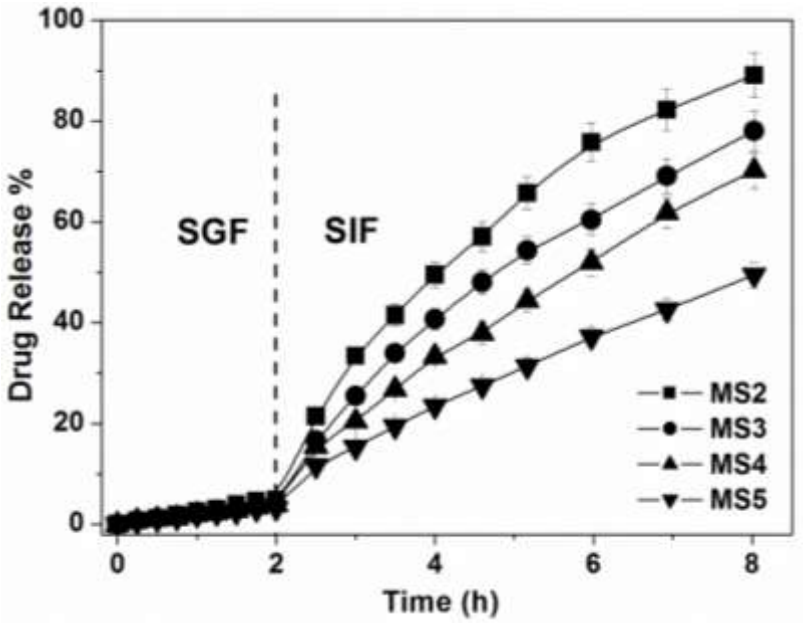

Figure 4.46. Drug release profiles of MS2, MS3, MS4 and MS5 microspheres in SGF and SIF at 37°C.

In order to imitate the conditions of the GIT, DX release from the microspheres was also studied in SGF and SIF. For further simulating the GIT conditions; the microspheres were immersed in SGF for 2 hours, and then transferred to SIF and the drug release was monitored. Figure 4.46 depicts the release pattern of DX from the

four microspheres in SGF and SIF environments. Approximately 5% of DX is released during the initial 2 h in SGF. However, when the microspheres were transferred to SIF, the rate of DX release increased significantly for all the four hydrogels. The release rate in the SIF was found to follow the same order as observed before *i.e.* MS2 > MS3 > MS4 > MS5. This release profile of dexamethasone fulfils the requirements of *US Pharmacopeia XXIV* for oral colon drug delivery.

Thus the synthesized microspheres could be effectively employed for the oral delivery of dexamethasone and their pH sensitivity could be exploited for the intestine-specific delivery. However, in order to achieve a controlled release of drug, the MS4 and MS5 microspheres are found to be more suitable. And MS5 was found to be the best of the lot for achieving sustained and intestinal delivery of DX.

4.10.5.2 DX Release Kinetics

The release data have been fitted to different empirical mathematical equations and shown in Table 4.9. The drug release data for MS2, MS3, MS4 and MS5 showed the best fit for the Ritger-Peppas equation with correlation coefficient values of 0.998, 0.998, 0.992 and 0.996 respectively. The diffusion exponent value '*n*' was found to be in the range of 0.76 to 0.85 for the microspheres indicating the anomalous nature of drug transport mechanism, which is the superimposition of diffusion-controlled and swelling controlled drug release.

The R/F plot showed a higher value of R/F for MS3, MS4 and MS5 microspheres in comparison to MS2 microspheres. This suggested that polymer relaxation played a major role in the drug release where CD is present. The MS5 microsphere exhibited the highest value of R/F.

Table 4.9. DX release parameters fitting to various mathematical models

Sample	Higuchi		Ritger-Peppas			Peppas-Sahlin			Zero-order	
	k ($h^{-0.5}$)	R^2	*n*	k'(h^{-n})	R^2	k_1 ($h^{-0.43}$)	k_2 ($h^{-0.86}$)	R^2	k'' (h^{-1})	R^2
MS2	0.319	0.822	0.85	0.236	0.998	–0.102	0.346	0.994	0.244	0.986
MS3	0.276	0.876	0.84	0.188	0.998	–0.034	0.218	0.994	0.167	0.989
MS4	0.227	0.849	0.76	0.175	0.992	–0.059	0.183	0.995	0.124	0.979
MS5	0.154	0.881	0.80	0.098	0.996	0.033	0.070	0.996	0.065	0.958

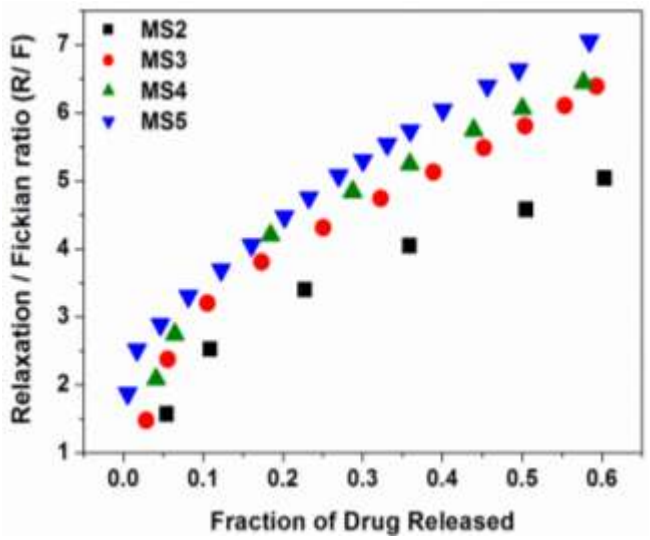

Figure 4.47. Plot of ratio of relaxation to the Fickian contribution (R/F) with the fraction of dug release for MS2, MS3, MS4 and MS5 microspheres.

4.10.6 Cytotoxicity assay

In order to ensure the biocompatibility of the synthesized microspheres, cytotoxicity assay was performed by MTT colorimetric technique. As shown in Figure 4.48, direct contact between L−929 cells and MS1 microspheres did not reveal any adverse effect. This suggested the compatibility of the synthesized microspheres with the living tissues thus validating these as possible delivery systems for the controlled delivery of DX.

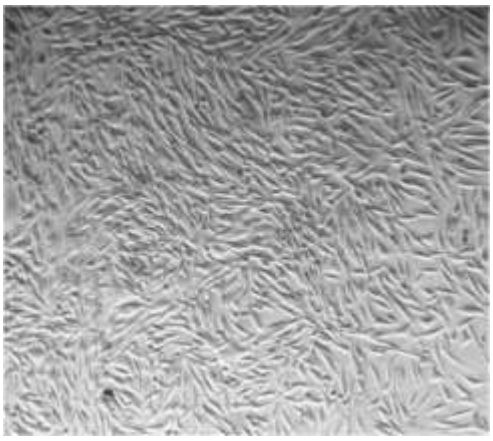

Figure 4.48. Optical Micrographs of L−929 cells cultured after 48 h incubation with MS1 microspheres.

4.11 CONCLUSIONS

- pH-Sensitive PVA-PAA microspheres cross-linked with GA were synthesized and studied for the delivery of the common anti-inflammatory and immunosuppressant drug DX.
- To regulate the release rate of DX, preformed solid inclusion complex of DX with CD was added into the hydrogel microspheres.
- In order to examine the effect of the method of preparation of inclusion complex on the release kinetics, the DX-CD inclusion complexes were prepared by two commonly used methods: the co-precipitation and freeze-drying method.
- The inclusion complexes were characterized by different spectroscopic techniques such as FTIR, XRD, DSC, SEM and ^{1}H NMR.
- Microspheres containing the free drug, the drug-CD physical mixture and the CD-complexed drug were synthesized and characterized by FTIR, XRD, DSC, SEM and their drug delivery efficacies were also investigated.
- The swelling characteristics indicated higher swelling in neutral pH than in acidic pH therefore indicating their pH-responsiveness.
- At pH 1.2, the amounts of DX released from all microspheres (MS2, MS3, MS4 and MS5) were much lower than the release amounts at pH 7.4. At pH 7.4 the rate of release of DX from these hydrogels follows the order: MS2 > MS3 > MS4 > MS5.
- Approximately 5% of DX released during the initial 2h in SGF but upon transfer to SIF, the rate of DX release increased significantly.

- The synthesized microspheres could be effectively employed for the controlled delivery of dexamethasone and their pH sensitivity could be exploited for the intestine-specific delivery.
- Moreover, the compatibility of the synthesized microspheres with the living tissues further validates them as promising drug delivery systems.
- MS5 containing the freeze-dried DX-CD inclusion complex was found to be the best of the lot for achieving a good control and intestine-specific delivery of DX.
- Thus, it can be proposed that the adverse side-effects of DX in the GIT could be minimized by using these microspheres as delivery vehicles.

CHAPTER 5

REGULATING THE DELIVERY OF 5–FLUOROURACIL FROM THERMO-RESPONSIVE GUAR GUM–PNIPAAm HYDROGELS

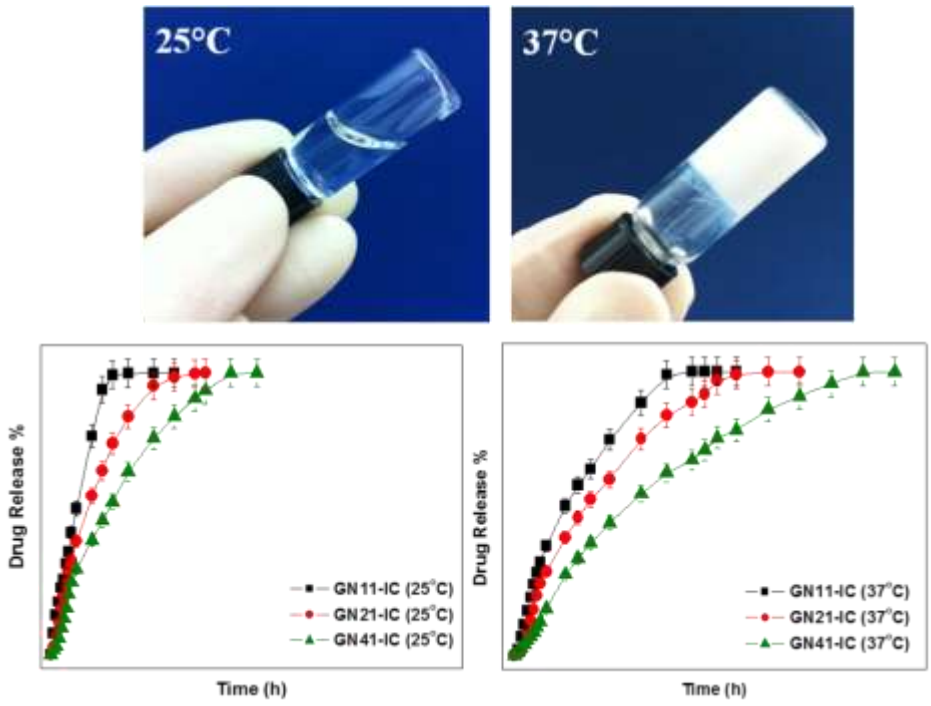

5.1 INTRODUCTION

Temperature-sensitive hydrogels are one of the most commonly studied classes of smart hydrogels in drug delivery research (Qiu and Park, 2001). Of the many temperature-sensitive polymers, poly(N-isopropylacrylamide) (PNIPAAm) is widely studied because of its lower critical solution temperature (LCST) around ~32°C, close to human body temperature. Block copolymers of PEO and PPO commercially available under the trade names of Pluronics® or Poloxamers® and Tetronics® have also been utilized in development of thermo-responsive drug delivery formulations. The excellent review article by Klouda and Mikos (2008) covers the developments in thermo-sensitive hydrogels for biomedical and pharmaceutical applications.

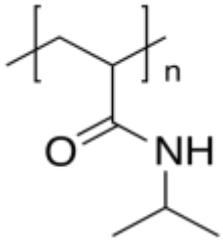

Figure 5.1. Chemical structure of poly(N-isopropylacrylamide) (PNIPAAm).

For hydrogels composed of thermo-sensitive polymers, the LCST is the deciding factor for their thermo-responsiveness. Polymeric materials that possess LCST-type phase diagram are composed of a mixture of hydrophilic and hydrophobic groups on their backbone and the LCST can be tailored as per requisites by adjusting the ratio of the hydrophilic and hydrophobic segments of the polymer (Qiu and Park, 2001). At temperatures below the LCST, the hydrogen bonding between the hydrophilic components of the polymer and the water is dominant and primarily responsible for the expansion of the hydrogel matrix. This leads to an increase in the water uptake capacity of the hydrogel thereby enhancing its swellability. At temperatures above the LCST, the intramolecular interactions become stronger while the polymer-water interaction (intermolecular) is weakened. Thus the hydrogel matrix is rendered

hydrophobic and the water is expelled out. This results in a contraction of the gel which directs to lower swelling characteristics and shrinking of the hydrogel (Wenceslau *et al.,* 2012). The phase transition temperature of PNIPAAm is known to change by the incorporation of small amount of ionizable groups into the gel network or by changing the solvent composition. Even copolymerization of PNIPAAm with other polymers has led to the formation of hydrogels with versatile properties including faster rate of shrinking of the gel (Qiu and Park, 2001). In drug delivery, the swelling/ shrinking behaviour of the thermo-sensitive PNIPAAm hydrogels have been used to obtain an on-off drug release profile in response to changes in temperature (Figure 5.2).

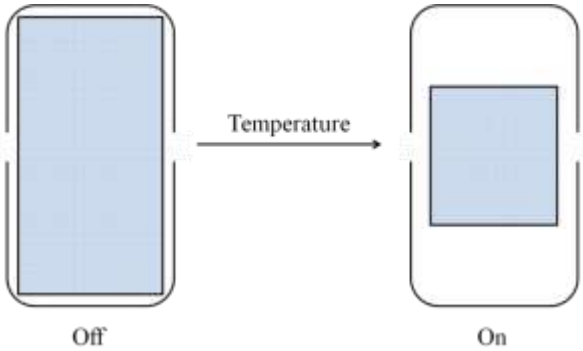

Figure 5.2. Schematic illustration of an on-off release for drug delivery.

From the viewpoint of biomedical purposes, pure PNIPAAm hydrogels are not appropriate candidates due to their poor mechanical stability (Muniz and Geuskens, 2001), low biocompatibility (Xiao *et al.,* 2009) and low biodegradability (Zhang *et al.,* 2004). Another serious limitation associated with the PNIPAAm hydrogel as a potential drug carrier, is the lack of sustained drug releasing ability *i.e.* the impregnated drug is usually released within a very short span of time when the polymer matrix undergoes the phase transition. The poor mechanical strength and the fast drug release from the conventional PNIPAAm hydrogel could be attributed to its lower polymer mass per unit volume that leads to opening of many channels and pores

for the drug to diffuse out rapidly. More so, the intermolecular hydrogen bonds in the swollen state are quite weak and tend to facilitate the drug release (Zhang *et al.*, 2004).

To overcome these deficiencies, copolymerization of PNIPAAm with hydrophobic co-monomers is usually carried out. However, this method is not advisable as it almost eliminates the inherent thermo-responsive properties of PNIPAAm. Copolymerization of PNIPAAm with AAc monomers had been carried out to confer pH-sensitivity and improve the mechanical characteristics of the hydrogel (Jones, 1999). It was observed that insertion of AAc units even in small amounts led to a disturbance of the continuous sequence of PNIPAAm and the cumulative hydrophobic interactions between the isopropyl groups were reduced. This eventually reduced the thermo-sensitivity of the resulting copolymer hydrogel. In order to obtain biocompatible and biodegradable hydrogels that preserve the temperature-sensitivity of PNIPAAm, natural polysaccharides have been roped into this context (Wang *et al.,* 2013).

Recently, the research in the areas pertaining to hydrophilic natural polysaccharides for the design of oral controlled drug delivery formulations has brewed into a huge territory. More so, the utility of natural polysaccharides in the fabrication of hydrogels for controlled delivery of drugs has blossomed largely. Polysaccharides are polymeric carbohydrates composed of long chain monosaccharide units joined together by glycosidic linkages. Natural polysaccharides have various sources of origin; algal (*e.g.* alginate), plant (*e.g.* pectin, cellulose, gum Arabic, inulin, *etc.*), microbial (*e.g.* dextran, xanthan gum) and animal (*e.g.* chitosan, chondroitin). Polysaccharides are generally associated with a wide range of molecular weights, varying chemical composition and a large number of reactive groups. These features hugely contribute to the diversity in structure and properties of the polysaccharides (Prabaharan, 2008).

Polysaccharides are abundant in nature and their processing is also cost-effective. Additionally, they are safe, non-toxic, biocompatible and biodegradable (Prabaharan and Jayakumar, 2009). Also, the hydrophilic groups such as hydroxyl, carboxyl, *etc.* present in the polysaccharides are capable of forming non-covalent bonds with the biological tissues forming bio-adhesion (Lee *et al.,* 2000). The utilization of natural polysaccharides in drug delivery systems has been a subject of intense investigation lately because of their biodegradability and biocompatibility.

IPNs of PNIPAAm with natural polymers were found to posses better mechanical properties in comparison to the parent homopolymer. Semi-IPNs of PNIPAAm and CS have been developed by Lee and Chen (2001) and it was found that the thermo-sensitivity of PNIPAAm remained unhindered even after addition of CS. PNIPAAm and CS have also been grafted into hydrogels and their physico-chemical properties and drug release characteristics were examined (Fang *et al.,* 2008). Hydrophilic and lipophilic drugs such as nalbuphine, indomethacin and nalbuphine prodrug were chosen as model drugs for the *in vitro* release experiments. The results suggested the controlled release of drugs from the hydrogels and the hydrogels were also found to be biocompatible in nature. Semi-IPN microspheres of PNIPAAm and NaAlg have been explored for the delivery of 5-Fluorouracil (Reddy *et al.,* 2008). The hydrogels exhibited both pH- and temperature sensitivity and the controlled release of drug was achieved at the physiological temperature of 37°C. Biodegradable hydrogel formulations based on PNIPAAm and dextran targeted towards controlled delivery of DOX exhibited remarkable drug releasing properties and thermo-sensitivity (Namkung and Chu, 2007). Hydrogels comprising xanthan-maleic anhydride and PNIPAAm were synthesized by solution polymerization technique and found to have potential applications in biopharmaceutical and biotechnology fields as these

hydrogels were very sensitive to minute changes in temperature (Long *et al.*, 2009). The LCST could be adjusted to be or near the body temperature by varying the precursor compositions. Pectin-g-PNIPAAm hydrogels have also been utilized for the colon-targeted delivery of theophylline (Assaf *et al.*, 2011). A plethora of research is dedicated towards development of formulations comprising of PNIPAAm and natural polysaccharides for controlled drug delivery (Ward and Georgion, 2011; Jing *et al.*, 2013).

Guar gum (GG), a galactomannan, is one such natural polysaccharide which is of particular interest in this regard. GG is a water soluble polysaccharide derived from the seeds of *Cyamopsis tetragonolobus*, family Leguminosae. It consists of linear chains of (1→4) β−D−mannopyranosyl units with α−D−galactopyranosyl units attached by (1→6) linkages. The non-toxic nature allows its usage in biomedical, pharmaceutical, food and cosmetic industries (Prabaharan, 2011). GG has been used as a binder, stiffener, disintegrant, thickening agent, suspending agent and as a stabilizer in various applications. GG hydrates in cold water producing a pseudo-viscous plastic solution which has greater low-shear viscosity than other hydrocolloids (Cheetham and Mashimba, 1990). This gelling property retards the release of the drug thereby helping to attain a sustained drug release profile.

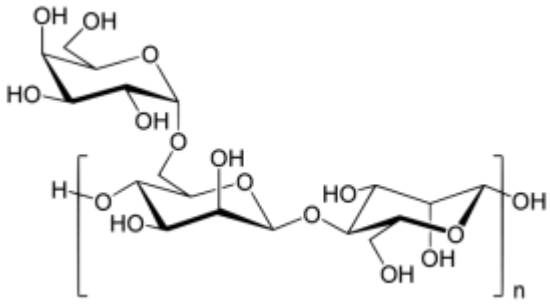

Figure 5.3. Chemical structure of guar gum (GG).

GG, as a drug delivery agent, has gained considerable significance because of its biocompatibility, physico-chemical stability and compressibility features. The susceptibility of GG to microbial degradation in the large intestine has drawn much attention towards oral drug delivery purposes. The potential use of GG as colon-specific, anti-hypertensive, protein and transdermal drug delivery systems has been well documented (Prabaharan, 2011). The flexibility of GG in drug delivery lies in tailoring its properties as per demand. Efforts in this direction have led to the development of a variety of dosage forms which include tablets, hydrogels, microspheres, beads, capsules, nanoparticles and others. Aminabhavi and co-authors (2014) have briefly summarized the advancement in the research endeavours on GG-based polymeric formulations for controlled delivery of therapeutics. However, the major hindrance in using GG matrices as platforms for controlled drug delivery is their high hydrophilic characteristics which leads to extensive swelling and facilitates the premature release of loaded drugs (Li *et al.*, 2008). GG has been often used in combination with a variety of other biodegradable polymers in the forms of copolymers, blends, grafts, IPNs, *etc.* Such polymers include PVA, PVP, polyacrylamide, NaAlg, HPMC, xanthan gum, PAA, CMC, NIPAAm, *etc*. (Ghosh and Wong, 2014).

GG, in the form of matrix tablets, has been investigated for the delivery of indomethacin to the colon because of its ability to sustain the physiological environment of the stomach (Prasad *et al.,* 1998). Microspheres of carboxymethyl GG have been prepared and explored for their controlled delivery of the anti-asthmatic drug theophylline (Phadke *et al.,* 2014). Recently, Bosio and co-workers (2014) observed sustained release of DOX from gel microbeads composed of alginate-carboxymethyl GG for oral controlled delivery. GG is also known to be efficient

delivery carriers for protein-based drugs. Kono *et al.*, (2014) developed GG hydrogels *via* esterification with 1, 2, 3, 4-butantetracarboxylic dianhydride as carrier materials for controlled protein delivery. The hydrogels adsorbed BSA and hen egg white lysozyme through electrostatic and hydrophobic interactions and exhibited slow and steady release of the proteins over a period of 24 h. Recently, Murali *et al.,* (2014) developed an injectable hydrogel system comprising biocompatible aminated GG and Fe_3O_4-ZnS core-shell nanoparticles for the delivery of DOX hydrochloride. The hydrogels were stable over a wide range of pH and displayed excellent drug release properties where upto 90% of the drug release was achieved after 20 days of incubation. Literature is abound with the versatility and applicability of GG formulations in drug delivery (Aminabhavi *et al.*, 2014).

In this regard, there are only a few reports relevant to hydrogels based on PNIPAAm and GG. Thermo-responsive blend hydrogel microspheres of NaAlg and PNIPAAm-g-GG were synthesized by emulsion cross-linking method using GA as cross-linker (Kajjari *et al.*, 2012). The *in vitro* release experiments assayed the thermo-sensitivity of the microspheres for controlled delivery of isoniazid. Li and co-authors (2008) have synthesized GG-PNIPAAm IPN hydrogels cross-linked by MBA and their physico-chemical properties have been investigated. The hydrogels possessed good thermo-sensitivity and the introduction of GG into the matrix led to an improvement in the mechanical stability. Thus there is a current need for the development of GG-PNIPAAm hydrogels and explore their drug releasing properties in greater details.

5FU is a hydrophobic drug that has been used in the treatment of colorectal cancer for many years (Figure 5.4). It is a powerful cytotoxic drug that acts as an anti-metabolite and successfully utilized for treatment of genital, urethral and intravaginal condylomata.

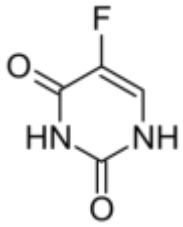

Figure 5.4. Chemical structure of 5-Fluorouracil (5FU).

However, it possesses moderate aqueous solubility, about 1g in 100 ml of water at room temperature (Bahaddi *et al.,* 1997) and is poorly absorbed after oral administration with erratic bioavailability therefore it is usually administered intravenously. Following parenteral administration of 5FU, there is a rapid distribution of drug followed by its brisk elimination with an apparent terminal half-life of about 8 to 20 min (Diasio and Harris, 1989). It has also been shown that when 5FU is applied topically to treat vaginal lesions; patient non-compliances occur due to chemoinflammation or epithelial erosion probably due to local high concentration of the drug (Syed *et al.,* 2000). Also severe gastrointestinal, neural, cardiac and dermatological toxic effects due to 5FU cytotoxicity have been reported (Diasio and Harris, 1989; Jin *et al.*, 2010). Thus lower doses of 5FU are generally warranted to reduce the side-effects and improve its bioavailability (Bilensoy *et al.,* 2011).

This work centres on the design of temperature sensitive GG−PNIPAAm IPN hydrogels cross-linked by tetraethyl orthoslilicate (TEOS), for the controlled release characteristics of 5FU. TEOS has been chosen as the cross-linker as alkoxysilanes and particularly TEOS are known to be nontoxic in nature and widely accepted for pharmaceutical purposes (Islam *et al.,* 2012; Rasool *et al.,* 2010). TEOS has been utilized to cross-link polyurethanes (Jena and Raju, 2008) and hydrogels of CS and PVA (Copello *et al.,* 2014; Islam *et al.,* 2013; Islam *et al.,* 2012; Kulkarni *et al.,* 2006). Thermo-sensitive gels with different content of TEOS have been prepared from NIPAAm and MBA by emulsion polymerization technique and the effect of cross-

linker on the hydrogels properties were investigated (Huang and Lee, 2009; Huang and Lee, 2010).

OBJECTIVES

The objectives of the present study constitute:

- Preparation of solid ICs of 5FU with CD and the characterization of the ICs.
- Synthesis of GG−PNIPAAm IPN hydrogels cross-linked by TEOS and their characterization.
- Evaluation of the temperature-responsive swelling properties of the hydrogels.
- To explore the drug releasing behaviour of the hydrogels containing the ICs for the controlled delivery of 5FU.
- To address the preliminary kinetics of drug release from the hydrogels and understand the importance of the presence and effect of CD on the drug release phenomenon.
- To asssay the cytotoxicity of the hydrogels on rat fibroblasts to ensure their biocompatibility with living tissues.

Hydrogels with different feed compositions of GG and NIPAAm were synthesized. Blank hydrogels without any free drug or IC were also synthesized for characterization purposes. The compositions and designations of the synthesized hydrogels are provided in Table 5.1.

Table 5.1. Composition and designation of synthesized GG−PNIPAAm hydrogels

Sample	GG: NIPAAm (wt%)	Sample Designation		
		GG−NIPAAm	GG−NIPAAm−5FU	GG−NIPAAm−IC
1	1:0	GG	GG-5FU	GG-IC
2	0:1	PNIPAAm	PNIPAAm-5FU	PNIPAAm-IC
3	1:1	GN11	GN11-5FU	GN11-IC
4	2:1	GN21	GN21-5FU	GN21-IC
5	4:1	GN41	GN41-5FU	GN41-IC

The concentration of 5FU released was estimated from the calibration plots obtained by observing the absorbance at λ_{max} = 265 nm.

5.2 RESULTS AND DISCUSSION

5.2.1 Inclusion Studies of 5FU in CD

5.2.1.1 UV−Vis Analysis

As illustrated in Figure 5.5, the absorbance of 5FU was found to increase with the gradual addition of CD. A slight blue shift in the absorption maximum was observed in the spectra upon increasing the amount of CD. This could be due to inclusion of the drug into the apolar cavity of CD indicating possible interactions between them. The increased absorbance of 5FU in presence of CD indicates the improved solubility of the hydrophobic drug in the aqueous medium due to 5FU-CD complexation.

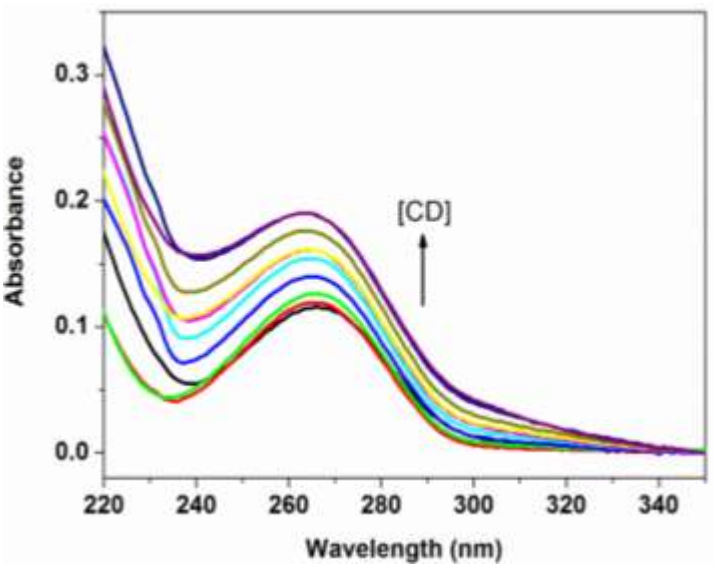

Figure 5.5. Absorption spectra of 5FU at varying concentrations of CD, [5FU] = 5×10^{-5} M, [CD] = 0−20 $\times10^{-3}$ M, pH=7.4.

5.2.1.2 FTIR Analysis

The FTIR spectra of CD, 5FU, PM and IC are illustrated in Figure 5.6.

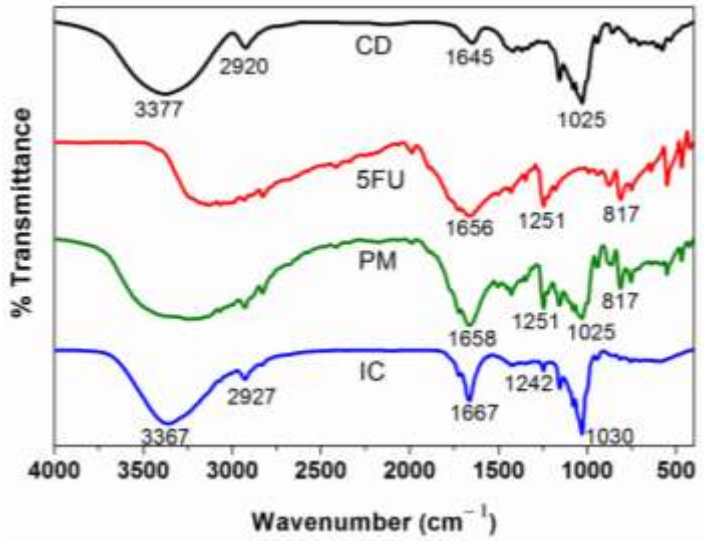

Figure 5.6. FTIR spectra of CD, 5FU, physical mixture (PM) and inclusion complex (IC).

The characteristics FTIR peaks of 5FU include the aromatic ring regions around 500−600 cm^{-1} and 2500−3000 cm^{-1} together with C=C stretching band at 1300−1500 cm^{-1} (Bilensoy *et al.,* 2007). The PM exhibited a spectrum corresponding to the superposition of the parent components. However the FTIR spectrum of the IC showed certain spectral shifts. A shift in the hydroxyl absorption position from 3377 cm^{-1} to 3355 cm^{-1} in the spectral profile of IC was evident. In particular, the key drug peak at 1645 $cm^{-1}$and 1251 cm^{-1} have shifted to 1667 $cm^{-1}$and 1242 cm^{-1}respectively in the spectrum of IC. These spectral shifts and modifications in the IC indicated the encapsulation of drug in CD cavity due to the formation of an IC (Bilensoy *et al.,* 2007).

5.2.1.3 XRD Analysis

Figure 5.7 shows the wide-angle XRD profiles of CD, 5FU, PM and IC. The crystalline nature of 5FU was established by its diffraction profile which shows a sharp peak at 2θ of 28.6°. The diffractogram of the PM revealed some new peaks along with the characteristic peaks of CD and 5FU, which could be attributed to some interaction of CD with 5FU in the PM. On the other hand, the diffractogram of IC was completely different as compared to the parent components. A somewhat amorphous

profile was observed for the IC, which might be due to the freeze-drying method of preparation.

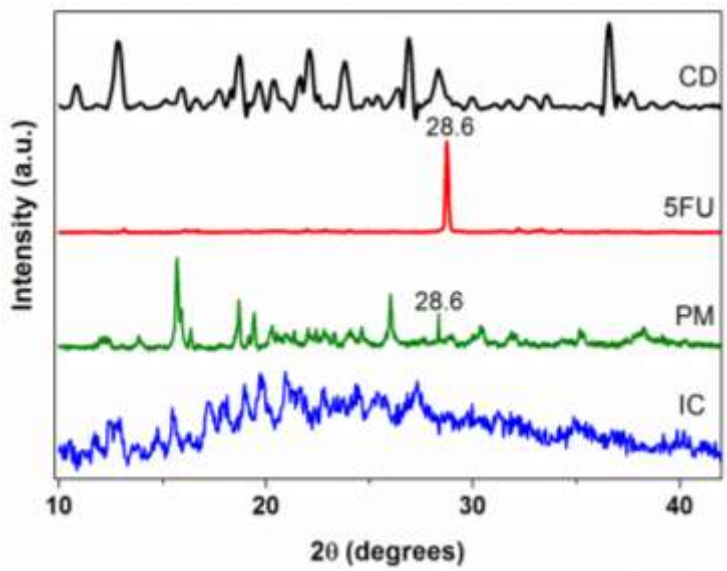

Figure 5.7. XRD profiles of CD, 5FU, physical mixture (PM) and inclusion complex (IC).

5.2.1.4 DSC Analysis

The DSC endotherms of CD, 5FU, PM and IC are displayed in Figure 5.8.

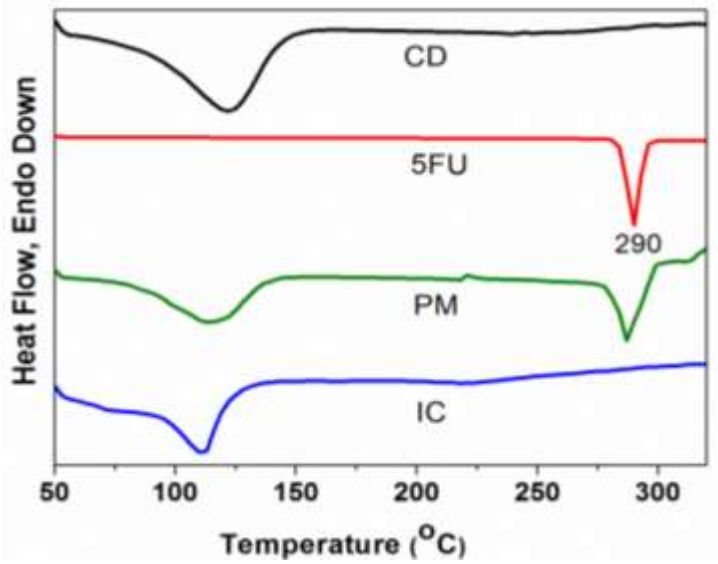

Figure 5.8. DSC thermograms of CD, 5FU, physical mixture (PM) and inclusion complex (IC).

The thermogram of 5FU was typical of a crystalline anhydrous substance showing an exothermic peak around 290°C indicating its melting point. For the PM, the

thermogram corresponding to both CD dehydration and DX melting was observed. The absence of the drug peak and the presence of the wide thermogram of CD in the DSC curve of the IC signified the inclusion of 5FU in CD cavity.

5.2.1.5SEM Analysis

The SEM images of CD, 5FU, PM and IC are presented in Figure 5.9. The images were taken at 5.00 kV and 500× magnification. The images demonstrate the typical crystals of CD (Figure 5.8 A) in polyhedral shapes while the particles of 5FU (Figure 5.8 B) appear as crystalline particles with larger dimensions. The PM (Figure 5.8 C) was found to contain both the crystals of CD and 5FU. However the particles of the IC (Figure 5.8 D) were found to be quite flaky in nature, unlike the morphologies of CD and 5FU. This agrees with the XRD studies which had previously established the amorphous nature for the IC. Thus the SEM analyses are indicative of the formation of new entities due to the complexation between 5FU and CD.

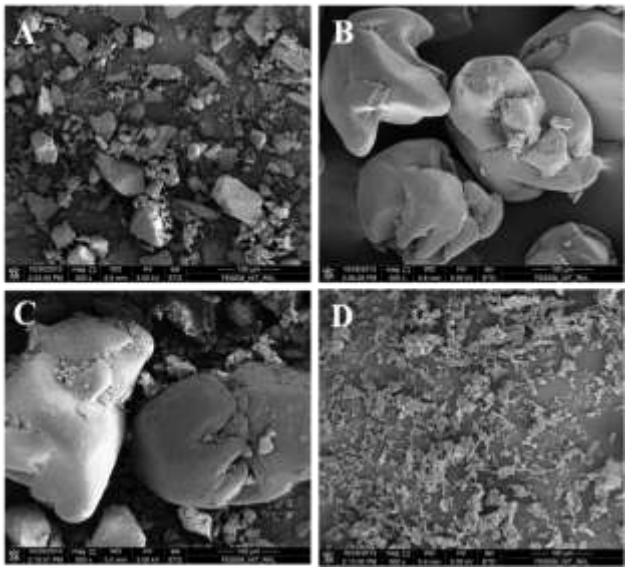

Figure 5.9. SEM images of (A) CD, (B) 5FU, (C) physical mixture (PM) and (D) inclusion complex (IC).

5.2.1.6 ^{1}H NMR studies

The ^{1}H NMR spectra for CD and IC obtained in D_2O are shown in Figure 5.10.

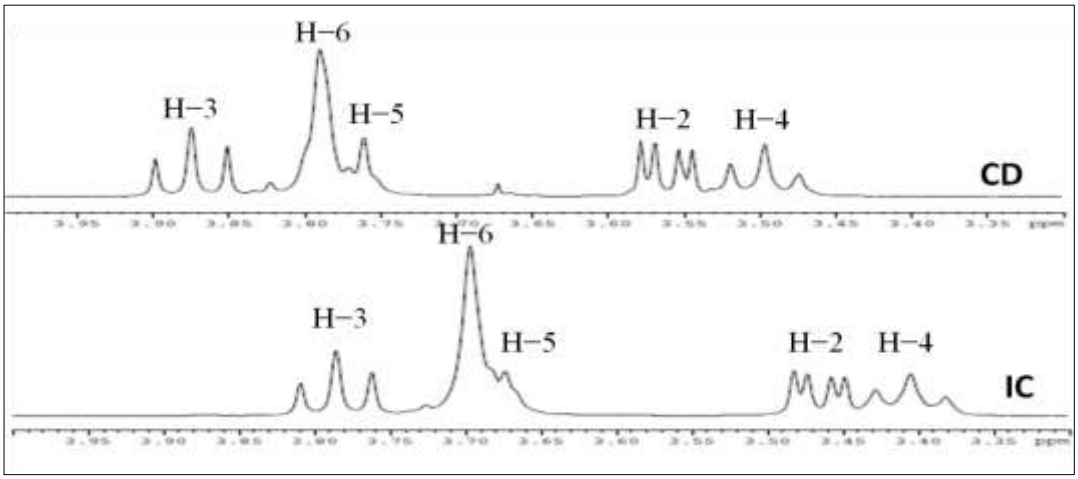

Figure 5.10. ^{1}H NMR spectra of CD and inclusion complex (IC) in D_2O at 298K.

The values of chemical shifts for the H−3 and H−5 protons of CD and IC are compared and their differences are listed in Table 5.2. From the table, [Δ(δH−3)] = [Δ(δH−5)] is clearly indicated. Thus the formation of IC is verified from the ^{1}H NMR spectral data and total inclusion of 5FU in CD cavity is confirmed.

Table 5.2. δ and Δδ of protons in CD and 5FU-CD IC

Protons	δ_{CD}	δ_{IC}	Δ (δ_{CD} and δ_{IC})
H−1	4.991	5.011	0.020
H−2	3.561	3.465	0.096
H−3	3.874	3.822	0.052
H−4	3.496	3.405	0.091
H−5	3.761	3.709	0.052
H−6	3.790	3.697	0.093

5.2.2 Characterization of Hydrogels

5.2.2.1 FTIR Analysis

The FTIR spectra of the hydrogels are represented in Figure 5.11. A strong hydroxyl stretching absorption characteristic appears at around 3400 cm^{-1} in all the hydrogels. This

band corresponds to the hydroxyl stretching of GG. The amide I band at 1658 cm^{-1} (C=O stretching) and the amide II band at 1538 cm^{-1} (N−H bending) of the amide group of PNIPAAm are also observed in all the IPN hydrogels. The spectra of the hydrogels also exhibited peaks in the region of 1000−1200 cm^{-1} which are attributed to the absorption bands of secondary alcohol or cyclic ether of the six-member rings on GG backbone (Li *et al.*, 2008).

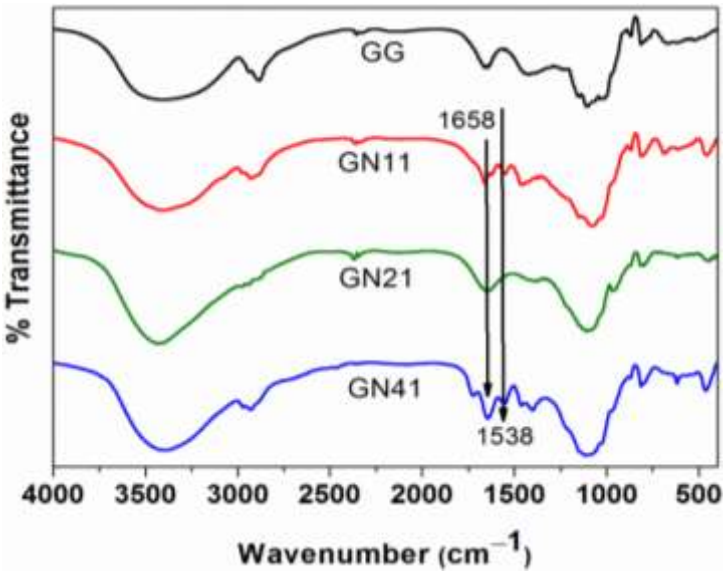

Figure 5.11.FTIR spectra of GG, GN11, GN21 and GN41 hydrogels.

5.2.2.2 XRD Analysis

The XRD profiles of the IPN hydrogels are displayed in Figure 5.12. GG presents a semi-crystalline nature with a broad diffraction pattern around 20^{o} and the crystalline regions are seen at 2θ of 29.6^{o} and 36^{o} which are the characteristics positions of the reflections from cellulose II (Zhang *et al.*, 2012). The IPN hydrogels exhibited almost similar diffraction profiles as that of the GG hydrogel but a slight decrease in the intensities of the crystalline peaks was observed probably due to the interpolymer interaction.

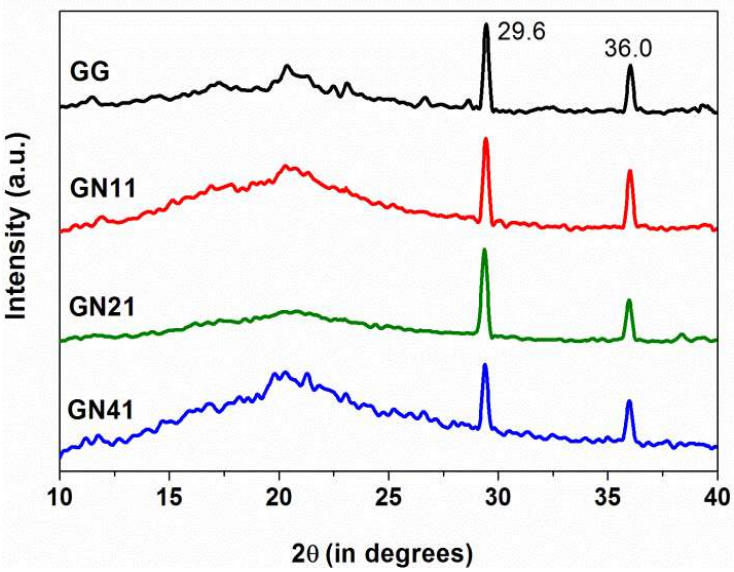

Figure 5.12.XRD profiles of GG, GN11, GN21 and GN41 hydrogels.

5.2.2.3 DSC Analysis

The LCSTs of the GG−PNIPAAm hydrogels were determined from their DSC thermograms and shown in Figure 5.13. The PNIPAAm hydrogel showed the LCST around 33°C, which matches with that of the reported value (Zhang *et al.*, 2004). The GN11, GN21 and GN41 hydrogels also exhibited LCST around 33°C. The invariance of the LCST with varying GG content implies that the arrangement of the PNIPAAm networks in the IPN hydrogels is more or less intact even after incorporation of GG. Previously it had been observed that copolymerization of a hydrophilic moiety into PNIPAAm hydrogel usually shifts the LCST to a higher temperature (Vernon *et al.*, 2007). Reversibly, the use of a hydrophobic moiety decreases the LCST (Koga *et al.*, 2001). In the present study, it could be inferred that no strong interactions were introduced into the PNIPAAm hydrogel by addition of GG and the thermo-sensitivity of the PNIPAAm was retained. It was also concluded that the incorporation of GG did not have a drastic impact on the LCST of the hydrogels. Similar results have also been observed earlier (Li *et al.*, 2008; Zhang *et al.*, 2005).

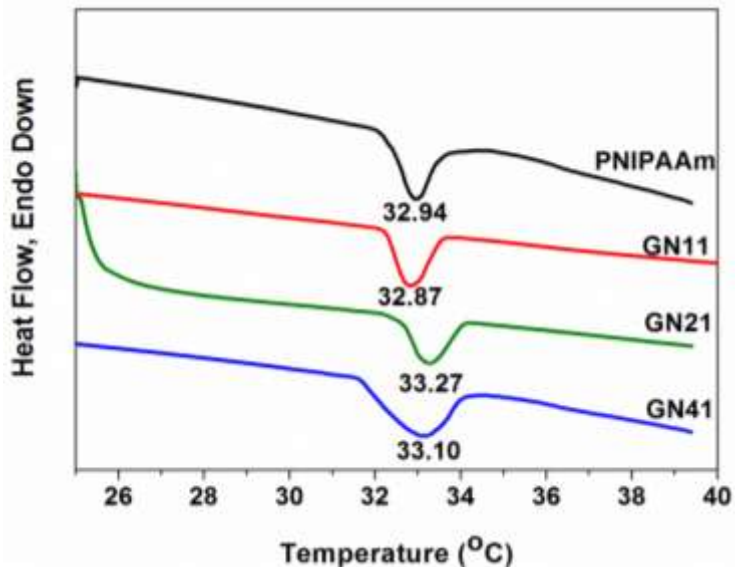

Figure 5.13. DSC thermograms of PNIPAAm, GN11, GN21 and GN41 hydrogels.

5.2.2.4 SEM Analysis

The morphology of the lyophilized hydrogels is represented in Figure 5.14.

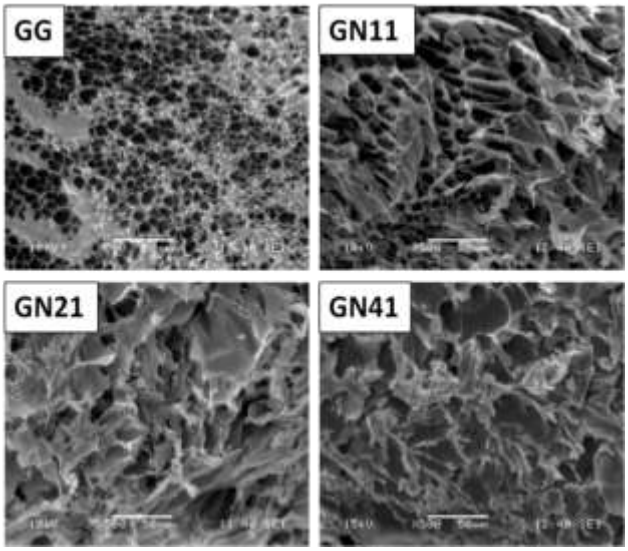

Figure 5.14. SEM images of GG, GN11, GN21 and GN41 hydrogels.

The SEM images reveal the highly porous morphology of the pure GG hydrogel. A distinct difference in the morphology of the IPN hydrogels and the GG hydrogel was observed. Though the IPN hydrogels also exhibited a somewhat porous nature, the porosity was greatly reduced in comparison to the GG hydrogel. An increase in the GG content led to the formation of a comparatively denser hydrogel network. This

increased network density could be attributed to the intermolecular hydrogen bonding between GG and PNIPAAm or intramolecular hydrogen bonding between the side-chains of GG and its backbones (Li *et al.*, 2008). Even the influence of cross-linking might be playing a role in the modification of the network structure. Thus the interplay of the above factors defines the morphology of the hydrogels.

5.2.3 Swelling Studies

5.2.3.1 Swelling in pH 7.4 buffer at 25°C and 37°C

The time-dependent swelling profiles of GN11, GN21 and GN41 hydrogels in pH 7.4 buffer at 25°C and 37°C, are illustrated in Figure 5.15 A and B, respectively.

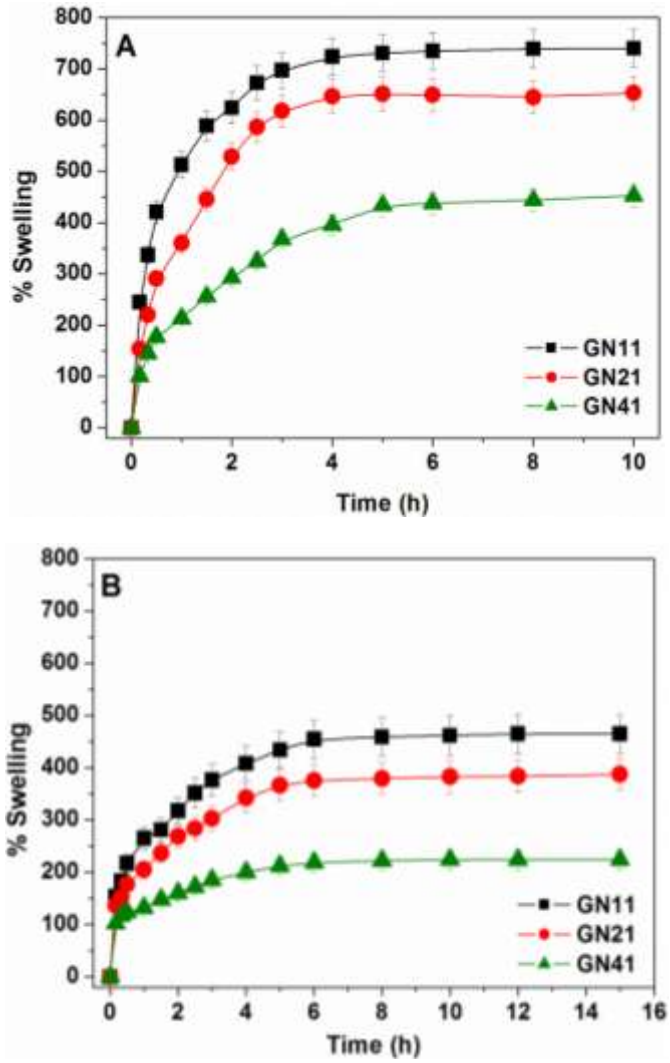

Figure 5.15. Time-dependent swelling profiles of GN11, GN21 and GN41 hydrogels in pH 7.4 buffer at (A) 25°C and (B) 37°C.

Higher swellability for the hydrogels was observed at 25°C than 37°C. The order of swelling of the hydrogels was found to be GN11 > GN21 > GN41. This implied that an increase in GG content in the matrix results in a decreased swelling capacity of the hydrogels. As evident from the SEM images, the GN41 hydrogel matrix structure was found to be relatively dense therefore it restricts the inflow of solvent molecules into the network which eventually leads to a lowering in its swelling ability.

5.2.3.2 Temperature−dependent Swelling

The equilibrium swelling ratios of the hydrogels in pH 7.4 buffer as a function of temperature is represented in Figure 5.16.

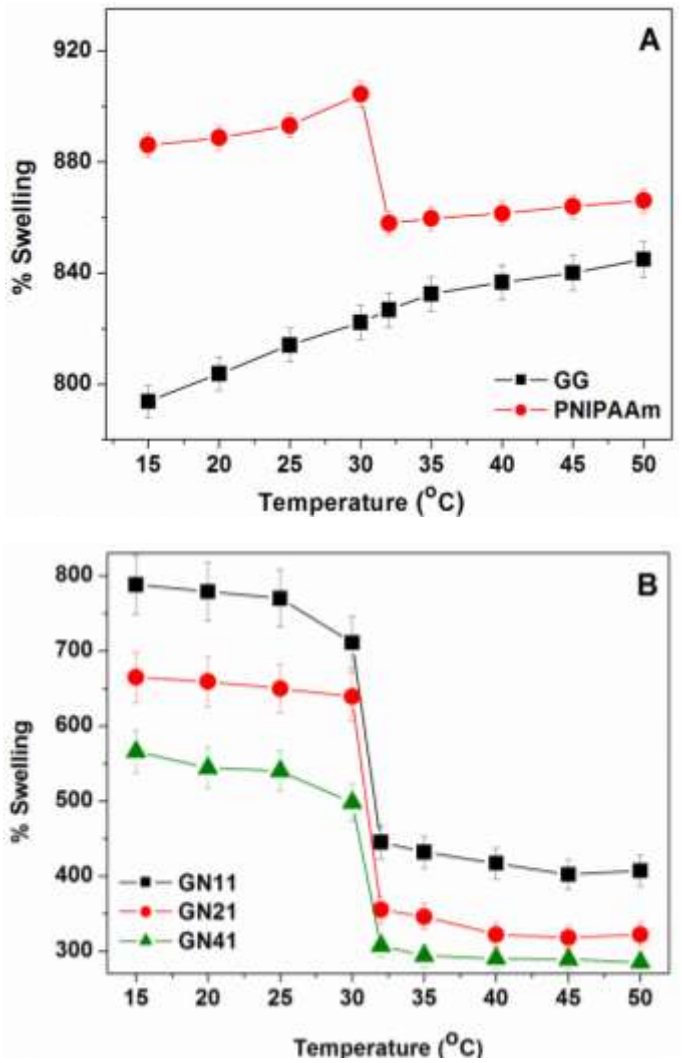

Figure 5.16. Temperature-dependent equilibrium swelling profiles of (A) GG, PNIPAAm and (B) GN11, GN21, GN41 hydrogels in pH 7.4 buffer.

Figure 5.16 A illustrates the swelling profiles of pure GG and PNIPAAm hydrogels in pH 7.4 buffer as a function of temperature. As evident, the GG hydrogel did not show any thermo-responsive behaviour; only a small increase in swelling percentage was observed due to the increased diffusion of water with temperature. However, a clear phase transition around 32°C is observed for the PNIPAAm hydrogel. The phase transition of PNIPAAm is the result of the balance between the hydrophobic and hydrophilic segments in the polymer chain (Otake *et al.*, 1990). PNIPAAm consists of the hydrophilic amido group (−CONH−) and a hydrophobic group (isopropyl−). Below LCST, the cooperative interaction (intermolecular hydrogen bonding) between the hydrophilic amide groups and the surrounding water molecules improve the hydrophilic characteristic of the hydrogel. Thus with decrease in temperature, the hydrophilic character is dominant and an enhanced swelling is observed (Zhang *et al.*, 2004). The water penetrating into the hydrogels is in a bound state at low temperatures. Upon increasing the temperature, the water molecules gain enthalpy and the intramolecular interaction becomes stronger while the intermolecular interactions between the polymer and water molecules weaken *i.e.* the hydrophobic force of the isopropyl group of the PNIPAAm chain increases. Thus the hydrophilic/ hydrophobic balance is disturbed in the PNIPAAm chains. The water present in the matrix is expelled out and the matrix experiences reduced swelling. In other words, the hydrogels showed contraction above the LCST, which is marked by the decrease in the swelling ratios. Both the hydrogels were found to be highly swelling matrices as indicated by their swelling values.

The swelling patterns of the IPN hydrogels are depicted in Figure 5.16 B. A region of minimum in the plots of swelling values with temperature occurs around 32°C in the GN11, GN21 and GN41 hydrogels. This indicates that the gel transition temperature

of PNIPAAm was not affected by the added GG component in the hydrogels. Among the IPN hydrogels, GN41 showed the least amount of water uptake may be due to the increased matrix density.

Photographs depicting the phase-transition of GN11 hydrogel is shown in Figure 5.17.

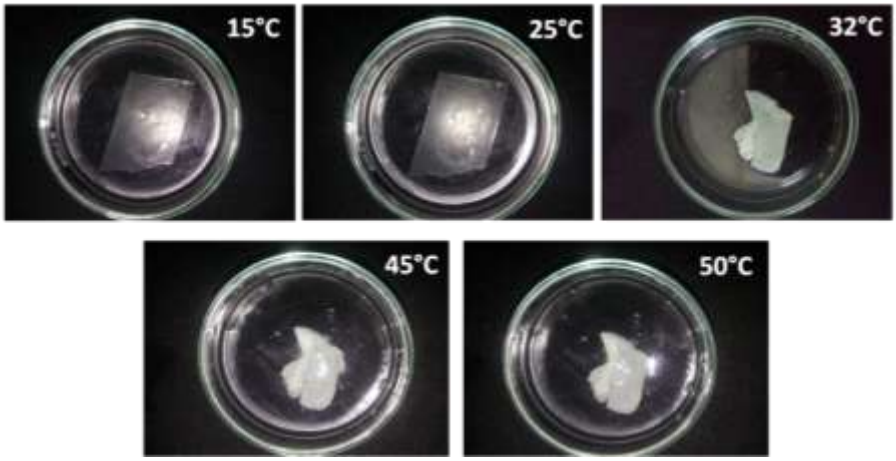

Figure 5.17. Photographs depicting the phase-transition ofGN11 hydrogel at different temperatures.

The photographs of the phase-transition of GN11 hydrogel swollen in pH 7.4 buffer at different temperatures of 15°C, 25°C, 32°C, 45°Cand 50°C are shown in Figure 5.17. The hydrogel, below the LCST, appears translucent. However, the hydrogel has shrunk in dimensions and appeared opaque at temperatures above the LCST of PNIPAAm. Thus the phase-transition of GN11 hydrogel is clearly visualized from the above photographs.

5.2.4 *In vitro* Drug Release Studies and Kinetics

5.2.4.1 *In vitro* 5FU Release Studies

The drug release patterns from GG-5FU, GG-IC, PNIPAAm-5FU and PNIPAAm-IC hydrogels and that from GN11-5FU and GN11-IC hydrogels in pH 7.4 buffer at the physiological temperature of 37°C are represented in Figures 5.18 A and Figures 5.18 B, respectively.

The release of 5FU from GG and PNIPAAm hydrogels were found to be very rapid and almost over by 2 h. Even for the GG-IC and PNIPAAm-IC hydrogels, where the drug is present in the form of IC with CD, the rate of drug release was almost similar to that of GG-5FU and PNIPAAm-5FU hydrogels containing the free drug. Thus, for the GG-IC and PNIPAAm-IC hydrogels, the role of CD was insignificant in controlling the drug release.

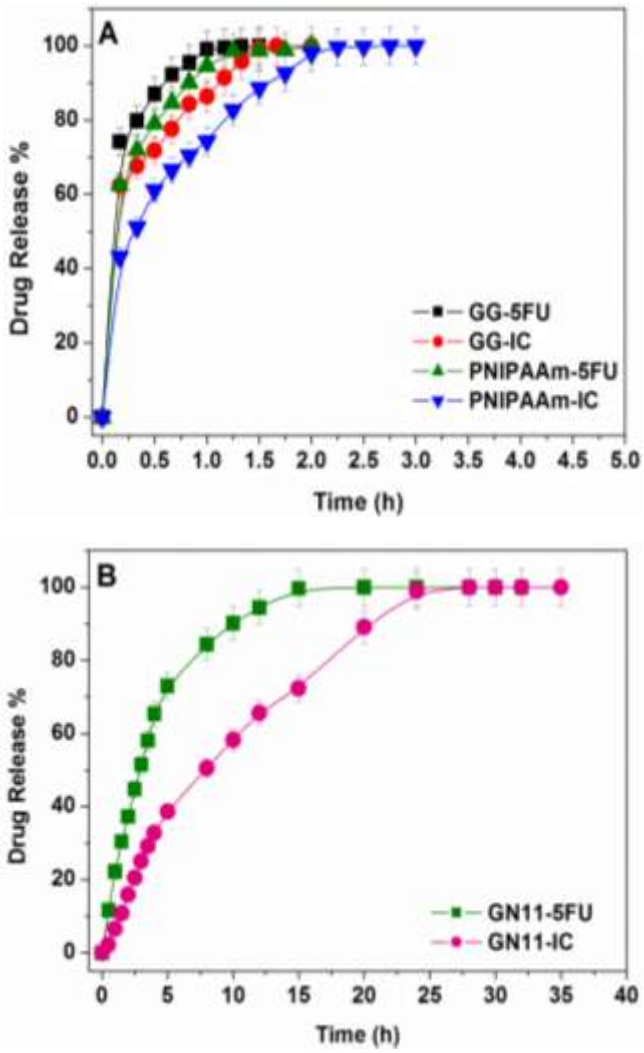

Figure 5.18. Drug release profiles of (A) GG-5FU, GG-IC, PNIPAAm-5FU, PNIPAAm-IC, and (B) GN11-5FU GN11-IC hydrogels in pH 7.4 buffer at 37°C.

As compared to the pure GG and PNIPAAm hydrogels the drug release was found to be significantly prolonged from the IPN hydrogels. Moreover, a remarkable difference was also observed in the release rates of 5FU from the GN11-5FU and GN11-IC

hydrogels. The GN11-IC hydrogel released the drug much slower than the GN11-5FU hydrogel containing the free drug. This could be attributed to the diffusion barrier imposed by CD on the drug diffusion from the GN11-IC hydrogel. From the above study it is clear that incorporation of IC into the hydrogel matrix is capable of controlling the drug release rate despite the fact that the matrix is undergoing a drastic morphological change above its LCST.

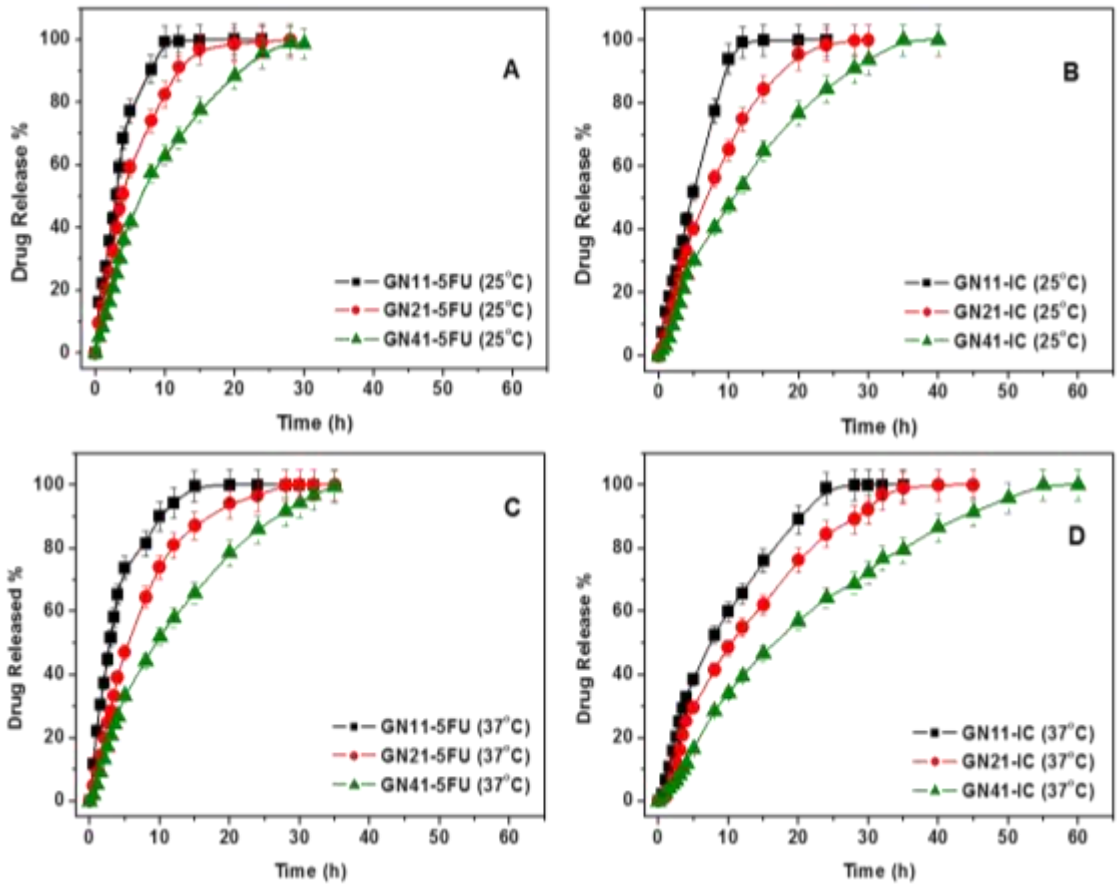

Figure 5.19. Drug release profiles of (A) GN11-5FU, GN21-5FU, GN41-5FU and (B) GN11-IC, GN21-IC, GN41-IC hydrogels in pH 7.4 buffer at 25°C and (C) GN11-5FU, GN21-5FU, GN41-5FU and (D) GN11-IC, GN21-IC, GN41-IC hydrogels in pH 7.4 buffer at 37°C.

To investigate the temperature-sensitivity of the synthesized hydrogels drug release experiments were performed at two different temperatures, below (25°C) and above (37°C) the LCST, in pH 7.4 buffer solutions. The release profiles of the drug from all

the synthesized GG−PNIPAAm IPN hydrogels in pH 7.4 buffer at 25°C and 37°C, are illustrated in Figure 5.19. The rate of drug release was found to be much slower at 37°C than at 25°C from all the hydrogels irrespective of whether they contained free 5FU or the IC. This could be explained by considering the temperature dependence in the swelling characteristics of the hydrogels. Since the hydrogels are in a contracted state at 37°C, the swellabilty is low and thus drug release is retarded. On the other hand, at 25^{o}C the hydrogels are in a swollen state therefore exhibiting a rapid release characteristic. However, at any time, the amount of drug released from the hydrogel containing IC is always less than that of the corresponding hydrogel with the free 5FU. This release profile signified the vital role of CD in the drug release phenomenon from the hydrogels and the temperature responsiveness of the hydrogels.

Figure 5.19 also illustrates the effect of GG content on the rate of drug release. The order of drug release from the hydrogels was found to be GN11-5FU > GN21-5FU > GN41-5FU. Similarly the IC containing hydrogels followed the order GN11-IC > GN21-IC > GN41-IC. This suggested that an increase in GG content led to a decrease in the rate of the drug release from the hydrogels. The above observations hold true for the release data conducted at both the experimental temperatures. The GN41-IC hydrogel was found to exhibit the slowest drug releasing characteristics and considered as the optimum hydrogel for the controlled delivery of 5FU. Thus controlled delivery of 5FU from the thermo-responsive GG−PNIPAAm IPN hydrogels is accomplished as a result of the synergistic effects of drug complexation with CD and the nature of the hydrogel matrix.

5.2.4.2 5FU Release Kinetics

The fitting parameters for the drug release data at 25°C and 37°C obtained by fitting to various mathematical models are tabulated in Tables 5.3 and 5.4, respectively. From Table 5.3, it is clear that the kinetics of drug release at 25°C mostly conform to Ritger-Peppas and Peppas-Sahlin models. The value of the diffusional exponent *n* lying between 0.77 and 0.89 specifies anomalous type of drug release from the hydrogels.

It is also evident from Table 5.4 that the drug release at 37°C also points to Ritger-Peppas and Peppas-Sahlin models. Anomalous type of drug release is indicated by the value of *n* lying between 0.74 and 0.96.

Table 5.3.5FU release parameters fitting to various mathematical models at 25°C

Sample	Higuchi		Ritger–Peppas			Peppas-Sahlin			Zero-Order	
	k ($h^{-0.5}$)	R^2	n	k' (h^{-n})	R^2	k_1 ($h^{-0.5}$)	k_2 (h^{-1})	R^2	k'' (h^{-1})	R^2
GN11-5FU	0.274	0.893	0.77	0.216	0.988	0.115	0.102	0.988	0.173	0.940
GN21-5FU	0.227	0.860	0.86	0.149	0.995	0.054	0.091	0.994	0.126	0.982
GN41-5FU	0.151	0.796	1.08	0.078	0.996	0.037	0.062	0.994	0.085	0.994
GN11-IC	0.193	0.865	0.86	0.128	0.995	0.080	0.050	0.996	0.107	0.980
GN21-IC	0.159	0.818	0.89	0.091	0.987	0.028	0.063	0.984	0.076	0.976
GN41-IC	0.129	0.831	0.86	0.065	0.987	0.028	0.039	0.983	0.049	0.963

Table 5.4.5FU release parameters fitting to various mathematical models at 37°C

Sample	Higuchi		Ritger–Peppas			Peppas-Sahlin			Zero-Order	
	k ($h^{-0.5}$)	R^2	n	k' (h^{-n})	R^2	k_1 ($h^{-0.5}$)	k_2 (h^{-1})	R^2	k'' (h^{-1})	R^2
GN11-5FU	0.277	0.899	0.79	0.216	0.999	0.106	0.110	0.997	0.176	0.961
GN21-5FU	0.185	0.839	0.86	0.112	0.992	0.067	0.047	0.988	0.088	0.972
GN41-5FU	0.149	0.892	0.74	0.093	0.992	0.073	0.028	0.990	0.054	0.905
GN11-IC	0.142	0.781	0.96	0.086	0.993	-0.017	0.091	0.994	0.073	0.962
GN21-IC	0.130	0.803	0.91	0.060	0.990	0.025	0.040	0.990	0.049	0.982
GN41-IC	0.106	0.838	0.89	0.039	0.990	0.016	0.025	0.992	0.029	0.980

In order to further demonstrate the importance of the polymer relaxation on the drug release mechanism from the hydrogels, plots of R/ F versus the fraction of drug released were constructed for the drug release data. Figure 5.20 presents the R/F plots for the drug release at 25°C and 37°C.

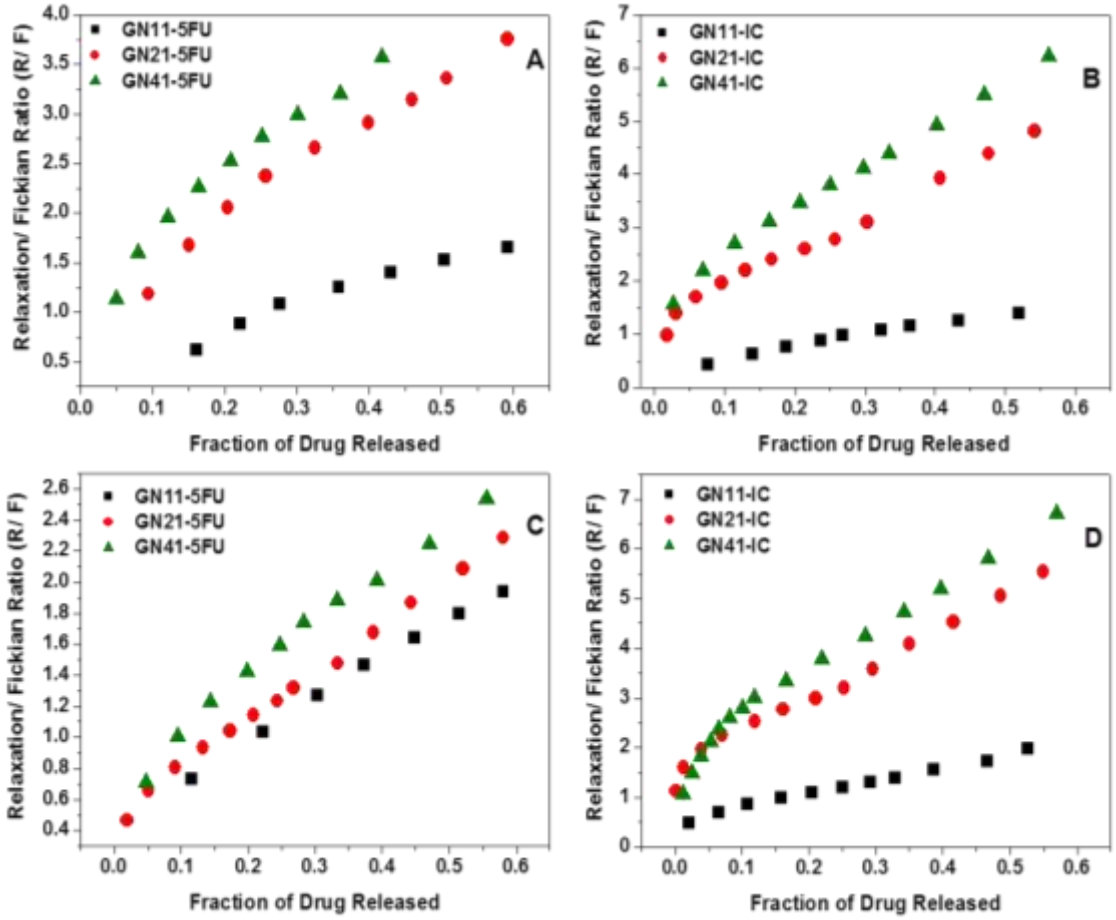

Figure 5.20. Plots of ratio of relaxation to the Fickian contribution (R/F) with the fraction of dug released from hydrogels (A) GN11-5FU, GN21-5FU, GN41-5FU; (B) GN11-IC, GN21-IC, GN41-IC hydrogels at 25°C and (C) GN11-5FU, GN21-5FU, GN41-5FU and (D) GN11-IC, GN21-IC, GN41-IC hydrogels at 37°C in pH 7.4 buffer.

In both the cases, the IC containing hydrogels were found to exhibit higher R/F values than the corresponding hydrogels containing the free drug. This indicated that the presence of CD influences the relaxation rate of the polymers which in turn retards the drug release. This can be explained by considering either the presence of hydrogen bonding interaction between the CDs and polymers or the CDs getting cross-linked to

some extent in the presence of the cross-linker TEOS. The value of R/F was found to be the maximum for the GN41-IC hydrogels irrespective of the temperature.

5.2.5 Cytotoxicity Assay

Since PNIPAAm is known to have poor biocompatibility, it is inevitable to test the cytotoxicity of the GG–PNIPAAm hydrogels before their use as drug delivery systems. The biocompatibility of GN41 hydrogel on L-929 rat fibroblasts was assayed by MTT colorimetric technique and the photograph obtained after 48 h incubation is shown in Figure 5.21.

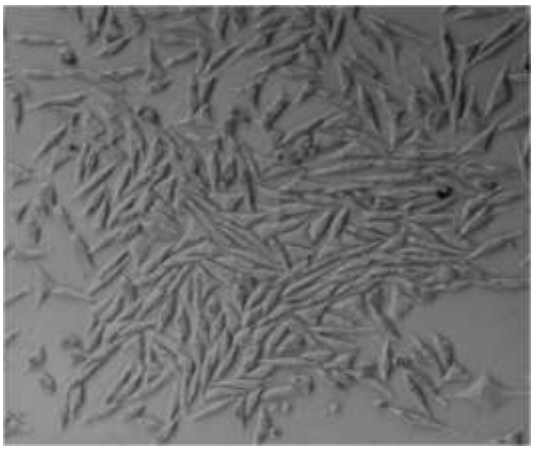

Figure 5.21. Optical micrographs of L−929 cells cultured after 48h incubation with GN41 hydrogel.

Direct contact between L-929 cells and the hydrogel did not reveal any adverse effect. This suggested the compatibility with the living tissues and non-toxicity of the hydrogel thus validating these as possible drug delivery systems.

5.3 CONCLUSIONS

- Solid ICs of 5FU in CD were prepared by the freeze drying/ lyophilization technique. The obtained ICs were characterized by FTIR, XRD, DSC, SEM and ^{1}H NMR studies. The formation of ICs was affirmed from the above analyses.

- Temperature-responsive GG−PNIPAAm hydrogels cross-linked by TEOS were synthesized by solution casting technique. The hydrogels were also characterized by various spectroscopic techniques such as FTIR, XRD, DSC and SEM.
- The FTIR analyses indicated the presence of amide-I and amide-II of PNIPAAm in the IPN hydrogels. An increase in GG content led to a decrease in the crystallinity of the hydrogels.
- The DSC thermograms indicated that the incorporation of GG did not disturb the arrangement of PNIPAAm chains and the LCST remained invariant.
- The hydrogels displayed temperature-dependent swelling characteristics. Higher swelling was observed at low temperatures (below the LCST of PNIPAAm) while a sudden drop in swelling ratio was observed around 32°C (LCST of PNIPAAm).
- The swelling behaviour indicated that the PNIPAAm present in the hydrogel had retained its thermo-sensitivity.
- The hydrogels also exhibited temperature dependence in their drug releasing characteristics. At higher temperature (above LCST) the release rate was considerably slower than that at lower temperature (below LCST).
- The rate of drug release was always slow from the hydrogels containing the ICs as compared to the hydrogels containing the free drug.
- Presence of IC in the hydrogel matrix is capable of significantly controlling the drug release rate despite the fact that the matrix is undergoing a drastic morphological change above its LCST.

- Higher amount of GG in the hydrogels led to a decrease in the release rate from the hydrogels. The order of drug release was found to be GN11 > GN21 > GN41.
- The GN41-IC hydrogel was found to be the optimum with slowest drug releasing characteristics.
- The preliminary analyses of drug release indicated Case II type of mechanism from the hydrogels at both the temperatures of 25°C and 37°C.
- Further analysis of R/ F values established the predominant effect of macromolecular relaxation on the drug release behaviour of the hydrogels.
- The presence of CD in the hydrogels as ICs was vital in influencing the polymer relaxation and retarding the drug release rate from the hydrogels containing the ICs.
- The cytotoxicity assay performed on rat fibroblasts certified the GG-PNIPAAm hydrogels to be safe, nontoxic and biocompatible with living tissues thereby validating their potential as controlled drug delivery systems.

CHAPTER 6

EVALUATING GUAR GUM–POLY(ACRYLIC ACID) HYDROGELS AS CONTROLLED DELIVERY SYSTEMS

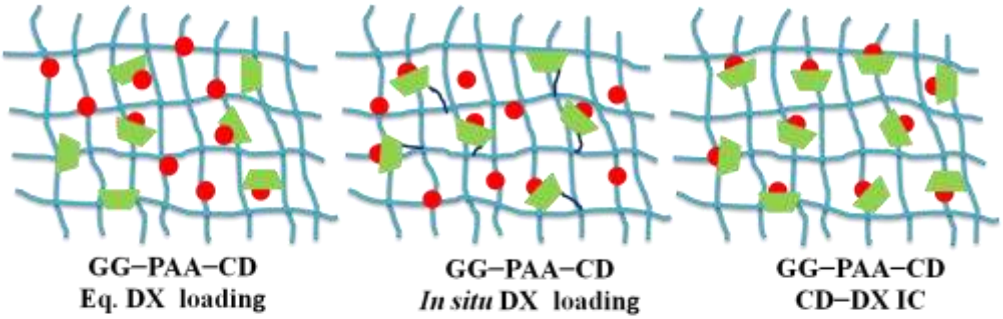

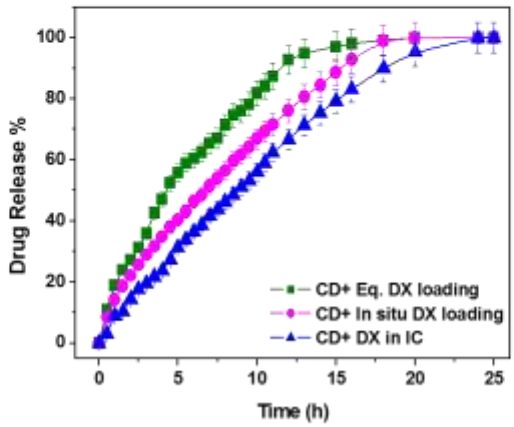

6.1 INTRODUCTION

Introduction of cyclodextrins into hydrogels plays a vital role in deciding the drug release profiles (Concheiro and Alvarez-Lorenzo, 2013; Crini *et al.,* 1998). Incorporation of cyclodextrins into polymeric drug release systems has been known to influence the mechanism by which the drug is released (Bibby *et al.,* 2000). A range of strategies have been explored to modify cyclodextrin integrated hydrogels to meet desired drug delivery profiles. Hydrogels in which CDs form a part of the network structure, can be obtained by cross-linking of CDs with the polymer backbone or by copolymerization of CD with the hydrogel network (Alvarez-Lorenzo *et al.,* 2011; Prabaharan and Gong, 2008; Prabaharan and Mano, 2005; Fulop *et al.,* 2013; Kobayashi *et al.,* 1989). Hydrogels bearing CDs as pendant groups have been constructed for modifying drug release rates (Liu *et al.,* 2004; Liu *et al.,* 2005; Szetjli *et al.,* 1978). CS hydrogels bearing CDs as pendant groups have been used as carriers for controlled protein release (Zhang *et al.,* 2009). Even hydrogels containing grafted CDs have been utilized in controlled drug delivery (Nielsen *et al.,* 2009; Zhang *et al.,* 2008; Salmaso *et al.,* 2007; Zhang *et al.,* 2004; Prabaharan and Mano, 2005). Hydrogels where CD has been blended with the polymer matrix have also shown potential to prolong drug release (Sreenivasan, 1997). The details regarding the various strategies employed for the integration of CDs with different hydrogels and their applications have been discussed in Chapter 1. Efforts are still being directed towards integrating CDs with different hydrogels to design novel drug delivery systems.

Mateen and Hoare (2014) have recently synthesized cyclodextrin-dextran hydrogels where CD is covalently attached to the polymer network through chemical cross-linking and utilized for the controlled delivery of DX. Machin and co-workers (2012)

prepared discs of insoluble CD polymers by cross-linking with EPI. The potential of the synthesized discs against two anti-inflammatory (NX and nabumetone) and antifungal drugs (naftifine and terbinafine) was investigated. Drug release data evidenced the suitability of these hydrogel as sustained release systems. Pinho and co-authors (2014) have recently illustrated the efficacy of CD-based hydrogels as wound dressing materials. A series of CD grafted carboxymethyl CS hydrogels have been constructed using 1-ethyl-3-(3-dimethylaminopropyl) carbodiimide hydrochloride as cross-linker in presence of N-hydroxysuccinimide (Kono and Teshirogi, 2015). The CD grafted hydrogels prolonged the release of acetylsalicylic acid (ASA) in comparison to ASA release from pure carboxymethyl CS hydrogel. Hydrogels based on the inclusion efficiency of CD have also been developed towards controlled delivery of drugs. Hybrid hydrogels based on host-guest interaction have been employed for the delivery of various anticancer drugs (Yu *et al.,* 2014; Yu *et al.,* 2014; Wu *et al.*, 2014). CD-based supramolecular assemblies for drug delivery purposes have been excellently reviewed by various research groups (Harada *et al.,* 2014; Tan *et al.*, 2014; Zhang and Ma, 2013; Chen and Jiang, 2011; Li and Loh, 2008). A plethora of literature is available regarding CD-integrated hydrogels towards controlled drug delivery applications. However, a comparative study of the drug delivery efficacy of hydrogels containing CD as a part of their network structure and hydrogels with preformed drug-CD ICs is yet to be explored.

OBJECTIVES

The focus of the present chapter is to evaluate GG-PAA-CD hydrogels, where CD is present as a part of the network structure, for the delivery of DX. Further, to compare the drug delivery efficacy of these hydrogels with that of the GG-PAA hydrogels containing preformed DX-CD ICs. GG matrices, as such are highly hydrophilic with

less mechanical strength (Li *et al.*, 2008). To improve the mechanical integrity, GG has been usually employed in an IPN with other polymers. GG IPN hydrogels have been developed in combination with PAA which improves the mechanical strength of the hydrogel (Huang *et al.*, 2007). Moreover, GG-PAA IPN hydrogels exhibit pH-sensitivity; therefore can be utilized as pH-responsive drug delivery vehicles.

The specific objectives of the present study are:

- Synthesis and characterization of TEOS cross-linked GG-PAA IPN hydrogels containing CD moieties.
- Synthesis of TEOS cross-linked GG-PAA hydrogels containing free DX as well as preformed DX-CD ICs.
- Evaluation of the swelling capacities and antimicrobial activities of the hydrogels.
- Estimation of the drug loading efficiencies of the hydrogels.
- Comparison of the drug delivery characteristics of the GG-PAA hydrogels containing CD in their networks and the hydrogels containing DX-CD ICs.
- Addressing the preliminary drug release kinetics.
- Cytotoxic assay of the hydrogels on L-929 mice fibroblasts.

The composition and designation of the synthesized hydrogels by varying the amounts of GG and PAA are listed in Table 6.1.

Table 6.1. Composition and designation of synthesized GG−PAA hydrogels

Sample	GG: AAc (%)	Sample Designation	
		GG-PAA (GP)	GG-PAA-CD (GP-CD)
1	1:0	GP10	GP10-CD
2	0:1	GP01	GP01-CD
3	1:1	GP11	GP11-CD
4	1:2	GP12	GP12-CD
5	1:4	GP14	GP14-CD
6	2:1	GP21	GP21-CD
7	4:1	GP41	GP41-CD

Hydrogels comprising GG and PAA are represented as GP and those containing CD are represented as GP-CD, in general. The numerical values represent the molar ratio of the parent components. The hydrogels containing the ICs of DX with CD have been designated accordingly. For the characterization and swelling studies, GP and GP-CD designation indicate the respective hydrogels without any drug. For the drug release studies, the GP and GP-CD hydrogels were loaded with DX. The ICs were prepared by the freeze drying method and a detailed discussion regarding the formation of ICs has been presented in Chapter 4.

6.2 RESULTS AND DISCUSSION

6.2.1 Hydrogel Characterization

6.2.1.1 FTIR Analysis

The FTIR spectra of GP10, GP10-CD, GP01 and GP01-CD hydrogels are presented in Figure 6.1 A. For GP10 and GP10-CD hydrogels, the bands around 3400 cm^{-1}, and 3000–2800 cm^{-1} are associated with the O−H and C−H stretching vibration modes, respectively and the peak at 1645 cm^{-1} is attributed to the ring stretching of the guar gum polymer backbone. The C−OH and the primary alcoholic CH_2OH stretching are observed in the region of 1120 cm^{-1}. The peak around 1400 cm^{-1} is due to the CH_2 deformation. The peaks observed in the 800−1200 cm^{-1} represent the highly coupled C−C−O, C−OH and the C−O−C stretching modes of the polymer (Mudgil *et al.,* 2012). The FTIR spectra of GP01 and GP01-CD show a broad band in the range 3500 – 3300 cm^{-1} owing to the hydroxyl stretching vibrations. The most important band is the 1640 cm^{-1} which is due to carbonyl stretching vibration, present in both the hydrogels. The band at 1417 cm^{-1} is associated with the bending vibrations of CH−CO groups. The bands at 1255 and 1192 cm^{-1} are attributed to the coupling between in-plane O−H bending and C−O stretching of the hydroxyl groups (Moharram and Khafagi, 2007).

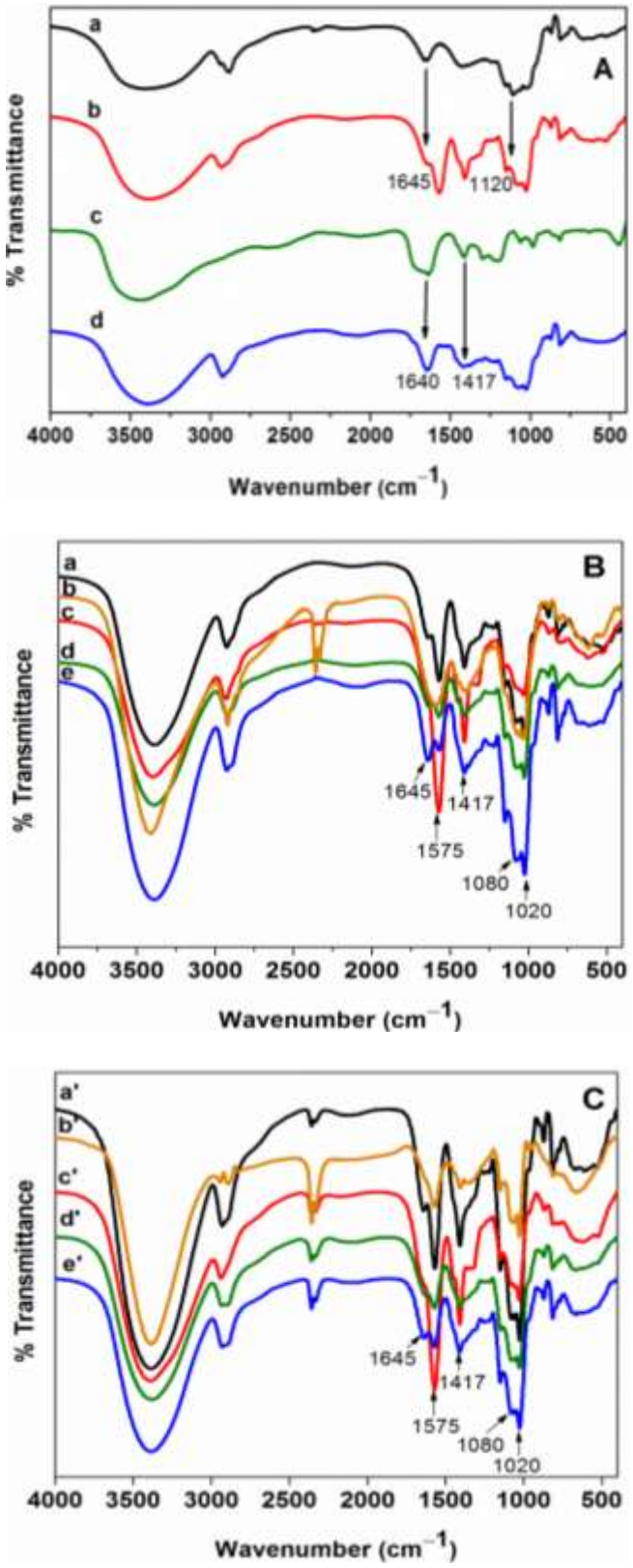

Figure 6.1. FTIR spectra of (A) (a) GP10, (b) GP10-CD, (c) GP01, (d) GP01-CD; (B) GP and (C) GP-CD hydrogels; (a) GP11, (b) GP12, (c) GP14, (d) GP21, (e) GP41, (a') GP11-CD, (b') GP12-CD, (c') GP14-CD, (d') GP21-CD, (e') GP41-CD hydrogels.

In comparison with the pure samples, a shift in the carbonyl stretching peak to 1575 cm^{-1} is observed in the spectra of the synthesized GP and GP-CD hydrogels (Figures 6.1 B and C) which can be assigned to the symmetric deformation of COO^- (Huang *et al.*, 2007). The characteristic 1417 cm^{-1} peak of PAA is also observed in the spectra of the hydrogels. This peak is most intense and sharp in GP14 and GP14-CD hydrogels but a decrease in the intensity of this particular peak is observed in the spectral profiles of GP21, GP21-CD, GP41 and GP41-CD hydrogels. This might be because of the dominant effect of GG in these hydrogels. Similar was the case observed with the peak at 1645 cm^{-1} due to the ring stretching of guar gum. The spectra of GP41 and GP41-CD hydrogels showed a more intense 1645 cm^{-1} peak than other hydrogels. Moreover, the peaks observed at 1020 and 1083 cm^{-1} in the spectra of all the synthesized hydrogels confirm the presence of the siloxane bond (Si−O−) resulting from the cross-linker TEOS (Islam and Yasin, 2012).

6.2.1.2 XRD Analysis

The X-ray diffraction profiles of the synthesized GP and GP-CD hydrogels are shown in Figures 6.2 A and B respectively. Results evidenced that all hydrogels except GP01 and GP01-CD presented a semi-crystalline nature. GP01 and GP01-CD hydrogels show a broad diffraction around 22° indicating the amorphous nature of the hydrogels. GP10 and GP10-CD hydrogels show a broad diffraction pattern around 20.5° and several crystalline peaks are observed at diffraction angles (2θ) 29.6°, 36°, 39.4°, 43.2° and 48.5°. Pure GG is known to present a broad diffraction pattern at 20.5° (Mudgil *et al.*, 2012) and the characteristics crystalline regions of the reflections from cellulose II (Hu and Hsieh, 1996). The GP and GP-CD hydrogels showed similar diffraction patterns as that of GP10 and GP10-CD hydrogels. However, a decrease in the intensity of the crystalline peaks was observed in the IPN hydrogels. This could be

attributed to the interpolymer interaction. Thus the XRD profiles clearly demonstrate the proper mixing of both the polymer components as well as CD in the resulting hydrogels.

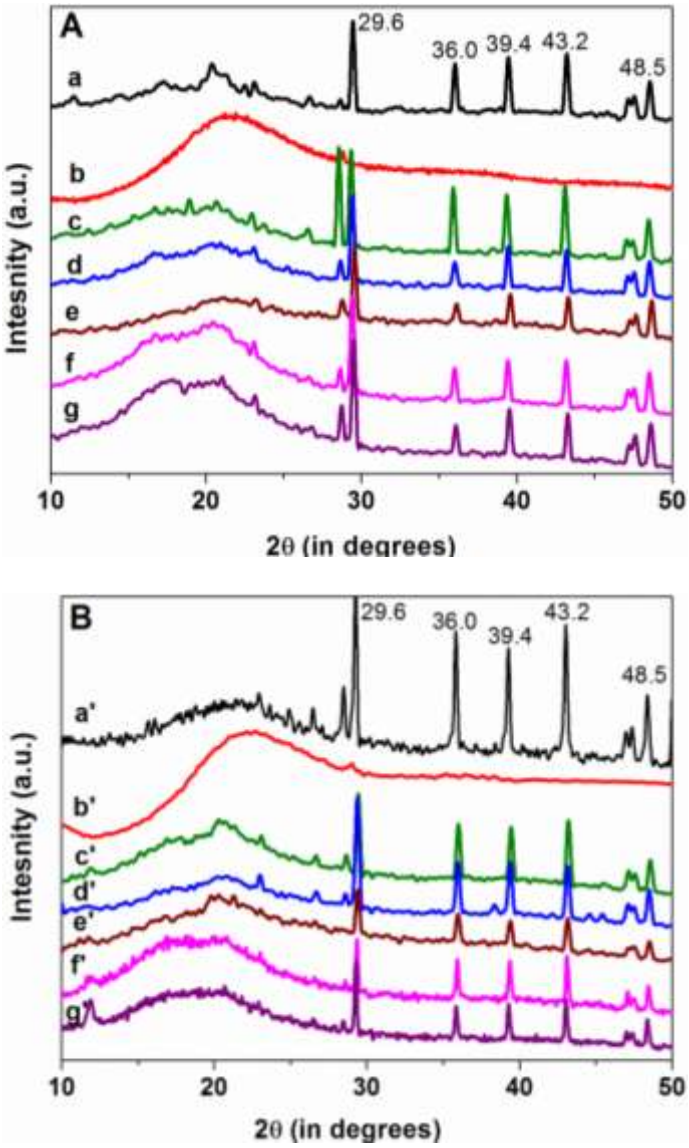

Figure 6.2. XRD profiles of (A) GP hydrogels; (a) GP10, (b) GP01, (c) GP11, (d) GP12, (e) GP14, (f) GP21 and (g) GP41,(B) GP-CD hydrogels; (a') GP10-CD, (b') GP01-CD, (c') GP11-CD, (d') GP12-CD, (e') GP14-CD, (f') GP21-CDand (g') GP41-CD.

6.2.1.4 DSC Analysis

The DSC thermograms of the synthesized hydrogels are shown in Figure 6.3.

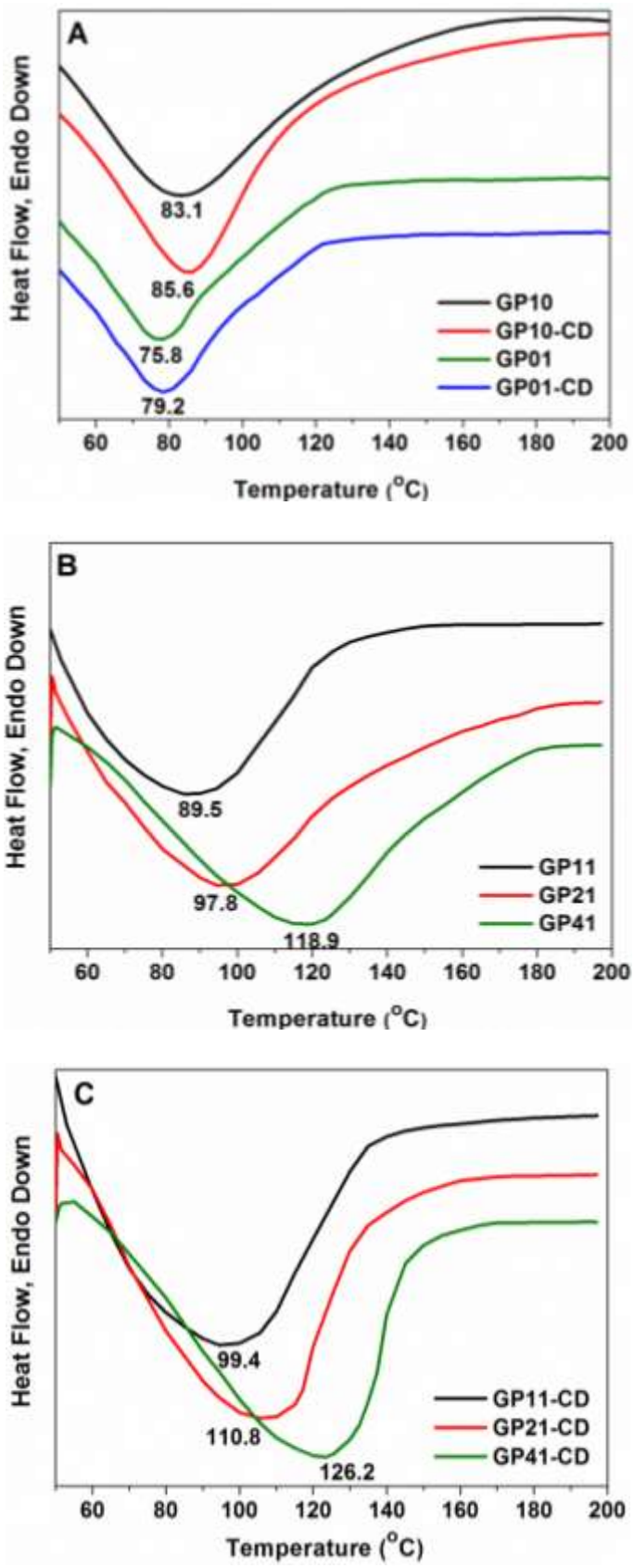

Figure 6.3. DSC thermograms of (A) GP10, GP10-CD, GP01, GP01-CD; (B) GP11, GP21, GP41, and (C) GP11-CD, GP21-CD, GP41-CD hydrogels.

The DSC thermograms of GP10 and GP01 reveal strong endothermic peaks around 83°C and 75°C respectively, which match with the reported T_g values for GG and PAA (Khutoryanskiy *et al.,* 2004; Singh, 2013). For the GP10-CD and GP01-CD hydrogels, the endotherms shifted to slightly higher temperatures at 86°C and 79°C, respectively. This can be probably due to the increased rigidity of the network structure upon incorporation of CDs in the hydrogels, which restrict the polymer chain mobility. The GP11 hydrogel showed a strong endothermic effect around 89.5°C, which is considerably higher than that of GP10 and GP01. This proved that the matrix of the resulting IPN is rigid in nature and possess higher thermal stability. For the GP11, GP21 and GP41 hydrogels (Figure 6.3 B); the endotherms shifted to higher temperatures with an increase in the GG content. Similar was the case observed for GP11-CD, GP21-CD and GP41-CD hydrogels (Figure 6.3 C). However, the T_g of the GP-CD hydrogels were always slightly higher than that of GP hydrogels, indicating an improved stability of these hydrogels due to the presence of CD in their network structures. In all IPN hydrogels, a single T_g indicates that the component polymers (GG and PAA) have good miscibility (Huang *et al.*, 2007).

6.2.1.5 SEM Analysis

Figure 6.4 displays the SEM images of the freeze-dried GP and GP-CD hydrogels. As evident, the GP10 (Figure 6.4 A) and GP01 (Figure 6.4 B) hydrogels exhibit highly porous matrix structures with spongy appearance. With an increase in PAA content in GP11 (Figure 6.4 C), GP12 (Figure 6.4 D) and GP14 (Figure 6.4 E) increase in the pore diameter of the hydrogels was observed although the matrix appeared relatively denser than the pure components.

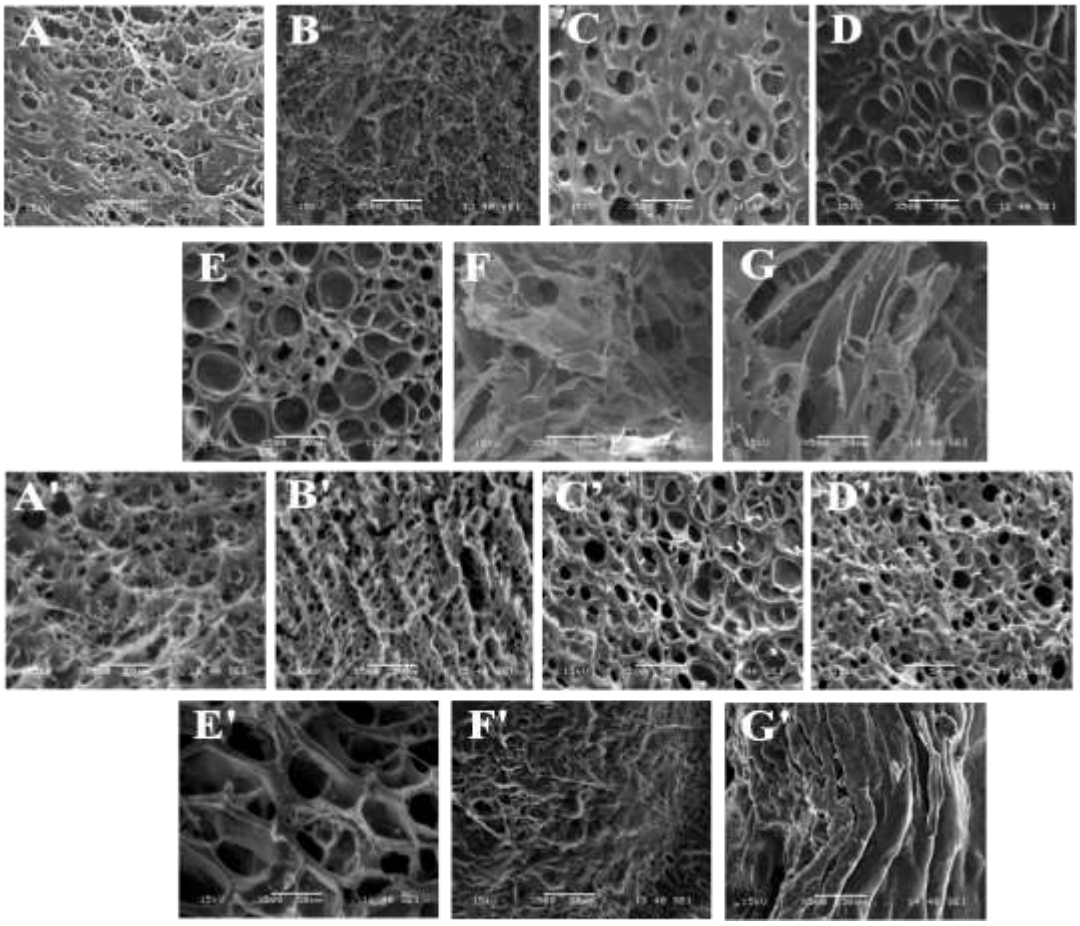

Figure 6.4. SEM images of (A) GP10, (B) GP01, (C) GP11, (D) GP12, (E) GP14, (F) GP21, (G) GP41, (A') GP10-CD, (B') GP01-CD, (C') GP11-CD, (D') GP12-CD, (E') GP14-CD, (F') GP21-CD and (G') GP41-CD hydrogels.

On the other hand, an increase in GG content led to the formation of a more compact and dense matrix for GP21 (Figure 6.4 F) and GP41 (Figure 6.4 G) hydrogels. For the hydrogels containing CD, almost similar morphological behaviour is observed as that of the corresponding hydrogels without CD, which indicates that the presence of CD did not have any significant effect on the morphology of the hydrogels.

6.2.2 Swelling Response of Hydrogels

6.2.2.1 Swelling in Water

The swelling characteristic is suggestive of the diffusion behaviour of molecules to and from the hydrogels. The swelling profiles of GP10, GP10-CD, GP01 and GP01-CD hydrogels are shown in Figure 6.5.

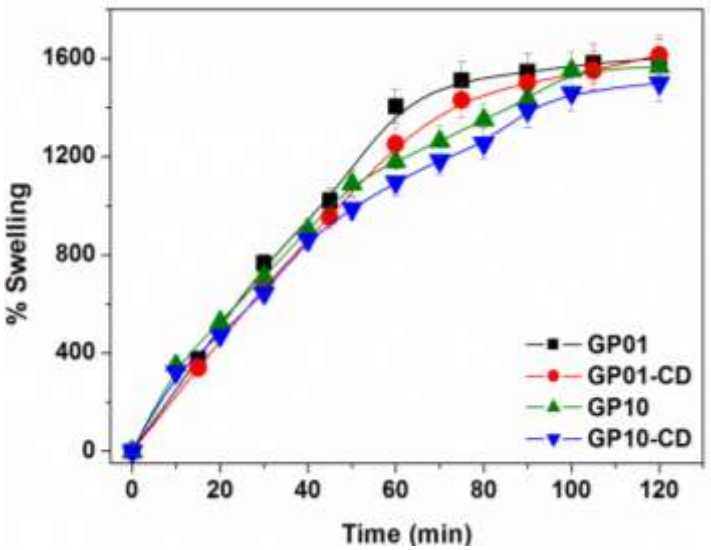

Figure 6.5. Time-dependent swelling behaviour of GP10, GP01, GP10-CD and GP01-CD hydrogels in water at 37°C.

As evident, the hydrogels undergo rapid swelling and maximum swelling was achieved within 2 h. The high extent of swelling in these hydrogels signifies their highly porous nature which was also observed from the SEM images. The presence of CD does not have any significant effect on the swellability of the hydrogels.

Time-dependent swelling of GP and GP-CD hydrogels in a buffer of pH 7.4 and at a temperature of 37°C were studied and illustrated in Figure 6.6 and Figure 6.7. As it is evident from the figures the swelling ability of the IPN hydrogels is significantly lower as compared to the hydrogels having single polymer component (*i.e.* GP10 and GP01). This can be explained considering the increased network rigidity induced by the IPN process, which was quite apparent from the SEM studies.

Effect of PAA Content on Swelling

Figures 6.6 A and B describe the effect of PAA content on the swelling behaviour of GP11, GP12, GP14 and GP11-CD, GP12-CD, GP14-CD hydrogels. Upon increase in PAA content, the swellability of the hydrogels increased, *i.e.* more the PAA content, more is the swelling. The increase in PAA amount results in increased number of ionizable groups in the polymer network; as a result of which the swelling ratio is also

enhanced. Similar increase in the swellability was also observed for GP11-CD, GP12-CD and GP14-CD hydrogels.

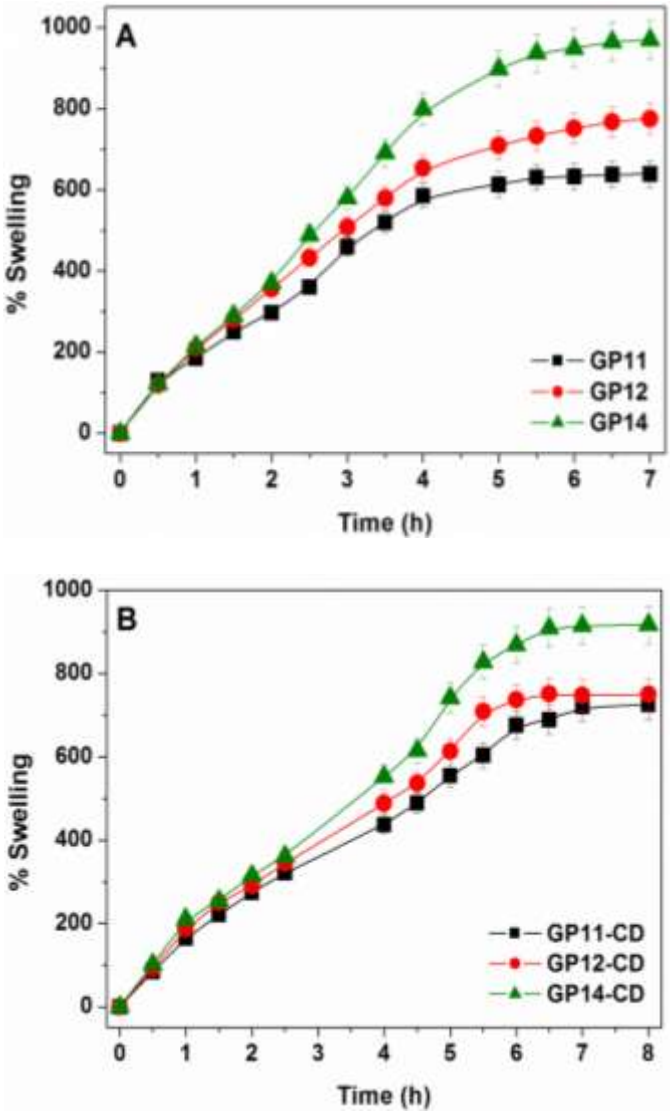

Figure 6.6. Time-dependent swelling behaviour of (A) GP11, GP12, GP14 and (B) GP11-CD, GP12-CD, GP14-CD hydrogels in water at 37°C.

Effect of GG Content on Swelling

The influence of GG on the swelling behaviour of GP and GP-CD hydrogels is demonstrated in Figure 6.7 A and B. With increased amount of GG in the hydrogels, the swelling ratio decreased. This might be attributed to formation of dense network structure due to inter-polymeric interaction between GG and PAA. More is the GG content, denser is the matrix which further leads to lower uptake of water and thus

swelling is reduced (Li *et al.*, 2006). This observation of swelling behaviour of the hydrogels with variation in PAA or GG content is also supported by the SEM data.

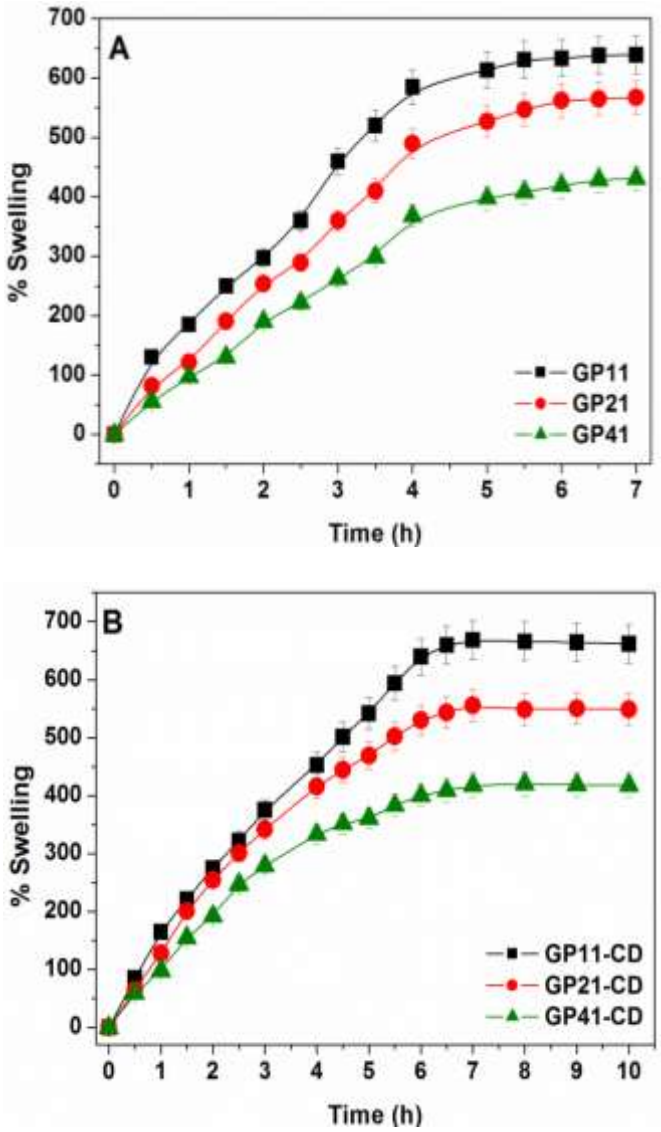

Figure 6.7. Time-dependent swelling behaviour of (A) GP11, GP21, GP41 and (B) GP11-CD, GP21-CD, GP41-CD hydrogels in water at 37°C.

6.2.2.2 pH-Dependent Swelling

The presence of ionic groups in the hydrogels is susceptible to changes in the environmental pH. Figure 6.8 A shows the swelling of GP11, GP12, GP14, GP21 and GP41 hydrogels at different pHs. As evident, the swelling ratios increased gradually from pH 2 to pH 7 and then a lowering is observed at alkaline pH. Again it is observed that more the PAA content higher is the swelling ratio irrespective of the pH. The pH-

sensitivity of these hydrogels is attributed to the presence of the ionizable carboxylic groups in PAA, which is a weak acid with an intrinsic pK_a of around 4.28. At low pH (pH < 4.28) the ionization of carboxylic groups is suppressed and there can be strong hydrogen bond interaction between the polymer chains that reduces the flexibility of the chains as a result the swelling capacity is lowered. At pH > 4.28, the water content of the hydrogels increases due to the ionization of the carboxylic groups. The increased ionic repulsion increases the free volume in the polymer matrix enhancing the water inflow. Additionally, the negative charge generated by the carboxylic groups drives the flow of cations into the hydrogel increasing the ionic swelling pressure and the degree of swelling. On further increase in pH (> 7), the effect of ionic strength surpasses the effect of electrostatic repulsion between the carboxylate groups by shielding the negative charges by high concentrations of counter ions thereby reducing the swelling (Huang *et al.,* 2007). The overall swelling behaviour of GP11-CD, GP12-CD, GP14-CD, GP21-CD and GP41-CD hydrogels were found to be very similar to the corresponding hydrogels without CD (Figure 4.50 B). This indicates that the presence of CD did not have any drastic effect on the swelling abilities of the hydrogels. For the IPN hydrogels the swelling ratio followed the order GP14 > GP12 > GP11 > GP21 > GP41, which is the same for the CD containing hydrogels as well.

The microstructures of the GP14 hydrogel swollen in solutions of different pHs were investigated by SEM. Figure 6.8 C displays the SEM images of the lyophilized GP14 hydrogel swollen in solutions of three different pHs, 2, 7.4 and 9. Since maximum swelling occurs in neutral pH, the hydrogel becomes highly porous in nature at this pH. As lower swelling takes place in pH 9, the hydrogel porosity is slightly decreased in comparison to pH 7.4. The hydrogel swells the lowest in acidic medium (pH 2),

thus a relatively compact morphology is evident. Similar morphological changes have been observed by Jin *et al.*, (2006) for PAA-PVP hydrogels.

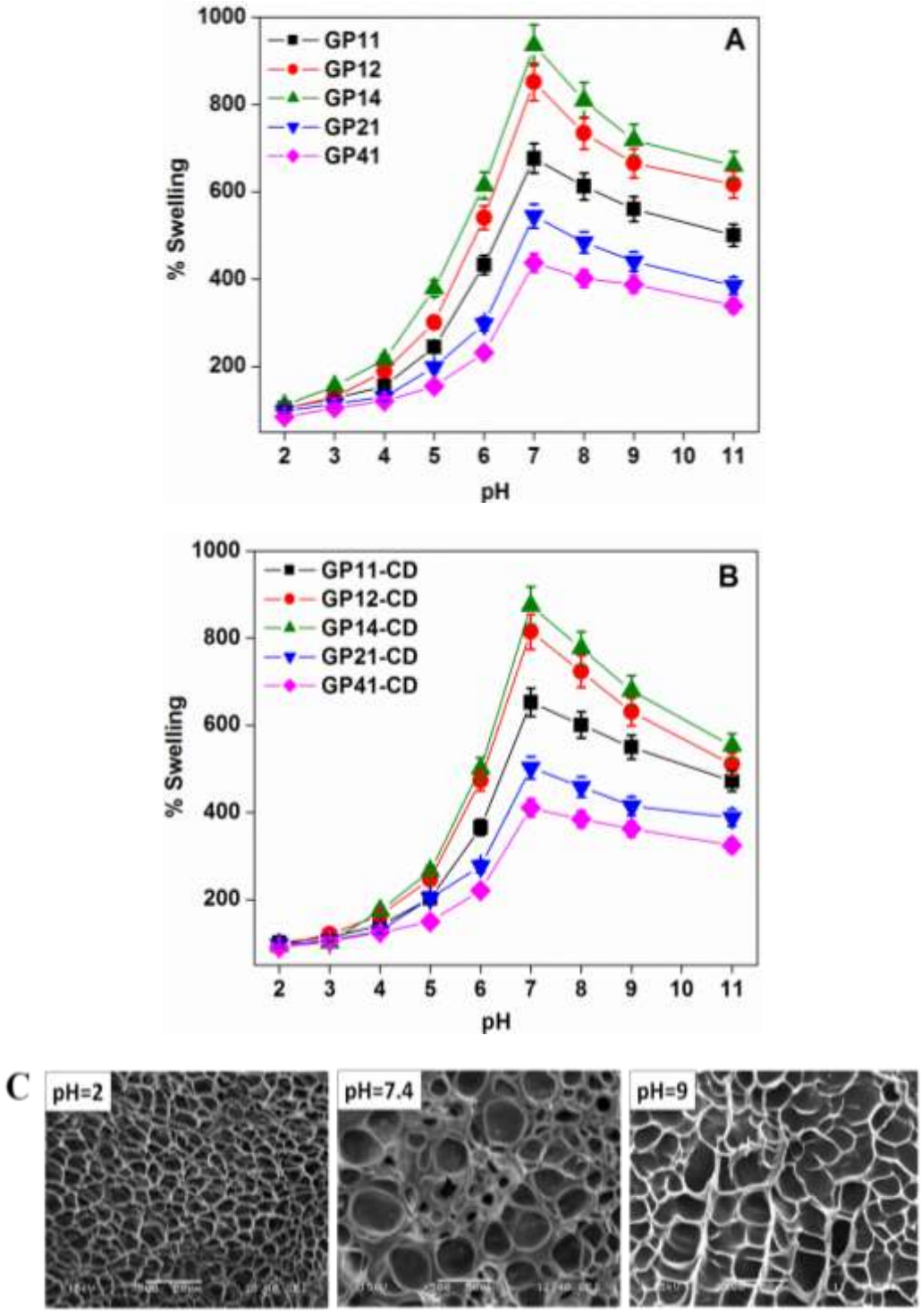

Figure 6.8. pH dependent swelling of (A)GP11, GP12, GP14, GP21, GP41 hydrogels and (B) GP11-CD, GP12-CD, GP14-CD, GP21-CD, GP41-CD hydrogels, and (C) SEM images of GP14 hydrogel swollen in pHs 2, 7.4 and 9.

6.2.3 Drug Loading Efficiency

The amount of drug that can be loaded when a hydrogel is immersed in a drug solution usually depends on both, the concentration of the soaking solution and the affinity of the drug for the hydrogel polymer network (Kim *et al.,* 1992). The equilibrium drug loading capacity of the synthesized hydrogels, with and without CD, was determined and listed in Table 6.2.

Table 6.2. Drug loading efficacies of GP and GP-CD hydrogels

Sample	DX Loading (%)
GP11	59 ± 2
GP11−CD	65 ± 3
GP12	50 ± 2
GP12−CD	58 ± 3
GP14	49 ± 4
GP14−CD	56 ± 2
GP21	56 ± 2
GP21−CD	58 ± 3
GP41	55 ± 2
GP41−CD	57 ± 3

It was observed that the presence of CD in the polymer matrix improved the drug loading capacitates of the hydrogels. For a particular PAA or GG content, the CD-containing hydrogel encapsulated more drug than the one without CD. This could be explained by taking into consideration the affinity of CD for hydrophobic guests (DX). It was also evident that the loading efficiency decreased with an increase in the PAA content. Since DX is mainly encapsulated in the hydrophobic cavity of CD, an increase in −COOH group implies an increase in the hydrophilic character of the hydrogel, which in turn, might decrease the loading efficiency of the hydrogel (Harada *et al.,* 1981). An increase in GG content also led to a decrease in the drug loading ability of the hydrogels. This effect could be possibly explained by formation of denser network structure with addition of GG which restricts the chain mobility and

reduction in the swellability, thereby preventing the in-flow of drug molecules during equilibrium loading.

6.2.4 *In vitro* Dexamethasone Release Studies and Kinetics

6.2.4.1 *In vitro* Dexamethasone Release Studies

Figure 6.9 shows the release profiles of DX from GP10, GP10-CD, GP01 and GP01-CD hydrogels at pH 7.4 and 37°C. DX release from GP10 and GP01 hydrogels, containing either GG or PAA, was found to be very fast and complete drug release takes place in a short period of time (< 2 h). This can be explained by considering the highly porous nature of these hydrogels leading to extensive swelling that result in rapid release of the drug. The GP10-CD and GP01-CD hydrogels showed a slightly prolonged release characteristic as compared to the corresponding hydrogels without CD. However, the presence of CD in these extensively swelling matrices does not have any significant effect on the release characteristics and the total release is over by 3 h.

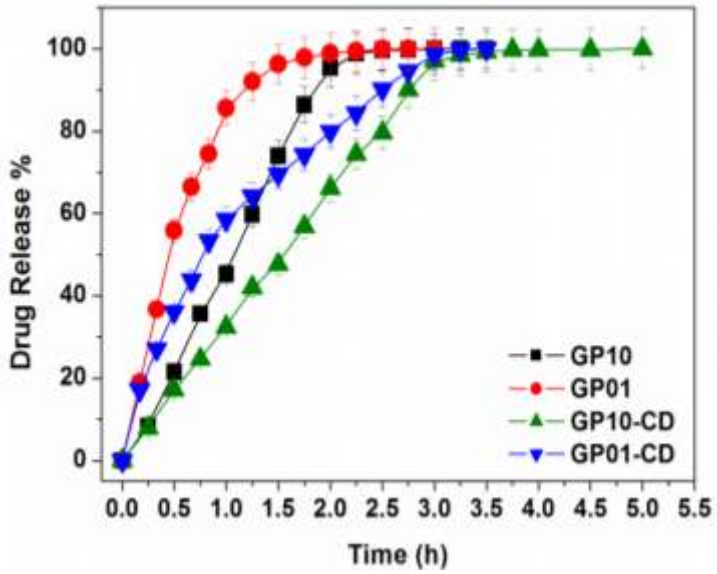

Figure 6.9. DX release profiles of GP10, GP01, GP10-CD, GP01-CD, hydrogels in pH 7.4 at 37°C.

Effect of PAA Content on DX Release from Hydrogels

Figures 6.10 A and B demonstrate the effect of PAA content on the drug release phenomenon from GP11, GP12, GP14 and GP11-CD, GP12-CD, GP14-CD hydrogels in pH 7.4 buffer at 37°C.

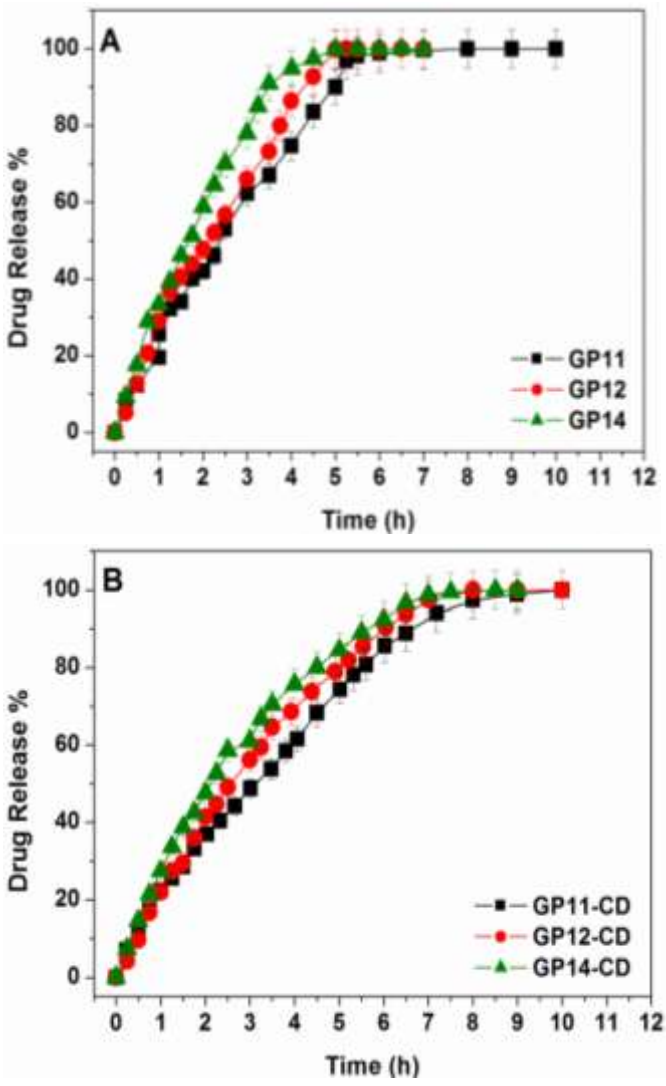

Figure 6.10. DX release profiles from (A) GP11, GP12, GP14 and (B) GP11-CD, GP12-CD, GP14-CD hydrogels in pH 7.4 buffer at 37°C.

Comparing the release profiles of GP11, GP12 and GP14 hydrogels, no significant difference is observed in the drug release rates with the increased PAA content. However, careful scrutiny of the release profiles indicate the drug release to follow the order GP14 > GP12 > GP11 *i.e.* with the increased PAA content a somewhat faster

release of DX is observed. This can be rationalized by considering the effect of PAA content on the swelling ratio. Since the increased amount of PAA leads to highly swellable matrix, the drug release also follows similar trend. The CD containing hydrogels show just a nominal increase in the release rate of DX as compared to the corresponding hydrogels without the CD. The DX release from these hydrogels also shows similar dependence on PAA content and follows the order: GP14-CD > GP12-CD > GP11-CD. However, the presence of CD does not have much control on the release rate from these highly swelling matrices.

Effect of GG Content on DX Release from Hydrogels

The effect of GG content on DX release from GP11, GP21, GP41 and GP11-CD, GP21-CD, GP41-CD hydrogels is clearly depicted in Figure 6.11 A and B, respectively. The drug release profiles are found to show a strong dependence on the GG content in the hydrogels. As the GG content increases, the rate of drug release decreases and the drug release is significantly prolonged. This can be explained by considering the dependence of drug release rate on the nature of the hydrogel matrix. Due to increased GG content, the hydrogel becomes denser and the swelling ratio decreases, which eventually inhibits the faster release of the drug. The effect of GG is more pronounced in case of the CD containing hydrogels. DX release is significantly prolonged from the GP41-CD hydrogel than that from GP11-CD and GP12-CD hydrogels. Moreover, the CD containing hydrogels show a considerably slow release of DX as compared to the corresponding hydrogels without the CD. The synergistic effect of the increased GG content and the presence of CD on the drug release process can be due to the combined effect of the increased matrix density and the influence of CD on the polymer relaxation process, which reduce the free volume available for the drug diffusion thus decreasing the release rate. In addition, the possibility of DX-CD

complex formation in the CD containing hydrogels should also be considered. In GP11, GP21 and GP41 hydrogels DX is freely dispersed in the matrix and can diffuse out of the matrix as the matrix swells, while in GP11-CD, GP21-CD and GP41-CD hydrogels some of the DX are freely dispersed and some are likely to be in a bound state with CD therefore prolonging the release rate. The GP41-CD hydrogel was found to exhibit the best of all for obtaining controlled release of DX.

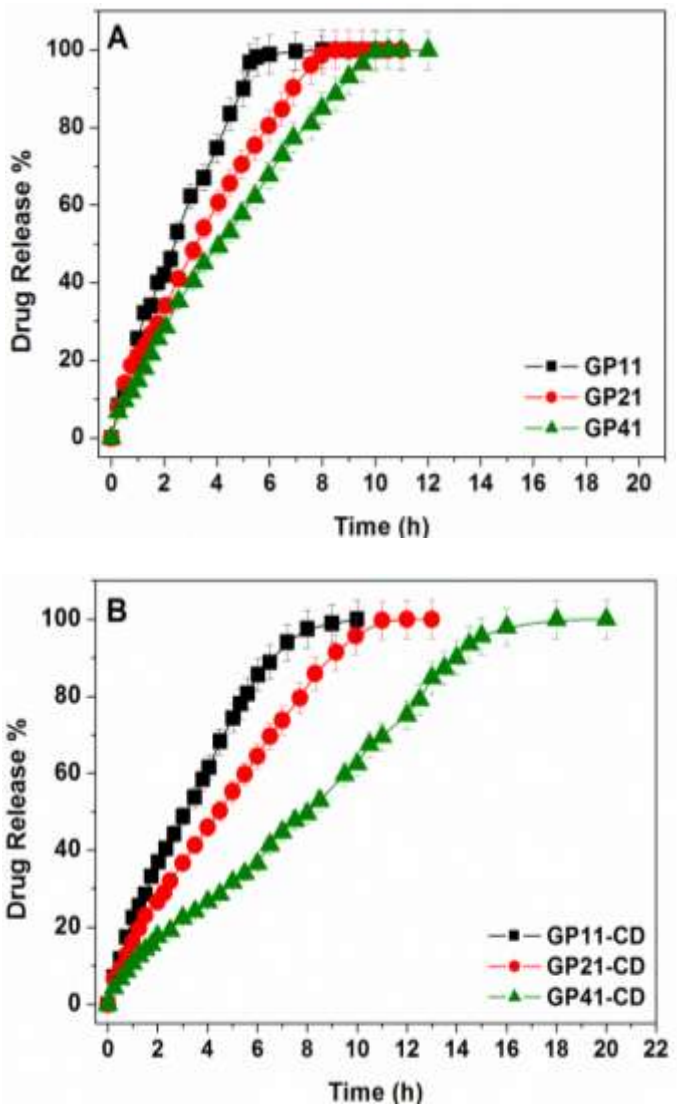

Figure 6.11. DX release profiles from (A) GP11, GP21, GP41 and (B) GP11-CD, GP21-CD, GP41-CD hydrogels in pH 7.4 at 37°C.

DX Release in SGF and SIF

In order to explore the drug release behaviour at pH conditions in the GIT, the release studies were carried out in the simulated fluids, SGF and SIF. For further imitating the GIT conditions; the GP41 and GP41-CD hydrogels were immersed in SGF for 2 hours, then transferred to SIF and the drug release was monitored (Figure 6.12).

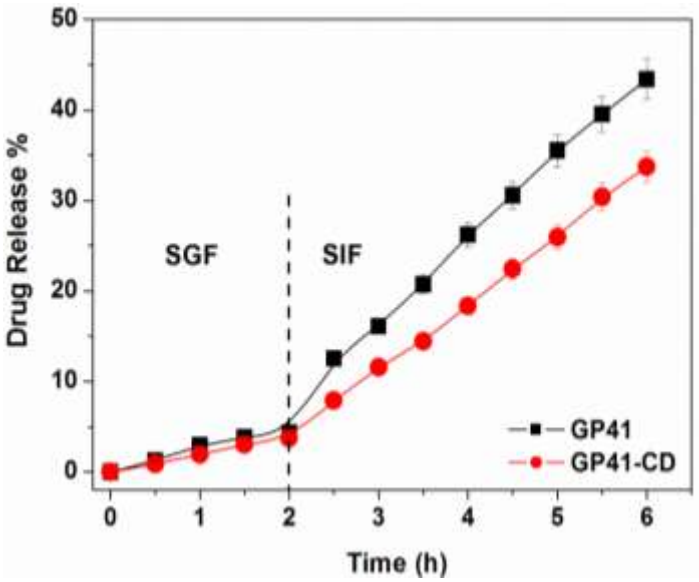

Figure 6.12. Drug release profiles of GP41, GP41-CD hydrogels in SGF and SIF at 37°C.

For all the hydrogels, less than 5% of DX was released during the initial 2 h in SGF. However, when the hydrogels were transferred to SIF, the release of DX increased significantly. It could be observed that the amount of DX released from the CD-containing hydrogels is considerably less than the hydrogels without CD at any given time. From the above study, it was proposed that GP41-CD could be employed as a controlled delivery vehicle for the delivery of dexamethasone to the intestine.

Drug Release from Hydrogels containing DX-CD ICs

In order to compare the efficacy of GG-PAA-CD hydrogels and GG-PAA-IC hydrogels, release experiments were also carried out from the hydrogels containing DX-CD ICs. The release profiles of GP01 and GP10 hydrogels containing the ICs showed almost similar release profiles as that of GP01-CD and GP10-CD hydrogels and the drug release was over by 3 h, due to the extensive swelling of the hydrogels.

Effect of PAA Content on DX Release from Hydrogels Containing DX-CD ICs

Figure 6.13 A describes the influence of increasing PAA content on the drug release process from the IC containing hydrogels. Similar to that observed earlier for GP-CD hydrogels, with increased PAA content, no significant difference in the rate of drug release occurred even in the presence of IC. GP11-IC, GP12-IC, and GP14-IC all showed similar release rate.

Effect of GG Content on DX Release from Hydrogels Containing DX-CD ICs

Figure 6.13 B illustrates the influence of GG content on DX release from GP11-IC, GP21-IC and GP41-IC hydrogels. The presence of GG in higher amounts in the hydrogel matrix remarkably prolongs the drug release rate which is very similar to that observed in case of the GP-CD hydrogels. GP41-IC hydrogel was found to be the best of the lot for controlled delivery of DX.

Therefore, it can be concluded that the hydrogel composition and the nature of the hydrogel matrix in terms of its network organization play vital roles in the drug release process, irrespective of whether CD is present as part of hydrogel network structure or added as an IC.

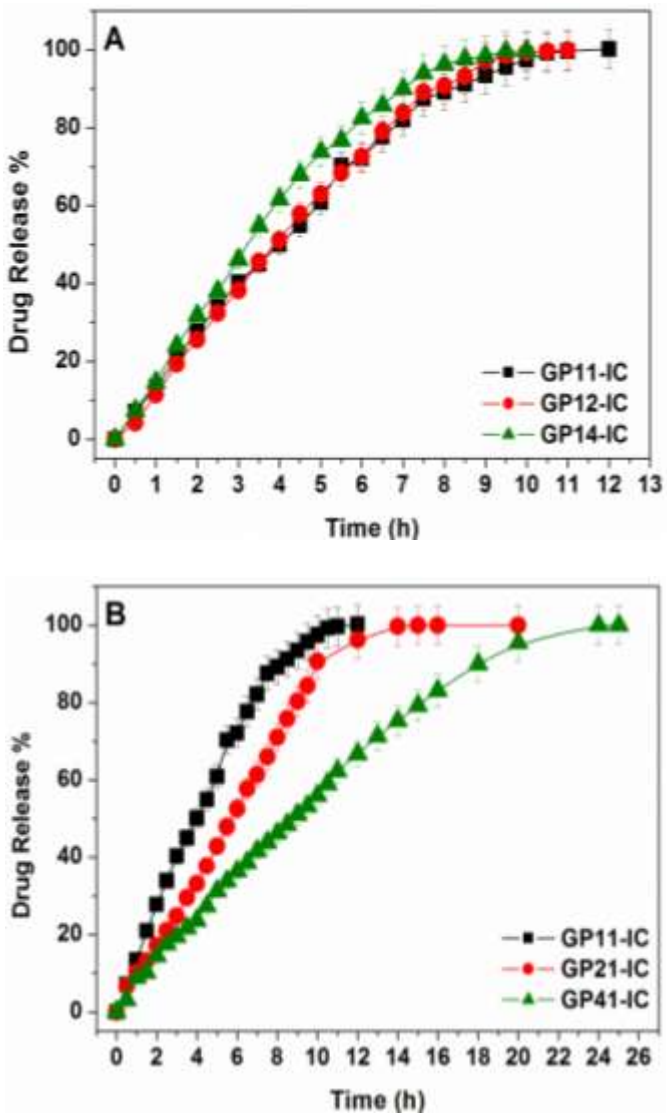

Figure 6.13. DX release profiles from (A) GP11-IC, GP12-IC, GP14-IC and (B) GP11-IC, GP21-IC, GP41-IC hydrogels in pH 7.4 at 37°C.

Effect of Method of Drug Incorporation in Hydrogels

To verify the influence of method of incorporation of drug into the hydrogel and the role of CD on the drug release characteristics, release studies were carried out from the following systems: (i) GP41-CD hydrogel where DX was added during the hydrogel synthesis, (ii) GP41 hydrogel containing the preformed solid DX-CD IC and (iii) GP41-CD (eq. loading) hydrogel where DX was loaded into the hydrogel through equilibrium loading process.

In the equilibrium loading method, the GP41-CD hydrogel was allowed to swell in the DX solution till equilibrium. Then the hydrogel was washed to remove the surface adhered drug. This hydrogel has been represented as GP41-CD (eq. loading); "eq. loading" in the parentheses indicates that the drug is loaded through equilibrium loading method.

Figure 6.14 represents the DX release profiles of GP41-CD, GP41-IC and GP41-CD (eq. loading) hydrogels at pH 7.4 and 37°C.

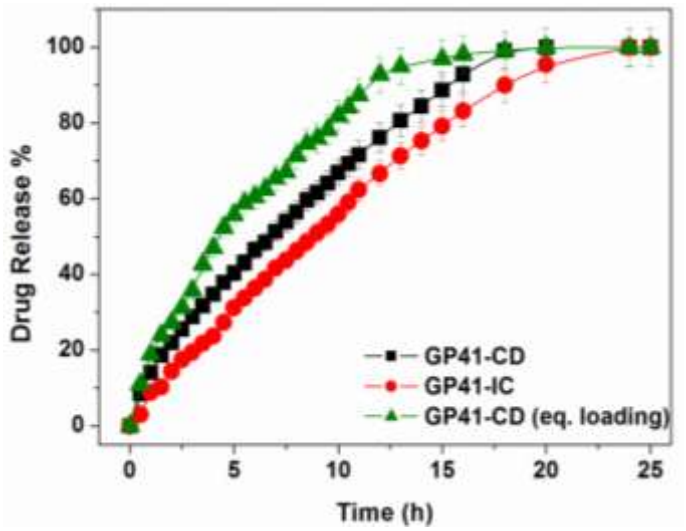

Figure 6.14. DX release profiles from GP41-IC, GP41-CD and GP41-CD (eq. loading) hydrogels at pH 7.4 and 37°C.

The DX release rate was found to follow the order GP41-CD (eq. loading) > GP41-CD > GP41-IC. The GP41-CD (eq. loading) hydrogel released the drug considerably faster in comparison to the other two hydrogels. The complete drug release from the equilibrium loaded hydrogel took around 12 h, from the GP41-CD hydrogel it took around 17 h whereas from the IC containing hydrogel the total drug release takes around 24 h. This could be attributed to the fact that during equilibrium loading it is likely that major fraction of DX is distributed freely in the hydrogel matrix and a few are in the bound state with the CD. For GP41-CD hydrogel, since the drug was incorporated *in situ i.e.* during the hydrogel synthesis, therefore it is expected that the

fraction of CD-bound drug to be higher than that the freely dispersed drug. But in case of GP41-IC hydrogel, it contains the drug mostly in the bound state therefore showing the slowest release characteristic. Similar results were also obtained for other GP hydrogels *i.e.* for all hydrogels the IC containing hydrogel showed relatively prolonged release than the corresponding hydrogel with CD as a part of the network.

Thus from the above studies it could be concluded that hydrogels containing ICs fare better in terms of controlled release characteristics than the hydrogels containing CD as a part of their matrix. Moreover the other benefits of loading drug in the form of IC are: (i) the drug can be protected from the harsh reaction conditions of hydrogel synthesis, (ii) it offers a control on the drug loading efficiency, and (ii) it can improve the solubility, stability and bioavailability of the drug.

6.2.4.2 *In vitro* DX Release Kinetics

Table 6.3 summarizes the kinetic and the fitting parameters for the DX release data fitted to various mathematical equations. It was also found that DX release data showed the best fit to the Ritger-Peppas model for almost all the hydrogels. The kinetic fittings for GP10, GP01, GP10-CD and GP01-CD hydrogels also showed good fit to the zero-order equation. The relative contribution from the diffusion and relaxation processes calculated from the Peppas-Sahlin equation for these hydrogels shows the predominant effect of the relaxation kinetic constant (k_2) over the diffusion kinetic constant (k_1). It has been observed that these hydrogels undergo extensive swelling in a very short period of time which can be due to the rapid polymer relaxation followed by water diffusion. Thus, the drug release from these hydrogels is controlled mostly by relaxation rate of the polymer chains. The diffusional exponent (n) was found to be 0.96 and 0.97 for GP10 and GP10-CD hydrogels which implied the Case II drug transport mechanism from these hydrogels. For the GP and GP-CD

hydrogels the value of *n* lie between 0.5 and 0.9 indicating the anomalous nature of drug release, where both diffusion and relaxation processes contribute.

Table 6.4 summarizes the kinetic and the fitting parameters for the DX release from GP-IC hydrogels which have been fit to various mathematical equations. The value of *n* lying between 0.87 and 0.95 indicate the drug transport mechanism to be of anomalous nature.

Table 6.3. DX release parameters from GP and GP-CD hydrogels fitting to various mathematical models

Sample	Higuchi		Ritger–Peppas			Peppas-Sahlin			Zero-Order	
	k ($h^{-0.5}$)	R^2	n	k' (h^{-n})	R^2	k_1 ($h^{-0.5}$)	k_2 (h^{-1})	R^2	k'' (h^{-1})	R^2
GP10	0.587	0.816	0.96	0.751	0.995	0.038	0.716	0.995	0.764	0.994
GP01	0.736	0.839	0.88	0.974	0.991	0.154	0.838	0.988	1.054	0.978
GP11	0.305	0.909	0.78	0.256	0.986	0.123	0.131	0.989	0.217	0.954
GP12	0.321	0.872	0.82	0.273	0.981	0.096	0.173	0.977	0.244	0.958
GP14	0.376	0.886	0.82	0.331	0.995	0.121	0.207	0.994	0.301	0.971
GP21	0.264	0.895	0.77	0.209	0.988	0.110	0.098	0.991	0.165	0.943
GP41	0.231	0.900	0.78	0.166	0.992	0.091	0.076	0.991	0.123	0.953
GP10-CD	0.505	0.817	0.97	0.561	0.995	0.017	0.543	0.995	0.563	0.995
GP01-CD	0.556	0.948	0.665	0.577	0.994	0.356	0.221	0.992	0.596	0.986
GP11-CD	0.27	0.903	0.76	0.218	0.993	0.122	0.096	0.994	0.173	0.934
GP12-CD	0.285	0.866	0.85	0.221	0.993	0.069	0.148	0.991	0.194	0.977
GP14-CD	0.321	0.883	0.83	0.271	0.998	0.092	0.175	0.996	0.244	0.978
GP21-CD	0.222	0.918	0.75	0.166	0.996	0.102	0.065	0.996	0.118	0.943
GP41-CD	0.158	0.897	0.82	0.094	0.991	0.051	0.043	0.994	0.063	0.972
GP41-CD (eq. loading)	0.231	0.985	0.713	0.172	0.993	0.122	0.054	0.993	0.113	0.917

Table 6.4. DX release parameters from GP-IC hydrogels fitting to various mathematical models

Sample	Higuchi		Ritger–Peppas			Peppas-Sahlin			Zero-Order	
	k ($h^{-0.5}$)	R^2	n	k' (h^{-n})	R^2	k_1 ($h^{-0.5}$)	k_2 (h^{-1})	R^2	k'' (h^{-1})	R^2
GP11-IC	0.234	0.863	0.88	0.148	0.997	0.046	0.102	0.996	0.126	0.988
GP12-IC	0.223	0.801	0.94	0.122	0.997	−0.017	0.138	0.998	0.128	0.989
GP14-IC	0.255	0.813	0.92	0.155	0.998	−0.011	0.155	0.998	0.154	0.982
GP21-IC	0.187	0.814	0.95	0.083	0.996	−0.025	0.087	0.995	0.086	0.985
GP41-IC	0.154	0.875	0.87	0.075	0.997	0.034	0.045	0.997	0.058	0.987

The R/ F plot for all the hydrogels has been drawn and shown in Figure 6.15.

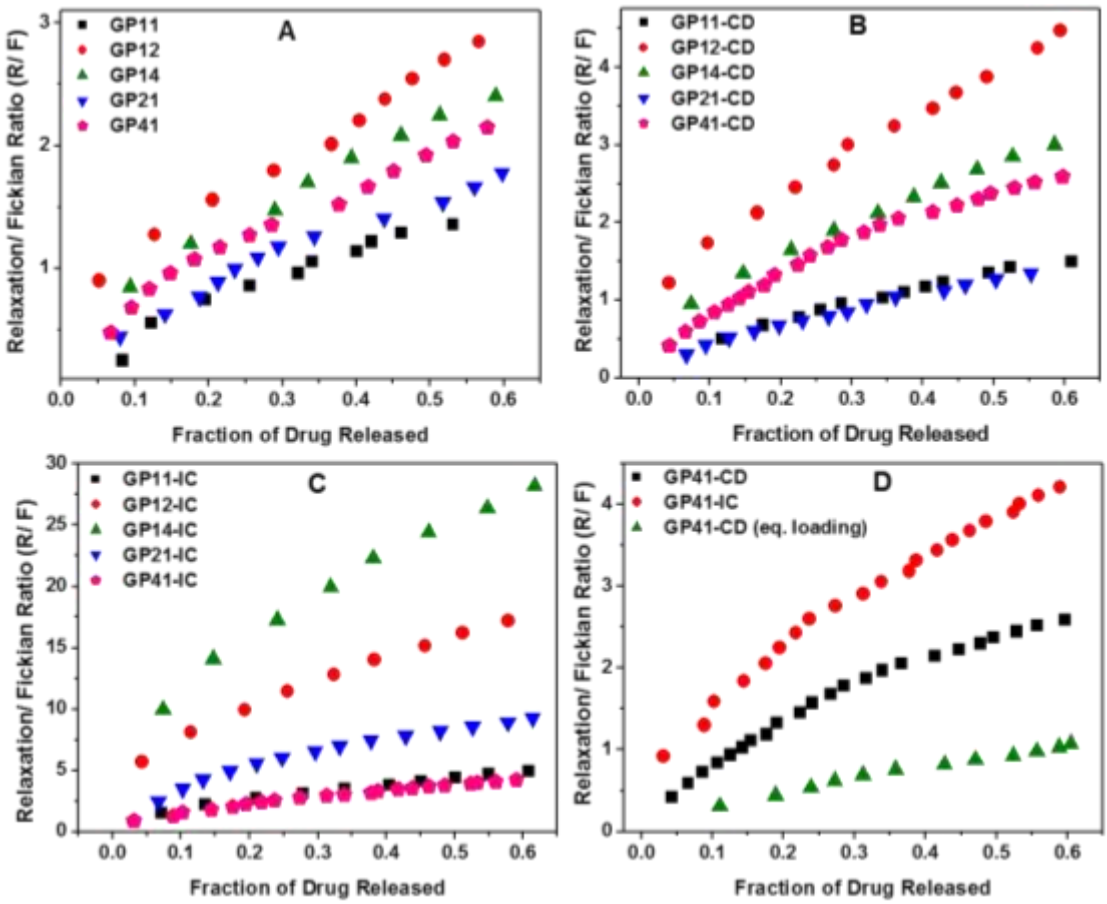

Figure 6.15. Plots of relaxation to the Fickian contribution (R/F) with the fraction of dug released for (A) GP11, GP12, GP14, GP21, GP41; (B) GP11-CD, GP21-CD, GP14-CD, GP21-CD, GP41-CD, (C) GP11-IC, GP12-IC, GP14-IC, GP21-IC, GP41-IC and (D) GP41-CD, GP41-IC, GP41-CD (eq. loading) hydrogels.

Figure 6.15 A illustrates the R/F plots for the GP11, GP12, GP14, GP21 and GP41 hydrogels, Figure 6.15 B that for GP11–CD, GP12–CD, GP14–CD, GP21–CD and GP41–CD hydrogels and Figure 6.15 C presents the R/F plots for GP11-IC, GP12-IC, GP14-IC, GP21-IC and GP41-IC hydrogels. For the IC containing hydrogels, predominant effect of macromolecular relaxation over the diffusion on the drug release is clearly witnessed from the considerably high values of R/F as compared to the other two systems. The CD containing hydrogels (GP-CD) showed a slightly

higher value of R/F as compared the corresponding GP hydrogels without CD. Therefore, it could be concluded that the presence of CD in the hydrogel matrix plays a vital role in modifying the drug release process (Bibby *et al.,* 2000).

Figure 6.15 D demonstrates the R/F plots for GP41-CD, GP41-IC and GP41-CD (eq. loading) hydrogels. As observed the dominance of polymer relaxation over diffusion is clearly indicated for GP41-IC than GP41-CD hydrogel. The fractional values of R/F for GP41-CD(eq. loading) hydrogel were suggestive of the fact that drug release from this hydrogel was predominantly diffusion-controlled. This is further supported by the reasonably good fit of the release data from this hydrogel to Higuchi model (Table 6.3).

6.2.5 Antimicrobial Assay

The design of complementary methods to inhibit the growth of pathogenic bacteria is an active area of research. Antimicrobial activity of GP-CD hydrogels against *E. coli* is shown in Figure 6.16. Hydrogel surface nanostructures and hydrophobic interactions are known to initiate bacterial cell phospholipids bilayer perforation. GG is known to exhibit antimicrobial activity due to hydrophobic interactions with the bacterial cell membrane (Das and Mukherjee, 2012; Qian *et al.,* 2011). Water has been used as negative control in this study. The hydrogels exhibited good bactericidal activity against *E. coli* and it was observed that the antimicrobial property of the hydrogels was not compromised by the introduction of PAA or CD in the matrix. Therefore the microbiocidal property of these hydrogels could be attributed to the surface hydrophobic interactions induced by GG and membrane perforation due to structural interactions. Thus these hydrogels could also be utilized as probable wound-dressing agents.

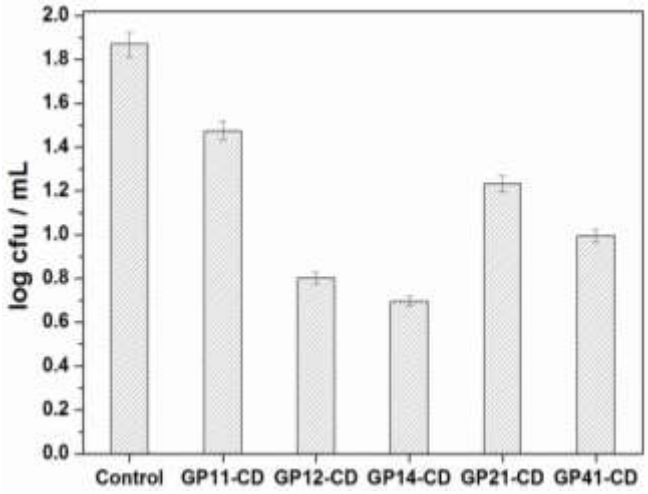

Figure 6.16. Antimicrobial activity of GP-CD hydrogels against *E. coli*.

6.2.6 Cytotoxicity Assay

The MTT colorimetric technique has been employed to evaluate the *in vitro* cytotoxicity of the hydrogels. In the direct contact method, optical microscopy revealed that the cells possess normal morphology even after 48 h incubation with the hydrogel samples. Figure 6.17 A represents the optical photomicrograph obtained after 48 h incubation of mouse fibroblasts cells in direct contact with GP41-CD hydrogel. Fibroblast cell viability assayed by MTT colorimetric technique (indirect method) after 24 h incubation with the GP14-CD and GP41-CD hydrogels is shown in Figure 6.17 C. It can be seen that the cell viabilities of the two hydrogels are all greater than 95% after incubation. According to GB/T 16886.5-2003 (ISO 10993-5:1999), samples with cell viability larger than 75% can be considered as showing no cytotoxicity (Yang *et al.*, 2009). Therefore these hydrogels can be considered as non-toxic in nature and thus biocompatible with living tissues therefore can be utilized as promising drug delivery systems.

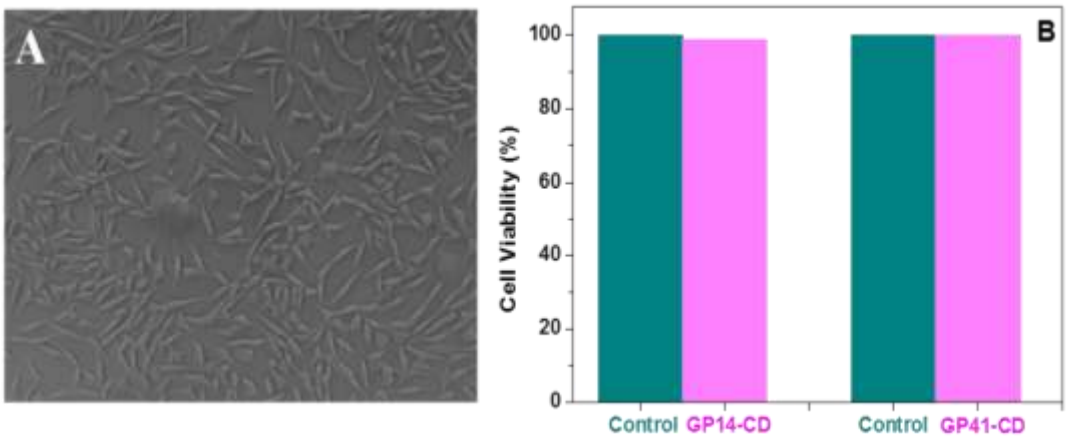

Figure 6.17. (A) Optical photomicrograph obtained after 48 h incubation of mouse fibroblasts cells in direct contact with GP41-CD and (B) Effects of GP14-CD and GP41-CD hydrogels on the cell viability of the fibroblasts after 24 h incubation determined by MTT assay.

6.3 CONCLUSIONS

- pH-Sensitive hydrogels composed of GG and PAA containing CD were synthesized using a non-toxic cross-linker, TEOS and explored for the delivery of DX.
- The hydrogels were characterized by various spectroscopic techniques.
- Hydrogels containing preformed DX-CD ICs were also synthesized and investigated for delivery of DX.
- The swelling studies revealed the pH-dependence and maximum swelling was observed at neutral pH. The incorporation of CD did not affect the swelling capacity of the hydrogels.
- Controlled release of DX was obtained from CD-incorporated hydrogels as opposed to the fast release from the hydrogels without CD. The GP41-CD hydrogel was found to be most suitable for the controlled delivery for DX.
- From the pH-responsive release studies it is concluded that these hydrogels could be employed as controlled delivery vehicles for the delivery of dexamethasone to the intestine.

- The incorporation of DX by equilibrium loading into GP41-CD hydrogel released the drug faster.
- The hydrogels containing the ICs fared better in terms of controlled delivery characteristics. Moreover, the utilization of IC is beneficial as it protects the drug without altering its properties.
- The preliminary kinetic analyses of the drug release presented the Case II type of drug release from the hydrogels. Moreover, the prevalence of the polymer relaxation process in the release phenomena was also established by the kinetic data.
- The MTT colorimetric assay indicated that the hydrogels are biocompatible and non-cytotoxic in nature certifying them as promising drug delivery systems.

CHAPTER 7

SUMMARY

7.1 Summary

Hydrogels are cross-linked hydrophilic polymers which retain their three-dimensional structure even after absorbing large amounts of water or biological fluids. In their fully swollen state, hydrogels are soft and have a rubbery consistency, therefore mimic the natural structure of the body's cellular makeup, rendering them importance for a wide variety of biomedical applications e.g. tissue engineering, artificial organ and contact lens designing and most importantly in drug delivery. Efforts have focused primarily on designing smart hydrogel systems that make use of changes in pH and temperature to expand and contract, forming a hydrogel "switch" that releases drug in a controlled fashion. However, the applicability of hydrogels as controlled delivery release systems is hindered due to their high hydrophilic characteristics which eventually lead to burst release of drug. More so, hydrogels are particularly inefficient for loading and sustained release of hydrophobic drugs. Recently growing interest has focused on overcoming the inherent pharmacological limitations of hydrogels by incorporating particulate systems (microspheres, microemulsions, micelles, microgel, liposomes, cyclodextrins, *etc.*) into the hydrogel matrix to form composite or ''plum pudding'' hydrogel networks. Cyclodextrins (CDs) are of interest in this context given their hydrophilic exterior and hydrophobic interior. The hydrophilic exterior can be useful for effective partitioning into the hydrogel matrix and maintaining the bulk hydrophilicity and swelling state of the hydrogel and the hydrophobic interior can facilitate the entrapment and controlled release of hydrophobic drugs. Incorporation of cyclodextrins into polymeric drug release systems has been known to influence the mechanism by which the drug is released. A range of strategies have been explored to modify cyclodextrin integrated hydrogels to meet desired drug delivery profiles.

The present research work aimed at employing a simple and easy strategy for incorporating CDs to hydrogel matrix by loading preformed drug−CD ICs directly into the hydrogel to design an array of controlled delivery systems and exploring this possibility in greater details.

To explore the efficacy of PVA hydrogels containing drug-CD ICs as controlled drug delivery systems, solid ICs of SA and IBF in CD were prepared and loaded to GA cross-linked PVA hydrogels. The formation of ICs was affirmed from FTIR, XRD, DSC, Optical Microscopy and ^{1}H NMR studies. The hydrogels were also characterized by several analytical techniques. The swelling evaluation indicated the decreased swelling with increasing GA content for both PVA and PVA-CD hydrogels. The presence of CD in the hydrogel significantly prolonged the release of drugs showing a sustained release pattern. The drug release profiles from the hydrogels containing the IC shows a strong dependence on the degree of cross-linking. Among all the hydrogels studied P4-CD, having maximum degree of cross-linking, was found to show the slowest release of SA. The release of IBF, a relatively hydrophobic drug in comparison to SA and having higher binding efficiency towards CD, was found to be further prolonged than that of SA. Thus the nature of drug in terms of its binding efficiency with the CD plays an important role in the drug release process from these hydrogels. The preliminary kinetic analysis revealed the anomalous nature of drug release from all the hydrogels except P4-IC. The P4-D hydrogel, however, showed Case II transport mechanism indicating the dominant relaxational process. Thus the role of CD in the drug release process from hydrogels is not only because of its inclusion ability but also due to its effect on the polymer relaxation. In other words, it is the combined effect of drug diffusion and polymer relaxation that controls the overall drug release process from the hydrogels containing ICs. The cytotoxicity tests

ensured the hydrogels to be non-toxic and hence can be utilized as controlled delivery systems.

Oral drug delivery systems targeting the lower part of the gastro intestinal track (GIT), including the intestine and colon, has attracted much interest for the delivery of an array of therapeutic agents. pH-Sensitive hydrogels with their unique ability to sense the differences in the pHs of GIT, have become quite an important class of systems used for controlled delivery formulations. With this rationale, pH-Sensitive CS−PVA IPN hydrogels with varying amount of PVA were synthesized, characterized and explored for the delivery of two NSAIDs; NX and DS. Hydrogels containing free drug and the ICs were prepared. The hydrogels exhibited pH-sensitive swelling with maximum swelling at neutral pH and lower swelling at acidic and alkaline pHs. The presence of CD did not have any significant effect on the swelling abilities of the hydrogel. The drug release from the hydrogels containing the ICs was much prolonged as compared to hydrogels containing the free drugs. The rate of drug release was found to decrease with increasing PVA content. The hydrogels released negligible amounts of drug in simulated gastric fluid (SGF) (< 5%) while the release amounts increased significantly in simulated intestinal fluid (SIF). The cytotoxic assay performed on the hydrogels ensured them to be nontoxic and biocompatible. Thus, it can be proposed that these hydrogels can be utilized as oral controlled delivery vehicles for the delivery of NSAIDs to the intestine.

PVA–PAA microspheres cross-linked with GA were synthesized and studied for the delivery of DX, one of the frequently used immunosuppressant drugs. The microspheres containing free DX, PM and ICs (CP and FD) were prepared in order to examine the effect of the method of preparation of IC on the release characteristics. The swelling studies indicated higher swelling in neutral pH than in acidic pH. At pH

1.2, the amounts of DX released from all microspheres were much lower than the release amounts at pH 7.4. Slowest release was observed from the microspheres which contained the FD. Approximately 5% of DX was released during the initial 2h in SGF but upon transfer to SIF, the rate of DX release increased significantly. Thus the synthesized microspheres containing ICs could be effectively employed for the controlled delivery of DX and their pH–sensitivity could be exploited for the delivery to the intestine. Moreover, the compatibility of the synthesized microspheres with the living tissues further validates them as promising drug delivery systems.

Controlled drug delivery features from thermo-responsive hydrogels comprising PNIPAAm and solid drug-CD ICs were also investigated. ICs of 5FU with CD were prepared by the freeze-drying method and characterized by different techniques. Temperature-responsive GG–PNIPAAm hydrogels cross-linked by TEOS were synthesized. The hydrogels displayed temperature-dependent swelling characteristics. Incorporation of GG did not disturb the arrangement of PNIPAAm chains and the LCST remained invariant. Higher swelling was observed below the LCST (~33^{o}C) while remarkable decrease in degree of swelling was seen above the LCST. The rate and amount of drug released at 25°C was always higher than that at 37°C. Presence of IC in the hydrogel matrix is capable of significantly controlling the drug release rate despite the fact that the matrix is undergoing a drastic morphological change above its LCST. Higher amount of GG in the hydrogels led to a decrease in the release rate from the hydrogels. The preliminary analyses of drug release indicated Case II type of mechanism from the hydrogels indicating the predominant effect of macromolecular relaxation on the drug release kinetics. The cytotoxicity assay certified these hydrogels to be safe, non-toxic and biocompatible with living tissues thereby establishing their potential as controlled drug delivery systems.

In order to evaluate the efficacy of hydrogels containing CD as part of network structure and those hydrogels containing drug-CD ICs, pH–sensitive hydrogels composed of GG and PAA were synthesized using TEOS as cross-linker by varying the ratio of GG and PAA. The corresponding GG−PAA−CD hydrogels with CD as a part of the network structure were also synthesized for comparison. The swelling characteristics revealed maximum swelling at neutral pH. The incorporation of CD did not have any significant effect on the swelling capacity of the hydrogels. Controlled release of drug was obtained from CD-incorporated hydrogels as opposed to the fast release from the hydrogels without CD. The hydrogel comprising GG to PAA ratio of 4:1 was found to be the best of the lot for controlled delivery of DX. Upon comparison it was found that the *in situ* method of incorporation of drug into the hydrogel matrix was found to be more favorable in terms of sustained release profile than loading the drug by equilibrium swelling. Moreover, hydrogels containing preformed ICs performed better in terms of controlled release characteristics than the hydrogels containing CD as a part of their network structure. The cytotoxicity study revealed the biocompatible and non-toxic nature of the hydrogels validating them as promising drug delivery systems.

7.2 Scope for Future Work

Considering the success of the strategy of incorporation of drug-CD ICs into the hydrogels to achieve a controlled delivery characteristic, this approach can be extended for the delivery of macromolecules such as proteins, peptides, growth factors and genes from hydrogels. Hydrogels with dual control *i.e.* pH as well as temperature sensitive, can be synthesized and similar work can be carried out. The possibilities of manipulating hydrogels to form a wide range of shapes and sizes, from nano to macro, and incorporating drug-CD ICs can open new perspectives for designing controlled

drug delivery systems. The hydrogel microspheres containing ICs can be subjected to surface functionalization for achieving target-specific controlled delivery of therapeutics.

REFERENCES

1. **Abd El-Rehim, H. A., Hegazy, E. A., Khalil, F. H. and Hamed, N. A.** (2007). *Nucl. Instr. Meth. Phys. Res. B,* **254,** 105-112.
2. **Abdelaal, M. Y., Abdel-Razik, E. A., Abdel-Bary, E. M. and El-Sherbiny, I. M.** (2007). *J. Appl. Polym. Sci.,* **103,** 2864-2874.
3. **Abdel-Halim, E. S. and Al-Deyab, S. S.** (2014). *React. Funct. Polym.,* **75,** 1-8.
4. **Abdel-Mohsen, A. M., Aly, A. S., Hrdina, R., Montaser, A. S. and Hebeish, A.** (2011). *J. Polym. Environ.,* **19,** 1005-1012.
5. **Abdoh, A. A., Zughul, M. B., Davies, J. E. D. and Badwan, A. A.** (2007). *J. Incl. Phenom. Macrocycl. Chem.,* **57,** 503-510.
6. **Acharya, G., Shin, C. S., McDermott, M., Mishra, H., Park, H., Kwon, I. C. and Park, K.** (2010). *J. Controlled Release,* **141,** 314-319.
7. **Aguilar, M. R. and Roman, J. S.** (2014). Smart Polymers and their applications, Woodhead Publishing, UK.
8. **Ahmed, E. M.** (2013). J. *Adv. Research.* DOI: 10.1016/j.jare.2013.07.006
9. **Ahsan, F., Arnold, J. J., Meezan, E. and Pillion, D. J.** (2001). *Pharm. Res.,* **18,** 608-614.
10. **Akala, E. O., Kopeckova, P. and Kpoecek, J.** (1998). *Biomaterials,* **19,** 1037-1047.
11. **Albin, G., Horbett, T. A. and Ratner, B. D.** (1985). *J. Controlled Release,* **2,** 153-164.
12. **Alinaghi, A., Rouini, M. R., Johari Daha, F. and Moghimi, H. R.** (201)3. *J. Liposome Res.,* **23,** 235–243.
13. **Altimari, I., Spizzirri, U. G., Iemma, F., Curcio, M., Puoci, F. and Picci, N.** (2012). *J. Appl. Polym. Sci.,* **125,** 3006-3013.
14. **Alvarez-Lorenzo, C., Bromberg, L. and Concheiro, A.** (2009). *Photochem. Photobiol.,* **85,** 848-860; *and references therein.*
15. **Alvarez-Lorenzo, C., Gomez-Amoza, J. L., Martinez-Pacheco, R., Souto, C. and Concheiro, A.** (1999). *Int. J. Pharm.,* **180,** 91-105.
16. **Aminabhavi, T. M., Nadagouda, M. N., Joshi, S. D. and More, U. A.** (2014). *Expert Opin. Drug Deliv.,* **11,** 753-766, *and references therein.*
17. **Ammar, H. O., Ghorab, M., Mostafa, D. M., Makram, T. S. and Ali, R. M.** (2013). *J. Incl. Phenom. Macrocycl. Chem.,* **77,** 121-134.
18. **Anderson, S., Chen, T., Iruela-Arispe, M. and Segura, T.** (2009). *Biomaterials,* **30,** 4618-4628.
19. **Angadi, S. C., Manjeshwar, L. S. and Aminabhavi, T. M.** (2011). *Ind. Eng. Chem. Res.,* **50,** 4504–4514.
20. **Anghelache, A., Teodorescu, M., Stanescu, P. O., Draghici, C. and Vuluga, D. M.** (2014). *Colloid Polym. Sci.,* **292,** 829-838.
21. **Anirudhan, T. and Mohan, A. M.** (2014). *RSC Adv.,* **4,** 12109-12118.
22. **Ankareddi, I. and Brazel, C. S.** (2007). *Int. J. Pharm.,* **336,** 241-7.
23. **Appel, E. A., del Barrio, J., Loh, X. J. and Scherman, O. A.** (2012). *Chem. Soc. Rev.,* **41,** 6195-6214, *and references therein.*
24. **Arancibia, J. A. and Escander, G. M.** (1999). *Analyst,* **124,** 1833-1838.

25. **Araujo, V., Gamboa, A., Caro, N., Abugoch, L., Gotteland, M., Valenzuela, F., Merchant, H. A., Basit, A. W. and Tapia C.** (2013). *J. Pharm. Sci.,* **102,** 2748-2759.
26. **Archana, D., Singh, B. K., Dutta, J. and Dutta, P. K.** (2013). *Carbohydr. Polym.,* **95,** 530-539.
27. **Assaf, S. M., Abul-Haija, Y. M. and Fares, M. M.** (2011). *J. Macromol. Sci.,* **48,** 493-502.
28. **Astakhova, A. V. and Demina, N. B.** (2004). *Pharm. Chem. J.,* **38,** 105-108, *and references therein.*
29. **Bahaddi, Y., Lelievre, F., Gareil, P., Maignan, J. and Galons, H.** (1997). *Carbohydr. Res.,* **303,** 229-232.
30. **Bai, H., Li, C., Wang, X. and Shi, G**. (2010). *Chem. Commun.,* **46,** 2376-2378.
31. **Bait, N., Grassl, B., Benaboura, A. and Derail, C.** (2013). *J. Adhes. Sci. Technol.,* **27,** 1032-1047.
32. **Bait, N., Grassl, B., Derail, C. and Benaboura, A.** (2011). *Soft Matter,* **7,** 2025-2032.
33. **Bajpai, S. K., Bajpai, M. and Dengre, R.** (2003). *J. Appl. Polym. Sci.,* **89,** 2277-2282.
34. **Baker, M. I., Walsh, S. P., Schwartz, Z. and Boyan, B. D.** (2012). *J. Biomed. Res. Part B,* **100B,** 145-1457, *and references therein.*
35. **Banik, A., Gogoi, P. and Saikia, M. D.** (2012). *J. Incl. Phenom. Macrocycl. Chem.,* **72,** 449-458.
36. **Barreiro-Iglesias, R., Alvarez-Lorenzo, C. and Concheiro, A.** (2001). *J. Controlled Release,* **77,** 59-75.
37. **Belder, D., Deege, A., Husmann, H., Kohler, F. and Ludwig, M.** (2001). *Electrophoresis,* **22,** 3813-3818.
38. **Belyakova, L. A. and Lyashenko, D. Y.** (2008). *J. Appl. Spectrosc.* **75,** 299-303.
39. **Belyakova, L. A., Varvarin, A. M., Lyashenko, D. Y., Khora, O. V. and Oranskaya, E. I.** (2007). *Colloid J.,* **69,** 586-591.
40. **Berkland C., Kim, K. and Pack, D. W.** (2003). *Pharm. Res.,* **20,** 1055-1062.
41. **Bezuidenhout, D., Oosthuysen, A., Davies, N., Ahrenstedt, L., Dobner, S., Roberts, P. and Zilla, P.** (2013). *J. Biomed. Mater. Res.,* **101A,** 1311-1318.
42. **Bhatia, S. K.** (2010). PEG-based biomaterials for wound closure. In: Biomaterials for clinical applications, Springer Science and Business Media, Springer, pp. 238-249.
43. **Bhattacharya, A.** (2000). *Prog. Polym. Sci.,* **25,** 371-401, *and references therein.*
44. **Bhattarai, N., Gunn, J. and Zhang, M.** (2010). *Adv. Drug Delivery Rev.,* **62,** 83-99, *and references therein.*
45. **Bibby, D. C., Davies, N. M. and Tucker, I. G.** (1999). *Int. J. Pharm.,* **187,** 243-250.

46. **Bibby, D. C., Davies, N. M. and Tucker, I. G.** (2000).. *Int. J. Pharm.,* **197,** 1-11, *and references therein.*
47. **Bilensoy, E., Cirpanli, Y., Sen, M., Dogan, A. L. and Calis, S.** (2007). *J. Incl. Phenom. Macrocycl. Chem.,* **57,** 363-370.
48. **Bilensoy, E., Moroy, P., Cirpanli, Y., Bilensoy, T., Dogan, Calis, S. and Mollamahmutoglu, L.** (2011). *J. Incl. Phenom. Macrocycl. Chem.,* **69,** 309-313.
49. **Bos, G. W., Hennink, W. E., Brouwer, L. A., den Otter, W., Veldhuis, T. F. J., van Nostrum, C. F. and van Lyun, M. J. A.** (2005). *Biomaterials,* **26,** 3901-3909.
50. **Bosio, V. E., Lopez, A. G., Mukherjee, A., Mechetti, M. and Castro, G. R.** (2014). *J. Mater. Chem. B,* **2,** 5178-5186.
51. **Boustta, M., Colombo, P. E., Lenglet, S., Poujol, S. and Vert, M.** (2014). *J. Control. Release,* **174,** 1-6.
52. **Brewster, M. E. and Loftsson, T.** (2007). Adv. *Drug Delivery Rev.,* **59,** 645-666, *and references therein.*
53. **Bromberg, L. E. and Ron, E. S.** (1998). *Adv. Drug Delivery Rev.,* **31,** 197-221, *and references therein.*
54. **Brunner, C. A. and Groner, R. W.** (2006). *Can. J. Plast. Surg.,* **14,** 151-154.
55. **Byun, J., Lee, Y. M. and Cho, C. S**. (1996). *J. Appl. Polym. Sci.,* **61**, 697-702.
56. **Caicco, M. J., Cooke, M. J., Wang, Y., Tuladhar, A., Morshead, C. M. and Shoichet, M. S.** (2013). *J. Controlled Release,* **166,** 197-202.
57. **Cappello, J., Crissman, J. W., Crissman, M., Ferrari, F. A., Textor, G., Wallis, O., Whiteledge, A. R., Zhou, X., Burman, D., Auckerman, L. and Stedronsky, E. R.** (1998). *J. Controlled Release,* **53,** 105-117.
58. **Cavalli, R., Bisazza, A., Trotta, M., Argenziano, M., Civra, A., Donalisio, M. and Lemdo, D.** (2012). *Int. J. Nanomed.,* **7,** 3309-3318.
59. **Cavalli, R., Trotta, F. and Tumiatti, W.** (2006). *J. Incl. Phenom. Macrocycl. Chem.,* **56**, 209-213.
60. **Celebi, N., Iscanoglu, M. and Degim, T.** (1991). *Pharamzie,* **46,** 863-865.
61. **Chadha, R., Gupta, S., Shukla, G., Jain, D. V. S. and Singh, S.** (2011). *J. Incl. Phenom. Macrocycl. Chem.,* **71,** 149-159.
62. **Challa, R., Ahuja, A., Ali, J. and Khar, R. K.** (2005). *AAPS PharmSciTech,* **6,** E329-E357, *and references therein.*
63. **Chang, C. and Zhang, L.** (2011). *Carbohydr. Polym.,* **84,** 40-53, *and references therein.*
64. **Chavanpatil**, **M. and Vavia, P. R.** (2003). *J. Incl. Phenom. Macrocycl. Chem.,* **44,** 137-140.
65. **Cheetham, N. W. H. and Mashimba, E. N. M.** (1990). *Carbohydr. Polym.,* **14,** 17-27.
66. **Chen, B., Wright, B., Sahoo, R. and Connon, C. J**. (2013). *Tissue Eng. Part C: Methods,* **19,** 568-576.
67. **Chen, G. and Jiang, M.** (2011). *Chem. Soc. Rev.,* **40,** 2254-2266, *and references therein.*

68. **Chen, J., Lu, W., Gu, W., Lu, S., Chen, Z., Cai, B. and Yang, X.** (2014). *Expert Opin. Drug Deliv.,* **11,** 565-577*, and references therein.*
69. **Chen, L., Kopecek, J. and Stewart, R. J.** (2000). *Bioconjugate Chem.,* **11,** 734.
70. **Chen, M. C., Huang, S. F., Lai, K. Y. and Ling, M. H.** (2013). *Biomaterials,* **34,** 3077-3086.
71. **Chen, P. C., Kohane, D. S., Park, Y. J., Bartlett R. H., Langer, R. and Yang, V. C.** (2004). *J. Biomed. Mater. Res., Part A,* **70,** 459-466.
72. **Chen, S., Liu, M., Jin, S. and Chen, Y.** (2014). *Polym. Bull.,* **71,** 719-734.
73. **Chen, X., Zhi, F., Jia, X., Zhang, X., Amberdekar, R., Meng, Z., Paradkar, A. R., Hu, Y. and Yang, Y.** (2013). *J. Pharm. Pharmacol.,* **65,** 807-816.
74. **Cheng, C. L., Gehrke, S. H. and Ritschel, W. A.** (1994). *Methods Find. Exp Clin. Pharmacol.,* **16,** 271-278.
75. **Chilajwar, S. V., Pednekar, P. P., Jadhav, K. R., Gupta, G. J. C. and Kadam, V. J.** (2014). *Expert Opin. Drug Deliv.,* **11,** 111-120*, and references therein.*
76. **Choi, J. J., Lee, J. H., Kang, B. J., Kim, S. H., Ahn, S. T., Yoon, W. J. and Lee, H. K.** (2010). *J. Comput. Assist. Tomogr.,* **34,** 449-455.
77. **Choudhary, K. P. R. and Dwarakanadha Reddy, P.** (2012). *J. Pharm. Res.,* **5,** 1799-1801.
78. **Choumerianou, D. M., Dimitriou, H. and Kalmanti, M.** (2008). *Tissue Eng. Part B Rev.,* **14,** 53-60.
79. **Chourasia, M. K. and Jain, S. K.** (2003). *J. Pharm. Pharmaceut. Sci.,* **6**, 33-40.
80. **Chrambach, A. and Rodbard, D.** (1971). *Science,* **172,** 440-451.
81. **Chui, Y. C., Cheng, M. H., Engel, H., Kao, S. W. and Larson, J.** (2011). *Biomaterials,* **32,** 6045-6051.
82. **Chung, Y. C., Su, Y. P., Chen, C. C., Jia, G., Wang, H. L., Wu, J. C. G. and Lin, J. G.** (2004). *Acta Pharmacol. Sinica,* **25,** 932-936.
83. **Cirri, M., Bragagni, M., Mennini, N. and Mura, P.** (2012). *Eur. J. Pharm. Biopharm.,* **80,** 46-53.
84. **Concheiro, A. and Alvarez-Lorenzo, C.** (2013). *Adv. Drug Delivery Rev.,* **65,** 1188-1203*, and references therein.*
85. **Connors, K. A.** (1995). *J. Pharm. Sci.,* **88,** 843-848.
86. **Constantin, M., Fundueanu, G., Bortolotti, F., Cortesi, R., Ascenzi, P. and Menegatti, E.** (2004). *Int. J. Pharm.,* **285,** 87-96.
87. **Copello, G. J., Villanueva, M. E., Gonzalez, J. A., Egues, S. L. and Diaz, L. E.** (2014). *J. Appl. Polym. Sci.,* DOI: 10.1002/ app.41005
88. **Courrier, H. M., Butz, N. and Vandamme, T. F.** (2002). *Crit. Rev. Ther. Drug Carrier Syst.,* **19,** 425-498*, and references therein.*
89. **Crini, G.** (2008).. *Dyes Pigments Int. J.,* **77,** 415-426.
90. **Crini, G. and Morcellet, M.** (2002). *J. Sep. Sci.,* **25,** 789-813.

91. **Crini, G., Bertini, S., Torri, G., Naggi, A., Sforzini, D., Vecchi, C., Janus, L., Lekchiri, Y. and Morcellet, M.** (1998). *J. Appl. Polym. Sci.,* **68,** 1973-1978.
92. **Crini, N. M. and Crini, G.** (2013). *Prog. Polym. Sci.,* **38,** 344-368 *and references therein.*
93. **Croisier, F. and Jerome, C.** (2013). *Eur. Polym. J.,* **49,** 780-792, *and references therein.*
94. **da Silva, M. A., Bode, F., Drake, A. F., Goldoni, S., Stevens, M. M. and Dreiss, C. A.** (2014). *Macromol. Biosci.,* **14,** 817-830.
95. **Das, A., Wadhwa, S. and Srivastava, A.** (2006). *Drug Delivery,* **13,** 139-142.
96. **Das, D. and Mukherjee, A.** (2012). *Bioresource Technol.,* **110,** 412-416.
97. **Dasan, K. P. and Rekha, C.** (2012). *Curr. Drug Deliv.,* **9,** 588-595, *and references therein.*
98. **Dash, M., Chiellini, F., Ottenbrite, R. M. and Chiellini, E.** (2011). *Prog. Polym. Sci.,* **36,** 981-1014, *and references therein.*
99. **Dastidar, S. G., Ganguly, K., Chaudhuri, K. and Chakrabarty, A. N.** (2000). *Int. J. Antimicrob. Agents,* **14,** 249-251.
100. **Del Toro-Sanchez, C. L., Ayala-Zavala, J. F., Machi, L., Santacruz, H., Villegas-Ochoa, M. A., Alvarez-Parrilla, E. and Gonzalez-Aguilar, G. A.** (2010). *J. Incl. Phenom. Macrocycl. Chem.,* **67,** 431-441.
101. **Diasio, R. B. and Harris, B. E.** (1989). *Clin. Pharm.,* **16,** 215-237.
102. **Dinerman, A. A., Cappello, J., El-Sayed, M., Hoag, S. W. and Ghandehari, H.** (2010). *Macromol. Biosci.,* **10,** 1235-1247.
103. **Doile, M. M., Fortunato, K. A., Schmucker, I. C., Schucko, S. K., Silva, M. A. S. and Rodrigues, P. O.** (2008). *AAPS PharmSciTech,* **9**, 314-321.
104. **Don, T. M., King, C. F. and Chiu, W. Y.** (2002). *J. Appl. Polym. Sci.,* **86,** 3057–3063.
105. **dos Santos, R., Jose-Fernando, R. Couceiro, A. Concheiro, Juan-Jose Torres-Labandeira, Alvarez-Lorenzo, C.** (2008). *Acta Biomater.,* **4,** 745-755.
106. **Doulabi, A. H., Mirzadeh, H., Imani, M. and Samadi, N.** (2013). *Carbohydr. Polym.,* **92,** 48-56.
107. **Dragan, E. S.** (2014). *Chem. Eng. J.,* **243**, 572-590, *and references therein.*
108. **Duncan, R. and Vincent, M. J.** (2013). *Adv. Drug Delivery Rev.,* **65,** 60-70.
109. **Dzinomwa, G. P. T., Wood, C. J. and Hill, D. J. T.** (1997). *Polym. Adv. Technol.,* **8,** 767-772.
110. **El-Leithy, E. S., Shaker, D. S., Ghorab, M. K. And Abdel-Rashid, R. S.** (2010). *AAPS PharmSciTech,* **11,** 1695-1702.
111. **El-Sherbiny, I. M., McGill, S. and Smyth H. D. C.** (2010). *J. Pharm. Sci.,* **99,** 2343-2356.
112. **Fang, J. Y., Chen, J. P., Leu, Y. L. and Hu, J. W.** (2008). *Eur. J. Pharm. Biopharm.,* **68,** 626-636.
113. **Fathy, M. and Sheha, M.** (2000). *Pharmazie,* **55,** 513-517.

114. **Fedorak, R. N., Haeberlin, B., Empey, L. R., Cui, N., Ill, H. N., Jewell, L. D. and Friend, D. R.** (1995). *Gastroenterology,* **108,** 1688-1699.
115. **Fei, J., Zhang, Z., Zhong, L. and Gu, L.** (2002). *J. Appl. Polym. Sci.,* **85**, 2423-2430.
116. **Ferry, J. D.** (1980). Viscoelstic properties of polymers, John Wiley & sons, New York, pp. 486-544.
117. **Figueiredo, K. C. S., Alves, T. L. M. and Borges, C. P.** (2009). *J. Appl. Polym. Sci.,* **111,** 3074-3080.
118. **Filipovic-Grcic, J., Voinovich, D., Moneghini, M., Becirevic-Lacan, M., Magaratto, L. and Jalsenjak, I.** (2000). *Eur. J. Pharm. Sci.,* **9,** 373-379.
119. **Freiberg, S. and Zhu, X. X.** (2004). *Int. J. Pharm.,* **282,** 1-18.
120. **Frijlink, H. W., Paiotti, S., Eissens, A. C. and Lerk, C. F.** (1992). *Eur. J. Pharm. Biopharm.,* **38,** 174-179.
121. **Fu, Y. and Kao, W. J.** (2011). *J. Biomed. Mater. Res.,* **98,** 201-211.
122. **Fucinos, C., Guerra, N. P., Teijon, J. M., Patrana, L. M., Rua, M. L. and Katime, I.** (2012). *J. Food Sci.,* **77,** N21-N28.
123. **Fulop, Z., Nielsen, T. T., Larsen, K. L. and Loftsson, T.** (2013). *Carbohydr. Polym.,* **97,** 635-642.
124. **Gajra, B., Pandya, S. S., Vidyasagar, G., Rabari, H., Dedania, R. R. and Rao, S.** (2012). *Int. J. Pharm. Research,* **4,** 20-26, *and references therein.*
125. **Gao, Y., Ren, F., Ding, B., Sun, N., Liu, X., Ding, X. and Gao, S.** (2011). *J. Drug Targeting,* **19,** 516-527.
126. **Gao, Z. W. and Zhao, X. P.** (2005). *J. Colloid Interface Sci.,* **289,** 56-62.
127. **Garzon, L. C. and Martinez, F.** (2004). *J. Solution Chem.*, **33,** 1379-1395.
128. **Gehrke, S. H. and Lee, P. I.** (1990). Hydrogels for drug delivery systems. In: *Encyclopaedia of Controlled Drug Delivery.* (Tyle, P., Eds), *Marcel Dekker*, 333 *and references therein.*
129. **George, M. and Abraham, T. E.** (2007). *Int. J. Pharm.*, **335,** 123-129.
130. **Ghandehari, H., Kopeckova, P. and Kpoecek, J.** (1997). *Biomaterials,* **18,** 861-872.
131. **Ghosh, A. and Wong, T. W.** (2014). Graft polymers of guar gum versus alginate: drug delivery applications and implications. In: Physical Chemistry of Macromolecules, Apple Academic Press, Oakville, Ontario, pp. 423-440.
132. **Giardina, G. and Inan, M. S.** (1998). *Biochim. Biophys. Acta,* **1401,** 277-288.
133. **Gil, E. S. and Hudson, S. M.** (2004). *Prog. Polym. Sci.,* **29,** 1173-1222, *and references therein.*
134. **Giri, A., Bhowmick, M., Pal, S. and Badyopadhyay, A.** (2011). *Int. J. Biol. Macromol.,* **49,** 885-893.
135. **Giri, T. K., Thakur, D., Alexander, A., Ajazuddin, Badwaik, H., Tripathy, M. and Tripathi, D. K.** (2013). *J. Mater. Sci. Mater. Med.,* **24,** 1179-1190.
136. **Gonzales, J. S. and Alvarez, V. A.** (2013). *Adv. Mater. Sci. Res.,* **15,** 231-249, *and references therein.*
137. **Gordon, M. K., Desantis, A., Deshmukh, M., Lacey, C., Hahn, R. A., Beloni, J., Anumolu, S. S., Schlager, J. J., Gallo, M. A., Gerecke, D. R.,**

Heindel, N. D., Svoboda, K. K., Babin, M. C. and Sinko, P. J. (2010). *J. Ocul. Pharmacology Ther.,* **26,** 407-419.

138. **Gordon, S., Young, K., Wilson, R., Rachel, R., Rizwan, S., Kemp, R., Rades, T. and Hook, S.** (2012). *J. Liposome Res.,* **22,** 193-204.
139. **Grande, D. A., Halberstadt, C., Naughton, G., Schwartz, R. and Manji, R.** (1997). *J. Biomed. Mater. Res.,* **34,** 211-220.
140. **Greatbanks, D. and Pickford, R.** (1987). *Magn. Reson. Chem.,* **25,** 208-215.
141. **Guan, Y., Zhao, H. B., Yu, L. X., Chen, S. C. and Wang, Y. Z.** (2014). *RSC Adv.,* **4,** 4955-4959.
142. **Gulbake, A. and Jain, S. K.** (2012). *Expert Opin. Drug Deliv.,* **9,** 713-729, *and references therein.*
143. **Guo, R. and Wilson, L. D.** (2012). *J. Appl. Polym. Sci.,* **125,** 1841-1854.
144. **Guo, R. and Wilson, L. D.** (2013). *Curr. Org. Chem.,* **17,** 14-21.
145. **Gupta, P., Vermani, K. and Garg, S.** (2002). *Drug Discov. Today,* **7,** 569-579, *and references therein.*
146. **Gupta, V., Davis, M., Hope-weeks, L. J. and Ahsan, F.** (2011*Pharm. Res.,* **28,** 1733-1749.
147. **Hacker, M. C. and Mikos, A. G.** (2011). Synthetic polymers. In: Principles of regenerative medicine, 2nd Ed., Elsevier Academic Press, San Diego, pp. 587-622.
148. **Hamidi, M., Azadi, A. and Rafiei, P**. (2008). *Adv. Drug Delivery Rev.,* **60,** 1638-1649, *and references therein.*
149. **Han, H. D., Kim, T. W., Shin, B. C. and Choi, H. S.** (2005). Release of *Macromol. Res.,* **13,** 54-61.
150. **Harada, A., Furue, M. and Nozakura, S.** (1981). *Polym. J.,* **13,** 777-781.
151. **Harada, A., Li, J. and Kamachi, M.** (1992). *Nature,* **356,** 325-327.
152. **Harada, A., Okada, M., Li, J. and Kamachi, M.** (1995). *Macromolecules,* **28,** 8406-8411.
153. **Harada, A., Takashima, Y. and Nakahata, M.** (2014). *Acc. Chem. Res.,* **47,** 2128-2140, *and references therein.*
154. **Harata, K.** (1998). *Chem. Rev.,* **98,** 1803-1828.
155. **Hari, P. R. and Sreenivasan, K.** (2001). *J. Appl. Polym. Sci.,* **82,** 143-149.
156. **Hassan, C. M. and Peppas, N. A.** (2000). *Adv. Polym. Sci.,* **153,** 37-65.
157. **Helary, C., Zarka, M. and Girad-Guille, M. M.** (2012). *J. Tissue Eng. Regener. Med.,* **6,** 225-237.
158. **Hennink, W. E. and van Nistrum, C. F.** (2002). *Adv. Drug Delivery Rev.,* **54,** 13-36, *and references therein.*
159. **Hennink, W. E., De Jong, S. J., Bos, G. W., Veldhuis, T. F. J., and van Nostrum, C. F.** (2004). *Int. J. Pharm.,* **277,** 99-104.
160. **Hergert, L. A. and Escandar, G. M.** (2003). *Talanta,* **60,** 235-246.
161. **Hickey, A. S. and Peppas, N. A.** (1995). *J. Membr. Sci.,* **107,** 229-237.
162. **Higuchi, T.** (1963). *J. Pharm. Sci.,* **52,** 1145-1149.
163. **Hladon, T., Pawlaczyk, J. and Szafran, B.** (2000). *J. Incl. Phenom. Macrocycl. Chem.,* **36,** 1-8.

164. **Hoare, T. R. and Kohane, D. S.** (2008). *Polymer,* **49**, 1993-2007, *and references therein.*
165. **Hoffman, A. S.** (2001). *Ann. N. Y. Acad. Sci.,* **944,** 62-73, *and references therein.*
166. **Hoffman, A. S.** (2002). *Adv. Drug Delivery Rev.,* **43,** 3-12.
167. **Holloway, J. L., Lowman, A. M. and Palmese, G. R.** (2013). *Soft Matter,* **9,** 826-833.
168. **Hosseinzadeh, H.** (2010). *J. Chem. Sci.,* **122,** 651-659.
169. **Hovgaard, L. and Brønsted, H.** (1995). *J. Controlled Release,* **36,** 159-166.
170. **Hsu, C. M., Yu, S. C., Tsai, F. J. and Tsai, Y.** (2013). *Carbohydr. Polym.,* **98,** 1422-1429.
171. **Hu, L., Sun, Y. and Wu, Y.** (2013). *Nanoscale,* **5,** 3103-3111,
172. **Hu, X. P. and Hsieh, Y.** (1996). *Polym. Sci. Part B: Polym. Phys.,* **34,** 1451.
173. **Huang, L. L. H., Lee, P. C., Chen, L. W. and Hseih, K. H.** (1998). *J. Biomed. Mater. Res.,* **39,** 630-636.
174. **Huang, W. J. and Lee, W. F.** (2009). *J. Appl. Polym. Sci.,* **111,** 2025-2034.
175. **Huang, W. J. and Lee, W. F.** (2010). *Polym. Compos.,* **31,** 887-896.
176. **Huang, X. and Brazel, C. S.** (2001). *J. Controlled Release,* **73,** 121-136.
177. **Huang, Y., Lu, J. and Xiao, C.** (2007). *Polym. Degrad. Stability,* **92,** 1072-1081.
178. **Huang, Y., Yu, H. and Xiao, C.** (2007).
179. **Huh, K. M., Kang, H. C., Lee, Y. J. and Bae, Y. H.** (2012). *Macromol. Res.,* **20,** 224-233.
180. **Hussein, K., Turk, M. and Wahl, M. A.** (2007). *Pharm. Res.,* **24,** 585-592.
181. **Ikada, Y., Jamshidi, K., Tsuji, H. and Hyon, S. H.** (1987). *Macromolecules,* **20,** 904-906.
182. **Indermun, S., Choonara, Y. E., Kumar, P., du Toit, L. C., Modi, G., Luttge, R. and Pillay V.** (2014). *Int. J. Pharm.,* **462,** 52-65.
183. **Irvin, D. J., Goods, S. H. and Whinnery, L. L.** (2001). *Chem. Mater.,* **13,** 1143-1145.
184. **Ishihara, K. and Matsui, K.** (1986). *J. Polym. Sci. Polym. Lett. Ed.,* **24,** 413-417.
185. **Islam, A. and Yasin, T.** (2012). *Carbohydr. Polym.,* **88,** 1055–1060.
186. **Islam, A., Riaz, M. and Yasin, T.** (2013). *Int. J. Biol. Macromol.,* **59,** 119-124.
187. **Islam, A., Yasin, T., Bano, I. and Riaz, M.** (2012). *J. Appl. Polym. Sci.,* **124,** 4184–4192.
188. **Islam, M. A., Firdous, J., Choi, Y. J., Yun, C. H. and Cho, C. S.** (2012). *Int. J. Nanomed.,* **7,** 6077-6093.
189. **Ito, Y., Casolaro, M., Kono, K. and Imanishi, Y.** (1989). *J. Controlled Release,* **10,** 195-203.
190. **Jackson, N., Cordero, N. and Stam F.** (2013). *J. Polym. Sci. Polym. Phys.,* **51,** 1523-1528.

191. **Jain, R. A., Rhodes, C. T., Railkar, A. M., Malik, A. W. and Shah, N. H.** (2000). *Eur. J. Pharm. Biopharm.,* **50,** 257-262.
192. **Jana, S. C., Maiti, S. and Biswas, S.** (2000). *J. Appl. Polym. Sci.,* **78**, 1586-1590.
193. **Jen, A. C., Wake, M. C. and Mikos, A. G.** (1996). *Biotechnol. Bioeng.,* **50,** 357-364, *and references therein.*
194. **Jena, K. K. and Raju, K. V. S. N.** (2008). *Ind. Eng. Chem. Res.,* **47,** 9214-9224.
195. **Jiang, C., Zhang, C., Bai, X., Liu, B. and Mu, J.** (2013). *J. Appl. Polym. Sci.,* DOI: 10.1002/app.39040.
196. **Jin, L., Liu, Q., Sun, Z., Ni, X. and Wei, M.** (2010). *Ind. Eng. Chem. Res.,* **49,** 11176-11181.
197. **Jin, R., Teixeira, L. S. M., Dijkstra, P. J., Karperien, M., Zhong, Z. Y. and Feijen, J.** (2008). *J. Controlled Release,* **132,** e24-e26.
198. **Jin, R., Teixeira, L. S. M., Dijkstra, P. J., van Blitterswijk, C. A., Karperien, M. and Feijen, J.** (2010). *Biomaterials,* **31,** 3103-3110.
199. **Jin, R., Teixeira, L. S. M., Dijkstra, P. J., van Blitterswijk, C. A., Karperien, M. and Feijen, J.** (2011). *J. Controlled Release,* **152,** 186-195.
200. **Jin, S., Gu, J., Shi, Y., Shao, K., Yu, X. and Yue, G.** (2013). *Eur. Polym. J.,* **49,** 1871-1880.
201. **Jin, S., Liu, M., Zhang, F., Chen, S. and Niu, A.** (2006). *Polymer,* **47,** 1526-1532.
202. **Jing, W., Zhou, X. and Xiao, H.** (2013). Structure and properties of cellulose/ PNIPAAm hydrogels prepared by SIPN strategy. *Carbohydr. Polym.,* **94,** 749-754.
203. **Jones, M. S.** (1999). *Eur. Polym. J.,* **35,** 795-801.
204. **Jose, S., Dhanya, K., Cinu, T. A., Litty, J. and Chacko, A. J.** (2009). *J. Young Pharm.,* **1,** 13-19.
205. **Jug, M. and Becirevic-Lacan, M.** (2008). *Drug Dev. Ind. Pharm.,* **34,** 817-826.
206. **Jug, M., Maestrelli, F. and Mura, P.** (2012). *J. Incl. Phenom. Macrocycl. Chem.,* **74,** 87-97.
207. **Jung, J., Arnold, R. D. and Wicker, L**. (2013). *Colloids Surf. B: Biointerfaces,* **104,** 116-121.
208. **Kaity, S., Issac, J. and Ghosh, A.** (2013). *Carbohydr. Polym.,* **94,** 456-467.
209. **Kajjari, P. B., Manjeshwar, L. S. and Aminabhavi, T. M.** (2012). *AAPS PharmSciTech,* **13,** 1147-1157.
210. **Kajjari, P. B., Manjeshwar, L. S. and Aminabhavi, T. M.** (2013). *Polym. Bull.,* **70,** 3387-3406.
211. **Kakuta, T., Takashima, Y. and Harada, A.** (2013). *Macromolecules,* **46,** 4575-4579.
212. **Kandoth, N., Mosinger, J., Gref, R. and Sortino, S.** (2013). *J. Mater. Chem. B,* **1,** 3458-3463.

213. **Kang-Mieler, J. J., Osswald, C. R. and Mieler, W. F.** (2014). *Expert Opin. Drug Deliv.,* **11,** 1647-1660, *and references therein.*
214. **Kanjickal, D., Lopina, S., Evancho-Chapman, M. M., Schmidt, S. and Donovan, D.** (2005). *J. Biomed. Mater. Res. Part A,* **74,** 454-460.
215. **Ke, X., Coady, D. J., Yang, C., Engler, A. C., Hedrick, J. L. and yang, Y. Y.** (2014). *Polym. Sci.,* **5,** 2621-2628.
216. **Khodaverdi, E., Tekie, F. S. M., Hadizadeh, F., Esmaeel, H., Mohajeri, S. A., Tabassi, S. A. S. and Zohuri, G.** (2014). *AAPS PharmSciTech,* **15,** 177-188.
217. **Khutoryanskiy, V. V., Cascone, M. G., Lazzeri, L., Barbani, N., Nurkeeva, Z. S., Mun, G. A. and Dubolazov, A. V.** (2004). *Polym. Int.,* **53,** 307-311.
218. **Kikuchi, M., Hirayama, F. and Uekama, K.** (1987). *Int. J. Pharm.,* **38,** 191-198.
219. **Kim, J. K., Kim, H. J., Chung, J. Y., Lee, J. H., Young, S. B. and Kim, Y. H.** (2014). *Arch. Pharmacal Res.,* **37,** 60-68, *and references therein.*
220. **Kim, S. J., Yoon, S. G., Lee, S. M., Lee, S. H. and Kim, S. I.** (2004). *J. Appl. Polym. Sci.,* **91,** 3613-3617.
221. **Kim, S. W., Bae, Y. H. and Okano, T**. (1992). *Pharm. Res.,* **9,** 283-290.
222. **Kim. H., Park, S. J. and Kim, S. J.** (2006). *Smart Mater. Struct.,* **15,** 1882-1886.
223. **Kimura, T., Iwai, S., Moritan, T., Nam, K., Mutsuo, S., Yoshizawa, H., Okada, M., Furuzono, T., Fujisato, T. and Kishida, A.** (2007 *J. Artif. Organs,* **10,** 104-108.
224. **Kleech, C. M.** (1990). Gels and jellies. In: *Encyclopaedia of Pharmaceutical Technology.* (Swarbrick, J., Boylan, J. C., Eds), *Marcel Dekker,* 415.
225. **Klouda, L. and Mikos, A. G.** (2008). *Eur. J. pharm. Biopharm.,* **68,** 34-45, *and references therein.*
226. **Kobayashi, J., Kikuchi, A., Sakai, K. and Okano, T.** (2003). *Anal. Chem.,* **75,** 3244-3249.
227. **Kobayashi, M. and Hyu, H. S.** (2010). *Materials,* **3,** 2753-2771.
228. **Kobayashi, N., Shirai, H. and Hojo, N.** (1989). *J. Polym. Sci.,* **27,** 191-195.
229. **Koga, S., Sasaki, S. and Maeda, H.** (2001). *J. Phys. Chem. B,* **105,** 4105-4110.
230. **Kolhe, P. and Kannan, R. M.** (2003). *Biomacromolecules,* **4,** 173-180.
231. **Kong, M., Chen, X. G., Xing, K. and Park, H. J.** (2009). *Int. J. Food Microbiol.,* **144,** 51-63, *and references therein.*
232. **Kong, S., Zhou, M., Ye, X. and Qian, X.** (2013). *Adv. Mater. Res.,* **718-720,** 172-175.
233. **Kono, H. and Teshirogi, T.** (2015). *Carbohydr. Polym.,* **72,** 299-308.
234. **Kono, H., Otaka, F. and Ozaki, M.** (2014). *Carbohydr. Polym.,* **111,** 830-840.
235. **Koopmans, C. and Ritter, H.** (2008). *Macromolecules,* **41,** 7418-7422.
236. **Kopecek, J.** (2009). *J. Polym. Sci., Polym. Chem.,* **47,** 5929-5946, *and references therein.*

237. **Kost, J. and Langer, R.** (1992). *Trends Biotechnol.,* **10,** 127-131., *and references therein.*
238. **Kowari, K., Hirosawa, I., Kurai, H., Utoguchi, N., Fujii, M. and Watanabe, Y.** (2002). *Biol. Pharm. Bull.,* **25,** 678-681.
239. **Kretschman, O., Choi, S. W., Miyauchi, M., Tomatsu, I., Harada, A. and Ritter, H.** (2006). *Angew. Chem.,* **45,** 4361-4365.
240. **Kudo, S., Otsuka, E. and Suzuki, A.** (2010). *J. Polym. Sci. Polym. Phys.,* **48,** 1978-1986.
241. **Kulkarni, S. S., Tambe, S. M., Kittur, S. A., Kariduraganavar, M. Y.** (2006). *J. Appl. Polym. Sci.,* **99,** 1380-1389.
242. **Kurkuri, M. D. and Aminabhavi, T. M.** (2004). *J. Controlled Release,* **96**, 9-20.
243. **Kushwaha, S. K., Saxena, P. and Rai, A.** (2012). *Int. J. Pharm. Investig.,* **2,** 54-60, *and references therein.*
244. **Kutyla, M. J., Lambert, L. K., Davies, N. M., McGeary, R. P., Shaw, P. N. and Ross, B. P.** (2013). *Int. J. Pharm.,* **28,** 175-184.
245. **Larsen, K. L.** (2002). *J. Incl. Phenom. Macrocycl. Chem.,* **43,** 1-13.
246. **Lasa, M., Brook, M., Saklatvala, J. and Clark, A. R.** (2001). *Mol. Cell. Biol.,* **21**, 771-780.
247. **Layre, A. M., Gosselet, N. M., Renard, E., Sebille, B. and Amiel, C.** (2002). *J. Incl. Phenom. Macro.,* **43,** 311-317.
248. **Le Corre, P., Le Guevello, P., Gajan, V., Chevanne, F. and Le Verge, R.** (1994). *Int. J. Pharm.,* **107,** 41-49.
249. **Lee, J. W., Park, J. H., Robinson, J. R.** (2000). *J. Pharm. Sci.,* **89,** 850-866.
250. **Lee, K. Y. and Mooney, D. J.** (2001). *Chem, Rev.,* **101,** 1869-1879.
251. **Lee, S. J., Kim, S. S. and Lee, Y. M.** (2000). *Carbohydr. Polym.,* **41,** 197-205.
252. **Lee, W. F. and Chen, Y. J.** (2001). *J. Appl. Polym. Sci.,* **82,** 2487-2496.
253. **Lejardi, A., Hernandez, R., Criado, M., Santos, J. I., Etxeberria, A., Sarasua, J. R. and Mijangos, C.** (2014). *Carbohyd. Polym.,* **103,** 267-273.
254. **Leslie, S. K., Cohen, D. J., Sedlaczek, J., Pinsker, E. J., Boyan, B. D. and Schwartz, Z.** (2013). *Biomaterials,* **34,** 8172-8184.
255. **Lesny, P., Croos, J. D., Pradny, M., Vacik, J., Michalek, J., Woerly, S. and Sykova, E.** (2002). *J. Chem. Neuron.,* **23,** 243-247.
256. **Li, G., Guo, L., Chang, X. and Yang, M.** (2012). *Int. J. Biol. Macromol.,* **50,** 899-904.
257. **Li, J.** (2010). *J. Drug Deliv. Sci. Technol.,* **20,** 399-405.
258. **Li, J. and Loh, X. J.** (2008). *Adv. Drug Delivery Rev.,* **60,** 1000-1017, *and references therein.*
259. **Li, J. and Zhang, X.** (2011). *J. Incl. Phenom. Macrocycl. Chem.,* **69,** 173-179.
260. **Li, J., Harada, A. and Kamachi, M.** (1994). *Polym. J.,* **26,** 1019-1026.
261. **Li, J., Xiao, H., Li, J. and Zhong, Y. P.** (2004). *Int. J. Pharm.,* **278,** 329-342.
262. **Li, S. and Liu, X.** (2008). *Polym. Adv. Technol.,* **19,** 1536-1542.
263. **Li, X., Wu, W. and Liu, W.** (2008). *Carbohydr. Polym.,* **71,** 394-402.

264. **Li, X., Wu, W., Wang, J. and Duan, Y.** (2006). *Carbohydr. Polym.,* **66,** 473-479.
265. **Liang, Z., Gong, T., Sun, X., Tang, J. Z. and Zhang, Z.** (2012). *Carbohydr. Polym.,* **87,** 2284-2290.
266. **Liechty, W. B., Kryscio, D. R., Slaughter, B. V. and Peppas, N. A**. (2010). Polymers for drug delivery systems. *Annu. Rev. Chem. Biomol. Eng.,* **1,** 149-173.
267. **Lin, C. C. and Metters, A. T. (2006).** *Adv. Drug Delivery Rev.,* **58**, 1379-1408., *and references therein.*
268. **Liu, L., and Guo, Q. X.** (2002). *J. Incl. Phenom. Macrocycl. Chem.,* **42,** 1-14.
269. **Liu, L., Fishman, M. L. and Hicks, K. B.** (2007). *Cellulose,* **14,** 15-24.
270. **Liu, S., Wang, Y., Cai, J., Ren, L., Wang, L. and Wang, Y.** (2013). *Polym. Int.,* **63,** 1930-1935.
271. **Liu, Y. Y. and Fan, X. D.** (2005). *Biomaterials,* **26,** 6367–6374.
272. **Liu, Y. Y., Fan, X. D. and Zhao, Y. B.** (2005). *J. Polym. Sci. Part A,* **43,** 3516-3524.
273. **Liu, Y. Y., Fan, X. D., Hu, H. and Tang, Z. H.** (2004). *Macromol. Biosci.,* **4,** 729-736.
274. **Liu, Y., Cui, Y. and Liao, M.** (2014). *J. Appl. Polym. Sci.,* **131,** 39781/1-39781/8.
275. **Loftsson, T. and Stefansson, E.** (1997). *Drug Dev. Ind. Pharm.,* **23,** 473-481.
276. **Loftsson, T., Jarho, P., Masson, M. and Jarvinen, T.** (2005). *Expert Opin. Drug Deliv.,* **2,** 335-351, *and references therein.*
277. **Long, Q., Pan, C., Meng, Y., Zhang, B. and Xu, C.** (2009). *J. Central South Univer. Technol.,* **16,** 66-72.
278. **Lu, Y., Sturek, M. and Park, K.** (2014). *Int. J. Pharm.,* **461,** 258-269.
279. **Lu, Y., Wang, D., Li, T., Zhao, X., Cao, Y., Yang, H. and Duan, Y. Y.** (2009). *Biomaterials,* **30,** 4143-4151.
280. **Lugao, A. B. and Malmonge, S. M.** (2001). *Nucl. Inst. Methods Phys. Res. B,* **185,** 37-42.
281. **Ma, G.** (2014). *J. Controlled Release,* **193,** 324-340.
282. **Ma, Y., Zhao, X., Li, J. and Shen, Q.** (2012). *Int. J. Nanomed.,* **7,** 559-570.
283. **Machin, R., Isasi, J. R. and Velaz, I.** (2012). *Carbohydr. Polym.,* **87,** 2024-2030, *and references therein.*
284. **Maestrelli, F., Zerrouk, N., Cirri, M., Mennini, N. and Mura, P.** (2006). *Eur. J. Pharm. Sci.,* **34,** 1-11.
285. **Manca, M. L., Zaru, M., Ennas, G., Valenti, D., Sinico, C., Loy, G. and Fadda, A. M.** (2005). *AAPS PharmSciTech.,* **6,** E464-E472.
286. **Manivannan, C., Vijay Solomon, R., Venuvanalingam, P. and Renganathan, R.** (2013). *Spectrochim. Acta A,* **103,** 18-24.
287. **Manokruang, K. and Lee, D. S.** (2013). *Macromol. Biosci.,* **13,** 1195-1203.
288. **Manzoori, J. L. and Amjadi, M.** (2003). *Spectrochim. Acta Part A,* **59,** 909-916.

289. **Mao, Y., Triantafillou, G., Hertlein, E., Towns, W., Stefanovski, M., Mo, X., Jarjoura, D., Phelps, M., Marcucci, G., Lee, L. J., Goldenberg, D. M., Lee, R. J., Byrd, J. C. and Muthusamy, N.** (2013). *Clin. Cancer Res.,* **19**, 347-356.
290. **Marques, H. C., Hadgraft, J. and Kellaway, I**. (1990). *Int. J. Pharm.,* **63**, 259-266.
291. **Marques, M. R. C., Loebenberg, R. and Almukainzi, M.** (2011). *Dissolut. Technol.,* 18, 15-28.
292. **Marras-Marquez, T., Pena, J. and Veiga-Ochoa, M. D.** (2014). *Carbohydr. Polym.,* **103,** 359-368.
293. **Martel, B., Ruffin, D., Weltrowski, M., Lekchiri, Y. and Morcellet, M.** (2005). *J. Appl. Polym. Sci.,* **97,** 433-442.
294. **Martin del Velle, E. M.,** (2004). *Process Biochem.,* **39,** 1033-1046.
295. **Martin del Velle, E. M., Galan, M. A. and Carbonell, R. G.** (2009). *Ind. Eng. Chem. Res.,* **48,** 2475-2486, *and references therein.*
296. **Mateen, R. and Hoare, T.** (2014). *J. Mater. Chem. B,* **2,** 5157-5167.
297. **Mather, M. L. and Tomlins, P. E.** (2010). *Regenerative Medicine,* **5,** 809-821.
298. **Matsuda, H. and Arima, H.** (1999). *Adv. Drug delivery Rev.,* **36,** 81-99.
299. **Matsuo, K., Ishii, Y., Kawai, Y., Saiba, Y., Quan, Y. S., Kamiyama, F., Hirobe, S., Okada, N. and Nakagawa, S.** (2013). *J. Pharm. Sci.,* **102,** 1936-1947.
300. **Matsusaki, M., Sakaquchi, H., Serizawa, T. and Akashi, M.** (2007). *J. Biomater. Sci. Polym. Ed.,* **18,** 775-783.
301. **Maziad, N. A., Abd El-Aal, S. E. and El-Kelesh, N. A.** (2009). *J. Appl. Polym. Sci.,* **111,** 1369-1380.
302. **McCormack, B. and Gregoriadis, G.** (1994). *Int. J. Pharm.,* **112,** 249-258.
303. **McCormack, B. and Gregoriadis, G.** (1994). *Drug Target.,* **2,** 449-454.
304. **McCormack, B. and Gregoriadis, G.** (1996). *Biochim. Biophys. Acta,* **1291,** 237-244.
305. **McLeod, A. D., Friend D. R. and Tozer, T. N.** (1994). *J. Pharm. Sci.,* **83,** 1284-1288.
306. **Merkus, F. W. H. M., Verhoef, J. C., Marttin, E., Romeijn, S. G., van der Kuy, P. H. M., Hermens, W. A. J. J. and Schipper, N. G. M.** (1999). *Adv. Drug Delivery Rev.,* **36,** 41-57, *and references therein.*
307. **Miguel, S. P., Ribeiro, M. P., Brancal, H., Coutinho, P. and Correia, I. J.** (2014). *Carbohydr. Polym.,* **111,** 366-373.
308. **Mino, G. and Kaizerman, S.** (1958). A new method for the preparation of graft copolymers. Polymerization initiated by ceric ion redox systems. *J. Appl. Polym. Sci.,* **31**, 242-243.
309. **Miyata, T., Uragami, T. and Nakamae, K.** (2002). *Adv. Drug Delivery Rev.,* **54,** 79-98, *and references therein.*
310. **Mocanu, G., Vizitiu, D. and Carpov, A.** (2001). *J. Bioact. Compat. Polym.,* **16,** 315-342, *and references therein.*

311. **Mohamadnia, Z., Zohuriaan-Mehr, A. J., Kabiri, K., Jamshidi, A. and Mobedi, H.** (2007). *J. Bioact. Compat. Polym.,* **22,** 342-356.
312. **Moharram, M. A. and Khafagi, M. G.** (2007). *J. Appl. Polym. Sci.,* **105,** 1888-1893.
313. **Mohit, V., Harshal, G., Neha, D., Vilasrao, K. and Rajashree, H.** (2010). *J. Incl. Phenom. Macrocycl. Chem.,* **67,** 39-47.
314. **Mok, E. Y. and Kim, J. C.** (2014). *Polym. Advanced Technol.,* **25,** 905-911.
315. **Morrison, P. W. J., Connon, C. J. and Khutoryanskiy, V. V.** (2013). *Mol. Pharmaceutics,* **10,** 756-762.
316. **Mudgil, D., Barak, S. and Khatkar, B. S.** (2012). *Int. J. Biol. Macromol.,* **50,** 1035-1039.
317. **Mufamadi, M. S., Pillay, V., Choonara, Y. E., Du Toit, L. C., Modi, G., Naidoo, D. and Ndesendo, V. M. K.** (2011). *J. Drug Deliv.,* 1–19.
318. **Muniz, E. C. and Geuskens, G.** (2001). *Macromolecules,* **43,** 4480-4484.
319. **Mura, P.** (2014). *JPBA Reviews,* **101,** 238-250, *and references therein.*
320. **Mura, P., Bettinetti, G. P., Manderioli, A., Faucci, M. T., Bramanti, G. and Sorrenti, A.** (1998). *Int. J. Pharm.,* **166,**189-203.
321. **Mura, P., Furlanetto, S., Cirri, M., Maestrelli, F., Corti, G. and Pinzauti, S.** (2005). *J. Pharm. Biomed. Anal.,* **37,** 987-994.
322. **Mura, P., Maestrelli, F., Cecchi, M., Bragagni, M. and Almeida, A.** (2010). *J. Microencapsul.,* **27,** 479-486.
323. **Murali, R., Vidhya, P. and Thanikaivelan, P.** (2014). *Carbohydr. Polym.,* **110,** 440-445.
324. **Murdan, S.** (2003). *J. Controlled Release,* **92,** 1-17, *and references therein.*
325. **Muzzarelli, R. A. A.** (1973). Natural chelating polymers: alginic acid, chitin and chitosan. Pergamon Press (Muzzarelli, R.A.A., Ed.), New York.
326. **Namkung, S. and Chu, C. C.** (2007). *J. Biomater. Sci. Polym.,* **18,** 901-924.
327. **Nazar, H., Caliceti, P., Carpenter, B., El-Mallah, A. I., Fatouros, D. G., Roldo, M., van der Merwe, S. M. and Tsibouklis, J.** (2013). *Biomater. Sci.,* **1,** 306-314.
328. **Ni, X., Cheng, A. and Li, J.** (2009). *J. Biomed. Mater. Res. A,* **88A,** 1031-1036.
329. **Nie, W., Yuan, X., Zhao, J., Zhou, Y. and Bao, H.** (2013). *Carbohydr. Polym.,* **96,** 342-348.
330. **Nielsen, A. L., Madsen, F. and Larsen, K. L**. (2009). *Int. J. Pharm.,* **16,** 92-101.
331. **Nishikawa, M., Onuki, Y., Isowa, K. and Takayama, K.** (2008). *AAPS PharmSciTech,* **9,** 1038-1045.
332. **Nonaka, N., Farr, S. A., Kageyama, H., Shioda, S. and Banks, W. A.** (2008). *J. Pharmacol. Exp. Ther.,* **325,** 513-519.
333. **Nonaka, N., Farr, S. A., Nakamachi, T., Morley, J. E., Nakamura, M., Shioda, S. and Banks, W. A.** (2012). *Peptides,* **36,** 168-175.
334. **Nugent, M. J. D. and Higginbotham, C. L.** (2007). *Eur. J. Pharm. Biopharm.,* 67, 377-386.

335. **Ogoshi, T., Takashima, Y., Yamaguchi, H. and Harada, A.** (2007). *J. Am. Chem. Soc.,* **129**, 4878–4879.
336. **Olson, S. T. and Chuang, Y. J.** (2002). *Trends Cardiovasc. Med.,* **12,** 331-338.
337. **Onuki, Y., Hoshi, M., Okabe, H., Fujikawa, M., Morishita, M. and Takayama, K.** (2005). *J. Controlled Release,* **108,** 331-340.
338. **Ooya, T., Ichi, T., Furubayashi, T., Katoh, M. and Yui, N.** (2007). *React. Funct. Polym.,* **67,** 1408-1417.
339. **Orienti, I., Bigucci, F., Gentilomi, G. and Zecchi, V.** (2001). *J. Pharm. Sci.,* **90,** 1435-1444.
340. **Osbun, J.W., Ellenbogen, R. G., Chesnut, R. M., Chin, L. S., Connolly, P. J., Cosgrove, G. R., Delashaw, J. B. Jr., J. A. and Wilberger, J. E.** (2012). *World Neurosurgery,* **78,** 498-504.
341. **Otake, K., Inomata, H., Konno, M. and Saito, S.** (1990). *Macromolecules,* **23,** 283-289.
342. **Otero-Espinar, F. J., Igea, S. A., Mendez, J. B. and Jato, J. L. V.** (1991). *Int. J. Pharm.,* **70,** 35-41.
343. **Otero-Espinar, F. J., Torrse-Labandeira, J. J., Alvarez-Lorenzo, C. and Blanco-Mendez, J.** (2010). *J. Drug Del. Sci. Tech.,* **20,** 289-301.
344. **Palanisamy, M., Khanam, J., Nagalingam, A. and Gani, N.** (2011). *Korean J. Chem. Eng.,* **28,** 1990-2001.
345. **Palmer, D., Levina, M., Douroumis, D., Maniruzzaman, M., Morgan, D. J., Farrell, T. P., Rajabi-Siaboomi, A. R. and Nokhodchi, A.** (2013). *Colloid Surf. B,* **104,** 174-180.
346. **Park, C. J., Clark, S. G., Lichtenstiger, C. A., Jamison, R. D. and Johnson, A. J.** (2009).. *Acta Biomater.,* **5,** 1926-1936.
347. **Park, J., Lim, E., Back, S., Na, H., Park, Y. and Sun, K**. (2010). *J. Biomed. Mater. Res. A,* **93A,** 1091–1099.
348. **Park, K., Lee, S., Joung, Y., Na, J., Lee, M. and Park, K.** (2009). *Acta Biomater.,* **5,** 1956-1965.
349. **Park, M. R., Seo, B. B. and Song, S. C.** (2013). *Biomaterials,* **34,** 1327-1336.
350. **Park, S. E., Nho, Y. C., Lim, Y. M. and Kim, H. I.** (2003). *J. Appl. Polym. Sci.,* **91,** 636-643.
351. **Parmar, V. J. and Lumbhani, A. N.** (2012). *Bull. Pharmaceut. Res.,* **2,** 167-174.
352. **Patterson, J., Slew, R., Herring, S., Lin, A., Guldberg, R. and Stayton, P.** (2010). *Biomaterials,* **31,** 6772-6781.
353. **Pearson, M., Allender, C., Brain, K., Anstey, A., Gateley, C., Wilke, N., Morrissey, A. and Birchall, J.** (2008). *Pharmaceut. Res.,* **25,** 407-416.
354. **Peppas, N. A.** (1986). Hydrogels of poly (vinyl alcohol) and its co-polymers. In: *Hydrogels in Medicine and Pharmacy.* (Peppas, N. A., Ed), *CRC Press,* Boca Raton, FL, **2,** 1-48.
355. **Peppas, N. A. and Merrill, E. W.** (1976). *J. Appl. Polym. Sci.,* **20,** 1457-1465.
356. **Peppas, N. A. and Sahlin, J. J.** (1989). *Int. J. Pharm.,* **57,** 169-172.

357. **Peppas, N. A., Bures, P., Leobandung, W. and Ichikawa, H.** (2000).. *Eur. J. Pharm. Biopharm.,* **50,** 27-46., *and references therein.*
358. **Peppas, N. A., Huang, Y., Torres, M-L., Ward, J. H. and Zhang, J.** (2000). *Annu. Rev. Biomed. Eng.,* **2,** 9-29, *and references therein.*
359. **Perchyonok, V. T. and Oberholzer, T.** (2012). *Curr. Org. Chem.,* **16,** 2365-2378, *and references therein.*
360. **Phadke, K. V., Manjeshwar, L. S. and Aminbhavi, T. M.** (2014). *Polym. Bull.,* **71,** 1625-1643.
361. **Pinho, E., Grootveld, M., Soares, G. and Henriques, M.** (2014). *Crit. Rev. Biotechnol.,* **34,** 328-37, *and references therein.*
362. **Pinho, E., Henriques, M. and Soares, G.** (2014). *Cellulose,* **21,** 4519-4530.
363. **Prabaharan, M.** (2008). *J. Biomater. Appl.,* **23,** 5-36,
364. **Prabaharan, M.** (2011). *Int. J. Biol. Macromol.,* **49,** 117-124, *and references therein.*
365. **Prabaharan, M. and Gong, S.** (2008). *Carbohydr. Polym.,* **73,** 117-125.
366. **Prabaharan, M. and Jayakumar, R.** (2009). *Int. J. Biol., Macromol.,* **44,** 320-325.
367. **Prabaharan, M. and Mano, J. F.** (2005). *Macromol. Biosci.,* **5,** 965-973.
368. **Preul, M. C., Campbell, P. K., Garlick, D. S. and Spetzler, R. F.** (2010). *J. Neurosurg. Spine,* **12,** 381-390.
369. **Pritchard, C. D., O' Shea, T. M., Seigwart, D. J., Calo, E., Anderson, D. G., Reynolds, F. M., Thomas, J. A., Slotkin, J. R., Woodard, E. J. and Langer R.** (2011). *Biomaterials,* **32,** 587-597.
370. **Priya, A. S., Sivakamavalli, J., Vaseeharan, B. and Stalin, T.** (2013). *Int. J. Biol. Macromol.,* **62,** 472-480.
371. **Puoci, F. and Curcio, M.** (2013). *RSC Smart Materials,* **2,** 153-179.
372. **Putnam, D.** (2006).. *Nat. Mater.,* **5,** 439-451.
373. **Qian, L., Xiao, H., Zhao, G. and He, B.** (2011). *ACS Appl. Mater. Interfaces,* **3,** 1895–1901.
374. **Qiu, Y. and Park, K.** (2001). *Adv. Drug Delivery Rev.,* **53**, 321-339.
375. **Quick, D. and Anseth, K.** (2004). *J. Controlled Release,* **96,** 341-351.
376. **Quintero, S. M. M., Ponce F., R. V., Cremona, M., Triques, A. L. C., d'Almeida, A. R. and Braga, A. M. B.** (2010). *Polymer,* **51,** 953-958.
377. **Raafat, A. I.** (2010). *J. Appl. Polym. Sci.,* **118,** 2642-2649.
378. **Raafat, A. I., Eid, M., El-Arnaouty, M. B.** (2012). *Nucl. Instr. Meth. Phys. Res. B,* **283,** 71-76.
379. **Raafat, D., von Bargen, K., Haas, A. and Sahl, H. G.** (2008). *Appl. Environ. Microbiol.,* **74,** 3764-3773.
380. **Ramı´rez, H. L., Cao, R., Fragoso, A., Torres-Labandeira, J. J., Dominguez, A., Schacht, E. H., Ban˜os, M. and Villalonga, R.** (2006). *Macromol. Biosci.,* **6,** 555–561.
381. **Ranganath, S. K., Kee, I., Krantz, W. B., Chow, P. K. and Wang, C. H.** (2009). *Pharmaceut. Res.,* **26,** 2101-2114.
382. **Ranjha, N. M. and Khan, S.** (2013). *J. Pharm. Alt. Med.,* **2,** 30-41.

383. **Rao, M. S., Kanatt, S. R., Chawla, S. P. and Sharma, A.** (2010*Carbohydr. Polym.,* **82,** 1243-1247.
384. **Rasool, N., Yasin, T., Heng, J. Y. Y. and Akhter, Z.** (2010). *Polymer,* **51,** 1687-1693.
385. **Raul, H., Victoria de Juan, H., Stephanie, C. and Guadalupe, Z.** (2012). Therapeutic use of contact lenses. In: *Ocular Surface.* (Herranz, R. M. and Herran, R. M. C., Eds), *CRC Press,* 288-296.
386. **Ravi Kumar, M. N. V.** (2000). *React. Funct. Polym.,* **46,** 1-27.
387. **Ravi, V., Pramod Kumar, T. M. and Siddaramaiah.** (2008). *Indian J. Pharm. Sci.,* **70,** 111-113.
388. **Ravichandran, P., Shantha, K. L. and Rao, K. P.** (1997). *Int. J. Pharm.,* **154,** 89-94.
389. **Ray, D., Gils, P. S., Mohanta, G. P., Manavalan, R. and Sahoo, P. K.** (2010). *J. Appl. Polym. Sci.,* **116,** 959-968.
390. **Reddy, K. M., Babu, V. R., Rao, K. S. V. K., Subha, M. C. S., Rao, K. C., Sairam, M. and Aminabhavi, T. M.** (2008). *J. Appl. Polym. Sci.,* **107,** 2820-2829.
391. **Riekes, M. K., Tagliari, M. P., Granada, A., Kuminek, G., Silva, M. A. S. and Stulzer, H. K.** (2007). *Mater. Sci. Engg.,* **30,** 1008-1013.
392. **Ritger, P. L. and Peppas, N. A.** (1987). *J. Controlled Release,* **5,** 37-42.
393. **Rodell, C. B., Kaminski, A. L. and Burdick, J. A.** (2013). *Biomacromolecules,* **14,** 4125-4134.
394. **Rodriguez-Tenreiro, C., Alvarez-Lorenzo, C., Rodriguez-Perez, A. and Concheiro, A.** (2007). *Eur. J. Pharm. Biopharm.,* **66,** 55-62.
395. **Rossi, D. D., Kajiwara, K., Osada, Y. and Yamauchi, A.** (1991). *J. Adhes.,* **37,** 271-272.
396. **Rotich, M. K., Brown, M. E. and Glass, B. D.** (2003). *J. Therm. Anal. Cal.,* **73**, 671.
397. **Roy, N., Saha, N., Kitano, T. and Saha, P.** (2012). *Carbohydr. Polym.,* **89,** 346-353.
398. **Saboktakin, M. A., Tabatabaie, R. M., Maharramov, A. and Ramazanov, M. A.** (2010). *J. Pharm. Sci.,* **99,** 4955-4961.
399. **Sadlej-Sosnowska, N.** (1997). *J. Incl. Phenom. Recog. Chem.,* **27,** 31-40.
400. **Sakaguchi, H., Serizawa, T. and Akashi, M.** (2006). *J. Nanosci. Nanotech.,* **6,** 1124-1127.
401. **Salmaso, S., Semenzato, A., Bersani, S., Metricardi, P., Rossi, F. and Caliceti, P.** (2007). *Int. J. Pharm.,* **345,** 42-50.
402. **Salústio, P. J., Feio, G., Figueirinhas, J. L., Pinto, J. F. and Cabral Marques, H. M.** (2009). *Eur. J. Pharm. Biopharm.,* **71,** 377-386.
403. **Salustio, P. J., Pontes, P., Conduto, C., Sanches, I., Carvalho, C., Arrais, J. and Marques, H. M. C.** (2011). *AAPS PharmSciTech,* **12,** 1276-1292.
404. **Samal, S. K., Dash, M., Vlierberghe, S. V., Kaplan, D. L., Chiellini, E., van Blitterswijk, C., Moroni, L. and Dubruel, P.** (2012). *Chem. Soc. Rev.,* **41,** 7147-7194, *and references therein.*

405. **Sareen, R., Jain, N. and Dhar, K. L.** (2013). *Curr. Drug Delivery,* **10,** 564-571.
406. **Schellekens, R. C. A., Stuurman, F. E., van der Weert, F. H. J., Kosterwink, J. G. W. and Frijlink, H. W.** (2007). *Eur. J. Pharm. Sci.,* **30,** 15-20.
407. **Scherman, O. A.** (2013). In: Polymeric and self assembled hydrogels: from fundamental understanding to applications, RSC, pp.167-196.
408. **Schild, H.** (1992). *Prog. Polym. Sci.,* **17,** 163-249.
409. **Schneider, H. J., Hacket, F., Rudiger, V. and Ikeda, H.** (1998). *Chem. Rev.,* **98,** 1755-1786 and references therein.
410. **Scriba, G. K. E.** (2008). *J. Sep. Sci.,* **31,** 1991-2011.
411. **Seidlits, S. K., Gower, R. M., Shephard, J. A. and Shea, L. D.** (2013). *Expert Opin. Drug Deliv.,* **10,** 599-509.
412. **Serra, L., Domenech, J. and Peppas, N. A.** (2006). *Biomaterials,* **27,** 5440-5451.
413. **Seuring, J. and Agarwal, S.** (2012). *Macromol. Rapid Comm.,* **33,** 1898-1920, *and references therein.*
414. **Sevillano, X., Isasi, J. R., Penas, F. J.** (2008). *Biodegradation,* **19,** 589-597.
415. **Shalmashi, A. and Eliassi, A.** (2008). *J. Chem. Eng. Data,* **53,** 199-200.
416. **Shang, J., Shao, Z. and Chen, X.** (2008). *Polymer,* **49,** 5520-5525.
417. **Sharma, N. and Baldi, A.** (2014). *Drug Delivery*, DOI:10.3109/ 10717544. 2014. 938839
418. **Sharma, N. and Harikumar, S. L.** (2013). *Int. J. Drug Develop. Res.,* **5,** 21-31, *and references therein.*
419. **Sharma, R., Rawal, R. K., Gaba, T., Singla, N., Malhotra, M., Matharoo, S. and Bhardwaj, T. R.** (2013). *Bioorg. Med. Chem. Lett.,* **23,** 5332-5338.
420. **Shazly, T. M., Baker, A. B., Naber, J. B., Bon, A., Vliet, K. J. V. and Edelman, E. R.** (2010). *J. Biomed. Mater. Res. A,* **95,** 1159-1169.
421. **Shen, E., Kipper, M. J., Dziadul, B., Lim, M. K. and Narasimhan, B.** (2002). *J. Controlled Release,* **82,** 115-125.
422. **Si, S., Zhou, R., Xing, Z., Xu, H., Cai, Y. and Zhang, Q.** (2013*Fibre Polym.,* **14,** 982-989.
423. **Siegel, R. A. and Rathbone, M. J.** (2012). Overview of controlled release mechanisms. In: Fundamentals and applications of controlled release drug delivery, Springer US, pp. 19-43.
424. **Siemoneit, U., Schmitt, C., Alvarez-Lorenzo, C., Luzardo, A., Otero-Espinar, F. and Concheiro, A.** (2006). *Int. J. Pharm.,* **312,** 66-74.
425. **Siepmann, J. and Peppas, N. A.** (2001). *Adv. Drug Delivery Rev.,* **48,** 139-157.
426. **Singh, A. V.** (2013). *J. Therm. Anal. Calorim.,* **112,** 791-793.
427. **Singh, A., Sharma, P. K., Garg, V. K. and Garg, G.** (2010). *Int. J. Pharm. Sci. Rev. Res.,* **4,** 97-105.
428. **Singh, B. and Sharma, V.** (2010). *Int. J. Pharm.,* **389,** 94-106.

429. **Singh, R. M., Kumar, A. and Pathak, K.** (2013). *AAPS PharmSciTech,* **14,** 412-424.
430. **Sinha, V. R., Mittal, B. R., Bhutani, K. K. and Kumria, R.** (2004). *Int. J. Pharm.,* **269,** 101-108.
431. **Song, B., Song, J., Zhang, S., Anderson, M. A., Ao, Y., Yang, C. Y., Deming, T. J. and Sofroniew, M. V.** (2012). *Biomaterials,* **33,** 9105-9116.
432. **Spiller, K. L., Liu, Y., Holloway, J. L., Maher, S. A., Cao, Y., Liu, W., Zhou, G. and Lowman, A. M.** (2012). *J. Controlled Release,* **157,** 39-45.
433. **Spiller, K. L., Liu, Y., Holloway, J. L., Maher, S. A., Cao, Y., Liu, W., Zhou, G. and Lowman, A. M.** (2012). *J. Controlled Release,* **157,** 39-45.
434. **Sreenivasan, K.** (1997). *J. Appl. Polym. Sci.,* **65,** 1829-1832.
435. **Stauffer, S. R. and Peppas, N. A.** (1992). *Polymer,* **33,** 3932-3936.
436. **Stella, V. J. and He, Q.** (2008). *Toxicol. Pathol.,* **36,** 30-42,
437. **Stella, V. J. and Rajeswski, R. A.** (1997). *Pharm. Res.,* **14,** 556-567.
438. **Sui, K., Gao, S., Wu, W. and Xia, Y.** (2010). *J. Polym. Sci. Polym. Chem.,* **48,** 3145-3151, *and references therein.*
439. **Sullad, A. G., Manjeshar, L. S. and Aminabhavi, T. M.** (2010). *Ind. Eng. Chem. Res.,* **49,** 7323-7329.
440. **Sullad, A. G., Manjeshwar, L. S. and Aminabhavi, T. M.** (2011). *Ind. Eng. Chem. Res.,* **50,** 11778-11784.
441. **Sutani, K., Kaetsu, I., Uchida, K. and Matsubara, Y.** (2002). *Radiat. Phys. Chem.,* **64,** 331-336.
442. **Syed, T. A., Qureshi, Z. A., Ahman, S. A. and Ali, S. M.** (2000). *Int. J. STD & AIDS,* **11,** 371-374.
443. **Szejtli, J.** (1998). *Chem. Rev.,* **98,** 1743-1753, *and references therein.*
444. **Szejtli, J.** (2004). *Pure Appl. Chem.,* **76,** 1825-1845.
445. **Szejtli, J., Fenyvesi, E. and Zsadon, B.** (1978). *Starch Starke,* **30,** 127-131.
446. **Tabassi, S. A. S., Tekie, F. S. M., Hadizadeh, F., Rashid, R., Khodaverdi, E. and Mohajeri, S. A.** (2014). *J. Sol-Gel Sci. Tech.,* **69,** 166-171.
447. **Takami, K., Watanabe, J., Takai, M. and Ishihara, K.** (2011). *J. Biomater. Sci. Polym Ed.,* **22,** 77-89.
448. **Tan, H. and Hu, X.** (2012). *J. Appl. Polym. Sci.,* **126,** E180-E186.
449. **Tan, H., Gao, X., Sun, J., Xiao, C. and Hu, X.** (2013). *Chem. Comm.,* **49,** 11554-11556.
450. **Tan, S., Ladewig, K., Fu, Q., Blencowe, A. and Qiao, G. G.** (2014). *Macromol. Rapid Comm.,* **35,** 1166-1184, *and references therein.*
451. **Tang, Y. F., Du, Y. M., Hu, X. W., Shi, X. W. and Kennedy, J. F.** (2007). *Carbohydr. Polym.,* **67,** 491-499.
452. **Tang, Y., Du, Y., Li, Y., Wang, X. and Hu, X.** (2009). *J. Biomed. Mater. Res. A,* **91,** 953-963.
453. **Thirumaleshwar, S., Kulkarni, P. K. and Gowda, D. V.** (2012). *Curr. Drug Therapy,* **7,** 212-218, *and references therein.*
454. **Tian, W. M., Zhang, C. L., Hou, S. P., Yu, X., Cui, F. Z., Xu, Q. Y., Sheng, S. L., Cui, H. and Li, H. D.** (2005).

455. **Tian, Z., Chen, C. and Allcock, H. R.** (2014). *Macromolecules,* **47,** 1065-1072.
456. **Tiwari, G., Tiwari, R. and Rai, A. K.** (2010). *J. Pharm. Bioallied Sci.,* **2,** 72-79*, and references therein.*
457. **Tomatsu, I., Peng, K. and Kros, A.** (2011). *Adv. Drug Delivery Rev.,* **63,** 1257-66*, and references therein.*
458. **Torelli-Souza, R. R., Bastos, L. A. C., Nunes, H. G. L., Camara, C. A. and Amorim, R. V. S.** (2012). *J. Appl. Polym. Sci.,* **126,** E408-E417.
459. **Torqersen, J., Ovsianikov, A., Mironov, V., Pucher, N., Qin, X., Li, Z., Cicha, K., Machacek, T., Liska, R., Jantsch, V. and Stampfl, J.** (2012).. *J. Biomed. Opt.,* **17,** 105008 (1-10).
460. **Torres, A. J., Zhu, C., Shuler, M. J. and Pannullo, S.** (2011). *Biotechnol. Prog.,* **27,** 1478-1487.
461. **Tubbs, R. K.** (1966). Sequence distribution of partially hydrolyzed poly (vinyl acetate). *J. Polym. Sci. Part A,* **4,** 623-629.
462. **Uchegbu, I. F., Carlos, M., McKey, C., Hou, X. and Schaetzlein, A. G.** (2014). *Polym. Int.,* **63,** 1145-1153.
463. **Uekama, K.** (2004). *Chem. Pharm. Bull.,* **52,** 900-915.
464. **Uekama, K., Kondo, T., Nakamura, K., Irie, T., Arakawa, K., Shibuya, M. and Tanaka, J.** (1995). *J. Pharm. Sci.,* **84,** 15-20.
465. **Uhrich, K. E., Cannizzaro, S. M., Langer, R. S. and Shakesheff, K. M.** (1999). *Chem. Rev.,* **99,** 3181-3198*, and references therein.*
466. **Urtti, A.** (2006). *Adv. Drug Delivery Rev.,* **58,** 1131-1135.
467. **Vadnerkar, G. and Dhaneshwar, S.** (2013). *Curr. Drug Delivery Technol.,* **10,** 16-24.
468. **Vaghani, S. S., Patel, M. M. and Satish, C. S.** (2012). *Carbohydr. Res.,* **347,** 76-82.
469. **Valade, D., Wong, L. K., Jeon, Y., Jia, Z. and Monteiro, M. J.** (2013). *J. Polym. Sci., Polym. Chem.,* **51,** 129-138.
470. **Valero, M. and Carrillo, C.** (2004). *J. Photochem. Photobiol. B: Biology,* **74**, 151-160.
471. **van de Manakker, F., Braeckmans, K., el Morabit, N., De Smedt, S. C., van Nostrum, C. F. and Hennink, W. E.** (2009). *Adv. Funct. Mater.,* **19,** 2992-3001.
472. **van de Manakker, F., Kroon-Batenburg, L. M. J., Vermonden, T., van Nostrum, C. F. and Hennink, W. E.** (2010). *Soft Matter,* **6,** 187-194.
473. **van de Manakker, F., van der Pot, M., Vermonden, T., van Nostrum, C. F. and Hennink, W. E.** (2008). *Macromolecules,* **41,** 1766-1773.
474. **van de Mannaker, F., Vermonden, T., van Nostrum, C. F. and Hennink, W. E.** (2009). *Biomacromolecules,* **10,** 3157-3175.
475. **van Dijk, M., Rijkers, D. T. S., Liskamp, R. M. J., van Nostrum, C. F. and Hennink, W. E.** (2009). *Bioconjugate Chem.,* **20,** 2001-2016.
476. **Vanic, Z., Hurler, J., Federber, K., Gasparovic, P. G., Skalko-Basnet, N. and Filipovic-Grcic, J.** (2014). *J. Liposome Res.,* **24,** 27-36.

477. **Varde, N. K. and Pack, D. W.** (2004). *Expert Opin. Biol. Ther.,* **4,** 35-51.
478. **Varghese, S. and Jamora, C.** (2012). *Expert Rev. Dermatol.,* **7,** 315-317.
479. **Vats, A. and Pathak, K.** (2013). *Expert Opin. Drug Deliv.,* **10**, 545-557.
480. **Veiga, F., Fernandes, C. and Teixeira, F.** (2000). *Int. J. Pharm.,* **202,** 165-171.
481. **Velaz, I., Sanchez, M., Martin, C., Martinez-Oharriz, M. C. and Zornoza, A.** (1997). *Int. J. Pharm.,* **153,** 211-217.
482. **Vermonden, T., Fedorovich, N. E., van Geeman, D., Alblas, J., van Nostrum, C. F. and Hennik, W. E.** (2008). *Biomacromolecules,* **9,** 919-926.
483. **Vernon, B., Kim, S. W. and Ba, Y. H.** (2000). *J. Biomed. Mater. Res.,* **51,** 69-79*, and references therein.*
484. **Vert, M., Doi, Y., Hellwich, K. H., Hess, M., Hodge, P., Kubisa, P., Rinuado, M. and Schue, F.** (2012). *Pure Appl. Chem.,* **84,** 377-410.
485. **Vianna, R. F. L., Bentley, M. V. L. B., Ribeiro, G., Carvalho, F. S., Neto, A. F., de Oliveira, D. C. R. and Collett, J. H.** (1998). *Int. J. Pharm.,* **167**, 205-213.
486. **Victor, S. P. and Sharma, C. P.** (**2002**). *J. Biomater. Appl.,* **17,** 125–134.
487. **Vieira, A. C. F., Serra, A. C., Carvalho, R. A., Gonsalves, A., Figueiras, A., Veiga, F. J., Basit, A. W. and Gonsalves, A. M. R.** (2013). *Carbohydr. Polym.,* **93,** 512-517.
488. **Villiers, A.** (1891). *C. R. Acad. Sci.,* **112,** 536-538.
489. **Vimala, K., Sivudu, K. S., Mohan, Y. M., Sreedhar, B. and Raju, K. M.** (2009). *Carbohydr. Polym.,* **75,** 463-471.
490. **Vyas, A., Saraf, S. and Saraf, S.** (2008). *J. Incl. Phenom. Macrocycl. Chem.,* **62,** 23-42*, and references therein.*
491. **Wanakule, P., Liu, G. W., Fleury, A. T. and Roy, K.** (2012). *J. Controlled Release,* **162,** 429-437.
492. **Wang, D., Li, H., Gu, J., Guo, T., Yang, S., Guo, Z., Zhang, X., Zhu, W. and Zhang, J.** (2013). *J. Pharm. Biomed. Anal.,* **83,** 141-148.
493. **Wang, H. D., Chu, L. Y., Yu, X. Q., Xie, R., Yang, M., Xu, D., Zhang, J. and Hu, L.** (2007). *Ind. Eng. Chem. Res.,* **46,** 1511-1518.
494. **Wang, J., Pham, D. T., Guo, X., Li, L., Lincoln, S. F., Luo, Z., Ke, H., Zheng, L. and Prud'homme, R. K.** (2010). *Ind. Eng. Chem. Res.,* **49,** 609-612.
495. **Wang, L., Li, J., Lin, Y. and Chen, C.** (2007). *J. Membr. Sci.,* **305,** 238-246.
496. **Wang, N., Zhang, J., Sun, L., Wang, P. and Liu, W.** (2014). *Acta Biomaterialia,* **10,** 2529-2538.
497. **Wang, Q., Zhang, J. and Wang, A.** (2009). *Carbohydr. Polym.,* **78,** 731-737.
498. **Wang, X., Yan, Y., Xiong, Z., Lin, F., Wu, R., Zhang, R. and Lu, Q.** (2005). *J. Biomed. Mater. Res. B Appl. Biomater.,* **75,** 91-98.
499. **Wang, Y., Cooke, M. J., Morshead, C. M. and Shoichet, M. S.** (2012). *Biomaterials,* **33,** 2681-2692.
500. **Wang, Z. and Chen, Y.** (2007). *Macromolecules,* **40,** 3402-3407.
501. **Ward, M. A. and Georgion, T. K.** (2011). *Polymers,* **3,** 1215-1242.

502. **Wasiak, I. and Ciach, T.** (2012). *Chem. Process Engg.,* **33,** 529-538.
503. **Wassmer, S., Rafat, M., Fong, W. G., Baker, A. N. and Tsilfids, C.** (2013). *Acta Biomater.,* **9,** 7855-7864.
504. **Watanabe, Y., Matsumoto, Y., Seki, M., Takase, M. and Matsumoto, M.** (1992). *Chem. Pharm. Bull.,* **40,** 3042-3047.
505. **Wei, L., Cai, C., Lin, J. and Chen, T.** (2009). *Biomaterials,* **30,** 2606-2613.
506. **Wei, L., Lin, J., Cai, C., Fang, Z. and Fu, W.** (2011). *Eur. J. Pharm. Biopharm.,* **78,** 346-354.
507. **Wenceslau, A. C., dos Santos, F. G., Ramos, E. R. F., Nakamura, C. V., Rubira, A. F. and Muniz, E. C.** (2012). *Mater. Sci. Engineering C,* **32,** 1259-1265.
508. **Wheeler, J. C., Woods, J. A., Cox, M. J., Cantrell, R. W., Watkins, F. H. and Edlich, R. F.** (1996). *J. Long Term Eff. Med. Implants,* **6,** 207-217.
509. **Wichterle, O. and Lim, D.** (1960). *Nature,* **185,** 117-118.
510. **Wu, D. Q., Wang, T., Lu, B., Xu, X. D., Cheng, S. X., Jiang, X. J., Zhang, X. Z. and Zhuo, R. X.** (2008). *Langmuir,* **24,** 10306-10312.
511. **Wu, Y., Guo, B. and Ma, P. X.** (2014). *ACS Macro Lett.,* **3,** 1145-1150.
512. **Wu, Y., Wei, W., Zhou, M., Wang, Y., Wu, J., Ma, G and Su, Z.** (2012). *Biomaterials,* **33,** 2351-2360.
513. **Wu, Y., Wu, S., Hou, L., Wei, W., Zhou, M., Su, Z., Wu, J., Chen, W. and Ma, G.** (2012). *Eur. J. Pharm. Biopharm.,* **81,** 486-497.
514. **Wu, Z., Sheng, Z., Sun, T., Geng, M., Li, J., Yao, Y. and Huang, Z.** (2003). *Chin. Med. J.,* **116,** 419-423.
515. **Xiao, C. and Zhou, G.** (2003). *Polym. Degrad. Stab.,* **81,** 297-301.
516. **Xiao, F., Chen, L., Xing, R. F., Zhao, Y. P., Dong, J., Guo, G. and Zhang, R.** (2009). *Colloid Surf. B,* **71,** 13-18.
517. **Xie, Y. T., Du, Y. Z., Yuan, H. and Hu, F. Q.** (2012). *Int. J. Nanomed.,* **7,** 3235-3244.
518. **Xing, Y. B., Chen, H. Y., Li, S. Y. and Guo, X. H.** (2014). *J. Liposome Res.,* **24,** 10-16.
519. **Xiong, X. Y., Li, Q. H., Li, Y. P., Guo, L., Li, Z. L. and Gong, Y. C.** (2013). *Colloids Surf. B.,* **111,** 282-288.
520. **Xu, J., Li, X., Sun, F. and Cao, P.** (2010). *J. Biomater. Sci. Polym. Ed.,* **21,** 1023-1038.
521. **Xu, L., Zhang, L. and Chen, H.** (2002). *Desalination,* **148,** 309-313.
522. **Xu, X. D., Wei, H., Zhang, X. Z., Cheng, S. X. and Zhuo, R. X.** (2006). *J. Biomed. Mater. Res.,* **81A,** 418-426.
523. **Yan, F., Li, B., Shen, F. and Fu, Q.** (2014). *Drug Delivery,* **27**, 1-7.
524. **Yang, X., Yang, K., Yu, F., Chen, X., Wu, S. and Zhu, Z.** (2009). *Polym. Int.,* **58,** 1291-1298.
525. **Ye, Y., Sun, Y., Zhao, H., Lan, M., Gao, F., Song, C., Lou, K., Li, H. and Wang, W.** (2013). *Int. J. Pharm.,* **458,** 110-117.
526. **Yin, R., Tong, Z., Yang, D. and Nie J.** (2012). *Carbohydr. Polym.,* **89,** 117-123.

527. **Yin, Y. H., Yang Y. J. and Xu, H. B.** (2001). *J. Polym. Sci. Part B: Polymer, Physics,* **39**, 3128-3137.
528. **Yokoyama, F., Masada, I., Shimamura, K., Ikawa, T. and Monobe, K.** (1986). *Colloid Polym. Sci.,* **264,** 2223-2229.
529. **Yoo, S. D., Yoon, B. M., Lee, H. S. and Lee, K. C.** (1999). *J. Pharm. Sci.,* **88,** 1119-1121.
530. **Yoshida, T., Lai, T. C., Kwon, G. S. and Sako, K.** (2013). *Expert Opin. Drug Deliv.,* **10,** 1-17.
531. **Yu, F., Cao, X., Li, Y., Zeng, L., Yuan, B. and Chen, X.** (2014). *Polym. Chem.,* **5,** 1082-1090.
532. **Yu, J., Ha, W., Chen, J. and Shi, Y.** (2014). *RSC Adv.,* **4,** 58982-58989.
533. **Yu, J., Ha, W., Sun, J. and Shi, Y.** (2014). *ACS Appl. Mater. Interfaces,* **6,** 19544-19551 *and references therein.*
534. **Zhang, H., Zhang, F. and Wu, J.** (2013). *Funct. Polym.,* **73,** 923-928.
535. **Zhang, J. and Ma, P. X.** (2013). *Adv. Drug Delivery Rev.,* **65,** 1215-1233.
536. **Zhang, J. T., Huang, S. W., Liu, J. and Zhuo, R. X.** (2005). *Macromol. Biosci.,* **5,** 192-196.
537. **Zhang, J. T., Xue, Y. N., Gao, F. Z., Huang, S. W. and Zhuo, R. X.** (2008). *J. Appl. Polym. Sci.,* **108,** 3031-3037.
538. **Zhang, M., Yang, Z., Chow, L. L. and Wang, C. H.** (2003). *J. Pharm. Sci.,* **92,** 2040-2056.
539. **Zhang, X. Z., Wu, D. Q. and Chu, C. C.** (2004). *Biomaterials,* **25,** 3793-3805.
540. **Zhang, X., Wang, Y. and Yi, Y.** (2004). *J. Appl. Polym. Sci.,* **94,** 860-864.
541. **Zhang, X., Wu, Z., Gao, X., Shu, S., Zhang, H., Wang, Z. and Li, C.** (2009). *Carbohydr. Polym.,* **77,** 394-401.
542. **Zhang, X., Zheng, S., Lin, Z. and Tan, S.** (2012). *J. Appl. Polym. Sci.,* **123,** 2250-2256.
543. **Zhang, Z. X., Liu, K. L. and Li, J.** (2013). *Angew. Chem. Int. Ed.,* **52,** 6180-6184.
544. **Zhang, Z., Chen, L., Zhao, C., Bai, Y., Deng, M., Shan, H., Zhuang, X., Chen, X. and Jing, X.** (2011). *Polymer,* **52,** 676-682.
545. **Zhao, W., Jin, X., Cong, Y., Liu, Y. and Fu, J.** (2013). *J. Chem. Technol. Biotechnol.,* **88,** 327-339.
546. **Zhao, Y., Zhang, Y., Chen, L., Feng, X. and Dong, J.** (2008). *Polym. Prepr.,* **49,** 1088-1094.
547. **Zheng, X. F., Lian, Q. and Song, S. T.** (2013). *Asian J. Chem.,* **25,** 5363-5366.
548. **Zhou, Q., Wei, X., Dou, W., Chou, G. and Wang, Z.** (2013). *Carbohydr. Polym.,* **95**, 733-739.
549. **Zhu, J.** (2010). *Biomaterials,* **31,** 4639-4656.
550. **Zingone, G. and Rubessa, F.** (2005). *J. Pharm.,* **291,** 3-10.

LIST OF PUBLICATIONS BASED ON RESEARCH WORK

A. Referred Journals

Subhraseema Das and Usharani Subuddhi (2013). Cyclodextrin mediated controlled release of naproxen from pH-sensitive chitosan/ poly(vinyl alcohol) hydrogels for colon targeted delivery. *Ind. Eng. Chem. Res.,* **52,** 14192-14200.

Subhraseema Das and Usharani Subuddhi (2014). Exploring poly(vinyl alcohol) hydrogels containing drug-cyclodextrin complexes as controlled drug delivery systems. *J. Appl. Polym. Sci.,* **131,** 40318 (1-8).

Subhraseema Das and Usharani Subuddhi (2014). Controlled delivery of dexamethasone to the intestine from poly(vinyl alcohol)−poly(acrylic acid) microspheres containing drug-cyclodextrin complexes: influence of method of preparation of inclusion complex. *RSC Adv.,* **4,** 24222-24231.

Subhraseema Das and Usharani Subuddhi (2015). Studies on the complexation of diclofenac sodium with β−cyclodextrin: influence of method of preparation. *J.Mol. Struct.,* **1099,** 482-489.

Subhraseema Das and Usharani Subuddhi (2015). Controlled and targeted delivery of diclofenac sodium to the intestine from pH-responsive chitosan/ poly(vinyl alcohol) IPN hydrogels. *Polym. Sci. Ser. A,* (In Press).

Subhraseema Das and Usharani Subuddhi (2015). Guar gum−Poly(acrylic acid)−β−Cyclodextrin hydrogels as controlled delivery vehicles for dexamethasone to the intestine. *Int. J. Biol. Macromol.,* **79,** 856-863.

B. Presentation in Conferences

Subhraseema Das and Usharani Subuddhi, Hydrogel Based Novel Drug Delivery Systems. 14th CRSI National Symposium in Chemistry (NSC-14), February 2-5, **2012**, NIIST, Trivandrum.

Subhraseema Das and Usharani Subuddhi, pH-responsive Chitosan Blends for Sustained Release of an Anionic Drug. International Conference on the Frontiers of Science & Technology, February 21-23, **2013**, Panjab University, Chandigarh.

Subhraseema Das and Usharani Subuddhi, β-Cyclodextrin Embedded Polyacrylic Acid Hydrogels as Sustained Drug Delivery Carriers. 3rd FAPS Polymer Science and MACRO, May 15-18, **2013**, Indian Institute of Science, Bangalore.

Subhraseema Das and Usharani Subuddhi, Controlled Drug Releasing Behaviour of PVA-PEG Hydrogels. National School on Sustainable Polymers and First Symposium on Advances in Sustainable Polymers, January 6-11, **2014**, Indian Institute of Technology, Guwahati.

Subhraseema Das and Usharani Subuddhi, Controlled and Colon Specific Delivery of Dexamethasone from Poly(vinyl alcohol) / Poly(acrylic acid) IPN Hydrogel Microspheres. Current Trends in Surface Science and Technology, February 28, **2014,** Sambalpur University, Orissa.

Subhraseema Das and Usharani Subuddhi, Colon Targeted Delivery of Dexamethasone from Poly(vinyl alcohol) / Poly(acrylic acid) Microspheres Containing Drug-Cyclodextrin Complexes: Influence of Method of Preparation of Inclusion Complex. Recent Developments in Chemical Science and Technology: Young Scientists' Meet, March 15-16, **2014,** National Institute of Technology, Rourkela, Orissa.